UNIVERSIDAD TÉCNICA FEDERICO SANTA MARÍA
DEPARTAMENTO DE FÍSICA
VALPARAÍSO - CHILE

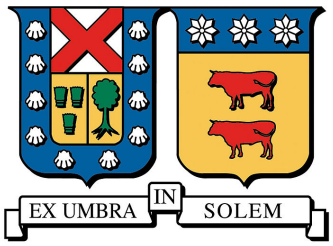

ANALYTIC QCD MODELS AND THEIR APPLICATIONS TO HADRONIC PROCESSES

CÉSAR AYALA NUÑEZ
MEMORIA DE TITULACION PARA OPTAR AL GRADO DE
DOCTOR EN CIENCIAS, MENCIÓN FÍSICA

PROFESOR GUÍA: GORAZD CVETIČ
PROFESOR CO-REFERENTES: SERGEY KOVALENKO Y ALFONSO ZERWEKH
PROFESOR CO-REFERENTE EXTERNO: MARCELO LOEWE

ENERO - 2014

To my wife
Macarena Diaz
and my Parents
Monica Nuñez and
Juan Carlos Ayala

Abstract

Analytic QCD represents QCD frameworks in which the running coupling parameter has the same analytic properties as the spacelike dimensionless physical quantities such as (derivatives) of current correlators, structure functions, dressing functions of propagators, etc. Stated otherwise, the running coupling in analytic QCD is an analytic (holomorphic) function in the plane of complex squared momenta Q^2 ($\equiv -q^2$) except on the timelike semiaxis $Q^2 < -M_{\rm thr}^2$ (where $M_{\rm thr} \sim 10^{-1}$ GeV). On the other hand, in the usual perturbative QCD the running coupling does not possess these holomorphic properties; on the contrary, it has unphysical (Landau) singularities, usually on the positive Q^2 axis in the infrared regime $0 < Q^2 < 1$ GeV^2. As a consequence, the perturbative QCD fails in the evaluation of low-energy physical QCD quantities. In this work, we review various analytic QCD models, and apply them to low-energy QCD phenomenology.

Resumen

QCD analítico corresponde a un topico de QCD en el cual el acoplamiento que corre con la energía es un parametro que posee las mismas propiedades analíticas que las cantidades físicas (medibles) tipo-espacio, tales como (derivadas de) correlador de corrientes, funciones de estructura, parte adimensional de propagadores, etc. En otras palabras, el acoplamiento que corre en QCD analítico es una función analítica (holomorfica) en el plano complejo del momentum al cuadrado Q^2 ($\equiv -q^2$), excepto en el semieje tipo-tiempo $Q^2 < -M_{\rm thr}^2$ (donde $M_{\rm thr} \sim 10^{-1}$ GeV). Por otro lado, en la QCD perturbativa, el acoplamiento que corre no posee dichas propiedades holomorficas, sino que posee una singularidad (Landau) no física, ubicada en el eje positivo de Q^2 en el régimen infrarojo $0 < Q^2 < 1$ GeV^2. Como consecuencia, la teoría de perturbación en QCD falla, que es, resultados erróneos para cantidades físicas de baja energía. En esta Tésis, revisarémos varios modelos de QCD anaítico y los aplicaremos a fenomenología de bajas energías.

Acknowledgments

First of all, I want to express my gratitude to my tutor Dr. Gorazd Cvetič, who provided me with the tools, knowledge and experience with which I could not have carried out this thesis. I appreciate his help, patience and dedication to me, not only his concern for the administrative aspects (scholarship applications, financial support, etc.) and scientific aspects (international contacts, excellent disposition to enter in new areas in my thesis, etc.), but also for his human support in hard and good times. I would like to thank Dr. Sergey Kovalenko for dedicating a lot of his time to teaching me the bases and more of my research.

Concerning my visits abroad, I must thank Dr. Dmitry V. Shirkov for hospitality and partial financial support during my visit in JINR (Dubna, Russia, in 2012); Dr. Gorazd Cvetič for trust and for giving me support from his FONDECYT and internal UTFSM projects; and to the MECESUP grant. In the research work abroad, I met excellent scientists whom I want to thank for their dedication: Dr. Antonio Pineda (UAB, Barcelona, Spain), Dr. Dmitry V. Shirkov, Dr. Anatoly V. Kotikov, Dr. Sergey V. Mikhailov, Dr. Alexander P. Bakulev (deceased) and Ms. Irina V. Potapova (all of JINR, Dubna, Russia).

I would like to express my deep gratitude and respect to my friends Gustavo Pulgar, Cristóbal Corral, Pedro Allendes, Felipe Rojas, Adolfo Toloza and Ligeia Aranguiz inter alia, for their fruitful discussions with me, for hospitality and unconditional help through my PhD, and I thank to Jorge Otálora and Jorge López for help in using calculational software.

I would like to thank my family, especially my parents Monica Nuñez and Juan Carlos Ayala for their unconditional support and continuous love during all my life.
I must thank my wife Macarena Diaz because without her love, companionship, and words of encouragement I would not have finished this thesis. She has been my livelihood and the best friend in hard and happy moments throughout my formation as physicist.

Contents

Introduction

It is well known that the perturbative approach to QCD (pQCD), while working well in evaluation of physical quantities at high momentum transfer ($|q^2| \gtrsim 10^1$ GeV^2), becomes increasingly unreliable at low momenta ($|q^2| \sim 1$ GeV^2). One of the main reasons for this is the singularity structure of the pQCD coupling parameter $a_{\rm pt}(Q^2) \equiv \alpha_s(Q^2)/\pi$ at spacelike low momenta q: $(0 <) \; Q^2 \equiv -q^2 \sim 1$ GeV^2. This singularity structure does not reflect correctly the analyticity structure of the (to be evaluated) spacelike observables $\mathcal{F}(Q^2)$. The latter, by the general principles of the (local) quantum field theory [13,14], must be analytic functions in the entire Q^2 plane except on the cut on the negative semiaxis: $Q^2 \in \mathbb{C}\backslash(-\infty, 0]$. Qualitatively the same analytic properties should have also the coupling parameter $\mathcal{A}_1(Q^2)$ that is used (instead of $a_{\rm pt}(Q^2)$) to evaluate the spacelike observables $\mathcal{F}(Q^2)$.

The first such analytic version (Analytic Perturbation Theory - APT) was constructed in by Shirkov, Solovtsov *et al.* in late nineties where the discontinuity function of pQCD $\rho_1^{\rm (pt)}(\sigma) = {\rm Im} a_{\rm pt}(Q^2 = -\sigma - i\epsilon)$ was kept unchanged on the entire negative axis in the Q^2-plane. Later on, other analytic QCD models were constructed, which fulfill certain additional physically motivated restrictions.

In this thesis, we review the subject of analytic QCD and various applications of it in low-energy QCD phenomenology, referring to works of various authors and including the works by this author.

In Part 1 of this thesis, we first review the usual perturbative QCD (pQCD), subsequently we present the APT of Shirkov, Solovtsov *et al.*, and then present other analytic QCD models (including one co-authored by this author [54]). In Part 2 we present applications of analytic QCD models to low-energy QCD phenomenology: the gluon propagator in the Landau gauge (including our work in arXiv form [69], to be submitted); calculation of the binding energy of heavy quarkonia and extraction of the masses of heavy quarks (one work co-authored by this author [105]); and deep inelastic scattering (including our work to be submitted [149]).

PART 1. Running Coupling Constant in QCD

Chapter 1

Running Coupling Constant in perturbative QCD

In this chapter we present the theoretical background in the description of QCD interaction. We will introduce the running coupling constant in the well known perturbative QCD that arises from the treatment of renormalization approach. After that, we will present several representative QCD models in the dispersive approach, namely Analytic Perturbation Theory (APT) and delta models. Later on we include of some other types of models.

1.1 Introduction

Perturbative quantum chromodynamics (pQCD) is a good tool for test the high energy processes that involves hadrons. This theory, based on the SU(3) gauge symmetry, describe the strong interaction between quarks (constituents of hadrons).
In this chapter, we will review the main steps of the renormalization approach on how to obtain the the pQCD coupling constant, and with this, an explicit dependence on transferred momenta (valid only for large momentum transfer Q^2).
We will analyze the applicability of perturbative expansion in QCD (pQCD), where asymptotic freedom and confinement are reviewed. In the last case, Landau pole become relevant.

1.2 Renormalization Theory

The renormalization procedure arises from the problem of how to deal with infinities in quantum fields theories (from loops in the perturbative expansion). In this sense we redefine the parameters and fields that appear in the original Lagrangian (unrenormalized or bare parameters), in order to obtain finite observables.
In the renormalization technique, we must evaluate some divergent integrals via regularization method. Here appears the ultraviolet cut off $\Lambda_{UV} \to \infty$ and an additional parameter μ which has its origin in the dimensionality in the aforementioned regularization method (both parameters have dimension of mass). Therefore, our renormalized parameters like coupling constant, masses and fields will depend on these quantities.
Of course, physical quantities D (like Adler function) in principle cannot depend on the choice of μ, but approximately they have some residual dependence on μ and on the renormalization scheme (RS) that tells us how to remove Λ_{UV}.
The condition of μ-independence of D can be implemented with the renormalization group equation (RGE), taking into account that D depends on an energy scale Q^2 characteristic of the process in question. Since D is dimensionless, it is a function of Q^2/μ^2 and $\alpha_s(\mu^2)$. By convention, the dependence on energy in perturbation theory of QCD is classified in two different regions, namely Euclidean region $Q^2 = -q^2 > 0$ (or spacelike) and Minkosky region $Q^2 = q^2 > 0$ (or timelike).
The RGE for the observable is the following:

$$\mu^2 \frac{d}{d\mu^2} D(Q^2/\mu^2, a) \equiv \left(\mu^2 \frac{\partial}{\partial \mu^2} + \mu^2 \frac{\partial a}{\partial \mu^2} \frac{\partial}{\partial a} \right) D = 0, \tag{1.1}$$

where by convenience we use for the running coupling constant the notation $a(\mu^2) = g_s(\mu^2)^2/(4\pi^2)$.
It can be rewritten in terms of $t = \ln(Q^2/\mu^2)$:

$$\left(-\frac{\partial}{\partial t} + \beta(a) \frac{\partial}{\partial a} \right) D(e^t, \alpha_s) = 0, \tag{1.2}$$

where

$$\beta(a) = \mu^2 \frac{\partial a^2}{\partial \mu^2} \tag{1.3}$$

The beta function $\beta(a(\mu^2))$ here is considered to be known, and leads to the following implicit solution for $a(\mu^2)$:

$$t \equiv \ln\left(\frac{Q^2}{\mu^2}\right) = \int_a^{a(Q^2)} \frac{dx}{\beta(x)}, \qquad a(\mu^2) \equiv a. \tag{1.4}$$

Here, $a(\mu^2)$ is related to the unrenormalized (bare) constant $a^0 \equiv a(\Lambda_{UV})$ in the standard way

$$a^0 = a(\mu^2) Z_g \left(a(\mu^2), \frac{\mu^2}{\Lambda^2_{UV}} \right) \tag{1.5}$$

Here Z_g is the renormalization constant that reflects the scale dependence.

1.3 The Beta Function

The differential equation that defines the beta function is given in Eq. (1.3), and at $\mu^2 = Q^2$ is

$$\beta(a(Q^2)) = Q^2 \frac{\partial a(Q^2)}{\partial Q^2}, \tag{1.6}$$

Now, in perturbation theory, we can solve it if we find their respectively renormalization constant that arise from either the quark gluon vertex, or ghost-ghost gluon vertex, or three gluon vertex, etc... In this calculus we have (with space dimension $d = 4 - \epsilon$) $\alpha_s^0 = \mu^\epsilon \alpha_s Z_g$ and we find from a series of diagrams the perturbative dependence in the form: $Z_g = 1 + \sum_{n=1}^{\infty} C_j^{(n)} \alpha_s^n$.
Therefore, the beta function takes the form of the corresponding perturbation expansion [with the notation: $a(Q^2) \equiv \alpha_s(Q^2)/\pi = g_s(Q^2)^2/(4\pi^2)$]

$$\beta(a) = -\sum_{j=2}^{\infty} \beta_{j-2} a^j \tag{1.7}$$

with (from Z_g calculus):

$$\begin{aligned}
\beta_0 &= \frac{1}{4}\left(11 - \frac{2}{3} n_f\right), \\
\beta_1 &= \frac{1}{16}\left(102 - \frac{38}{3} n_f\right), \\
\beta_2 &= \frac{1}{64}\left(\frac{2857}{2} - \frac{5033}{18} n_f + \frac{325}{54} n_f^2\right), \\
\beta_3 &= \frac{1}{256}\left[\left(\frac{149753}{6} + 3564\zeta_3\right) - \left(\frac{1078361}{162} + \frac{6508}{27}\zeta_3\right) n_f \right. \\
&\quad \left. + \left(\frac{50065}{162} + \frac{6472}{81}\zeta_3\right) n_f^2 + \frac{1093}{729} n_f^3\right]
\end{aligned} \tag{1.8}$$

where ζ_ν is the Riemann zeta function, in particular $\zeta_3 \simeq 1,202057$; n_f = number of active quarks flavors .

This result is in the $\overline{MS}$ scheme. The first two beta coefficients (β_0 and β_1) are scheme independent, we say they are universal (only if quarks are massless). While the next coefficients ($\beta_2, \beta_3, \ldots$) are scheme dependent (or scheme sensitive).
The first consequence of the use of non-Abelian theory (QCD) was seen in the beta function, because at one loop it is evident that β_0 coefficient in QED and QCD have the opposite signs for $n_f \leq 33/2 \approx 16$ (and $n_f = 8$ for two-loop β_1 coefficient). This is a consequence ofthe asymptotically freedom of QCD, that is the beta function has a stable UV fixed point.

1.4 Running Coupling

Combining Eq. (1.6) and (1.7) we have

$$Q^2 \frac{\partial a}{\partial Q^2} = -\sum_{j=2}^{\infty} \beta_{j-2} a^j. \tag{1.9}$$

The beta function (on the right hand side of (1.9)) is usually written as a truncated perturbation series of coupling a, the resulting differential equation for a is then solved, either analytically (if possible) or numerically.
For example, the one-loop order equation can be integrated

$$\int_{a(\mu^2)}^{a(Q^2)} \frac{da}{a^2} = -\beta_0 \int_0^{\frac{1}{2}\ln(Q^2/\mu^2)} d\ln(Q^2/\mu^2), \tag{1.10}$$

giving the well known solution

$$a(Q^2) = \frac{a(\mu^2)}{1 + \beta_0 a(\mu^2) \ln(Q^2/\mu^2)}. \tag{1.11}$$

It is usual to re-express (in a more modern notation) this quantity in terms of a new invariant mass parameter Λ ($\sim 10^{-1}$GeV)

$$a(Q^2) = \frac{1}{\beta_0 \ln(Q^2/\Lambda^2)}, \qquad \Lambda^2 = \mu^2 e^{-1/(\beta_0 a(\mu^2))}. \tag{1.12}$$

With the explicit value of β_0 this become

$$a(Q^2) = \frac{12}{(33 - 2n_f)\ln(Q^2/\Lambda^2)} \tag{1.13}$$

One way to solve the RGE to two loops is iterating with respect to the one-loop formula, which gives us an approximate coupling as an expansion in powers of L^{-1}, where $L \equiv \ln(Q^2/\Lambda^2)$, and explicitly we obtain

$$a^{(2)}(Q^2) = \frac{1}{\beta_0 L}\left(1 - \frac{\beta_1}{\beta_0^2}\frac{\ln(L)}{L}\right) \tag{1.14}$$

this approximation is valid for $L \gg 1$, that is the high energy region.
The iterative method can be performed to any loops, and is straightforward to find the next level, that is to three loops in the form

$$a^{(3)}(Q^2) = \frac{1}{\beta_0 L}\left(1 - \frac{\beta_1}{\beta_0^2}\frac{\ln(L)}{L} + \frac{\beta_1 \ln^2(L) - \beta_1 \ln(L) + \beta_2\beta_0 - \beta_1^2}{\beta_0^4 L^2}\right) \tag{1.15}$$

and in the analogous way, we have for four loop case

$$\begin{aligned} a^{(4)}(Q^2) &= \frac{1}{\beta_0 L}\left\{1 - \frac{\beta_1}{\beta_0^2}\frac{\ln(L)}{L} + \frac{1}{\beta_0^2 L^2}\left[\frac{\beta_1^2}{\beta_0^2}(\ln^2(L) - \ln(L) - 1) + \frac{\beta_2}{\beta_0}\right] + \right. \\ &\quad \frac{1}{\beta_0^3 L^3}\left[\frac{\beta_1^3}{\beta_0^3}\left(-\ln^3(L) + \frac{5}{2}\ln^2(L) + 2\ln(L) - \frac{1}{2}\right)\right. \\ &\quad \left.\left. -3\frac{\beta_1\beta_2}{\beta_0^2}\ln(L) + \frac{\beta_3}{2\beta_0}\right]\right\} \end{aligned} \tag{1.16}$$

There is a way to find the two loop coupling as a solution of RGE exactly. RGE to two loop lead a transcendental equation. Namely, integrating (1.9) we have

$$\int_{a(\mu^2)}^{a(Q^2)} \frac{da}{a^2\left(1 + \frac{\beta_1}{\beta_0}a\right)} = -\beta_0 \int_0^{\frac{1}{2}\ln(Q^2/\mu^2)} d\ln(Q'^2/\mu^2). \tag{1.17}$$

So, the transcendental equation gets the form

$$\ln(Q^2/\mu^2) = C + \frac{1}{\beta_0 a(Q^2)} + \frac{\beta_1}{\beta_0^2}\ln(a(Q^2)) - \frac{\beta_1}{\beta_0^2}\ln\left(1 + \frac{\beta_1}{\beta_0}a(Q^2)\right), \tag{1.18}$$

here C contains the coupling in μ^2.
Now we want to introduce (in the same way as in the one-loop case) a new invariant mass parameter Λ, given by

$$\begin{aligned} \ln(Q^2/\Lambda^2) &= \frac{1}{\beta_0 a(Q^2)} - \frac{\beta_1}{\beta_0^2}\ln\left(\frac{\beta_1}{\beta_0^2} + \frac{1}{\beta_0 a(Q^2)}\right), \\ \Lambda^2 &= \mu^2 \exp\left[C - \frac{\beta_1}{\beta_0^2}\ln(\beta_0)\right]. \end{aligned} \tag{1.19}$$

At this stage, we need to invert this relation, but this is difficult and serious problems related to the singularity structure appear(we lose an explicit form for the singularities).
The solution was made with the help of the so-called Lambert W function defined by

$$W(z)\exp[W(z)] = z \tag{1.20}$$

The singularity structure of the Lambert function is made up of infinite number of branches; it satisfies the following symmetry relation: $W^*_{-n}(y^*) = W_n(y)$.
With this function the solution to the coupling is

$$a^{(2)}(Q^2) = -\frac{1}{c_1}\frac{1}{1+W_{\mp 1}(z_\pm)}, \tag{1.21}$$

where $c_1 = \beta_1/\beta_0$, $Q^2 = |Q^2|\mathrm{e}^{i\phi}$, and the upper sign refers to the case $0 \le \phi \le +\pi$, the lower sign to $-\pi \le \phi \le 0$, and

$$z_\pm = \frac{1}{c_1 \mathrm{e}}\left(\frac{|Q^2|}{\Lambda^2}\right)^{-\beta_0/c_1} \exp\left[i\left(\pm\pi - \frac{\beta_0}{c_1}\phi\right)\right]. \tag{1.22}$$

This idea can be extended to the three-loop case, using an approximation via Padé for the beta function

$$\beta_{app}(a) = -\beta_0 a^2(Q^2)\frac{1+(c_1 - c_2/c_1)a(Q^2)}{1-(c_2/c_1^2)a(Q^2)}. \tag{1.23}$$

With this, the solution of the coupling to three loops in terms of the Lambert function takes the form

$$a^{(3)}(Q^2) = -\frac{1}{c_1}\frac{1}{1-c_2/c_1^2 + W_{\mp 1}(z_\pm)} \tag{1.24}$$

The Lambert function $W = W(z)$ is defined via the inverse relation (1.20), cf. Fig. 1.1(a). The two branches $W_{\mp 1}(z)$ of the Lambert function are related via complex-conjugation

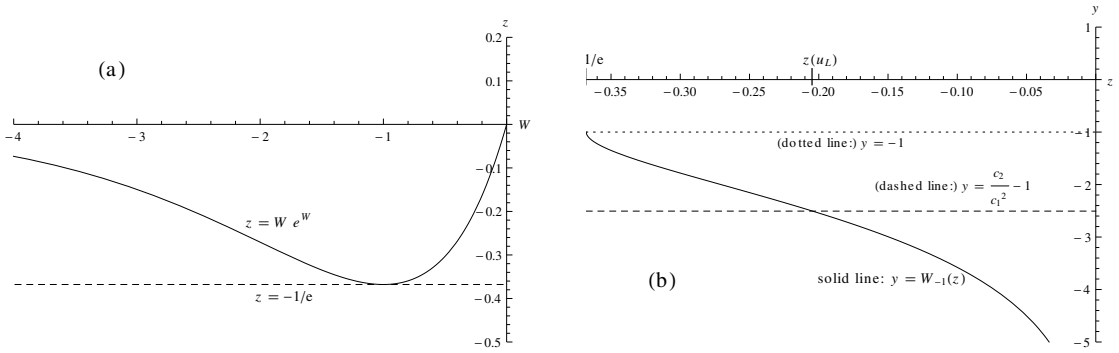

Figure 1.1: (a) The defining relation $z = We^W$ for the Lambert function $W(z)$, for $-1/e < z < 0$; (b) The branch $W_{-1}(z)$ for the same z-interval; when $c_2 < 0$, the denominator of Eq. (1.24) becomes zero at a $z(u_\mathrm{L})$ in this interval.

$W_{+1}(z^*) = W_{-1}(z)^*$, and the point $z = -1/e$ is the branching point of these functions. In the interval $-1/e < z < 0$, $W_{-1}(z)$ is a decreasing function of z, cf. Fig. 1.1(b). When $z \to -0$, the scale Q^2 tends to $Q^2 \to +\infty$, and $W_{-1}(z) \to -\infty$, this reflecting

the asymptotic freedom of $a_{\rm pt}(Q^2)$ of Eq. (1.24). In our considered case of low-energy QCD (i.e., with number of quark flavors $n_f = 3$), the solution (1.24) has unphysical (Landau) singularities along the positive Q^2 axis, for any c_2. An extension of such beta function to the effective four- and five-loop case, such that the solution is explicit and involving Lambert functions, was made in [2]. For more details on the Lambert functions, we refer to Refs. [2–6].

1.5 Thresholds

Until now, the coupling that we are considering has been running in the whole range of energy without taking into account the heavy mass thresholds. The latter provide us a more accurate formula for the running coupling.
In order to incorporate these mass (decoupled) effects, we note that the flavor dependence (n_f) is via the beta coefficients (1.8). We will consider the following convention: n_l massless quarks with $m_q \ll \mu$ ($n_l = n_f - 1$), and the n'_fth quark flavor has a mass m_h that is supposed to be much larger than the energy scale μ.
The most simple way to consider the mass effects is by imposing continuity on the coupling in the Euclidean region at threshold scales $\mu_{thr} \sim m_h$. Introducing the notation

$$a(Q^2) \equiv f_{N_f}(Q^2/\Lambda^2_{n_f}) \ , \tag{1.25}$$

at positive "threshold" values $Q^2 = \mu_{thr} = Q^2_{n_f-1 \mapsto n_f} > 0$ chosen to be for $n_f = 4, 5, 6$ the squares of the current heavy quark masses m_h: $m_c \equiv m_4$, $m_b \equiv m_5$ and $m_t \equiv m_6$, respectively [7]

$$f_{N-1}(m^2_N/\Lambda^2_{N-1}) = f_N(m^2_N/\Lambda^2_N) \qquad (N \equiv n_f = 4, 5, 6) \ . \tag{1.26}$$

Further, it is assumed that, for complex Q^2, the values of $a(Q^2)$ involve the scale $\overline{\Lambda}_{N_f}$ determined by the absolute value $|Q^2|$

$$a(Q^2) = f_N(Q^2/\overline{\Lambda}^2_N) \qquad \text{for}: m^2_N < |Q^2| < m^2_{N+1} \ . \tag{1.27}$$

In a more rigurous way, we need to take the matching between the coupling in the QCD and a coupling in an effective theory. In this way, we have an effective theory with n_l flavors by requiring consistency with the n_f QCD theory at an energy that corresponds to the heavy mass threshold $\mu^{(n_f)} = \mathcal{O}(m_h)$. Following the formulae in [8, 10, 11] up to three loops, and taking explicit formulas to four loops from [12] we have the matching scale $\mu^{(n_f)}$ in units of the RG-invariant $\overline{\rm MS}$ mass $\mu_h = m_h(\mu_h)$

$$\begin{aligned} \frac{a'}{a} &= 1 - a\frac{\ell_h}{6} + a^2\left(\frac{\ell_h^2}{36} - \frac{19}{24}\ell_h + c_2\right) + a^3\left[-\frac{\ell_h^3}{216}\right. \\ &- \left.\frac{131}{576}\ell_h^2 + \frac{\ell_h}{1728}(-6793 + 281\, n_l) + c_3\right] , \end{aligned} \tag{1.28}$$

Table 1.1: Comparison between different values of the lambda QCD for $n_f = 3, 4, 5$ in the $\overline{\rm MS}$ scheme and the different values of the coupling at three loop order in the threshold masses.

Method	Lambda QCD			Running Coupling (3 loops)			
	$\overline{\Lambda}_5$	$\overline{\Lambda}_4$	$\overline{\Lambda}_3$	$a^{(n_f=5)}(m_b^2)$	$a^{(n_f=4)}(m_b^2)$	$a^{(n_f=4)}(m_c^2)$	$a^{(n_f=3)}(m_c^2)$
Decoupled	0.208	0.289	0.329	0.0713	0.0714	0.1220	0.1223
Shirkov	0.208	0.287	0.326	0.0712	0.0712	0.1216	0.1216

where $\ell_h = \ln[(\mu^{(n_f)})^2/\mu_h^2]$, $a' = a^{(n_l)}(\mu^{(n_f)})$, $a = a^{(n_f)}(\mu^{(n_f)})$ and

$$c_2 = \frac{11}{72}, \quad c_3 = -\frac{82043}{27648}\zeta(3) + \frac{564731}{124416} - \frac{2633}{31104}n_l. \tag{1.29}$$

Here, ζ is Riemann's zeta function ($\zeta(3) \approx 1.202\,057$). And in terms of the pole mass M_h with $\mathcal{L}_h = \ln[(\mu^{(n_f)})^2/M_h^2]$

$$\begin{aligned} \frac{a'}{a} &= 1 - a\frac{\mathcal{L}_h}{6} + a^2\left(\frac{\mathcal{L}_h^2}{36} - \frac{19}{24}\mathcal{L}_h + C_2\right) + a^3\left[-\frac{\mathcal{L}_h^3}{216}\right. \\ &- \left.\frac{131}{576}\mathcal{L}_h^2 + \frac{\mathcal{L}_h}{1728}(-8521 + 409\,n_l) + C_3\right], \end{aligned} \tag{1.30}$$

where

$$\begin{aligned} C_2 = -\frac{7}{24}, \quad C_3 &= -\frac{80507}{27648}\zeta(3) - \frac{2}{3}\zeta(2)\left(\frac{1}{3}\ln 2 + 1\right) \\ &- \frac{58933}{124416} + \frac{n_l}{9}\left[\zeta(2) + \frac{2479}{3456}\right]. \end{aligned} \tag{1.31}$$

In order to test the first model (more easy) with the rigorous analysis of the treatment of the thresholds, we obtained the values of $\overline{MS}$ lambda at $k = 3, 4, 5$ (flavors).

In Table 1, the value for $\overline{\Lambda}_5$ was taken from the well-known world average value of the coupling: $a^{(n_f=5)}(M_z^2) = 0.118/\pi$ that implies: $\overline{\Lambda}_5 = 0.208$ in the $\overline{MS}$ renormalization scheme to three loops order.
Besides, the values of the more simple approach differ by about 1% with respect to the last method. This small effect in the coupling implies that when we will work in analytic QCD models, we prefer the more simple method and therefore we define the coupling as a "global" in the form

$$\begin{aligned} a^{glob.}(Q^2) &= a^{n_f=3}(Q^2;\Lambda_3)\Theta(Q^2 \le m_4^2) + a^{n_f=4}(Q^2;\Lambda_4)\Theta(m_4^2 \le Q^2 \le m_5^2) + \\ &\quad a^{n_f=5}(Q^2;\Lambda_5)\Theta(m_5^2 \le Q^2 \le m_6^2) + a^{n_f=6}(Q^2;\Lambda_6)\Theta(m_6^2 \le Q^2) \end{aligned} \tag{1.32}$$

1.6 Confinement and Asymptotic Freedom

In QCD we have a familiar behavior of the running coupling that decreases logarithmically at large momentum transfer $Q^2 \to \infty$ (see Eq. (1.12)). It is familiar because the perturbation theory is reliable at these scales, so this is only a consequence of a mathematical procedure. On the other hand, the theoretical explanation of this fact is that the interaction at small distance is negligible.
We can see this effect in the beta function too. The asymptotic freedom occurs if $\beta_0 > 0$, that is for $n_f \leq 16$, therefore the asymptotic freedom in QCD is valid since $n_f \leq 16$.
Asymptotic freedom is inherent in the nature of nonabelian Yang-Mills theory, because of gauge boson self-interactions.
On the contrary, when we go to low energy scales, the running coupling constant begins to increase, and perturbative QCD becomes unreliable. Such growth of the coupling explains the nature of the strong interaction.
Confinement in QCD means that free quarks and gluons cannot be observes in the real world.
Confinement is a tendency of the perturbative coupling; in the next section we will see that is natural to have an infrared (IR) fixed point, i.e. that the running coupling freezes at $Q^2 \to 0$.
In Fig. (1.2) we can see the perturbative running coupling at three flavors in a wide region of energy scale. From here is evident the aforementioned properties of asymptotic freedom and confinement are evident confirmed by the experiments (we used the normalization at $n_f = 5$ from the world average value).

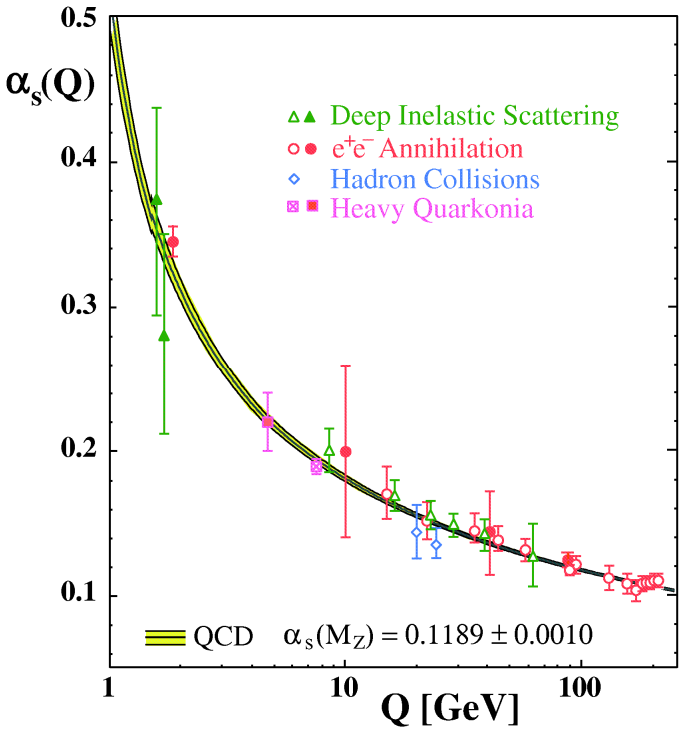

Figure 1.2: Runing coupling constant versus Q^2, compared with different experiments from different sources taken from Ref. [15]

1.7 Landau Poles

The one-loop running coupling constant (1.12), has a pole singularity at the spacelike point $Q^2 = \Lambda^2$ due to the logarithmic behavior called "Landau pole". Here the application of perturbative expansion is not reliable.
A similar phenomenon we can see at two loop (see Eq. (1.14)) $a^{(2)}(Q^2) \sim 1/\sqrt{\ln(Q^2/\Lambda^2)}$, where a pole and a branching point appear. When we go to higher orders, the singularities at spacelike $Q^2 \sim \Lambda^2$ remain.
Based on these arguments, at $Q^2 \approx 3\text{GeV}^2$ scales, the perturbative QCD (pQCD) coupling $a(Q^2)$ is marginally reliable; at $Q \approx 1$ GeV it is unreliable. This is so because the pQCD coupling $a(Q^2)$ suffers from unphysical (Landau) singularities at low spacelike q^2 ($\equiv -Q^2$), i.e., at $0 < Q^2 < \Lambda^2$ where $\Lambda^2 \sim 10^{-1}$ GeV^2; for $Q^2 \sim 1$ GeV^2 it is dangerously close to these singularities, and thus unreliable.
The aforementioned Landau singularities are not physical because they do not possess the analytic properties of the spacelike observables $\mathcal{D}(Q^2)$ (such as the Adler function), the latter properties being dictated by the general properties of quantum field theories [13, 14] including causality. Namely, $\mathcal{D}(Q^2)$ must be an analytic function in the entire complex Q^2 plane, with the exception of the timelike semiaxis $Q^2 < -M_{\text{thr}}^2$,

where $M_{\rm thr} \sim 10^{-1}$ GeV is a particle production threshold. Specifically, the evaluation of spacelike quantities $\mathcal{D}(Q^2)$ in pQCD, as a (truncated) power series of the perturbative running coupling (couplant) $a_{\rm pt}(\kappa Q^2) \equiv \alpha_s(\kappa Q^2)/\pi$ (with $\kappa \sim 1$), does not respect these important analytic properties of $\mathcal{D}(Q^2)$

Chapter 2

Analytic Perturbation Theory (APT)

2.1 Introduction

The analytic perturbation theory (APT) was introduced by Shirkov and Solovtsov [16–19] (for more details see the reviews in Refs. [20, 21]). This was the first QCD model based on the dispersion relation or Källen-Lehmann representation to the running coupling, and represents one of the most known analytic QCD models (analytic in the sense that the coupling $a(Q^2)$ is analytic/holomorphic function).
We saw that in the IR domain, the RGE method gives us nonphysical (Landau) singularities, and the main idea of all analytic models is to eliminate them.
The Källen-Lehmann representation can be derived by applying the Cauchy theorem, choosing an appropriate contour in the complex Q^2-plane displayed in Fig. (2.1). Taking $f(Q'^2) \equiv \frac{a(Q'^2)}{Q'^2-Q^2}$ in Fig. (2.1) we get the following analytic coupling:

$$\mathcal{A}_1(Q^2) \equiv a(Q^2)_{(an.)} = \frac{1}{\pi}\int_0^\infty d\sigma \frac{\rho_1^{pt}(\sigma)}{\sigma + Q^2}, \tag{2.1}$$

where

$$\rho_1^{pt}(\sigma) \equiv \frac{1}{2i}[a(-\sigma - i\epsilon) - a(-\sigma + i\epsilon)] = \mathrm{Im}(a(-\sigma - i\epsilon)). \tag{2.2}$$

This new coupling is called APT analytic coupling. Via this dispersive approach all the unphysical singularities are removed in a natural way, and it is straightforward to generalize this approach to any powers. In this sense, the new analytic version of

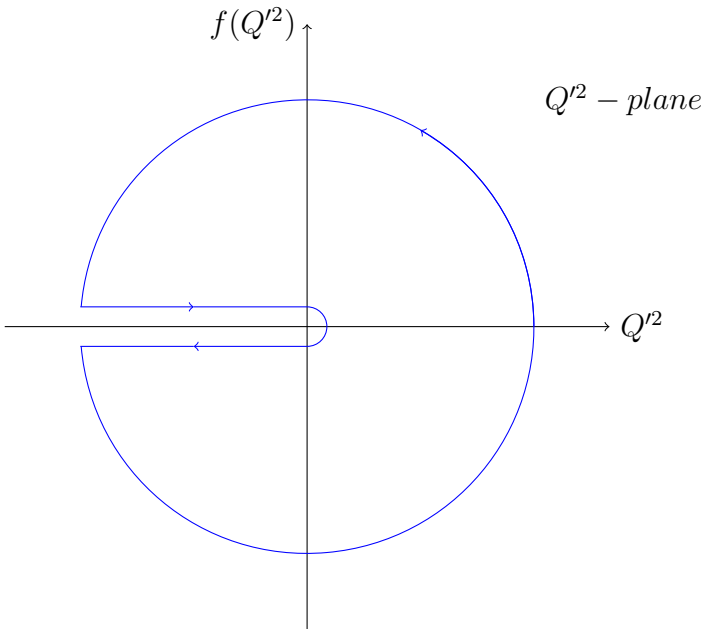

Figure 2.1: Contour needed to derive the analytic APT coupling (with radius $r \mapsto \infty$)

the powers of the coupling are in general nonpowers [16, 19, 20, 22–25] and obeys the following linear operation (that is, in the region: $Q^2 \equiv -q^2 \in \mathbb{C}\ \ (-\infty, \infty]$) A_E:

$$A_E[a^n_{(l)}] = \mathcal{A}^{(l)}_n(Q^2) \equiv \frac{1}{\pi}\int_0^\infty d\sigma \frac{\rho^{(l)}_n(\sigma)}{\sigma + Q^2}. \tag{2.3}$$

Here, the spectral density generalized to l-loops and takes the form

$$\rho^{(l)}_n(\sigma) = \mathrm{Im}[a^n_{(l)}(-\sigma - i\epsilon)]. \tag{2.4}$$

In analogous way, we can find the running analytic coupling in the Minkowskian region ($s = q^2 > 0$) via linear operation A_M

$$A_M[a^n_{(l)}] = \mathfrak{A}^{(l)}_n(s) \equiv \frac{1}{\pi}\int_s^\infty d\sigma \frac{\rho^{(l)}_n(\sigma)}{\sigma}, \tag{2.5}$$

Now, these two analytic couplings can be related one to another via the following two integral transformations: $\hat{D}$ from Minkowski to Euclidean and $\hat{R}$ from Euclidean to Minkowski.

$$\begin{aligned} \hat{D}[\mathfrak{A}^{(l)}_n] &= \mathcal{A}^{(l)}_n \equiv Q^2 \int_0^\infty d\sigma \frac{\mathfrak{A}^{(l)}_n(\sigma)}{(\sigma + Q^2)^2}, \\ \hat{R}[\mathcal{A}^{(l)}_n] &= \mathfrak{A}^{(l)}_n \equiv \frac{1}{2\pi i}\int_{-s-i\epsilon}^{-s+i\epsilon} d\sigma \frac{\mathcal{A}^{(l)}_n(\sigma)}{\sigma}, \end{aligned} \tag{2.6}$$

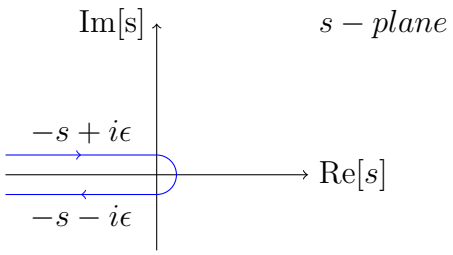

Figure 2.2: Contour for $\hat{R}$ transformation

where the contour of Fig. (2.2) was implemented to the case of $\hat{R}$ transformation.

2.2 Physical Observables in APT

The Adler function $D(Q^2)$ represents a typical observable in physical processes in the spacelike regime (Euclidean region). In the standard perturbative QCD the Adler function takes the form [22, 26]

$$D(Q^2) = \sum_n d_n a_{(l)}^n(Q^2), \tag{2.7}$$

where the renormalization point $\mu^2 = Q^2$ is understood.
With this form of the Adler function, the analytization of this quantity is direct via the aforementioned (defined in the last section) linear transformation $A_E[D] \equiv \mathcal{D}_A$, with

$$\begin{aligned} \mathcal{D}_A &= A_E\left[\sum_n d_n a_{(l)}^n(Q^2)\right] \\ &= \sum_n d_n A_E[a_{(l)}^n(Q^2)] \\ &= \sum_n d_n \mathcal{A}_n^{(l)}(Q^2). \end{aligned} \tag{2.8}$$

We can perform the second step since the coefficients d_n are independent of the momentum transfer Q^2. In general, we must take such a step in the dispersive approach.
In an analogous way, we can deal with observables in the timelike regime (Minkowski region) such as Drell function $R(s)$. In the perturbative expansion in QCD, this function is given by

$$R(s) = \sum_m r_m a_{(l)}^m(s), \tag{2.9}$$

where the condition $\mu^2 = s$ was assumed.
The analytization in the timelike region is made with the help of the aforementioned linear operation $A_M[R] \equiv \mathcal{R}$

$$\begin{aligned}\mathcal{R} &= A_M\left[\sum_m r_m a^m_{(l)}(s)\right] \\ &= \sum_m r_m A_M[a^m_{(l)}(s)] \\ &= \sum_m r_m \mathfrak{A}^{(l)}_m(s). \end{aligned} \tag{2.10}$$

where r_m coefficients are s independent.
Now, the connection between these two quantities is like in the case of the coupling in the two regimes

$$\hat{R}[\mathcal{D}_A] = \mathcal{R}; \qquad \hat{D}[\mathcal{R}] = \mathcal{D}_A \tag{2.11}$$

2.3 Nonpower Expansion

In the previous section, analytic Adler and Drell functions in terms of analytic coupling were presented, these expansions incorporate a linear transformation upon powers of coupling resulting in nonpower analytic couplings (given by Eq. (2.6)). This gave the explicit expressions in (2.8) and (2.10) which were obtained in [19, 23, 26] We can find recursive relation based on the renormalization group (since we can analytize the beta function) for higher orders of the analytic coupling

$$\frac{1}{k}\frac{d\mathcal{A}^{(l)}_k(Q^2)}{d\ln Q^2} = -\sum_{j=1}^{n}\beta_{j-1}\mathcal{A}^{(l)}_{k+j}(Q^2); \qquad \frac{1}{k}\frac{d\mathfrak{A}^{(l)}_k(s)}{d\ln s} = -\sum_{j=1}^{n}\beta_{j-1}\mathfrak{A}^{(l)}_{k+j}(s). \tag{2.12}$$

It is often more easy to use this relation for calculations of higher orders instead of use the dispersive approach directly.
We present below the derivation of the first relation in (2.12). In pQCD we have

$$\begin{aligned}\frac{da^k(Q^2)}{d\ln(Q^2)} &= \frac{da^k}{da}\frac{da}{d\ln(Q^2)} = ka^{k-1}\beta(a) \\ &= -k\beta_0 a^{k+1} - k\beta_1 a^{k+2} - k\beta_2 a^{k+3} + \cdots . \end{aligned} \tag{2.13}$$

Applying the imaginary part on both sides of (2.13) and taking $Q^2 \in \mathbb{C}$ & $Q^2 = -\sigma - i\epsilon$ ($d\ln(Q^2) \to d\ln\sigma$), we obtain

$$\frac{1}{k}\frac{d\mathrm{Im}a^k(-\sigma - i\epsilon)}{d\ln\sigma} = -\sum_{n\geq 1}\beta_{n-1}\mathrm{Im}\left[a^{k+n}(-\sigma - i\epsilon)\right]$$

$$\Longrightarrow \frac{1}{\pi k}\int_0^\infty d\sigma \frac{\sigma \frac{d}{d\sigma}\mathrm{Im}a^k(-\sigma - i\epsilon)}{\sigma + Q^2} = -\sum_{n\geq 1}\beta_{n-1}\mathcal{A}_{k+n}(Q^2), \tag{2.14}$$

and we can rewrite the l.h.s of (2.14) in the following form:

$$\begin{aligned}
\frac{1}{\pi k}\int_0^\infty d\sigma \frac{\sigma \frac{d}{d\sigma}\mathrm{Im}a^k(-\sigma - i\epsilon)}{\sigma + Q^2} &= -\frac{1}{\pi k}\int_0^\infty d\sigma \mathrm{Im}a^k(-\sigma - i\epsilon)\frac{d}{d\sigma}\left(\frac{\sigma}{\sigma + Q^2}\right) \\
&= \frac{1}{\pi k}\int_0^\infty d\sigma \frac{(-Q^2)}{(\sigma + Q^2)^2}\mathrm{Im}a^k(-\sigma - i\epsilon) \\
&= \frac{1}{\pi k}\frac{d}{d\mathrm{ln}Q^2}\int_0^\infty d\sigma \frac{\mathrm{Im}a^k(-\sigma - i\epsilon)}{(\sigma + Q^2)} \\
&= \frac{1}{k}\frac{d\mathcal{A}_k(Q^2)}{d\mathrm{ln}Q^2}
\end{aligned} \tag{2.15}$$

Therefore with (2.14) and (2.15) we obtain the first recursion relation in (2.12). The procedure to find the recursion relation in the Minkowski region can be performed in an analogous way.
The relations (2.12) are valid also in any other analytic QCD model, and define the power analogous $\mathcal{A}_k$ as combination of logarithmic derivatives $d^n\mathcal{A}_1(Q^2)/d(\mathrm{ln}Q^2)^n$; this construction of $\mathcal{A}_k$'s in general analytic QCD models was proposed and presented in Refs. [35, 36].

2.4 One-Loop APT Coupling

A first (and more basic) application of the dispersion relation is for the running coupling to one-loop order (1.12).
The spectral density is given by [20, 21]

$$\begin{aligned}
\rho_1^{(1)} &= \mathrm{Im}\left[\frac{1}{\beta_0 \mathrm{ln}(-\sigma/\Lambda^2)}\right] = \frac{1}{\beta_0}\mathrm{Im}\left[\frac{1}{\mathrm{ln}(\sigma/\Lambda^2) - i\pi}\right] \\
&= \frac{\pi}{\beta_0(\mathrm{ln}^2(\sigma/\Lambda^2) + \pi^2)}.
\end{aligned} \tag{2.16}$$

We replace this in (2.3). The analytic coupling to one loop is

$$\begin{aligned}
\mathcal{A}_1^{(1)}(Q^2) &= \frac{1}{\beta_0 \mathrm{ln}(Q^2/\Lambda^2)} - \frac{1}{2\pi i}\int \frac{dQ'^2 a(Q'^2)}{Q^2 - Q'^2} \\
&= \frac{1}{\beta_0 \mathrm{ln}(Q^2/\Lambda^2)} - \frac{1}{\beta_0}\left(\frac{\Lambda^2}{\Lambda^2 - Q^2}\right),
\end{aligned} \tag{2.17}$$

where for simplicity, we apply the Cauchy theorem, with the second term in the r.h.s. of (2.17) corresponding to the residue in the Landau pole $Q^2 = \Lambda^2$. Therefore, the analytic coupling corresponds to perturbative coupling minus the Landau pole.
In the Minkowskian region, we apply the relation (2.5) or the transformation $\hat{R}$ (see Eq. (2.6)) upon (2.17), and this gives

$$\begin{aligned}\mathfrak{A}_1^{(1)}(s) &= \frac{1}{\pi\beta_0}\arctan\left(\frac{\pi}{\ln(s/\Lambda^2)}\right)\\ &= \frac{1}{\pi\beta_0}\arccos\left(\frac{\ln(s/\Lambda^2)}{\sqrt{\ln(s/\Lambda^2)+\pi^2}}\right)\end{aligned} \tag{2.18}$$

The expressions for higher orders are found via recursive relations (2.12) taking into account that $\beta_0 \neq 0$ and $\beta_{i>0} = 0$:

$$\begin{aligned}\mathcal{A}_2^{(1)}(Q^2) &= \frac{1}{\beta_0^2}\left(\frac{1}{\ln^2(Q^2/\Lambda^2)} - \frac{Q^2}{\Lambda^2(Q^2/\Lambda^2-1)^2}\right),\\ \mathcal{A}_3^{(1)}(Q^2) &= \frac{1}{\beta_0^3}\left(\frac{1}{\ln^3(Q^2/\Lambda^2)} - \frac{1}{2}\frac{Q^2/\Lambda^2(1+Q^2/\Lambda^2)}{(Q^2/\Lambda^2-1)^3}\right)\end{aligned} \tag{2.19}$$

and for the Minkowski coupling

$$\begin{aligned}\mathfrak{A}_2^{(1)}(s) &= \frac{1}{\beta_0}\frac{1}{\ln^2(s/\Lambda^2)+\pi^2},\\ \mathfrak{A}_3^{(1)}(s) &= \frac{1}{\beta_0^3}\frac{\ln^2(s/\Lambda^2)}{(\ln^2(s/\Lambda^2)+\pi^2)^2},\end{aligned} \tag{2.20}$$

where from (2.12) we used (iteratively) to one loop

$$\begin{aligned}\mathcal{A}_2^{(1)}(Q^2) &= -\frac{1}{\beta_0}\frac{d\mathcal{A}_1^{(1)}(Q^2)}{d\ln(Q^2/\Lambda^2)}\\ \mathcal{A}_3^{(1)}(Q^2) &= -\frac{1}{2\beta_0}\frac{d\mathcal{A}_2^{(1)}(Q^2)}{d\ln(Q^2/\Lambda^2)} = \frac{1}{2\beta_0^2}\frac{d^2\mathcal{A}_1^{(1)}(Q^2)}{d\ln(Q^2/\Lambda^2)^2}\\ &\vdots\\ \mathcal{A}_k^{(1)}(Q^2) &= \frac{(-1)^{k-1}}{\beta_0^{k-1}(k-1)!}\frac{d^{k-1}}{d\ln(Q^2/\Lambda^2)^{k-1}}\mathcal{A}_1^{(1)}(Q^2); \qquad k\geq 2\end{aligned} \tag{2.21}$$

and

$$\mathfrak{A}_k^{(1)}(s) = \frac{(-1)^{k-1}}{\beta_0^{k-1}(k-1)!}\frac{d^{k-1}}{d\ln(s/\Lambda^2)^{k-1}}\mathfrak{A}_1^{(1)}(s); \qquad k\geq 2 \tag{2.22}$$

We compare the analytic couplings in the Euclidean and Minkowskian regions (see Fig. 2.3), by summarizing the following properties:

- There is an IR fixed point, that is $\mathfrak{A}_1(0) = \mathcal{A}_1(0) = 1/\beta_0$, with $\beta_0 = \frac{1}{4}(11 - 2n_f/3)$.
- Asymptotic freedom is satisfied: $\mathfrak{A}_1(\infty) = \mathcal{A}_1(\infty) = 0$
- In general, the coupling (at any order) changes when we go from the Minkowskian to Euclidean region. This property is known as "distorting mirror".
- Higher order analytic couplings by construction are different from powers of $\mathcal{A}_1$ (or $\mathfrak{A}_1$). Therefore, we have an expansion in nonpower function.

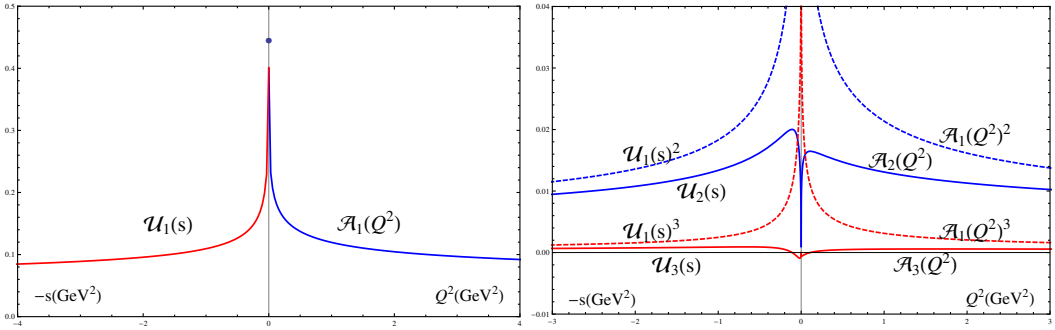

Figure 2.3: Analytic couplings in APT to one-loop order for spacelike $\mathcal{A}_1(Q^2)$ and timelike $\mathcal{U}_1(s) \equiv \mathfrak{A}_1(s)$ in the left panel. In the right panel we show the higher powers $\mathcal{A}_1(Q^2)^2$, $\mathcal{A}_1(Q^2)^3$ (dashed lines) compared with the nonpower analogous $\dashv_2(Q^2)$, $\dashv_3(Q^2)$ (lines), and analogously for the timelike couplings

.

2.5 Two-Loop APT Coupling

We know the exact solution for the two-loop running coupling constant in pQCD via Lambert function as in Eq. (1.21). Unfortunately, the APT analytization of the two-loop running coupling has no simple solution. Therefore, we can only extract numerical information with the following spectral function (we will show another way to obtain the analytic two-loop form in general, where we generalize the analytic nonpowers with the power index real and noninteger):

$$\tilde{\rho}_n^{(2)}(t) = \left(\frac{1}{c_1}\right)^n \mathrm{Im}\left[\frac{-1}{1 + W_1(z(t))}\right]^n, \tag{2.23}$$

with

$$z(t) = \frac{\beta_0}{\mathrm{e}c_1} \exp\left[-\frac{t}{c_1}\beta_0 + i\pi\left(\frac{\beta_0}{c_1} - 1\right)\right] \tag{2.24}$$

and

$$t = \ln(\frac{\sigma}{Q^2}), \qquad \sigma = \Lambda^2 \mathrm{e}^t.$$

In this particular case. we used in the analytic coupling the change of variable $\sigma \to t$, this leave the spectral function unchanged ($\tilde{\rho}_1^{(2)}(t) = \rho_1^{(2)}(\sigma)$) and

$$\mathcal{A}_n^{(\ell)}(Q^2) = \frac{1}{\pi}\int_0^\infty \frac{\rho_n^{(\ell)}(\sigma)}{\sigma + Q^2} d\sigma = \frac{1}{\pi}\int_{-\infty}^\infty \frac{\mathrm{e}^t}{\mathrm{e}^t + Q^2/\Lambda^2}\tilde{\rho}_n^{(\ell)}(t)dt. \tag{2.25}$$

That is general to ℓ-loops.
In order to obtain an explicit formula for the analytic running to two loops, we have an alternative form (although it is not exact) which is using the iterative solution (1.14) for the coupling; the spectral function is given in this case by

$$\rho^{(2)}(\sigma) = \frac{1}{\beta_0}\frac{I(t)}{I^2(t) + R^2(t)} \tag{2.26}$$

with

$$\begin{aligned} I(t) &= \pi + \frac{c_1}{\beta_0}\arccos\left(\frac{c_1/\beta_0 + t}{\sqrt{(c_1/\beta_0 + t)^2 + \pi^2}}\right) \\ R(t) &= t + \frac{c_1}{\beta_0}\ln\left(\frac{\sqrt{(c_1/\beta_0 + t)^2 + \pi^2}}{c_1/\beta_0}\right) \end{aligned} \tag{2.27}$$

This is an alternative approximate solution for the two.loop APT analytic coupling.

2.6 Thresholds in APT (Global APT)

As was mentioned in the previous section, the threshold effects will be introduced via global running coupling given by Eq. (1.32) in their continuous form (1.25)-(1.27). This was motivated by Shirkov et al. where the coupling is considered at the one- and two-loop level only, therefore this implementation of the thresholds is formally valid for the underlying pQCD coupling $a(Q^2)$.
In this sense, we have the spectral density in the continuous form (for n-th power)

$$\begin{aligned} \rho_n^{glob.}(\sigma) &= \rho_n^{n_f=3}(\sigma;\Lambda_3)\Theta(\sigma \le m_4^2) + \rho_n^{n_f=4}(\sigma;\Lambda_4)\Theta(m_4^2 \le \sigma \le m_5^2) + \\ &\quad \rho_n^{n_f=5}(\sigma;\Lambda_5)\Theta(m_5^2 \le \sigma \le m_6^2) + \rho_n^{n_f=6}(\sigma;\Lambda_6)\Theta(m_6^2 \le \sigma), \end{aligned} \tag{2.28}$$

where $\rho_n^{n_f}(\sigma,\Lambda_{n_f}) = \mathrm{Im}\left\{a^n(-\sigma - i\epsilon,\Lambda_{n_f})\right\}$ and $a(Q^2,\Lambda_{n_f}) = f_{n_f}(Q^2/\Lambda_{n_f}^2)$.

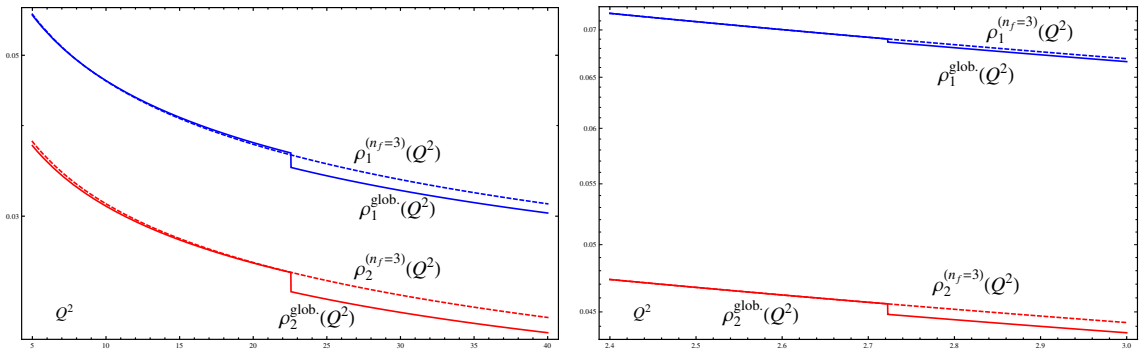

Figure 2.4: Global spectral density of the first and second powers, $\rho_{1,2}(Q^2)$, at one-loop level corresponding to three flavors comparing with (global) and without (dashed lines) taking threshold into account

With the corresponding global analytic coupling

$$\mathcal{A}_n^{glob.}(Q^2) = \int_0^\infty \frac{\rho_n^{glob.}(\sigma)}{\sigma + Q^2} d\sigma \tag{2.29}$$

The global analytic effective charges in the Minkowskian region is, by the same taken

$$\mathfrak{A}_n^{glob.}(s) = \int_s^\infty \frac{\rho_n^{glob.}(\sigma)}{\sigma} d\sigma. \tag{2.30}$$

2.7 Fractional Analytic Perturbation Theory (FAPT): From integer to general powers counting

The procedure to generalize the analytization of of powers a^ν in APT to any $\nu \in \mathbb{R}$ (i.e., noninteger) is via Laplace representation in APT, and was called fractional analytic perturbation theory or FAPT [28, 29] (for a general analytic QCD model this was performed in [27]).
First, to one loop the Laplace representation is written in the following way (for convenience we will use $L \equiv \ln(Q^2/\Lambda^2)$):

$$\mathcal{A}_1(L) = \int_0^\infty \mathrm{e}^{-tL} \tilde{\mathcal{A}}_1(t) dt, \tag{2.31}$$

where

$$\tilde{\mathcal{A}}_1(t) = \frac{1}{\beta_0} \left[1 - \sum_{m=1}^{\infty} \delta(t-m) \right]. \tag{2.32}$$

Using this idea we can generalize (where the clue is to replace $(k-1)! \mapsto \Gamma(\nu)$ for the continuation in the index ν) (2.21) in the form ($k \mapsto \nu$)

$$\mathcal{A}_\nu(L) = \frac{1}{\beta_0^{\nu-1}\Gamma(\nu)}\left(-\frac{d}{dL}\right)^{\nu-1}\mathcal{A}_1(L) = \frac{1}{\beta_0^{\nu-1}}\int_0^\infty \mathrm{e}^{-Lt}\frac{t^{\nu-1}}{\Gamma(\nu)}\tilde{\mathcal{A}}_1(t)dt. \tag{2.33}$$

Therefore, the Laplace transform of the analytic image of the effective coupling $\mathcal{A}_\nu(L)$ is given by

$$\tilde{\mathcal{A}}_\nu(t) = \frac{t^{\nu-1}}{\beta_0^{\nu-1}\Gamma(\nu)}\tilde{\mathcal{A}}_1(t) = \frac{t^{\nu-1}}{\beta_0^{\nu}\Gamma(\nu)}\left(1-\sum_{m=1}^{\infty}\delta(t-m)\right). \tag{2.34}$$

Finally, combining Eqs. (2.34) and (2.33) gives the result

$$\begin{aligned}\mathcal{A}_\nu(L) &= \frac{1}{\beta_0^\nu}\left(\frac{1}{L^\nu}-\frac{1}{\Gamma(\nu)}\sum_{m=1}^{\infty}\mathrm{e}^{-mL}m^{\nu-1}\right)\\ &= \frac{1}{\beta_0^\nu}\left(\frac{1}{L^\nu}-\frac{\mathrm{e}^{-L}}{\Gamma(\nu)}\Phi(\mathrm{e}^{-L},1-\nu,1)\right),\end{aligned} \tag{2.35}$$

where $\Phi(z,\nu-1,1)$ is the Lerch trascendental function. We can to rewrite (2.35) noticing that $\Phi(z,\nu,1) = \mathrm{Li}_\nu(z)/z$, where $Li_\nu(z)$ is the polylogarithmic function

$$\mathcal{A}_\nu(L) = \frac{1}{\beta_0^\nu}\left(\frac{1}{L^\nu}-\frac{\mathrm{Li}_{1-\nu}(\mathrm{e}^{-L})}{\Gamma(\nu)}\right). \tag{2.36}$$

In an analogous way, we find the analytic coupling in the Minkowskian region (with for convenience we take instead of Q^2: $L_s \equiv \ln(s/\Lambda^2)$, $s>0$)

$$\mathfrak{A}_\nu(L_s) = \frac{\sin[(\nu-1)\arccos(L_s/\sqrt{\pi^2+L_s^2})]}{\pi\beta_0^\nu(\nu-1)(\pi^2+L_s^2)^{(\nu-1)/2}}. \tag{2.37}$$

From these analytic couplings (2.36) and (2.37) we can extract the following properties:

- The analytic coupling satisfies a symmetric relation (for $\nu = m \geq 2, m \in \mathbb{N}$)

$$\begin{aligned}\mathcal{A}_m(L) &= (-1)^m\mathcal{A}_m(-L),\\ \mathfrak{A}_m(L_s) &= (-1)^m\mathfrak{A}_m(-L_s).\end{aligned} \tag{2.38}$$

- The asymptotic condition is ($\nu = m, m \in \mathbb{N}$)

$$\begin{aligned}\mathfrak{A}_m(-\infty) &= \mathcal{A}_m(-\infty) = \frac{1}{\beta_0}\delta_{m,1},\\ \mathfrak{A}_m(\infty) &= \mathcal{A}_m(\infty) = 0.\end{aligned} \tag{2.39}$$

- $\mathcal{A}_{m+2}$ has m zeros at positive L in the vicinity of the point $L = 0$.
- For negative index, corresponding to "inverse nonpower" (that is the analytization of $a^{-\nu}(Q^2)$) the expression are given by

$$\begin{aligned} \mathcal{A}_{-\nu}(L) &= \beta_0^\nu \left(L^\nu - \frac{\mathrm{Li}_{\nu+1}(\mathrm{e}^{-L})}{\Gamma(-\nu)} \right), \\ \mathfrak{A}_{-\nu}(L_s) &= \beta_0^\nu \left(\frac{(\pi^2 + L_s^2)^{(\nu+1)/2} \sin[(\nu+1)\arccos(L_s/\sqrt{\pi^2 + L_s^2})]}{\pi(\nu+1)} \right) \end{aligned} \tag{2.40}$$

- In the point $L = 0$ we have

$$\mathcal{A}_\nu(0) = -\frac{\xi(1-\nu)}{\beta_0 \Gamma(\nu)}; \qquad \mathfrak{A}_\nu(0) = \frac{\sin[(\nu-1)\pi/2]}{\beta_0^\nu (\nu-1)\pi^\nu}, \tag{2.41}$$

  or, relating these two quantities

$$\mathcal{A}_\nu(0) = \left[\frac{(\nu-1)\xi(\nu)}{2^{\nu-1}} \right] \mathfrak{A}_\nu(0) \tag{2.42}$$

Another analytization that can be obtained in FAPT is that of the terms containing logarithmics: $a^\nu \ln(a)$ or the more general expression $a^\nu \ln^k(a)$. These expressions appear typically in perturbation expansion of some observables (for example when we solve the renormalization group equations).
For convenience (for more understanding of the analytization procedure) we rewrite the logarithmic terms as derivatives of the running coupling in the form

$$a^\nu \ln^k(a) = \frac{d^k}{d\nu^k} a^\nu. \tag{2.43}$$

The analytization can be applied directly to $a^\nu(Q^2)$ due to linearity of the differential operator, therefore

$$\mathcal{L}_{\nu;k}(L) \equiv \left[\frac{d^k}{d\nu^k} a^\nu(L) \right]_{an} = \frac{d^k}{d\nu^k} \mathcal{A}_\nu(L). \tag{2.44}$$

2.7.1 Two-loop FAPT and higher orders

Theoretically speaking, the higher orders can be made based on the one-loop coupling, in order to find an explicit expression (numerically, we can do it without problem by numerical evaluation of the dispersion integral).

At two loops for example, from RGE we have a transcendental equation for the two-loop pQCD running coupling $a_{(2)}$

$$\frac{1}{\beta_0 a_{(2)}} + \frac{c_1}{\beta_0} \ln\left[\frac{\beta_0 a_{(2)}}{1 + c_1/\beta_0 a_{(2)}}\right] = L. \tag{2.45}$$

As a consequence, we can express $a_{(2)}$ as a power series in the one-loop running coupling: $a_{(1)} = 1/(\beta_0 L)$

$$\begin{aligned} a_{(2)} &= a_{(1)} + c_1 a_{(1)}^2 \ln(\beta_0 a_{(1)}) + c_1^2 a_{(1)}^3 [\ln^2(\beta_0 a_{(1)}) + \ln(\beta_0 a_{(1)}) - 1] \\ &\quad + O(a_{(1)}^4 \ln^3(a_{(1)})). \end{aligned} \tag{2.46}$$

Therefore, the analytization gives us [28, 29]

$$\begin{aligned} \mathcal{A}_1^{(2)}(L) &= \mathcal{A}_1^{(1)}(L) + c_1 \mathcal{A}_2^{(1)}(L) \ln(\beta_0) + c_1 \left.\frac{d}{d\nu} \mathcal{A}_\nu^{(1)}(L)\right|_{\nu=2} \\ &\quad + c_1^2 \mathcal{A}_3^{(1)}(L)(\ln^2(\beta_0) + \ln(\beta_0) - 1) + c_1^2 \left.\frac{d}{d\nu} \mathcal{A}_\nu^{(1)}(L)\right|_{\nu=3} (\ln(\beta_0) + 1) \\ &\quad + c_1^2 \left.\frac{d^2}{d\nu^2} \mathcal{A}_\nu^{(1)}(L)\right|_{\nu=3} + \cdots \end{aligned} \tag{2.47}$$

2.8 Global FAPT: Crossing thresholds

The generalization of taking the thresholds into account is straightforward, with the global analytic coupling being a generalization of Eqs. (2.29)- (2.30) by substitution $n \mapsto \nu$

$$\begin{aligned} \mathcal{A}_\nu^{glob.,(\ell)}(L) &= \int_{-\infty}^{\infty} \frac{\rho_\nu^{glob.,(\ell)}(L_\sigma)}{1 + \mathrm{e}^{L - L_\sigma}} dL_\sigma, \\ \mathfrak{A}_\nu^{glob.,(\ell)}(L_s) &= \int_{L_s}^{\infty} \rho_\nu^{glob.,(\ell)}(L_\sigma) dL_\sigma, \end{aligned} \tag{2.48}$$

where $L \equiv \ln(Q^2/\Lambda_3^2)$, $L_\sigma \equiv \ln(\sigma/\Lambda_3^2)$ and as in Eq. (2.28)

$$\begin{aligned} \rho_\nu^{glob.,(\ell)}(L_\sigma) &= \rho_\nu^{(\ell)}(L_\sigma; \Lambda_3)\Theta(L_\sigma < L_4) + \rho_\nu^{(\ell)}(L_\sigma; \Lambda_4)\Theta(L_4 \le L_\sigma < L_5) \\ &\quad + \rho_\nu^{(\ell)}(L_\sigma; \Lambda_5)\Theta(L_5 \le L_\sigma < L_6) + \rho_\nu^{(\ell)}(L_\sigma; \Lambda_6)\Theta(L_6 \le L_\sigma) \end{aligned} \tag{2.49}$$

and $L_N \equiv \ln(\Lambda_N^2/Lambda a_3^2)$, $\rho_\nu^{(\ell)}(L_\sigma; \Lambda_N) \equiv \mathrm{Im} a(-\sigma - i\epsilon; \Lambda_N)^\nu$ [we recall: $a(Q^2, \Lambda_N) = f(Q^2/\Lambda_N^2)$].

Finally, in the analogous procedure as before (in the global APT), we have for the terms involving logarithms of the pQCD coupling:

$$\mathcal{A}_{\nu,k}(L) = \int_{-\infty}^{\infty} \frac{\rho_{\nu,k}^{glob;(\ell)}(L_\sigma)}{1+\mathrm{e}^{L-L\sigma}} dL_\sigma, \tag{2.50}$$

and

$$\mathfrak{A}_{\nu,k}(L) = \int_{L_s}^{\infty} \rho_{\nu,k}^{glob;(\ell)}(L_\sigma) dL_\sigma, \tag{2.51}$$

the spectral density here is $\rho_{\nu,k}^{glob;(\ell)}(L_\sigma) = \mathrm{Im}\{a(L_\sigma)^\nu \ln^k a(L_\sigma)\}$.

Chapter 3

Other Analytic QCD Models

3.1 Introduction

Most of the analytic QCD (anQCD) models suffer from one or both of the following problems:

- Analytic QCD models with few free parameters usually severely underestimate the experimental value of the (strangeless) semihadronic tau decay ratio r_τ. For example, (F)APT gives values for r_τ by at least 10σ below the experimental value, cf. Ref. [30,37]. The value of r_τ is at present the most precisely measured low-energy QCD observable, with the squared momentum of the process $s = |Q^2| = m_\tau^2 \approx 3$ GeV^2.
- The deviation of the analytic coupling $\mathcal{A}_1(Q^2)$ from the perturbative coupling $a_{\rm pt}(Q^2)$, at high $Q^2 \gg \Lambda^2$, can be appreciable: $\mathcal{A}_1(Q^2) - a_{\rm pt}(Q^2) \sim (\Lambda^2/Q^2)^k$ ($k = 1$, or 2, ...); in (F)APT $k = 1$. This implies that such analytic QCD models give nonperturbative contributions $\sim (\Lambda^2/Q^2)^k$ which are at least partly from the ultraviolet (UV) regime. Such UV nonperturbative contributions are in disagreement with the Operator product expansion (OPE) philosophy of the ITEP (Institute of Theoretical and Experimental Physics) group [38], which stipulates that the nonperturbative contributions come only from the infrared (IR) regime.

The perturbative coupling $a(Q^2) \equiv \alpha_s(Q^2)/\pi$ has singularities (cut) along the real Q^2 axis at $Q^2 \leq Q_b^2$ ($\sim \Lambda^2$) in the complex plane, where Q_b^2 is the branching point. Application of the Cauchy theorem gives the following general dispersion relation for

$a(Q^2)$:

$$a(Q^2) = \frac{1}{\pi}\int_{-Q_b^2-\eta}^{+\infty} d\sigma \frac{\rho_1^{(\mathrm{pt})}(\sigma)}{(\sigma+Q^2)} \ , \tag{3.1}$$

where $\rho_1^{(\mathrm{pt})}(\sigma) = \mathrm{Im}\ a(Q^2 = -\sigma - i\epsilon)$ is the perturbative discontinuity function, and $\eta \to +0$. In the previous chapter we saw the (F)APT model of Shirkov and Solovtsov [16, 22, 30] and this consists of removing the offending cut at positive Q^2 ($0 < Q^2 \leq Q_b^2$), i.e., for $-Q_b^2 \leq \sigma < 0$ we have the form (2.1). In analogous way, the higher order couplings $\mathcal{A}_n$ ($n = 2, 3, \ldots$) are given by Eq. (2.3).

As mentioned before, once the parameter $\overline{\Lambda}$ (the $\overline{\mathrm{MS}}$ Λ-scale is referred to in this notation, for convenience) is adjusted in APT so that the high-energy QCD phenomenology is reproduced. However, then the value of the semihadronic tau decay ratio r_τ (strangeless and massless) is predicted to be about 0.14, much lower [36, 37] than the well measured experimental value $r_\tau \approx 0.203 \pm 0.004$. Another possibly unattractive aspect of APT is that its coupling $\mathcal{A}_1(Q^2)$ has singularities along the entire nonpositive Q^2 axis ($Q^2 \leq 0$, i.e., $\sigma \geq 0$) in the complex Q^2-plane. This does not reflect closely the analyticity properties of spacelike observables $\mathcal{D}(Q^2)$ which have nonanalyticity cut along negative Q^2 axis starting at a negative threshold value $-M_{\mathrm{thr}}^2$: $Q^2 \leq -M_{\mathrm{thr}}^2$ (i.e., $\sigma \geq M_{\mathrm{thr}}^2$). The value of the threshold mass M_{thr} is typically (multiple of) a mass of light mesons. One possibility to incorporate such behavior in the analytic coupling is to eliminate certain IR interval $0 \leq \sigma < M_{\mathrm{thr}}^2$ of the cut in the dispersive relation (2.1), resulting in a "modified" APT (mAPT) coupling

$$\mathcal{A}_1^{(\mathrm{mAPT})}(Q^2) = \frac{1}{\pi}\int_{M_{\mathrm{thr}}^2}^{+\infty} d\sigma \frac{\rho_1^{(\mathrm{pt})}(\sigma)}{(\sigma+Q^2)} \ . \tag{3.2}$$

Such type of change was proposed in Refs. [32].[1] In general analytic QCD the application of the Cauchy theorem gives the following general dispersion relation for the analytic (holomorphic) $\mathcal{A}(Q^2)$:

$$\mathcal{A}_1(Q^2) = \frac{1}{\pi}\int_{M_{thr}^2}^{+\infty} \frac{d\sigma \rho_1(\sigma)}{\sigma+Q^2}, \tag{3.3}$$

where $\rho_1(\sigma) \equiv \mathrm{Im}(Q'^2 = -\sigma - i\epsilon)$.

In Ref. [40] (motivated by the work of Peris [41]), it was pointed out that the coupling (3.2) and (3.3) is a Stieltjes function, and that, as a consequence, the paradiagonal Padé approximants $[M-1/M](Q^2)$ of such a coupling systematically con-

[1] The authors of [32] used for $\mathcal{A}_1$, before eliminating an IR-cut, a "second" APT model [31], which is obtained by minimal analytization of the right-hand side of the following form of the perturbative renormalization group equation (RGE): $d\ln a/d\ln Q^2 = -\beta_0 a - \beta_1 a^2 - \beta_2 a^2 - \cdots$. Their numerical analysis is then performed at the one-loop level.

verge to the exact values $\mathcal{A}_1(Q^2)$ when the Padé index M increases.[2] The latter fact was checked numerically, and it was also shown there that the aforementioned Padé approximations are equivalent to approximating the mAPT discontinuity function $\rho_1^{(mAPT)}(\sigma) \equiv \mathrm{Im}\mathcal{A}_1^{(mAPT)}(-\sigma - i\epsilon) = \rho_1^{(pt)}(\sigma)\Theta(\sigma - M_{thr}^2)$ by a sum of M delta terms

$$\frac{1}{\pi}\rho_1^{(\mathrm{mAPT})}(\sigma)_{[M-1/M]} = \Theta(\sigma - M_{\mathrm{thr}}^2) \times \mathrm{Im}\ a(Q^2 = -\sigma - i\epsilon) \tag{3.4}$$

$$\approx \sum_{n=1}^{M} f_n^2 \Lambda^2 \delta(\sigma - M_n^2) = \sum_{n=1}^{m} f_n^2 \delta(s - s_n)\ , \tag{3.5}$$

where $s = \sigma/\Lambda^2$, $s_n = M_n^2/\Lambda^2$ and f_n are positive dimensionless quantities, and $M_{\mathrm{thr}} \approx M_1 < M_2 < \cdots$. Stated otherwise the $[M-1/M]$ Padé approximation to $\mathcal{A}_1^{(mAPT)}$ is

$$[M-1/M]_{\mathcal{A}_1^{(mAPT)}}(Q^2) = \frac{1}{\pi}\int_0^\infty \frac{d\sigma \rho_1^{(mAPT)}(\sigma)_{[M-1/M]}}{\sigma + Q^2}$$

$$= \sum_{n=1}^{M} \frac{f_n^2 \Lambda^2}{Q^2 + M_n^2} = \sum_{n=1}^{M} \frac{f_n^2}{s + s_n}. \tag{3.6}$$

Therefore, it was argued that, although a sum of delta functions appears to be a very crude approximation for the (continuous) function $\rho_1^{(mAPT)}(\sigma)$, it gives increasingly better expressions for the coupling $\mathcal{A}_1(Q^2)$ when the number M of deltas in the sum (3.5) increases. We only know the approximate behavior of the true $\rho_1(\sigma)$ at high $\sigma \gg \Lambda^2$ [$\rho_1(\sigma) \approx \rho_1^{(\mathrm{pt})}(\sigma)$], and we do not know the behavior in the IR regime $\sigma \sim \Lambda^2$. Therefore, as was also argued in Ref. [40], in the regime of low positive σ we can expect that parametrization of the true $\rho_1(\sigma)$ in terms of one or a few delta functions may lead to a reasonably realistic behavior of $\mathcal{A}_1(Q^2)$ at low $|Q^2|$. We will show in the next sections the construction of a model by parametrization via one and two deltas and finally the construction, in this kind of models (analytic models in general), of analytic analogous $\mathcal{A}_\nu(Q^2)$ [and $\mathfrak{A}_\nu(s)$] of powers $a_{pt}(Q^2)^\nu$ (where ν can be noninteger).

[2] Padé approximant $[N/M](x)$ to a function $f(x)$ is, by definition, a ratio $P_N(x)/Q_M(x)$ of polynomials of degree N and M, respectively, such that the Taylor expansions of $[N/M](x)$ and of $f(x)$ around $x = 0$ agree up to (and including) the term $\sim x^{N+M}$.

3.2 One-delta Analytic QCD model

This model was introduced in Ref. [53].
One delta function in the IR regime of σ's is used in the form:

$$\rho_1^{1\delta}(\sigma) = \pi f_1^2 \Lambda^2 \, \delta(\sigma - M_1^2) + \Theta(\sigma - M_0^2) \times \rho_1^{(\mathrm{pt})}(\sigma) \, , \tag{3.7}$$

$$= \pi f_1^2 \, \delta(s - s_1) + \Theta(s - s_0) \times r_1^{(\mathrm{pt})}(s) \, , \tag{3.8}$$

where $s = \sigma/\Lambda^2$, $s_1 = M_1^2/\Lambda^2$, $s_0 = M_0^2/\Lambda^2$, and $r_1^{(\mathrm{pt})}(s) = \rho_1^{(\mathrm{pt})}(\sigma) = \mathrm{Im}\ a(Q^2 = -\sigma - i\epsilon)$. We may expect[3] $0 < M_1 < M_0$, i.e., the actual threshold mass is M_1. The discontinuity function $\rho_1(\sigma)$, Eq. (3.7), is depicted in Figs. 3.1 (a), (b), for the choice of two sets of values of the parameters (M_1, M_0 and Λ), which will be motivated later.

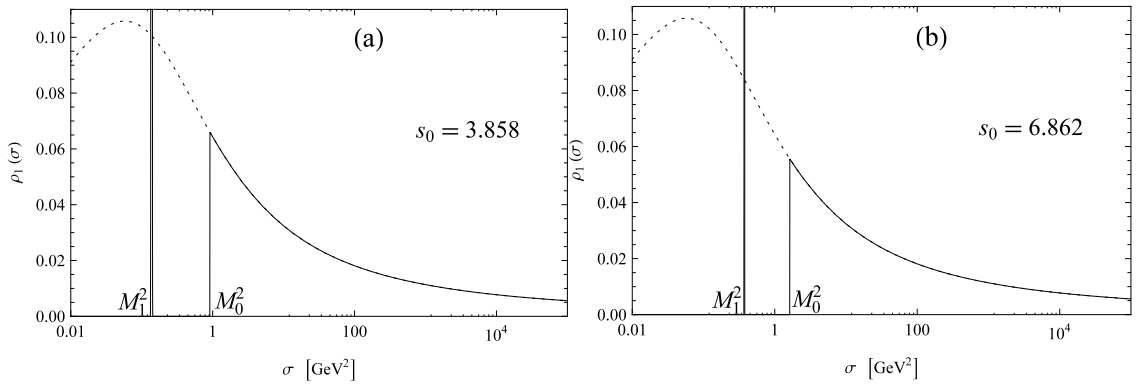

Figure 3.1: The discontinuity function $\rho_1(\sigma)$, Eq. (3.7) taking from Ref. [53], for the values of scale parameters $\Lambda = 0.487$ GeV and: (a) $M_1 = 0.371$ GeV and $M_0 = 0.956$ GeV ($s_1 \equiv M_1^2/\Lambda^2 = 0.581$ and $s_0 \equiv M_0^2/\Lambda^2 = 3.858$); (b) $M_1 = 0.612$ GeV and $M_0 = 1.275$ GeV ($s_1 \equiv M_1^2/\Lambda^2 = 1.579$ and $s_0 \equiv M_0^2/\Lambda^2 = 6.862$). For comparison, perturbative discontinuity function $\rho_1^{\mathrm{pt}}(\sigma)$ at positive σ is also included as a dotted curve [in $\beta_2 = \beta_3 = \cdots = 0$ renormalization scheme (RSch), and with $n_f = 3$].

A physical interpretation of the ansatz (3.7)-(3.8) is also possible: If the discontinuity function $\rho_1(\sigma)$ is to simulate, in the first approximation, the spectral functions $\rho_{\mathcal{D}}(\sigma) = \mathrm{Im}\ \mathcal{D}(Q^2 = -\sigma - i\epsilon)$ of spacelike observables $\mathcal{D}(Q^2)$, the delta-term in Eqs. (3.7)-(3.8) and in Figs. 3.1 can be regarded as a narrow width approximation (NWA) of the dominant low-energy resonance.[4] For an application of NWA ansatz directly to the spectral function of the vector current-current correlator ($\Leftrightarrow$ Adler function), see Ref. [41].

[3] Although we do not impose the condition $0 < M_1 < M_0$, it will turn out to be true in our model.

[4] For two simpler-minded analytic QCD models involving delta-function in $\rho_1(\sigma)$, see Refs. [35,36].

Furthermore, in Ref. [42] a similar idea was applied directly to the spectral function $v_1(\sigma)$ of the vector current-current correlator. The ansatz for $v_1(\sigma)$ there is similar to the ansatz (3.7)-(3.8). However, instead of approximating the low-energy regime ($\sigma < M_0^2$) by a simple delta function, the known measured low-energy values of $v_1(\sigma)$ of the ALEPH and OPAL collaborations [43–45] were used. The threshold value of the onset of perturbative QCD (M_0^2), and the perturbative coupling strength ($\Leftrightarrow \overline{\Lambda}$) were then fixed by two conditions: the correct measured value of the (strangeless) r_τ has to be reproduced, and the higher-twist terms of the resulting massless Adler function have no terms of dimension two ($\propto 1/Q^2$). The work of Ref. [42] is a generalization and refinement of an earlier work Ref. [46].

The dispersion relation applied to the discontinuity function (3.7)-(3.8) then gives us the following expression for the analytic coupling $\mathcal{A}_1^{(1\delta)}(Q^2)$:

$$\mathcal{A}_1^{(1\delta)}(Q^2) \;=\; \frac{1}{\pi}\int_0^{+\infty} d\sigma\, \frac{\rho_1^{1\delta}(\sigma)}{(\sigma+Q^2)} = \frac{f_1^2}{u+s_1} + \frac{1}{\pi}\int_{s_0}^{\infty} ds\, \frac{r_1^{(\rm pt)}(s)}{(s+u)}\;, \qquad (3.9)$$

where we use the notation

$$u = Q^2/\Lambda^2, \qquad s = \sigma/\Lambda^2\;. \qquad (3.10)$$

In the renormalization scheme (RSch) with the beta function coefficients $\beta_2 = \beta_3 = \cdots = 0$, the discontinuity function is explicitly known in terms of Lambert function $W_{\pm 1}$ Eqs. (1.21)-(1.22), Ref. [4] (see also Refs. [5,6] on the use of Lambert functions in evaluation of the n-loop coupling)

$$\begin{aligned} r_1^{(\rm pt)}(s) \;&=\; {\rm Im}\left[\frac{1}{c_1}\frac{1}{\left[1+W_{-1}\left(\frac{1}{c_1 e}s^{-\beta_0/c_1}\exp[-i\pi(\beta_0/c_1-1)]\right)\right]}\right] \\ &=\; {\rm Im}\left[\frac{-1}{c_1}\frac{1}{\left[1+W_{+1}\left(\frac{1}{c_1 e}s^{-\beta_0/c_1}\exp[+i\pi(\beta_0/c_1-1)]\right)\right]}\right]\;, \qquad (3.11) \end{aligned}$$

where $s = \sigma/\Lambda^2$, and β_0 and $c_1 = \beta_1/\beta_0$ are the two (universal) coefficients in the renormalization group equation and $n_f = 3$ is taken. It is in this renormalization scheme that we will asume the form (3.8) of the discontinuity function, and consequently, the form (3.9) of $\mathcal{A}_1^{(1\delta)}(Q^2)$. The Λ scale appearing implicitly in these expressions and in Eq. (1.22) is the Lambert Λ, and it is related with the $\overline{\rm MS}$ scale $\overline{\Lambda}$ at $n_f = 3$ via

$$\Lambda \approx \overline{\Lambda}\exp(0.3205)\;. \qquad (3.12)$$

The coupling $a(Q^2)$ in the $\beta_2 = \beta_3 = \cdots = 0$ renormalization scheme has a Landau cut along $0 < Q^2 < Q_b^2$, where Q_b^2 is the branching point $Q_b^2 = \Lambda^2 s_b$, where $s_b = c_1^{-c_1/\beta_0} \approx$

0.635 when $n_f = 3$. The perturbative coupling $a(Q^2)$ in this renormalization scheme is known (1.21)-(1.22). It can be numerically checked that the dispersion relation (3.1) holds for $a(Q^2)$ in this renormalization scheme, using for the discontinuity function the expressions (3.11) at $s \equiv \sigma/\Lambda^2 > 0$, and for $-s_b < s \equiv \sigma/\Lambda^2 < 0$ the expression

$$r_1^{(\rm pt)}(s) \;=\; {\rm Im}\left[\frac{1}{c_1}\frac{1}{\left[1 + W_{-1}\left(\frac{-1}{c_1 e}|s|^{-\beta_0/c_1} + i\epsilon\right)\right]}\right] \;. \tag{3.13}$$

One peculiar feature in most of the analytic QCD models is that at large $|Q^2|$ ($\gg \Lambda^2$) the analytic coupling $\mathcal{A}_1(Q^2)$ differs from the perturbative coupling $a(Q^2)$ by an inverse power of Q^2:

$$|\mathcal{A}_1(Q^2) - a(Q^2)| \sim \left(\frac{\Lambda^2}{Q^2}\right)^k \qquad (|Q^2| \gg \Lambda^2) \;. \tag{3.14}$$

In APT ([16–25]), and in the "second APT" [31], this power is $k = 1$, i.e., relatively large deviation.

However, power deviations (3.14) are not in accordance with the philosophy of the operator product expansion (OPE) as promoted by the ITEP group [38]. According to that philosophy, all nonperturbative contributions such as $(\Lambda^2/Q^2)^k$ to (inclusive) observables originate from the infrared (IR) regimes $|Q^2| \lesssim \Lambda^2$. Consequently, the OPE of spacelike inclusive observables is interpreted in this approach as superposition of perturbative contributions coming from the ultraviolet regime $|Q^2| \gg \Lambda^2$ (Wilson coefficients) and nonperturbative contributions coming from the IR regime (vacuum expectation values of operators). Once we have power deviations of the type (3.14), this implies that a theory with such $\mathcal{A}_1(Q^2)$ will give us, in evaluations of inclusive spacelike observables, nonperturbative terms (of the type Λ^2/Q^2) coming at least partly from the UV regime, thus contravening the ITEP philosophy.

More specifically, the authors of Ref. [47] argued in the following way that the terms $\sim (\Lambda^2/Q^2)^k$ in the deviation Eq. (3.14) contravene the ITEP philosophy of OPE. Namely, let us consider the leading-β_0 summation of an inclusive spacelike observable $\mathcal{D}(Q^2)$

$$\mathcal{D}^{(\rm LB)}(Q^2) \equiv \int_0^\infty \frac{dt}{t}\, F_{\mathcal{D}}(t)\, a(tQ^2 e^{\overline{\mathcal{C}}}) \;. \tag{3.15}$$

Here, $F_{\mathcal{D}}(t)$ is the characteristic function of the observable and $\overline{\mathcal{C}} = -5/3$. The quantity $tQ^2 e^{\overline{\mathcal{C}}}$ is the square of internal loop momenta appearing in the resummation. In the UV regime $t > 1$, the deviation (3.14) then produces power term contributions of UV origin in the observable (see also Ref. [48])

$$\delta\mathcal{D}^{(\rm LB)}(Q^2) \sim (\Lambda^2/Q^2)^k \int_1^\infty \frac{dt}{t^{k+1}}\, F_{\mathcal{D}}(t) \sim (\Lambda^2/Q^2)^k \;. \tag{3.16}$$

For more discussion on these aspects, we refer to Ref. [39]. The aforementioned OPE condition then implies

$$|\mathcal{A}_1(Q^2) - a(Q^2)| < \left(\frac{\Lambda^2}{Q^2}\right)^k \qquad (|Q^2| \gg \Lambda^2; k = 1, 2, \ldots). \tag{3.17}$$

This condition can be interpreted as a requirement that the analytic QCD model be formally perturbative (analytic) QCD at high momenta. We want to construct here a simple analytic QCD model with the discontinuity function $\rho_1(\sigma)$ of the type (3.7) which is as close as possible to perturbative QCD (in renormalization scheme $\beta_2 = \beta_3 = \cdots = 0$) [53]. In such a model, all the measured values of the high-energy QCD observables (with $|Q^2| > 10^1$ GeV^2) are then reproduced just as in perturbative QCD. In such a model, we have to ensure only that the values of the well measured low-energy observables, particularly r_τ (with $|Q^2| = m_\tau^2 \approx 3$ GeV^2), are reproduced.

We will construct here an analytic QCD model of Eqs. (3.7)-(3.9), which only approximately fulfills the condition (3.17), namely for $k = 1, 2..$ The best low-energy condition is the reproduction is the measured value of the canonical $(V + A)$ nonstrange and massless semihadronic τ-lepton decay ratio r_τ, [43–45].[5] When we remove the (measured) strangeness-changing contribution, the color and CKM factors and the electroweak effects, and the chirality-violating higher twist (quark mass) contributions, the following value is obtained (cf. [60, 62, 133], and Appendix B of Ref. [39] for details):

$$r_\tau(\triangle S = 0, m_q = 0)_{\rm exp.} = 0.203 \pm 0.004 \ . \tag{3.18}$$

Numerical analyses of the measured data indicate that the chirality-conserving higher-twist effects, such as gluon-condensate contributions, are negligible in the case of the considered $V + A$ decay channel. Although such analyses have been performed within pQCD+OPE approach, we will assume that they remain valid when an analysis is performed with the presented anQCD two-delta model + OPE. This assumption appears to be reasonable because the considered anQCD coupling $\mathcal{A}_1(Q^2)$ is very close to the pQCD coupling $a(Q^2)$ (in the considered scheme) at momenta $|Q^2| \gtrsim 1$ GeV^2. Therefore, in the calculation of the discussed r_τ, Eq. (3.18), in the presented anQCD model, the (chirality-conserving) higher-twist contributions will be ignored. We note that the model of Eqs. (3.7)-(3.9) at first contains three free dimensionless positive parameters (f_1^2, s_1, s_0), in addition to the energy scale parameter Λ. The parameters f_1^2, s_1 will be fixed by requiring: the condition that

$$|\mathcal{A}_1(Q^2) - a(Q^2)| \sim \left(\frac{\Lambda^2}{Q^2}\right)^3 \qquad (|Q^2| \gg \Lambda^2). \tag{3.19}$$

instead[6] of the generic $\sim \left(\frac{\Lambda^2}{Q^2}\right)^1$. The scale Λ is obtained by the requiring the correct

[5] The "canonical" means that the normalization is used such that $(r_\tau)_{\rm pt} = a + \mathcal{O}(a^2)$.

[6] This condition, with $k = 3$, is also fulfilled in the model for $\mathcal{A}_1(Q^2)$ of Ref. [33].

perturbative QCD value of $\mathcal{A}_1(Q^2)$ at $Q^2 = (3m_c)^2$. This is approximately the highest value of Q^2 where the number of active quark flavors can still reasonably safely be kept $n_f = 3$ in perturbative QCD with four-loop RGE-running and three-loop matching conditions [12].[7]

A consistent accounting of the threshold effects fully within analytic QCD, when $n_f \mapsto (n_f + 1)$, is not yet known for general analytic QCD models. However, in APT of Refs. [16, 30], such an accounting can be made systematically as was presented in Section 2.6 for APT (namely global APT) and in Section 2.8 for FAPT (namely global FAPT). This threshold matching procedure could be implemented also in the present model (in the renormalization scheme $\beta_2 = \beta_3 = \cdots = 0$) by making $\rho_1(\sigma)$ accordingly step-like discontinuous at $\sigma_{\rm thr}$'s. However, by assuming that at $Q^2_{\rm thr} = (3m_c)^2$ the present $n_f = 3$ analytic QCD model merges with perturbative QCD does not result in any appreciable error, due to the condition that in the relation (3.14) we have $k = 3$.

Throughout this model, we assume that we are in the regime of three active quark flavors ($n_f = 3$), and that the three quarks u, d and s are (almost) massless. The "approximate perturbative QCD" condition $k = 3$ in Eq. (3.19) can be expressed via the following two conditions:

$$\frac{1}{\pi} \int_{-s_b}^{+s_0} ds \; r_1^{(\rm pt)}(s) \;\; = \;\; f_1^2 \; , \tag{3.20}$$

$$\frac{1}{\pi} \int_{-s_b}^{+s_0} ds \; s \; r_1^{(\rm pt)}(s) \;\; = \;\; s_1 f_1^2 \; , \tag{3.21}$$

where $s_b = c_1^{-c_1/\beta_0} = Q_b^2/\Lambda^2$, Q_b^2 being the (Landau) branch point of $a(Q^2)$ in the complex Q^2-plane. Conditions (3.20)-(3.21) mean that the coefficient at (Q^2/Λ^2) and $(Q^2/\Lambda^2)^2$ in the deviation $\mathcal{A}_1(Q^2) - a(Q^2)$ is zero, respectively. Equations (3.20)-(3.21) were obtained by subtracting Eq. (3.9) from Eq. (3.1)

$$a(Q^2) - \mathcal{A}_1(Q^2) = -\frac{f_1^2}{u + s_1} + \frac{1}{\pi} \int_{-s_b}^{+s_0} ds \; \frac{r_1^{(\rm pt)}(s)}{(s + u)} \; , \tag{3.22}$$

and expanding in powers of $(1/u) = (\Lambda^2/Q^2)$.

In addition to the two conditions (3.20)-(3.21), there is a condition that the theory merge with the perturbative coupling at higher renormalization scales μ^2. Since we do

[7] If we apply the four-loop RGE-running in $\overline{\rm MS}$ renormalization scheme with three-loop matching conditions according to Ref. [12] at $Q^2 = (\kappa m_c)^2$ and $Q^2 = (\kappa m_b)^2$, and choose a fixed initial value $a(m_c^2, \overline{\rm MS}; n_f = 3) = 0.12945$ at the initial $Q_0^2 = m_c^2$ [which gives: $a((3m_c)^2, \overline{\rm MS}; n_f = 3) = 0.07245$, i.e., the value we use in this paper], we obtain the values $\alpha_s(M_Z^2, \overline{\rm MS}) = 0.1190, 0.1191, 0.1193$, when choosing for the threshold parameter κ the values $\kappa = 3, 2, 1$, respectively. For the quark masses we use the values $m_c = 1.27$ GeV and $m_b = 4.20$ GeV [49].

not yet know a consistent exact threshold conditions within analytic QCD models, we assume that our analytic QCD model coupling $\mathcal{A}_1(\mu^2)$ has the number of active quarks $n_f = 3$ up to the renormalization scale (RScl) $\mu^2 = (3m_c)^2$ (with $m_c \approx 1.27$ GeV) and that at that scale it practically merges with the value of the perturbative coupling $a((3m_c)^2; \beta_2 = \beta_3 = \cdots = 0; n_f = 3)$ such as implied by the high energy QCD experiments. Specifically, high energy QCD implies $a(M_Z^2, \overline{\rm MS}) \approx 0.119/\pi$, Ref. [49]. We then run this value, by perturbative four-loop RGE in $\overline{\rm MS}$ renormalization scheme, down to renormalization scale $\mu^2 = (3m_c)^2$, and incorporate quark thresholds at $\mu^2 = (3m_q)^2$ $(q = b, c)$ by three-loop matching conditions Ref. [12]. We obtain in this way $\overline{a}_{\rm pt} \equiv a((3m_c)^2, \overline{\rm MS}, n_f = 3) = 0.07245$. Changing renormalization scheme from $\overline{\rm MS}$ to $\beta_2 = \cdots = 0$ by the subtracted form (Ref. [51], Appendix A there) of the integrated perturbative QCD RGE (see Ref. [52], Appendix A there) then results in[8]

$$a_{\rm in} \equiv a((3m_c)^2; \beta_2 = 0, \beta_3 = 0, \ldots; n_f = 3) = 0.07050 \ . \tag{3.23}$$

As stated above, we require that $\mathcal{A}_1(\mu^2)$ of our analytic QCD model, at $\mu^2 = (3m_c)^2$, agrees with the value Eq. (3.23), i.e., the analytic QCD model merges with perturbative QCD starting at the scale $\mu^2 = (3m_c)^2$ upwards

$$\mathcal{A}_1(\mu^2 = (3m_c)^2) = a_{\rm in} \quad (= 0.07050) \ . \tag{3.24}$$

This then fixes our Lambert scale Λ ($\Lambda \approx 0.487$GeV).

One may worry that the replacement of the presented analytic QCD model by perturbative QCD at $Q^2 \geq (3m_c)^2$ [and with $n_f = 3 \mapsto 4$ perturbative threshold at $Q^2 = (3m_c)^2$] may not be a good approximation, i.e., that the analytic coupling $\mathcal{A}_1(Q^2)$ of the theory, say at fixed $n_f = 3$, behaves at high scales $Q^2 \sim M_Z^2$ significantly different than the perturbative coupling $a(Q^2)$. It turns out that this is not the case. Namely, if we formally keep fixed $n_f = 3$ (in order not to worry about threshold effects in analytic QCD), the perturbative RGE-running (in the renormalization scheme $\beta_2 = \cdots = 0$) from the initial value $a((3m_c)^2; n_f = 3) = 0.070502 = 0.221487/\pi$ [Eq. (3.23)] at the scale $Q^2 = (3m_c)^2$ to the high final scale $Q^2 = M_Z^2$ gives the value $a(M_Z^2; n_f = 3) = 0.033694 = 0.105852/\pi$. The analytic coupling, for both representative values of parameter s_0 used later in this model ($s_0 = 3.858, 6.862$), gives the same value $0.221487/\pi$ at $Q^2 = (3m_c)^2$, and almost the same values at $Q^2 = M_Z^2$: $\mathcal{A}_1(M_Z^2) = 0.105853/\pi, 0.105856/\pi$, respectively.[9] This strongly indicates

[8] We use for the $\overline{\rm MS}$ beta function $\beta(a(Q^2))$ at $Q^2 = (3m_c)^2$ and $n_f = 3$ the Padé $[2/3]_\beta(a)$ based on the 4-loop polynomial $\overline{\rm MS}$ beta function; if using the latter (polynomial) form, we obtain slightly different value $a_{\rm in}$ [$\equiv a((3m_c)^2; \beta_2 = 0, \beta_3 = 0, \cdots; n_f = 3)$] $= 0.07054$. It appears that, at such relatively large values of a, the Padé $[2/3]_\beta(a)$ is a better approximation to the full (yet unknown) $\overline{\rm MS}$ beta function.

[9] The values of $\mathcal{A}_1(Q^2)$, for various values of the parameter s_0, differ from the values of the perturbative coupling only at low $Q^2 < 10$ GeV^2; for example, the relative difference $a(Q^2)/\mathcal{A}_1(Q^2) - 1$ is a monotonously decreasing function of Q^2 for $Q^2 < 10$ GeV^2; in the interval 1 GeV$^2 < Q^2 <$ 5 GeV^2 it falls from 0.02 to 0.0004 when $s_0 = 3.858$, and from 0.05 to 0.001 when $s_0 = 6.862$.

Table 3.1: The dimensionless nonnegative parameters $s_1 = M_1^2/\Lambda^2$ and f_1^2 as functions of the cutoff parameter $s_0 = M_0^2/\Lambda^2$ (> 0). The scale Λ is practically independent of s_0: $\Lambda \approx 0.487$ GeV. The penultimate column shows the leading-β_0 resummed (LB) contributions to r_τ; in parentheses the leading order (LO) contribution. The last column shows the sum of the LB and the beyond-the-leading-β_0 contribution (LB+bLB) to r_τ; in parentheses the LO and beyond-leading-order contribution (LO+bLO) to r_τ (for details on r_τ, see the next section).

s_0	s_1	f_1^2	$r_\tau^{(\mathrm{LB})}$ $(r_\tau^{(\mathrm{LO})})$	$r_\tau^{(\mathrm{LB+bLB})}$ $(r_\tau^{(\mathrm{LO+bLO})})$
1.958	0.0000	0.1721	0.2522 (0.1315)	0.2399 (0.1892)
2.000	0.0121	0.1732	0.2509 (0.1315)	0.2386 (0.1893)
3.000	0.3117	0.1970	0.2290 (0.1316)	0.2166 (0.1915)
3.858	0.5812	0.2156	0.2156 (0.1317)	0.2030 (0.1939)
4.000	0.6267	0.2186	0.2137 (0.1317)	0.2010 (0.1943)
5.000	0.9523	0.2387	0.2016 (0.1319)	0.1885 (0.1975)
6.000	1.2861	0.2576	0.1916 (0.1321)	0.1781 (0.2006)
6.862	1.5788	0.2732	0.1844 (0.1323)	0.1704 (0.2030)

that $\mathcal{A}_1(Q^2)$ of the analytic QCD model presented in this here, at both mentioned values of s_0, is practically indistinguishable from the perturbative $a(Q^2)$ at scales $Q^2 > (3m_c)^2$. This conclusion even gets generalized to any higher order couplings of this analytic QCD and the perturbative QCD.

Altogether, the three conditions (3.20), (3.21), and (3.24) eliminate three of the four otherwise free parameters $s_0, s_1, f_1^2, \Lambda^2$ of our analytic QCD model. We are thus left with only one free parameter, e.g., the dimensionless parameter s_0 in Eq. (3.9) for $\mathcal{A}_1(Q^2)$. In Table 3.1 we present the numerical dependence of the parameters s_1, f_1^2 on s_0. It turns out that the value of the scale $\Lambda \approx 0.487$ GeV is practically independent of the value of s_0, it varies by less than 0.1% for the range of the s_0-values presented in Table 3.1, the reason being that $\mathcal{A}_1((3m_c)^2) = a((3m_c)^2)$ ($= 0.07050$) behaves at such scales practically as perturbative coupling a due to "approximate perturbative QCD" conditions (3.20)-(3.21).[10] In the last two columns of Table 3.1 are included various evaluated contributions to the strangeless and massless semihadronic tau decay ratio r_τ [11], see Appendix B of Ref. [53].

[10] For example, for the two input values $s_0 = 3.858, 6.862$ used later in the text, we have $\Lambda = 0.48679, 0.48687$ GeV, respectively; the perturbative value of Λ (at $n_f = 3$) is $\Lambda_{pQCD} = 0.48676$ GeV.

[11] The value of $s_0 = 3.858$ results from the requirement of the reproduction of the central value of the experimental result $r_\tau(\Delta S = 0, m_q = 0)_{\mathrm{exp}} = 0.203 \pm 0.004$ when the leading-β_0 (LB) and the beyond-the-leading-β_0 (bLB) contributions are evaluated and added together.

In Table 3.1 we see that the cutoff parameter $s_0 = M_0^2/\Lambda^2$ cannot fall below $s_0 \approx 1.96$ because in such a case $s_1 = M_1^2/\Lambda^2$ turns out to be negative and the coupling acquires a Landau singularity (at $Q^2 = -s_1 > 0$). In Appendix B of Ref. [53] we calculate the inclusive low energy observable is calculated, in particular (for our purpose) the semihadronic tau decay ratio r_τ (ratio between decays $\tau^- \to \nu_\tau X$ (or $\tau^- \to \nu_\tau \gamma$) and $\tau^- \to \nu_\tau e^- \overline{\nu_e}$ (or $\tau^- \to \nu_\tau e^- \gamma$)) in two different ways, first in the case when the leading-β_0 resummation is performed ($s_0 = 3.858$) in the evaluation, and in the case when it is not performed ($s_0 = 6.862$).

3.3 Two-delta Analytic QCD model

This model was introduced in Ref. [54]. It is an improvement of the one-delta QCD model, in the sense that $\rho_1(\sigma) \equiv \mathrm{Im}\mathcal{A}_1(-\sigma - i\epsilon)$ is the low-σ unknown regime by two deltas. The ansatz for the discontinuity function $\rho_1(\sigma) \equiv \mathrm{Im}\ \mathcal{A}_1(Q^2 = -\sigma - i\epsilon)$ (for $\sigma > 0$) agrees with the perturbative counterpart $\rho_1^{(\mathrm{pt})}(\sigma) \equiv \mathrm{Im}\ a(Q^2 = -\sigma - i\epsilon)$ at sufficiently high scales $\sigma \geq M_0^2$ ($M_0^2 \sim 1$ GeV^2); and in the low-scale regime $0 < \sigma < M_0^2$ its otherwise unknown behavior is parametrized as a linear combination of (two) delta functions

$$\rho_1^{(2\delta)}(\sigma; c_2) = \pi \sum_{j=1}^{2} f_j^2 \Lambda^2\, \delta(\sigma - M_j^2) + \Theta(\sigma - M_0^2) \times \rho_1^{(\mathrm{pt})}(\sigma; c_2) \qquad (3.25)$$

$$= \pi \sum_{j=1}^{2} f_j^2\, \delta(s - s_j) + \Theta(s - s_0) \times r_1^{(\mathrm{pt})}(s)\ , \qquad (3.26)$$

where we denoted $s = \sigma/\Lambda^2$, $s_j = M_j^2/\Lambda^2$ ($j = 0, 1, 2$), and $r_1^{(\mathrm{pt})}(s; c_2) = \rho_1^{(\mathrm{pt})}(\sigma; c_2) = \mathrm{Im}\ a(Q^2 = -\sigma - i\epsilon; c_2)$. Here, Λ^2 ($\lesssim 10^{-1}$ GeV^2) is the Lambert scale appearing in expression (1.24) for a. The underlying pQCD coupling is taken in the more general form (1.24) with the scheme parameter β_2 ($\equiv \beta_0 c_2$) nonzero in general [cf. Eqs. (1.22)-(1.23)].

The aforementioned branching point of nonanalyticity $z(s_\mathrm{L}) = -1/e$ corresponds (as was seen at the final paragraph in Section 1.4), according to Eq. (1.22), to the scale $Q^2(s_\mathrm{L}) = \Lambda^2 s_\mathrm{L}$ with $s_\mathrm{L} = c_1^{-c_1/\beta_0}$ ($s_\mathrm{L} = 0.6347$ when $n_f = 3$), and the interval $Q^2 \in (0, \Lambda^2 s_\mathrm{L})$ represents the interval of the unphysical (Landau) singularities of $a(Q^2)$ of Eq. (1.24). If the scheme parameter c_2 is chosen to be negative (this will be our case), then there is an additional pole-type Landau singularity [12] at a somewhat higher

[12] I wanted to recall at this point that this aforementioned singularity is an additional non-physical pole.

scale $Q^2(u_{\rm L}) = \Lambda^2 u_{\rm L}$ ($\Leftrightarrow \;\; z = z(u_{\rm L}) = -u_{\rm L}^{-\beta_0/c_1}/(c_1 e)$) at which the denominator of Eq. (1.24) becomes zero, cf. Fig. 1.1(b), i.e., when

$$-1 + c_2/c_1^2 = W_{-1}\left(\frac{-1}{c_1 e}|u_{\rm L}|^{-\beta_0/c_1} + i\epsilon\right) \; . \tag{3.27}$$

When $n_f = 3$ and $c_2 = -4.76$ (this will be our central choice of the scheme later), we get $u_{\rm L} = 1.0095$ ($> s_{\rm L}$). For this case, the underlying pQCD coupling a is presented in Fig. 3.2(a) as a function of z (for $-1/e < z < 0$, i.e., $s_{\rm L}\Lambda^2 < Q^2 < \infty$), and in Fig. 3.2(b) as a function of $t = -\ln(-z) = 1.266\ln(Q^2/\Lambda^2) + 1.575$.

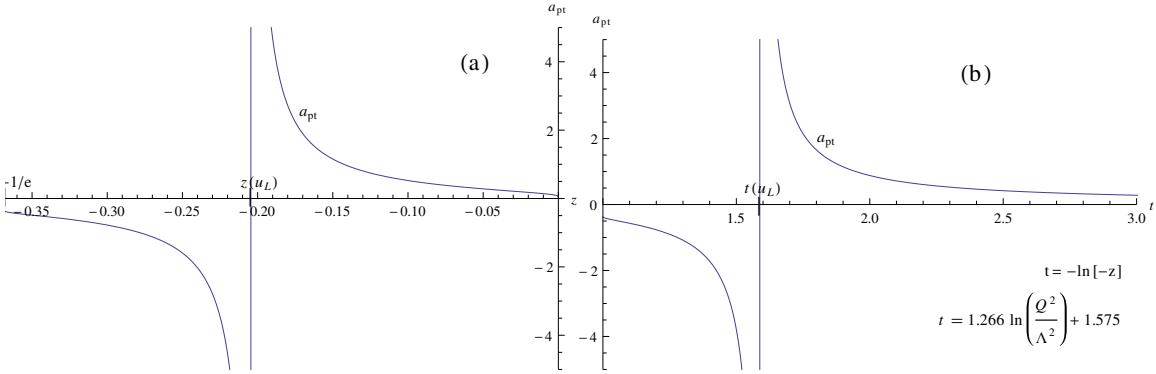

Figure 3.2: (a) The perturbative coupling a of Eq. (1.24) as a function of z, for $-1/e < z < 0$; (b) as a function of $t = -\ln(-z)$. The curves are for the case of $n_f = 3$ and $c_2 = -4.76$ ($\Rightarrow \;\; t = 1.266\ln(Q^2/\Lambda^2) + 1.575$).

It can be checked that, as a result of application of the Cauchy theorem to the function $a(Q'^2)/(Q'^2 - Q^2)$ in the complex-Q'^2 plane, the following dispersion relation for a holds:

$$a(Q^2; c_2) = \frac{1}{\pi}\int_{\sigma=-Q^2_{\rm min}-\eta'}^{\infty} d\sigma \; \frac{{\rm Im}\; a(-\sigma - i\epsilon; c_2)}{(\sigma + Q^2)} = \frac{1}{\pi}\int_{s=-u_{\rm min}-\eta}^{\infty} ds \; \frac{r_1^{\rm (pt)}(s; c_2)}{(s + Q^2/\Lambda^2)}, \tag{3.28}$$

where $\eta, \eta' \to 0$, and the integration covers the entire cut, i.e., starting at a sufficiently low negative value $\sigma_{\rm min} = -Q^2_{\rm min}$ ($Q^2_{\rm min} \lesssim 1$ GeV^2). The perturbative discontinuity function is denoted as $r_1^{\rm (pt)}(s; c_2) = {\rm Im}\; a(Q^2 = -s\Lambda^2 - i\epsilon; c_2)$. Since the cut of the coupling $a(Q'^2, c_2)$, Eq. (1.24) with $c_2 < 0$, includes also the pole $Q'^2_{\rm L} = u_{\rm L}\Lambda^2$ of the coupling, the contour of integration in the complex (Q'^2/Λ^2)-plane is of the type as presented in Fig. 3.3 (with the outer radius going to infinity). Therefore, the

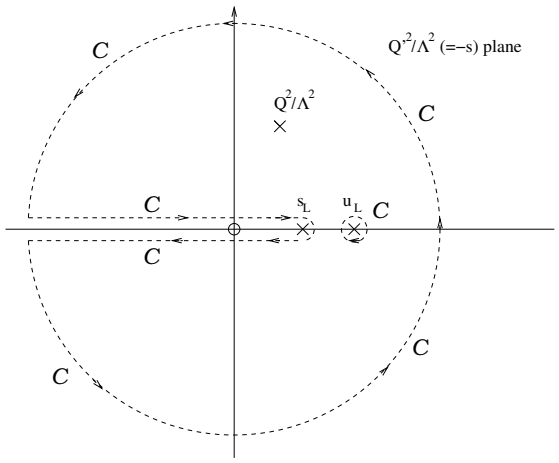

Figure 3.3: The path of contour integration in $(Q^{'2}/\Lambda^2)$-plane leading to the expression (3.29).

dispersive relation (3.28) obtains a slightly generalized form

$$a(Q^2) = \frac{1}{\pi}\int_{s=-s_{\rm L}-\eta}^{\infty} ds\ \frac{r_1^{(\rm pt)}(s;c_2)}{(s+Q^2/\Lambda^2)} + \frac{\Delta u}{2\pi}\int_{\Phi=-\pi}^{\pi} d\Phi\ e^{i\Phi}\ \frac{a\left((u_{\rm L}+\Delta u e^{i\Phi})\Lambda^2;c_2\right)}{[(Q^2/\Lambda^2)-u_{\rm L}-\Delta u e^{i\Phi}]} \quad (3.29)$$

$$= \frac{1}{\pi}\int_{s=-s_{\rm L}-\eta}^{\infty} ds\ \frac{r_1^{(\rm pt)}(s;c_2)}{(s+Q^2/\Lambda^2)} + \frac{{\rm Res}_{(z=u_{\rm L})}a(z\Lambda^2;c_2)}{(-u_{\rm L}+Q^2/\Lambda^2)}\ . \quad (3.30)$$

In Eq. (3.29), $\Delta u\Lambda^2$ is a sufficiently small (but otherwise arbitrary) radius of integration around the point $u_{\rm L}\Lambda^2$ in the complex $Q^{'2}$-plane, cf. Fig. 3.3. In Eq. (3.30), this integration is expressed by the residue of the function $a(z\Lambda^2)$ at this point.

The perturbative discontinuity function $r_1^{(\rm pt)}(s;c_2) = {\rm Im}\ a(Q^2=-s\Lambda^2-i\epsilon;c_2)$, which is nonzero for $-s_{\rm L} < s < +\infty$, has the specific form

$$r_1^{(\rm pt)}(s;c_2) = {\rm Im}\left[\frac{(-1)}{c_1}\frac{1}{\left[1-(c_2/c_1^2)+W_{+1}\left(\frac{-1}{c_1 e}|s|^{-\beta_0/c_1}-i\epsilon\right)\right]}\right]\ (s<0)\ , \quad (3.31)$$

$$= {\rm Im}\left[\frac{(-1)}{c_1}\frac{1}{\left[1-(c_2/c_1^2)+W_{+1}\left(\frac{-1}{c_1 e}|s|^{-\beta_0/c_1}\exp(i\beta_0\pi/c_1)\right)\right]}\right]\ (s>0) \quad (3.32)$$

The analytic (spacelike) coupling $\mathcal{A}_1^{(2\delta)}(Q^2;c_2)$ of the two-delta anQCD model is constructed on the basis of the discontinuity function (3.25)-(3.26) [cf. Eq. (3.32)] using

the dispersion relation (3.3). This gives

$$\mathcal{A}_1^{(2\delta)}(Q^2;c_2) = \sum_{j=1}^{2} \frac{f_j^2}{(u+s_j)} + \frac{1}{\pi}\int_{s_0}^{\infty} ds\, \frac{r_1^{(\mathrm{pt})}(s;c_2)}{(s+u)} \ , \tag{3.33}$$

where $u = Q^2/\Lambda^2$.

In the presented two-delta anQCD model, we will consider the first three quark flavors to be massless, and will consider that the momenta in the $n_f = 3$ regime in the anQCD model reach up to the threshold $|Q^2| = (2m_c)^2$ (≈ 6.45 GeV^2). Further, the anQCD model will be constructed in such a way as to practically merge with pQCD at such sufficiently high momenta. Therefore, we will consider that the value of the Lambert scale Λ^2 used in our analytic coupling $\mathcal{A}_1(Q^2;c_2)$ coincides with the perturbative Lambert scale Λ^2, the latter being determined by the condition $a^{(\overline{\mathrm{MS}})}(M_Z^2) = 0.1184/\pi$, i.e., by the central value of the world average [56] in the same way as for one delta approach. Therefore, Λ^2 is determined by RGE-evolving this a down to $a^{(\overline{\mathrm{MS}})}((2m_c)^2; n_f = 3)$, using the four-loop polynomial form of $\beta^{(\overline{\mathrm{MS}})}(a)$, and the three-loop matching conditions [12] at quark thresholds $\mu^2 = (2m_q)^2$ ($q = b, c$); and then changing from the $\overline{\mathrm{MS}}$ scheme to the "Lambert" scheme [$\equiv (c_2, c_3 = c_2^2/c_1, \ldots)$] defined by the beta function (as explained, e.g., in Refs. [39, 53]).

The conditions we impose to fix the parameters are the following:

1. The analytic coupling $\mathcal{A}_1(Q^2;c_2)$ acquires the aforementioned pQCD value of the scale Λ^2 of $a(Q^2;c_2;n_f=3)$

$$\Lambda^2 = \Lambda^2_{\mathrm{pt}}(n_f = 3) \ . \tag{3.34}$$

2. While in general we expect $\mathcal{A}_1(Q^2;c_2)$ to differ from $a(Q^2;c_2)$ at $Q^2 > \Lambda^2$ by $\sim (\Lambda^2/Q^2)^1$, we impose the condition

$$\mathcal{A}_1(Q^2;c_2) - a(Q^2;c_2) \sim (\Lambda^2/Q^2)^{n_{\max}} \quad \text{with } n_{\max} = 5 \ . \tag{3.35}$$

The condition (3.35) represents in practice four conditions (like in the case of one delta $n_{max} = 3$ implies two conditions).

These conditions appear when we subtract from the perturbative coupling (3.30) the analytic coupling (3.33)

$$a(Q^2;c_2) - \mathcal{A}_1(Q^2;c_2) = \frac{\mathrm{Res}_{(z=u_{\mathrm{L}})} a(z\Lambda^2)}{(u-u_{\mathrm{L}})} - \sum_{j=1}^{2} \frac{f_j^2}{(u+s_j)} + \frac{1}{\pi}\int_{s_{\mathrm{L}}-\eta}^{s_0} ds\, \frac{r_1^{(\mathrm{pt})}(s;c_2)}{(s+u)} \ . \tag{3.36}$$

Table 3.2: Values of the parameters of the considered 2δanQCD model. We consider $c_2 = -4.76$ ($M_0 = 1.25$ GeV) as the central representative case. The Lambert scale values in the corresponding cases are for the QCD coupling parameter value $\alpha_s^{(\overline{\rm MS})}(M_Z^2) = 0.1184$.

$c_2 = \beta_2/\beta_0$	s_0	s_1	f_1^2	s_2	f_2^2	Λ [GeV]	M_0	$\mathcal{A}_1(0)$
-2.10	17.09	12.523	0.1815	0.7796	0.3462	0.363	1.50	0.544
-4.76	23.06	16.837	0.2713	0.8077	0.5409	0.260	1.25	0.776
-5.73	25.01	18.220	0.3091	0.7082	0.6312	0.231	1.15	1.00

Expanding the left-hand side in powers of $(1/u) = (\Lambda^2/Q^2)$, the imposition of the condition (3.35) gives us the conditions that the terms of $\sim (\Lambda^2/Q^2)^{1+k}$ ($k = 0, 1, 2, 3,$) in this expansion are zero, i.e., we have the following four conditions

$$\frac{1}{\pi}\int_{s_{\rm L}-\eta}^{s_0} ds\; s^k\; r_1^{({\rm pt})}(s; c_2) + (-u_{\rm L})^k\; {\rm Res}_{(z=u_{\rm L})} a(z\Lambda^2) \;\; = \;\; s_1^k f_1^2 + s_2^k f_2^2\;. \quad (3.37)$$

Altogether, Eqs. (3.34) and (3.37) represent five conditions. Once the scheme c_2 parameter is chosen, we have altogether six parameters in the model: f_1^2, f_2^2, s_1, s_2, s_0, and the scale Λ. Therefore, yet another condition should be imposed. This condition is chosen to be the reproduction of the correct value of $r_\tau(\Delta S = 0, m_q = 0)_{exp} = 0.203 \pm 0.004$.
The scheme parameter c_2 ($\equiv \beta_2/\beta_0$) can still be varied. Guided by various physical considerations, we can restrict the pQCD-onset scale M_0 to be $M_0 \leq 1.5$ GeV, and the coupling at $Q^2 = 0$ to be not too large: $\mathcal{A}_1(0) \leq 1.0$. This gives us the variation of c_2 in the interval $-5.73 < c_2 < -2.1$. In table 3.2 we present the results for the parameters of the model for three different c_2 in this interval. Our preferred choice is $c_2 = -4.76$ where $M_0 = 1.25$

For historical reasons, we conserve the notation $\mathcal{A}_n(Q^2)$ for the first and the most popular model based on the spectral perturbative representation of the coupling that is APT. Therefore hereafter we use the superscript (1δ) or (2δ) for the model based on one or two deltas respectively.

3.4 Effective charge

We can define a coupling directly from the experiment, without resorting to the (not well defined) perturbation expansion in powers of a in the whole energy range. Therefore, we expect to obtain a "real" (or physical) coupling and in principle this

should be finite (or zero) as the momentum goes to zero.
In this sense, the new coupling is defined as [63]

$$a_{eff}(s) = \mathcal{R}(s) = \sum_m r_m a^m_{(\ell)}(s), \tag{3.38}$$

that is the "physical coupling", where $\mathcal{R}(s)$ is, for example, the Drell ratio(e^+e^- annihilation into hadrons) that is defined in the timelike region. We can go from timelike to spacelike region with the integral relation (2.6).
The most notable properties of this approach can be summarize as follow:

1. It includes both, the perturbative and nonperturbative effect (completely).
2. It is analytic in the whole momentum range.
3. It has a finite value at zero momentum scale (freezing).
4. It is analytic across the quark threshold flavor and nonsingular.
5. It is different for each observable, this implies that we lose the prediction for other observables.

The disadvantage (5) has a simple solution, since we can relate two different couplings via perturbation expansion, but of course, the accuracy will depend on how many terms we consider, and how weak or strong are the nonperturbative contributions which cannot be accounted for in the perturbation expansion.

3.5 "Massive" Perturbative QCD

In order to obtain a "regular" coupling (that is finite at zero momentum energy) the author of Ref. [65] proposed a simple change in the momentum:

$$Q^2 \mapsto Q^2 + m^2_{gl}. \tag{3.39}$$

The mass scale m^2_{gl} is, in principle, (in this ansatz) a constant and is associated with an "effective gluonic mass".
The one-loop ($\ell = 1$) expression takes the simple form

$$\mathcal{A}^{(\ell=1)}_{1,MPT}(x;\xi) = \frac{1}{\beta_0 \ln(\xi + x)}, \tag{3.40}$$

where the dimensionless variables are $\xi = \frac{m^2_{gl}}{\Lambda^2} = \mathrm{e}^{1/\beta_0 a_{crit}}$; $a_{crit} = \mathcal{A}_{1,MPT}(0;\xi)$ and $x = Q^2/\Lambda^2$.

And at two-loop level

$$\mathcal{A}^{(\ell=2)}_{1,MPT}(x;\xi)=\frac{a_s}{1+a_s\beta_0\ln(1+\phi x)+a_s\frac{\beta_1}{\beta_0}\ln[1+a_s\beta_0\ln(1+\phi x)]}, \tag{3.41}$$

where the logarithm for low-energy scales is written as $\ln(\xi+x)=\ln\xi+\ln(1+\xi x)=\frac{1}{a_s\beta_0}+\ln(1+\xi x)$, and $\phi=1/\xi$.
As this model is analytic, the higher power analogs of the coupling $\mathcal{A}^{(\ell=1)}_{1,MPT}(x;\xi)$ are constructed with the nonpower series mechanism presented in Section 2.3, which is applicable to any analytic QCD model (not just APT) as explained in Refs. [35, 36].
This simple analytic QCD model instead of removing the Landau singularities, moves them to low negative (timelike) Q^2. In this way, if the dynamical gluon mass is m_{gl}, then the (Landau) pole becomes $Q^2_p=\Lambda^2-m^2_{gl}$, having two possibilities:

$$m^2_{gl}\to\begin{cases} >\Lambda^2 & \Rightarrow Q^2_p<0 \qquad (MPT)\\ \leq\Lambda^2 & \Rightarrow Q^2_p\geq 0 \qquad (MPT+FAPT)\end{cases} \tag{3.42}$$

On the other hand, if $Q^2_p-m^2_{gl}>0$, we can use FAPT (with MPT) in order to remove this pole. In the first case ($Q^2_p-m^2_{gl}<0$) we do not have a pole in the physical region (in the Euclidean regime of course), therefore MPT is sufficient.
We have typically $Q_p\leq 300$MeV and $m_{gl}=700-1000$MeV.
This model was applied with a preliminary estimation in the polarized $\Gamma_1^{p-n}(Q^2)$ form factor of the Bjorken Sum Rules, giving a very good agreement in comparison with JLab data [65].

3.6 Non integer Powers: A general treatment

This formalism was introduced in Ref. [27].
Strictly speaking, the dispersion relation (3.3) in a general analytic QCD model (beyond APT) involves the discontinuity function

$$\rho_1(\sigma)=\text{Im }\mathcal{A}_1(Q^2=-\sigma-i\varepsilon)\ , \tag{3.43}$$

defined for $\sigma\geq 0$; usually, the discontinuity cut is nonzero below a threshold value $-\sigma\leq -M^2_{\text{thr}}$ where $M_{\text{thr}}\sim M_\pi$. Therefore Q^2 can have any value in the complex plane except the cut $(-\infty,-M^2_{\text{thr}}]$. The logarithmic derivatives are defined as

$$\widetilde{\mathcal{A}}_{n+1}(Q^2)\equiv\frac{(-1)^n}{\beta_0^n n!}\frac{\partial^n\mathcal{A}_1(Q^2)}{\partial(\ln Q^2)^n}\ , \qquad (n=0,1,2,\ldots)\ . \tag{3.44}$$

We note that for $n = 0$ equation (3.44) gives $\widetilde{\mathcal{A}}_1 \equiv \mathcal{A}_1$. We can write the logarithmic derivatives in the following form:

$$\widetilde{\mathcal{A}}_{n+1}(Q^2) = \frac{1}{\pi}\int_0^\infty \frac{d\sigma}{\sigma}\rho_1(\sigma)\frac{1}{\beta_0^n\Gamma(n+1)}\frac{d^n}{d(\ln z)^n}\left(\frac{z}{1+z}\right)\Big|_{z=\sigma/Q^2} . \tag{3.45}$$

It turns out that the integrand is the known polylogarithm function

$$\frac{d^n}{d(\ln z)^n}\left(\frac{z}{1+z}\right) = \left(z\frac{d}{dz}\right)^n \sum_{m=1}^\infty (-1)^{m+1}z^m = \sum_{m=1}^\infty (-1)^{m+1}m^n z^m = (-1)\mathrm{Li}_{-n}(-z) , \tag{3.46}$$

which brings equation (3.45) in the following form:

$$\widetilde{\mathcal{A}}_{n+1}(Q^2) = \frac{1}{\pi}\frac{(-1)}{\beta_0^n\Gamma(n+1)}\int_0^\infty \frac{d\sigma}{\sigma}\rho_1(\sigma)\mathrm{Li}_{-n}(-\sigma/Q^2) . \tag{3.47}$$

This relation is valid for $n = 0, 1, 2, ...$ Analytic continuation in $n \mapsto \nu$ gives us[13] the logarithmic noninteger derivatives

$$\widetilde{\mathcal{A}}_{\nu+1}(Q^2) = \frac{1}{\pi}\frac{(-1)}{\beta_0^\nu\Gamma(\nu+1)}\int_0^\infty \frac{d\sigma}{\sigma}\rho_1(\sigma)\mathrm{Li}_{-\nu}\left(-\frac{\sigma}{Q^2}\right) \quad (-1 < \nu) . \tag{3.48}$$

We note that the integral converges for $\nu > -1$. Namely, at high σ ($|z| \gg 1$ where $z \equiv \sigma/Q^2$) we have in the integrand of equation (3.48): $\rho_1(\sigma) \approx \rho_1^{(\mathrm{pt})}(\sigma) \sim \ln^{-2}\sigma \sim \ln^{-2} z$ and $\mathrm{Li}_{-\nu}(-z) \sim \ln^{-\nu} z$ (for noninteger ν). Therefore, the integral converges at $\sigma \to \infty$ if $\nu > -1$. The integral obviously converges at low σ, too.

In principle, a continuation to arbitrary ν, as performed by the transition from equation (3.47) to equation (3.48), could in principle miss some terms, such as terms proportional to $\sin^k(\nu\pi)$. However, such terms will be excluded because they are finite oscillatory when $\nu \to \pm\infty$.

It is interesting that the recursive relation

$$\widetilde{\mathcal{A}}_{\nu+2}(Q^2) = \frac{(-1)}{\beta_0(\nu+1)}\frac{d}{d\ln Q^2}\widetilde{\mathcal{A}}_{\nu+1}(Q^2) , \tag{3.49}$$

which for positive integer $\nu = n = 0, 1, 2, \ldots$ is a direct consequence of the definition (3.45), remains valid even for noninteger ν as a consequence of the relation (3.48) and the known[14] relation $z(d/dz)\mathrm{Li}_{-\nu}(z) = \mathrm{Li}_{-\nu-1}(z)$.

[13] In Mathematica [55], the $\mathrm{Li}_{-\nu}(z)$ function is implemented as PolyLog$[-\nu, z]$. However, at large $|z| > 10^7$, PolyLog$[-\nu, z]$ appears to be unstable. For such z we should use the identities relating $\mathrm{Li}_{-\nu}(z)$ with $\mathrm{Li}_{-\nu}(1/z)$, which can be found, for example, in [57].

[14] This relation can be obtained, for example, by applying $d/d\ln z$ to the power series $Li_{\nu'}(z)_{\mathrm{ser.}} = \sum_{m=1}^\infty z^m m^{-\nu'}$.

We can recast the result (3.48) into an alternative form involving the spacelike coupling $\mathcal{A}_1$ instead of the discontinuity function $\rho_1(\sigma)$. This can be performed in the following way.

We can use the following integral form of $\mathrm{Li}_{-\nu}$ function [15] [58] appearing in equation (3.48):

$$\mathrm{Li}_{-\nu}(z) = \frac{z}{\Gamma(-\nu)} \int_0^\infty \frac{dt\; t^{-\nu-1}}{(e^t - z)} = \frac{z}{\Gamma(-\nu)} \int_0^1 \frac{d\xi}{1-z\xi} \ln^{-\nu-1}\left(\frac{1}{\xi}\right) \quad (\nu < 0)\ . \quad (3.50)$$

The last expression on the right-hand side was obtained by the change of variable $t = \ln(1/\xi)$. Since we have in our result (3.48) $\mathrm{Li}_{-\nu}$ with $-1 < \nu$ (and not just: $-1 < \nu < 0$), we extend the integral representation to higher $\nu > 0$. This is achieved by using in equation (3.50) the aforementioned relation $(d/d\ln z)\mathrm{Li}_{-\nu} = \mathrm{Li}_{-\nu-1}$. We thus obtain, for $\nu = n + \delta$, with $0 < \delta < 1$ and $n = -1, 0, 1, 2, \ldots$, the following integral form, [59]:

$$\mathrm{Li}_{-n-\delta}(z) = \left(\frac{d}{d\ln z}\right)^{n+1} \left[\frac{z}{\Gamma(1-\delta)} \int_0^1 \frac{d\xi}{1-z\xi} \ln^{-\delta}\left(\frac{1}{\xi}\right)\right]\ . \quad (3.51)$$

Inserting the representation (3.51), for $\nu = n + \delta$, into our general formula (3.48), and exchanging the order of integration, gives us

$$\widetilde{\mathcal{A}}_{\nu+1}(Q^2) = \frac{1}{\beta_0^\nu \Gamma(n+1+\delta)\Gamma(1-\delta)} \left(-\frac{d}{d\ln Q^2}\right)^{n+1} \int_0^1 \frac{d\xi}{\xi} \ln^{-\delta}\left(\frac{1}{\xi}\right) \times \int_0^\infty \frac{d\sigma \rho_1(\sigma)}{\pi(\sigma + Q^2/\xi)}\ . \quad (3.52)$$

The last integral over $d\sigma$ is the spacelike coupling $\mathcal{A}_1(Q^2/\xi)$ due to the dispersion relation (2.1). Therefore, we obtain the alternative form of the result (3.48), for $\nu = n + \delta$, with $0 < \delta < 1$ and $n = -1, 0, 1, 2, \ldots$,

$$\begin{aligned} \widetilde{\mathcal{A}}_{\nu+1}(Q^2) &\equiv \widetilde{\mathcal{A}}_{n+1+\delta}(Q^2) \\ &= \frac{1}{\beta_0^\nu \Gamma(1+\nu)\Gamma(1-\delta)} \left(-\frac{d}{d\ln Q^2}\right)^{n+1} \int_0^1 \frac{d\xi}{\xi} \mathcal{A}_1(Q^2/\xi) \ln^{-\delta}\left(\frac{1}{\xi}\right) \quad (3.53) \\ &= \frac{1}{\beta_0^\nu} \frac{\Gamma(1+\delta)}{\Gamma(n+1+\delta)} \frac{\sin(\pi\delta)}{(\pi\delta)} \left(-\frac{d}{d\ln Q^2}\right)^{n+1} \int_0^\infty \frac{dt}{t^\delta} \mathcal{A}_1(Q^2 e^t)\ , \quad (3.54) \end{aligned}$$

[15] Equation (3.50) can be proven by expanding the integrand in powers of e^{-t} and using the basic integral expression for the $\Gamma(\nu')$ function (where $\nu' \equiv -\nu > 0$): $\int_0^\infty du\; e^{-u} u^{\nu'-1} = \Gamma(\nu')$. In this way, the (convergent for $|z| < 1$) series $\sum_{m=1}^\infty z^m m^{-\nu'}$ is generated, which is just the polylogarithm function $\mathrm{Li}_{\nu'}(z) \equiv \mathrm{Li}_{-\nu}(z)$.

where the last form (3.54) was obtained from the previous one by the substitution $t = \ln(1/\xi)$ and using the identity $\Gamma(1+\delta)\Gamma(1-\delta) = \pi\delta/\sin(\pi\delta)$.

Furthermore, for the special FAPT case the explicit result obtained in [28] is satisfied

$$\widetilde{\mathcal{A}}_{\nu+1}(Q^2)^{(\mathrm{FAPT},1-\ell)} = \mathcal{A}_{\nu+1}(Q^2)^{(\mathrm{FAPT},1-\ell)} = \frac{1}{\beta_0^{\nu+1}} \left(\frac{1}{\ln^{\nu+1}(Q^2/\Lambda^2)} - \frac{\mathrm{Li}_{-\nu}(\Lambda^2/Q^2)}{\Gamma(\nu+1)} \right) , \tag{3.55}$$

where the scale Λ appears in the one-loop FAPT analytic coupling $\mathcal{A}_1(Q^2)^{(\mathrm{FAPT},1-\ell)}$ and in its discontinuity function $\rho_1(\sigma)^{(1-\ell)}_{\mathrm{pt}}$

$$\mathcal{A}_1(Q^2)^{(\mathrm{FAPT},1-\ell)} = \frac{1}{\beta_0} \left(\frac{1}{\ln(Q^2/\Lambda^2)} - \frac{\Lambda^2}{(Q^2-\Lambda^2)} \right) , \tag{3.56}$$

$$\begin{aligned} \rho_1(\sigma)^{(1-\ell)}_{\mathrm{pt}} &= \mathrm{Im} a_{\mathrm{pt}}(-\sigma - i\epsilon)^{(1-\ell)} = \mathrm{Im}\mathcal{A}_1(-\sigma - i\epsilon)^{(\mathrm{FAPT},1-\ell)} \\ &= \frac{1}{\beta_0} \mathrm{Im} \frac{1}{(\ln(\sigma/\Lambda) - i\pi)} = \frac{\pi}{\beta_0} \frac{1}{\left(\ln^2(\sigma/\Lambda) + \pi^2\right)} . \end{aligned} \tag{3.57}$$

When replacing $\mathcal{A}_1(Q^2/\xi)$ in the integrand of the expression (3.53) by the second term of the expression (3.56) for $\mathcal{A}_1(Q^2/\xi)^{(\mathrm{FAPT},1-\ell)}$, and using the integral form (3.51) for $\mathrm{Li}_{-\nu}$, we obtain immediately

$$\begin{aligned} \frac{1}{\beta_0^{\nu}\Gamma(1+\nu)\Gamma(1-\delta)} \left(-\frac{d}{d\ln Q^2} \right)^{n+1} \int_0^1 \frac{d\xi}{\xi} \ln^{-\delta}\left(\frac{1}{\xi}\right) \frac{1}{\beta_0} \frac{(-1)\Lambda^2}{(Q^2/\xi - \Lambda^2)} \\ = \frac{(-1)}{\beta_0^{\nu+1}\Gamma(\nu+1)} \mathrm{Li}_{-\nu}(\Lambda^2/Q^2) . \end{aligned} \tag{3.58}$$

On the other hand, when replacing $\mathcal{A}_1(Q^2/\xi)$ in the integrand of the expression (3.54) by the first term of the expression (3.56) for $\mathcal{A}_1(Q^2/\xi)^{(\mathrm{FAPT},1-\ell)}$, we obtain in a direct manner[16]

$$\begin{aligned} \frac{1}{\beta_0^{\nu}} \frac{\Gamma(1+\delta)}{\Gamma(n+1+\delta)} \frac{\sin(\pi\delta)}{(\pi\delta)} \left(-\frac{d}{d\ln Q^2} \right)^{n+1} \int_0^{\infty} \frac{dt}{t^{\delta}} \frac{1}{\beta_0} \frac{1}{[t + \ln(Q^2/\Lambda^2)]} \\ = \frac{1}{\beta_0^{\nu+1} \ln^{\nu+1}(Q^2/\Lambda^2)} . \end{aligned} \tag{3.59}$$

[16] We can use the integration variable $y = t/t_0$, where $t_0 = \ln(Q^2/\Lambda^2)$, and the exact solution of the following integral:

$$\int_0^{\infty} \frac{dy}{y^{\delta}(y+1)} = \frac{\pi}{\sin(\pi\delta)} , \qquad \text{where } 0 < \delta < 1 .$$

Combining the results (3.58) and (3.59), we obtain the full result (3.55) for $\mathcal{A}_{\nu+1}(Q^2)$ in the one-loop approach of FAPT, for any noninteger ν such that $-1 < \nu$ (when ν is nonnegative integer, the limit $\delta \to 0$ can be made in the derivation). This (one-loop FAPT) result, was obtained for the first time by Bakulev, Mikhailov and Stefanis (BMS) in [28]. The result (3.55) is explicit and allows us to apply it even for $\nu \leq -1$, and even for complex ν; this is a kind of analytic continuation in ν. We can thus use this result, by adding and subtracting it from of our general integral expression (3.48), thus extending the ν-regime of applicability of our expression

$$\begin{aligned} \widetilde{\mathcal{A}}_{\nu+1}(Q^2) &= \widetilde{\mathcal{A}}_{\nu+1}(Q^2)^{(\mathrm{FAPT},1-\ell)} + \frac{1}{\pi}\frac{(-1)}{\beta_0^\nu \Gamma(\nu+1)} \\ &\quad \times \int_0^\infty \frac{d\sigma}{\sigma}\left[\rho_1(\sigma) - \rho_1(\sigma)_{\mathrm{pt}}^{(1-\ell)}\right] \mathrm{Li}_{-\nu}\left(-\frac{\sigma}{Q^2}\right) \\ (-2 < \nu)\ , & \end{aligned} \tag{3.60}$$

where $\widetilde{\mathcal{A}}_{\nu+1}(Q^2)^{(\mathrm{FAPT},1-\ell)}$ and $\rho_1(\sigma)_{\mathrm{pt}}^{(1-\ell)}$ are given in equations (3.55) and (3.57), respectively. Now the integral converges also for $-2 < \nu < -1$, because, due to asymptotic freedom, the difference $[\rho_1(\sigma) - \rho_1(\sigma)_{\mathrm{pt}}^{(1-\ell)}]$ behaves at large σ as $\sim \ln\ln\sigma/\ln^3\sigma$ and not as $1/\ln^2\sigma$. Further, the expression (3.60) implies that $\widetilde{\mathcal{A}}_0(Q^2)$ $[\equiv \lim_{\nu\to-1}\widetilde{\mathcal{A}}_{\nu+1}(Q^2)] = 1$ for all complex Q^2, because: $\mathrm{Li}_{-\nu}(z)/\Gamma(\nu+1) \to 0$ when $\nu \to -1$, and $\widetilde{\mathcal{A}}_0(Q^2)^{(\mathrm{FAPT},1-\ell)} \equiv 1$.

In turns out that the relations (2.12) between the logarithmic derivatives of $\mathcal{A}_1$ and it was shown there that the power analogs $\mathcal{A}_n = (a^n)_{an}$ are valid in any anQCD, not only (F)APT, as pointed out in Refs. [35, 36]. In Ref. [27] these relations are generalized to $n \mapsto \nu$ (real ν), and the power analogs $\mathcal{A}_\nu \equiv (a^\nu)_{an}$ can be constructed as linear combinations of $\widetilde{\mathcal{A}}_{\nu+m}$'s:

$$\mathcal{A}_\nu = \widetilde{\mathcal{A}} + \sum_{m\geq 1} \tilde{k}_\nu(m)\widetilde{\mathcal{A}}_{\nu+m}, \tag{3.61}$$

where the coefficients $\tilde{k}_\nu(m)$ were obtained in [27] for general ν.

3.6.1 An Equivalent Formulation

The central results (3.45) and (3.60) were obtain above in the way presented in Ref. [27]. However, we can obtain the formula (3.45) in an alternative way, using Laplace transforms.

We can apply the same idea of Ref. [28] (see Section 2.7 for details), where

$$\mathcal{A}_1(L) = \int_0^\infty \mathrm{e}^{-Lt}\mathcal{A}_1'(t)dt. \tag{3.62}$$

Applying this to (3.44) we find a more simple form, where the derivatives converts to powers of t in the Laplace transform. Therefore, we not have problem to make the analytic continuation from n to ν ($\nu \in \Re$), taking into account that $\Gamma(n) = (n-1)!$

$$\begin{aligned}\tilde{\mathcal{A}}_{n+1}(L) &= \frac{1}{\beta_0^n\Gamma(n+1)}\int_0^\infty t^n\mathrm{e}^{-Lt}\mathcal{A}_1'(t)dt \\ &\to \frac{1}{\beta_0^\nu\Gamma(\nu+1)}\int_0^\infty t^\nu\mathrm{e}^{-Lt}\mathcal{A}_1'(t)dt \end{aligned}\tag{3.63}$$

The general dispersion representation (3.3) then gives for the Laplace transform

$$\mathcal{A}_1'(L) = -\frac{1}{\pi}\int_{M_{thr}^2/\Lambda^2}^{+\infty} ds r_1(s)\sum_{m=0}^\infty\left(\frac{-1}{s}\right)^{m+1}\delta(t+m), \tag{3.64}$$

where $r_1(s)$ is the dimensionless discontinuity (spectral) function, i.e. $r_1(s) \equiv \rho_1(\sigma = \Lambda^2 s)$. Hence, $\widetilde{\mathcal{A}}_{\nu+1}(L)$ of (3.63) can be written in terms of the spectral function, too

$$\begin{aligned}\tilde{\mathcal{A}}_{\nu+1}(L) &= \frac{1}{\beta_0^\nu\Gamma(\nu+1)}\int_0^\infty t^\nu\mathrm{e}^{-Lt}\left(-\frac{1}{\pi}\int_{M_{thr}^2/\Lambda^2}^{+\infty} ds r_1(s)\sum_{m=0}^\infty\left(\frac{-1}{s}\right)^{m+1}\delta(t+m)\right)dt \\ &= \frac{1}{\pi\beta_0^\nu\Gamma(\nu+1)}\sum_{m=0}^\infty(-1)^m\int_0^\infty dt t^\nu\mathrm{e}^{-Lt}\delta(t+m)\int_{M_{thr}^2/\Lambda^2}^{+\infty}\frac{ds}{s^{m+1}}r_1(s) \\ &= \frac{1}{\pi\beta_0^\nu\Gamma(\nu+1)}\sum_{m=0}^\infty(-1)^m\int_0^\infty dt t^\nu\mathrm{e}^{-Lt}\delta(t+m)\int_{L_{s_0}}^{+\infty} dL_s\mathrm{e}^{-mL_s}r_1(L_s) \\ &= \frac{(-1)^\nu}{\pi\beta_0^\nu\Gamma(\nu+1)}\int_{L_{s_0}}^{+\infty} dL_s r_1(L_s)\sum_{m=0}^\infty\frac{(-\mathrm{e}^{L+L_s})^m}{m^{-\nu}} \\ &= \frac{(-1)^\nu}{\pi\beta_0^\nu\Gamma(\nu+1)}\int_{L_{s_0}}^{+\infty} dL_s r_1(L_s)\mathrm{Li}_{-\nu}(-\mathrm{e}^{L+L_s}), \end{aligned}\tag{3.65}$$

where $L_{s_0} \equiv \ln(M_{thr}^2/\Lambda^2)$ and we used from the definition of polylogarithmic function that $\mathrm{Li}_{-\nu}(-z) = \sum_{m=0}^\infty m^\nu(-z)^m$.
The expression (3.65) coincides with (3.48) and we demostrated that both approaches give the same result. Therefore, one has the freedom (choice by convenience) to start with the discontinuity function or the Laplace representation of the analytic model. Any analytic QCD model is defined either by $\rho_1(\sigma)$, or $\widetilde{\mathcal{A}}_1(Q^2)$.

3.7 General Evaluation Approach in Analytic QCD Model

The truncated pQCD series

$$D_{pt}^{[N]}(Q^2) = a^{\nu}(Q^2) + d_1 a^{\nu+1}(Q^2) + d_2 a^{\nu+2}(Q^2) + \ldots + d_{N-1} a^{\nu+N-1}(Q^2), \quad (3.66)$$

of a spacelike observable $D(Q^2)$ is evaluated in general anQCD model as

$$\begin{aligned} D_{pt}^{[N]}(Q^2) &= \mathcal{A}_{\nu}(Q^2) + d_1 \mathcal{A}_{\nu+1}(Q^2) + \ldots + d_{N-1} \mathcal{A}_{\nu+N-1}(Q^2), \\ &= \widetilde{\mathcal{A}}_{\nu}(Q^2) + \tilde{d}_1 \widetilde{\mathcal{A}}_{\nu+1}(Q^2) + \ldots + \tilde{d}_{N-1} \widetilde{\mathcal{A}}_{\nu+N-1}(Q^2), \end{aligned} \quad (3.67)$$

where the aforementioned connections between $\mathcal{A}_{\nu'}$ and $\mathcal{A}_{\nu''}$'s are used in the correspondingly truncated form (truncated at $\sim \widetilde{\mathcal{A}}_{\nu+N-1} \sim \mathcal{A}_{\nu+N-1}$)

$$\mathcal{A}_{\nu+K} = \widetilde{\mathcal{A}}_{\nu+K} + \sum_{m=1}^{N-1-K} \tilde{k}_{\nu+K}(m) \widetilde{\mathcal{A}}_{\nu+K+m}, \quad (K = 0, 1, \ldots, N-1), \quad (3.68)$$

and the corresponding inverse relations are

$$\widetilde{\mathcal{A}}_{\nu+K} = \mathcal{A}_{\nu+K} + \sum_{m=1}^{N-1-K} k_{\nu+K}(m) \mathcal{A}_{\nu+K+m}, \quad (3.69)$$

with the coefficients $k_{\nu+K}(m)$ and $\tilde{k}_{\nu+K}(m)$ obtained in Ref. [27] (see also Ref. [66]) for the general case of real index ν.
Further more, when ν is integer and the truncation index N is even, a generalization of the diagonal Padé method (Refs. [66,67,132]) is a very efficient evaluation method of $D(Q^2)$ in any analytic QCD, it gives a convergent sequence of values as $N(= 2M)$ increases. The latter method, which was introduced in Ref. [68] in the context of pQCD, usually fails in pQCD due to the vicinity of the Landau singularities (they are absent in analytic QCD).

PART 2. Applications of Analytic QCD Models

Chapter 4

The Gluon Propagator

This chapter is mainly based on the work of Ref. [54].

4.1 The Perturbative Scenario

Our first task is to derive the Gluon Propagator in analytic QCD models in two differents ways, beginning with the usual dispersion relation (or unsubtracted dispersion relation), and after that with the subtracted dispersion relation.
In QCD we have the gluon propagator in the Landau gauge

$$D^{ab}_{\mu\nu}(q) = \delta^{ab}(g_{\mu\nu} - q_\mu q_\nu/q^2)D(-q^2), \tag{4.1}$$

with the propagator in the space-like momentum notation (that is $Q^2 \equiv -q^2$)

$$D(Q^2) = \frac{1}{Q^2}Z(Q^2). \tag{4.2}$$

The propagator is normalized at a Euclidean (spacelike) point $Q^2 = \mu^2$, in the form: $Z(Q^2) \equiv d(Q^2/\mu^2)|_{Q^2=\mu^2} = 1$.
On the other hand, we can give an extension of this formula for a possible presence of a gluon mass. This we will discuss in a model where a dynamical gluon mass is introduced, reflecting strong interaction effects in the infrared; this propagator is

$$D(Q^2) = \frac{Z^{(NP)}(Q^2)}{Q^2 + M(Q^2)^2} \tag{4.3}$$

In general, the propagator is obtained perturbatively from the Callan-Symanzik equation (or invariance under the renormalization group equation (RGE)) with a mass scale dependence too. And in general this mass is renormalization scale dependent. We will focus for the moment on the non-massive gluon propagator, with the RGE solution in the form,

$$Z(Q^2) = \exp\left(\int_{a_{pt}(Q_0^2)}^{a_{pt}(Q^2)} \frac{\gamma_v(x)}{\beta(x)} dx\right). \tag{4.4}$$

The anomalous dimension (in the Landau gauge) and the beta function have in perturbative QCD (pQCD) the following form:

$$\gamma_v(a_{pt}) = -\left(\gamma_0 a_{pt} + \gamma_1 a_{pt}^2 + \ldots\right), \tag{4.5}$$

$$\beta(a_{pt}) = -\left(\beta_0 a_{pt}^2 + \beta_1 a_{pt}^3 + \ldots\right), \tag{4.6}$$

where $\gamma_0 = (13 - 4n_f/3)/8$, $\gamma_1 = (531/8 - 61n_f/6)/16$ and $\beta_0 = (11 - 2n_f/3)/4$, $\beta_1 = (102 - 38n_f/3)/16$.
As a consequence, the gluon propagator residue (dressing) function (dimensionless) at N-loop level has the following expression:

$$Z(Q^2) = c_v \sum_{n=0}^{N-1} d_n a_{pt}^{n+\nu}, \tag{4.7}$$

where $\nu = \gamma_0/\beta_0$, and c_v is a constant that depends on the initial condition.
In order to prove Eq. (4.7), first we note that the ratio between N-loop anomalous dimension and beta function can be rewritten as a ratio of two polynomials, which can always be written in the partial fraction form, as we show below

$$\begin{aligned}
\frac{\gamma_v(a_{pt})}{\beta(a_{pt})} &= \frac{\sum_{n=0}^{N-1} \gamma_n a_{pt}^{n+1}}{\sum_{n=0}^{N-1} \beta_n a_{pt}^{n+2}} \\
&= \frac{\gamma_0}{\beta_0 a_{pt}} \left(\frac{1 + \sum_{n=1}^{N-1} (\gamma_n/\gamma_0) a_{pt}^n}{1 + \sum_{n=1}^{N-1} (\beta_n/\beta_0) a_{pt}^n}\right) \\
&= \frac{\gamma_0}{\beta_0 a_{pt}} \sum_{n=0}^{N-1} \frac{A_n}{1 + B_n a_{pt}} \\
&= \sum_{n=0}^{N-1} \frac{\tilde{A}_n}{a_{pt}} - \sum_{n=0}^{N-1} \frac{\tilde{A}_n B_n}{1 + B_n a_{pt}}
\end{aligned} \tag{4.8}$$

Where $\tilde{A}_n \equiv (\gamma_0/\beta_0)A_n$. In the partial fraction approximation we have additional constraints, namely in the limits of a_{pt}. When $a_{pt} \to 0 \Rightarrow \sum_{n=0}^{N-1} A_n = 1$; and when $a_{pt} \to \infty \Rightarrow \left(\tilde{A}_0 = \gamma_{N-1}/\beta_{N-1}; B_0 = 0\right)$.
Using Eq. (4.4), the residue function $Z(Q^2)$ obtains the form (with notation: $a_{pt} = a_{pt}(Q^2)$ and $a_{pt,0} = a_{pt}(Q_0^2)$):

$$\begin{aligned} Z(Q^2) &= \exp\left\{\int_{a_{pt,0}}^{a_{pt}} \left(\sum_{n=0}^{N-1} \frac{\tilde{A}_n}{x} - \sum_{n=0}^{N-1} \frac{\tilde{A}_n B_n}{1+B_n x}\right) dx\right\} \\ &= \prod_{n=0}^{N-1} \left(\frac{a_{pt}}{a_{pt,0}}\right)^{\tilde{A}_n} \left(\frac{1+B_n a_{pt}}{1+B_n a_{pt,0}}\right)^{-\tilde{A}_n} \\ &\simeq \left(\frac{a_{pt}}{a_{pt,0}}\right)^{\nu} \left(\frac{1+d_1 a_{pt}+d_2 a_{pt}^2+\ldots}{1+d_1 a_{pt,0}+d_2 a_{pt,0}^2+\ldots}\right) \\ &= c_v \sum_{n=0}^{N-1} d_n a_{pt}^{n+\nu} \end{aligned} \tag{4.9}$$

We note that: $\nu \equiv \sum_{n=0}^{N-1} \tilde{A}_n = (\gamma_0/\beta_0) \sum_{n=0}^{N-1} A_n = \gamma_0/\beta_0$. Also, we performed an expansion in the third line of Eq. (4.9), resulting in $d_1 \equiv -\sum_{n=0}^{N-1} \tilde{A}_n B_n$, $d_2 \equiv (1/2) \sum_{n=0}^{N-1} \tilde{A}_n B_n^2 (1+\tilde{A}_n)$, etc... .
And we have a factor that depends on initial condition at $Q^2 = Q_0^2$, that is: $c_v = \{a_{pt,0}^{\nu}(1 + d_1 a_{pt,0} + d_2 a_{pt,0}^2 + \ldots)\}^{-1}$

4.2 The Gluon Propagator Revised

4.2.1 Gluon Propagator (GP) by M. Frasca

Mapping the IR region by Massless Scalar Field

The main goal of his work is to analyze the infrared limit of quantum field theory. In the case of Yang-Mills theory, it is possible to make a map from solution of the IR Yang-Mills theory to a $\lambda\phi^4$ theory taking some restrictions into account (for more details we refer to Refs. [70, 71] , especially to Ref. [72]), namely we must choose the gauge boson A_μ^a with some components being zero and all others being equal, and $\lambda = Ng^2$, where g is the coupling constant.

The equivalence between Yang-Mills (QCD without quarks) and $\lambda\phi^4$ theories is exact at the classical level, but does not hold at the quantum level (due to quantum fluctuations). In the latter case, the author uses the functional integral form in the limit $\lambda \to \infty$.
Based on this model, the gluon propagator in the infrared limit (that is the two-point Green function) is given by [70, 71]

$$D_{gl}(t) \equiv G(t) = \theta(t) \left(\frac{2}{\lambda}\right)^{1/4} \text{sn}\left[\left(\frac{\lambda}{2}\right)^{1/4} t, i\right], \tag{4.10}$$

where

$$\text{sn}(u,i) = \frac{2\pi}{K(i)} \sum_{n=0}^{\infty} \frac{(-1)^n e^{-(n+1/2)\pi}}{1+e^{-(2n+1)\pi}} \sin\left[(2n+1)\frac{\pi u}{2K(i)}\right], \tag{4.11}$$

is the Jacobi sinoidal elliptical function and $K(i) \sim 1.3111028777$ is a constant.
There is another solution, $t \mapsto -t$, and it represents the backward propagating Green function (gluon propagator).
The solution (4.10) can be inserted in the expression for the scalar field

$$\begin{aligned} \phi(t) &= \sum_{n=0}^{\infty} a_n \int dt' G(t-t')(t-t')^n j(t') \\ &= \sum_{n=0}^{\infty} a_n \left(\frac{2}{\lambda}\right)^{\frac{n+2}{4}} I(t,\lambda) \end{aligned} \tag{4.12}$$

where

$$I(t,\lambda) = \int dt' \theta(t_1) \text{sn}(t_1, i) t_1^n j\left(t - \left(\frac{2}{\lambda}\right)^{1/4} t_1\right) \tag{4.13}$$

The important thing here is that the propagator can be expressed as an asymptotic series with respect to λ. In this sense, the Fourier transform of the gluon propagator is given by an expansion in λ, too

$$D_{gl}(\omega^2) \equiv G(\omega) = \sum_{n=0}^{\infty} \frac{B_n}{\omega^2 - \omega_n^2 + i\epsilon} \tag{4.14}$$

with the coefficient

$$B_n = (2n+1)\frac{\pi^2}{K^2(i)} \frac{(-1)^{n+1} e^{-(n+1/2)\pi}}{1+e^{-(2n+1)\pi}}, \tag{4.15}$$

and where the mass spectrum in the IR limit (where all the higher corrections are neglected, therefore we consider only the leading order term) is of the form

$$\omega_n = \left(n + \frac{1}{2}\right) \frac{\pi}{K(i)} \left(\frac{\lambda}{2}\right)^{1/4} \Lambda \tag{4.16}$$

with Λ is a constant.
In this approach, the gluon propagator in the IR limit is

$$D_{gl}(\omega) = \sum_{n=0}^{\infty}(2n+1)\frac{\pi^2}{K^2(i)}\frac{(-1)^{n+1}e^{-(n+1/2)\pi}}{1+e^{-(2n+1)\pi}}\frac{1}{\omega^2-\omega_n^2+i\epsilon} \tag{4.17}$$

where the mass spectrum ω_n is given by (4.16), with the replacement $\lambda \to Ng^2$ as was mentioned.
Due to the fact that the ghost field decouples in the IR, its propagator is that of a free particle

$$D_G(\omega, \mathbf{k}) = \frac{1}{|\mathbf{k}|^2-\omega^2-i\epsilon} \tag{4.18}$$

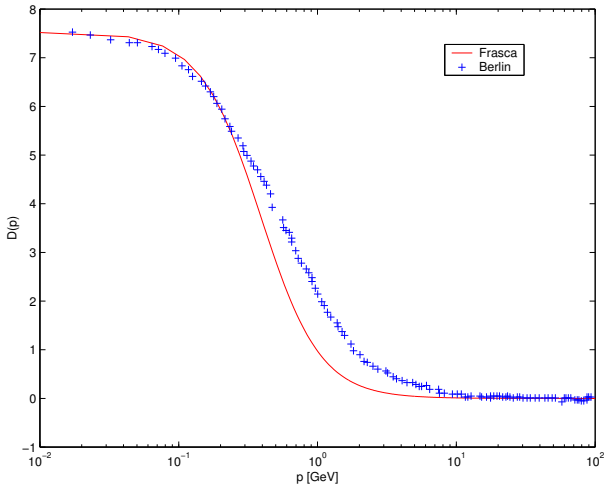

Figure 4.1: Comparison of the Yang-Mills Gluon propagator, between lattice simulation [75] and this method, taken from [70].

In Fig. (4.1) we see that this method agrees well with lattice [75] at very low energies and high energies, but in the intermediate region $(0.1 - 10$ GeV) there is some disagreement.

Källen-Lehmann Representation (K-L) to GP

In this case, the idea is to compare the K-L representation with the method presented in the previous section. Considering a theory with a mass gap, the propagator have a pole in $Q^2 = -m_0^2$. And their K-L representation takes the form [74]

$$D(Q^2) = \frac{Z_0}{Q^2+m_0^2-i\epsilon} + \int_{m_1^2}^{\infty} d\mu^2 \frac{\sigma(\mu^2)}{Q^2+\mu^2-i\epsilon} \tag{4.19}$$

with $m_0 < m_1$ and Z_0 a renormalization constant. In this form, we need to isolate the gluon mass (m_0) in the IR limit, that is, the spectral function must vanish there $\sigma(0) = 0$. This implies that the propagator is

$$D(Q^2 \to 0) = \frac{Z_0}{m_0^2} + \int_{m_1^2}^{\infty} d\mu^2 \frac{\sigma(\mu^2)}{\mu^2} = \text{constant} \tag{4.20}$$

And in the UV limit ($Q^2 \to \infty$) we deduce the well known condition:

$$Z_0 + \int_{m_1^2}^{\infty} d\mu^2 \sigma(\mu^2) = 1 \tag{4.21}$$

In the formalism based on the method of the previous section, we have the spectral function $\sigma(\mu^2) = \sum_n Z_n \delta(\mu^2 - m_n^2)$, and looking at Eq. (4.21) we have two possibilities:

1. Positivity condition for spectral representation implies that all Z_n's are positive.
2. With (4.21) we have the condition $\sum_n Z_n = 1$ and this implies that the Z_n's have alternating signs.

The conditions (4.20) and (4.21) show the agreement with the method of mapping the IR sector.

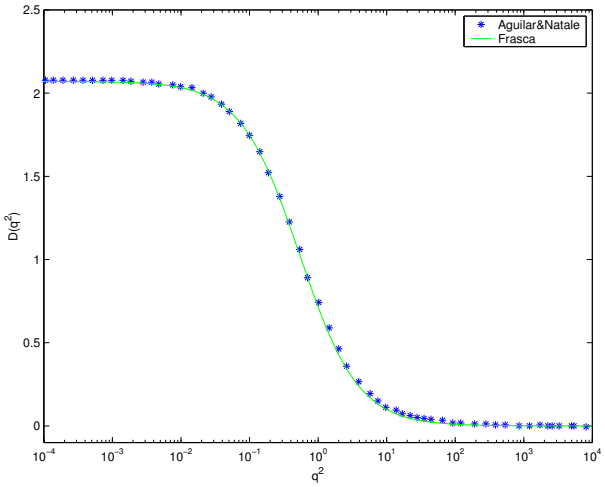

Figure 4.2: Comparison between DSE simulation and this method taken from [72]. The normalization of the curve of this method is adjusted so that it coincides with SDE result at $q^2 = 0$.

The comparison between DSE [73] and this model [70, 71] is depicted in Fig. (4.2), and the agreement is evident.

4.2.2 Running Gluon Mass and Lattice by Bicudo and Oliveira

The basis of this work is to consider three different scenarios [76] (IR and UV constant gluon mass and momentum-dependent gluon mass, see the subsections below) assuming the existence of a dynamically generated gluon mass as a function of the momentum [77]. They justified it in a frame beyond the perturbation theory where the mass appears by diffractive phenomena [78] and inclusive radiative decays of J/ψ and Υ [79].
The lattice calculations (as in the works by Bogolubsky et.al. [80]) are performed with the following bare lattice propagator inspired by the one-loop results [76]:

$$D(Q^2)_{latt.} = \frac{K}{Q^2}\left(\ln\frac{Q^2}{\Lambda^2}\right)^{-\gamma}, \tag{4.22}$$

where the renormalized propagator is $D(Q^2) = Z_R D(Q^2)_{latt.}$. The renormalization constant Z_R comes from the fit of the parameters K and Λ in (4.22). The simulation performed by the author is presented in Fig. 4.3 for the gluon propagator $D(Q^2)$ and in Fig. 4.4 for the gluon dressing function $Q^2D(Q^2)$, where they fix the renormalization constant at $\mu = 3$GeV.

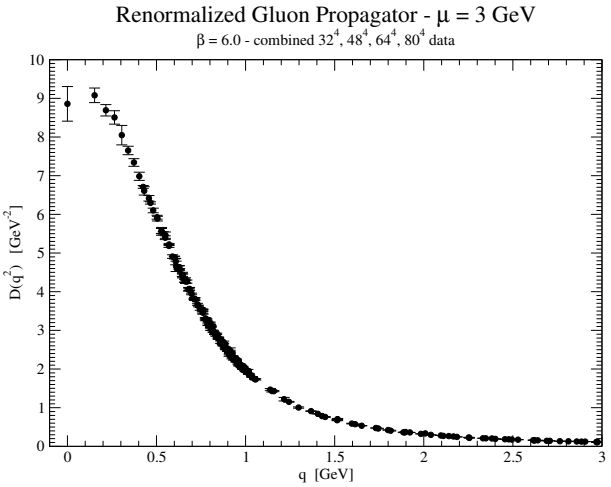

Figure 4.3: Lattice simulation for the gluon propagator $D(Q^2)$ taken from [76]

In this lattice calculus, the Gribov copies are not taken into account, because they do not change significantly the gluon propagator, i.e., these contributions are within the statistical errors.
In the following, we will present the two different scenarios , where one of them can be analyzed in the two limits of the momentum (IR and UV), given three different scenarios altogheter.

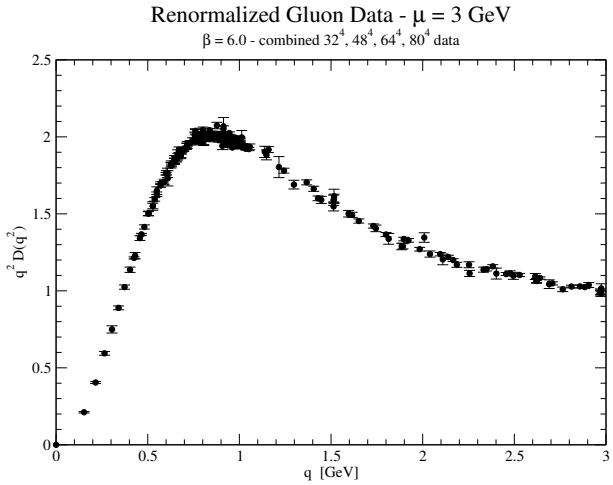

Figure 4.4: Lattice simulation for the gluon dressing function $Q^2D(Q^2)$ taken from [76]

Table 4.1: The fit value for different parameters found in [76]

	$D(0)$ included[MeV] ($Q_{min} = 0$)	$D(0)$ excluded[MeV] ($Q_{min} > 0$)
Q_{max}	~ 500	~ 500
Z	4.044(78)	4.49(10)
M	648(7)	723(11)

Constant Gluon Mass

In this first and more simple case, we take Eq. (4.3) with M and Z constant in certain momentum range where the approximation is valid ($Q^2_{min} \leq Q^2 \leq Q^2_{max}$). These can be fit with the lattice results for the two limiting momentum scales.
This gives a good agreement at low energies, but at high energies the approximation fails.

IR constant gluon mass

In this case they found two different values for the constant, depending on whether they take ($Q_{min} = 0$) or do not take ($Q_{min} > 0$) the zero momentum point into account. The different fits are given in Table 4.1, where both methods are feasible up to $Q \sim 500$MeV.

- UV gluon constant mass:
  Unfortunately in this case the gluon mass takes negative values (after a fitting

procedure): $M^2 < 0$, which is in contradiction with physical principles of QFT. Other work takes the ansatz [81, 82]:

$$D(Q^2) = \frac{Z}{Q^2 + M^2} \left\{ \frac{Q^2 M^2}{(Q^2 + M^2) \ln \sqrt{Q^2 + M^2}} \right\}^{\gamma} \tag{4.23}$$

Here, the mass takes a non-vanishing positive value, but in principle we want to have a zero gluon mass in the UV region and the only possibility to have such a scenario is with the mass that depends on the momentum region and this is presented in the next subsection.

Momentum-Dependent Gluon Mass

In order to have an agreement of the expression of the gluon propagator with the lattice date, a good approximation to the gluon dressing function and the mass in the two limits is given by

$$\begin{aligned} Z(Q^2) &= \frac{Z_0}{[A + \ln(Q^2 + m_0^2)]^{\gamma}}, \\ M^2(Q^2) &= \begin{cases} Q^2 & Q^2 \gg \Lambda_{QCD} \\ Q^2 \ln Q^2 & Q^2 \lesssim \Lambda_{QCD}. \end{cases} \end{aligned} \tag{4.24}$$

Here, $\gamma = 13/22$ is the anomalous gluon dimension and $m_0^2 \approx 1.6\text{GeV}^2$.
The form of the gluon effective mass in the low energy regime comes from the works of Cornwall [77].
Now, we present the other well known models in order to incorporate the aforementioned gluon mass. The usual perturbative QCD (pQCD) and the analytic methods (lattice and Dyson-Schwinger (DS) approach):

- $M^2(Q^2)$ pQCD inspired:
  A good approximation from the pQCD point of view is to translate the Landau pole to the origin. This is made by changing the effective coupling given in the gluon dressing function by

$$Z(Q^2) = z \left[\ln \left(1 + \frac{Q^2}{\Lambda^2} \right) \right]^{-\gamma} \tag{4.25}$$

  Hence the gluon propagator is

$$D(Q^2) = \frac{z}{Q^2} \left[\ln \left(1 + \frac{Q^2}{\Lambda^2} \right) \right]^{-\gamma} \tag{4.26}$$

Therefore, the gluon mass is defined by taking the lattice propagator

$$D(Q^2) = \frac{z}{Q^2 + M^2(Q^2)} \left[\ln\left(1 + \frac{Q^2}{\Lambda^2}\right) \right]^{-\gamma} \tag{4.27}$$

Unfortunately, here $Q_{min} = 3\text{GeV}$ in order to recover the perturbative behavior.

- $M^2(Q^2)$ from lattice and DS results:
  The dressing function is taken from the decoupling solution of the DS equations [83–87] which are solved numerically, and the best numerical fit of this solution gives the form

$$Z(Q^2) = \frac{z_0}{\ln^{\gamma}\left(\frac{Q^2 + r m_0^2}{\Lambda}\right)} \tag{4.28}$$

  And for the numerical fit of the gluon mass, we present two cases:

  – Aguilar & Papavassiliou: They make a naive extension of the perturbative dressing function toward the IR [84–87], keeping $Z(Q^2)$ always finite:

$$M^2(Q^2) = m^2(Q^2, m_0^2) \left[\frac{\ln\left(\frac{Q^2 + f(Q^2, m_0^2)}{\Lambda^2}\right)}{\ln\left(\frac{f(0, m_0^2)}{\Lambda^2}\right)} \right] \tag{4.29}$$

    where

$$f(x, m_0^2) = \rho_1 m_0^2 + \rho_2 m^2(x, m_0), \qquad m^2(x) = \frac{m_0^4}{x + m_0^2} \tag{4.30}$$

    Here $\rho_1 = 1/2; \rho_2 = 5/2$ and $M^2_{pert}(q^2)$ runs from $\sim 1.2\text{GeV}$ for $Q^2 = 0$ and down to zero for $\sqrt{Q^2} \sim 932\text{GeV}$.

  – Decoupling-type solution of the gluon-ghost DSE: Here the gluon mass was found as a decreasing function of Q^2, becoming massless in the UV region, and the explicit form is the following

$$M^2(Q^2) = \frac{m_0^2}{Q^2 + m_0^2} \tag{4.31}$$

    The fits can't distinguish between (4.29) and (4.31), finding $m_0 = 671(9)\text{MeV}$. Besides, these two functional forms have a good behavior in the range of $\sqrt{Q^2}$ from 0 to 4.2GeV.

4.2.3 Running coupling via the dressing functions by von Smekal and Lerche

In the Landau gauge, in the Wick-rotated formulation ($q^2 \mapsto -Q^2$, where q^2 is in Minkowski metric, and Q^2 in Euclidean), and in the theory with the UV cutoff Λ_{uv}, the gluon propagator has the form (4.2) with $Z(Q^2) \equiv Z_{\rm gl}^{(\Lambda_{uv})}(Q^2)$, and the ghost propagator is

$$D_G(Q) = -Z_{\rm gh}^{(\Lambda_{uv})}(Q^2)\frac{1}{Q^2}. \tag{4.32}$$

We introduced the superscript (Λ_{uv}) which indicates that the theory has the UV momentum cutoff Λ_{uv}.

The first and the second Kugo-Ojima (KO) [88] criterium for confinement can be expressed, respectively, as

$$\lim_{Q^2\to 0} Z_{\rm gl}^{(\Lambda_{uv})}(Q^2)/Q^2 \;<\; \infty \quad \text{(KO1)} \;, \tag{4.33a}$$

$$Z_{\rm gh}^{(\Lambda_{uv})}(0) \;=\; \infty \quad \text{(KO2)} \;. \tag{4.33b}$$

However, the first condition gets additionally restricted by the conclusion of Zwanziger [89] about the effects of proximity of the Gribov horizon $-\partial_\mu D^\mu(A) = 0$ in the Landau gauge formulation for the generating functional

$$\lim_{Q^2\to 0} Z_{\rm gl}^{(\Lambda_{uv})}(Q^2)/Q^2 = 0 \;. \tag{4.34}$$

The conditions (4.33b) and (4.34) imply that in the Dyson-Schwinger equation (DSE) for the gluon propagator, in the Landau gauge, the loop contribution with ghost propagators is the dominant one in the IR regime. In the work [90] it was demonstrated that in this approximation in the Landau gauge, the DSE's for the ghost and gluon propagators have a solution which has the scaling behavior in the IR regime

$$Z_{\rm gl}^{(\Lambda_{uv})}(Q^2) \sim (Q^2)^{2\kappa} \;, \quad Z_{\rm gh}^{(\Lambda_{uv})}(Q^2) \sim (Q^2)^{-\kappa} \;, \tag{4.35}$$

where $1/2 < \kappa < 1$. It is interesting that the Gribov approach [91] gives such a scaling solution as well, with $\kappa = 1$.

The renormalization group (RG) equation for the gluon and ghost propagator residues (dressing functions) has the form

$$\left(\Lambda_{uv}\frac{\partial}{\partial\Lambda_{uv}} + \beta(g)\frac{\partial}{\partial g} - 2\gamma_{\rm gl,gh}(g)\right) Z_{\rm gl,gh}^{(\Lambda_{uv})}(Q^2) = 0 \;, \tag{4.36}$$

where Λ_{uv} is the UV cutoff of the theory (renormalization scale), and $\gamma_{\rm gl}$ and $\gamma_{\rm gh}$ are the respective anomalous dimensions, and $g = g(\Lambda_{uv})$. The solution is (where we replace the UV cutoff Λ_{uv} by the usual notation μ, the UV renormalization scale of the theory)

$$Z_{\rm gl}^{(\mu)}(Q^2) = \exp\left\{-2\int_{g(\mu)}^{g(Q)} d\bar{g}\frac{\gamma_{\rm gl}(\bar{g})}{\beta(\bar{g})}\right\} \equiv \mathcal{Z}_3(Q,\mu)\ , \tag{4.37a}$$

$$Z_{\rm gh}^{(\mu)}(Q^2) = \exp\left\{-2\int_{g(\mu)}^{g(Q)} d\bar{g}\frac{\gamma_{\rm gh}(\bar{g})}{\beta(\bar{g})}\right\} \equiv \widetilde{\mathcal{Z}}_3(Q,\mu)\ , \tag{4.37b}$$

The usual multiplicative normalization constants are $Z_3(\mu) = \mathcal{Z}_3(\mu,\Lambda_{uv})$ and $\widetilde{Z}_3(\mu) = \widetilde{\mathcal{Z}}_3(\mu,\Lambda_{uv})$. In the exponentials of the expressions (4.37), the integration in the IR regime is not well known. Therefore, in Ref. [90], the integral in the regime $\bar{g} = g(K)$ with $Q < K < \Lambda_{ir}$ ($\Lambda_{ir} = \Lambda_{QCD} \sim 1$ GeV) is parametrized in power series of (Q^2/Λ_{ir}^2)

$$Z_{\rm gl}^{(\mu)}(Q^2) = \exp\left\{-2\int_{g(\mu)}^{g(\Lambda_{ir})} d\bar{g}\frac{\gamma_{\rm gl}(\bar{g})}{\beta(\bar{g})}\right\}\left[e_0\left(\frac{Q^2}{\Lambda_{ir}^2}\right)^{\epsilon_0} + \cdots\right]\ , \tag{4.38a}$$

$$Z_{\rm gh}^{(\mu)}(Q^2) = \exp\left\{-2\int_{g(\mu)}^{g(\Lambda_{ir})} d\bar{g}\frac{\gamma_{\rm gh}(\bar{g})}{\beta(\bar{g})}\right\}\left[d_0\left(\frac{Q^2}{\Lambda_{ir}^2}\right)^{\delta_0} + \cdots\right]\ , \tag{4.38b}$$

For the running coupling $a(Q^2) = g(Q)^2/(4\pi^2)$ we have in general

$$\frac{a(Q^2)}{a(\Lambda_{ir}^2)} = Z_g^{(\Lambda_{ir})}(Q^2)^{-2} = \frac{Z_{\rm gl}^{(\Lambda_{ir})}(Q^2)Z_{\rm gh}^{(\Lambda_{ir})}(Q^2)^2}{\widetilde{Z}_1^{(\Lambda_{ir})}(Q^2)^2}\ , \tag{4.39}$$

where $\widetilde{Z}_1^{(\Lambda_{ir})}(Q^2) \equiv \widetilde{\mathcal{Z}}_1(Q,\Lambda_{ir})$ is the gluon-ghost vertex renormalization parameter. This parameter is in the Landau gauge equal to one, at all energies, i.e., nonrenormalization of the gluon-ghost vertex takes place in the Landau gauge to all orders in perturbation theory, Refs. [90, 92].

A central assumption in this approach is that in nonperturbative effects of the IR regime do not change this conclusion, i.e., $\widetilde{Z}_1^{\Lambda_{ir}}(Q^2) = 1$ remains unchanged at low $|Q^2|$. Therefore,

$$\frac{a(Q^2)}{a(\mu^2)} = Z_{\rm gl}^{(\mu)}(Q^2)Z_{\rm gh}^{(\mu)}(Q^2)^2\ , \tag{4.40}$$

where we replaced Λ_{ir} by a general UV renormalization scale μ. The DSE's in the Landau gauge, in the mentioned ghost dominance approximation, and under the condition that the ghost-ghost-gluon vertex is of the tree-level form in the symmetric

configuration [$A_\mu(Q^2;Q^2,Q^2) = iQ_\mu$, nonrenormalization of the vertex, [92]], give as a solution the gluon and ghost residue functions in the IR regime (4.38) with

$$\delta_0 = -\kappa, \quad \epsilon_0 = 2\kappa \ , \quad 1/2 < \kappa < 1 \ . \tag{4.41}$$

This, in conjuntion with the relations (4.38), implies the relations (4.35). The relations (4.35) imply in Eq. (4.40) that the running coupling freezes in the IR

$$\lim_{Q\to 0} a(Q^2) = a_0 < \infty \ , \tag{4.42}$$

where $a_0 \neq 0$.

If, on the other hand, the horizon condition (4.34) were not fulfilled, but rather the more general confinement condition (4.33a) (finite gluon propagator in the IR, in the Landau gauge), then DSE's satisfying such conditions also exist [85] and give in the IR regime the behavior

$$Z_{\rm gl}^{(\Lambda_{uv})}(Q^2) \sim (Q^2)^1 \ , \quad Z_{\rm gh}^{(\Lambda_{uv})}(Q^2) \sim (Q^2)^0 \ . \tag{4.43}$$

This is a so called decoupling behavior, and it gives, according to the relation (4.40): $a(Q^2) \to 0$ when $Q^2 \to 0$.

4.2.4 Gauge Invariant Truncation Scheme By Aguilar and Papavassiliou

This approach is based on pinch technique and the correspondence with background field method (BFM), where the DSEs are derived by an expansion about the free-field vacuum.
The (fundamental) problem that arise from the DSE is the choice of a self-consistent truncation scheme [85] as a consequence of the aforementioned expansion. In this sense, the authors of Ref. [85] want to show that the application of a novel gauge-truncation scheme to DSE leads, in Landau gauge(LG), to an infrared finite gluon propagator and a divergent ghost propagator, in qualitative and quantitative (approximately) agreement with recent lattice data of Refs. [93, 94].

In this scheme the new DS series are [95] (with the notation: $D(Q^2) \equiv \Delta(Q^2) = Z_{gl}(Q^2)/Q^2$ for the gluon propagator and $D_G(Q^2)$ for the ghost propagator)

$$\begin{aligned}
\Delta^{-1}(Q^2)P_{\mu\nu}(Q) &= \frac{Q^2 P_{\mu\nu}(Q) + i\sum_{i=1}^4 (a_i)_{\mu\nu}}{[1+G(Q^2)]^2}, \\
iD_G^{-1}(P^2) &= P^2 + i\lambda \int_k \Gamma^\mu \Delta_{\mu\nu}(K)\Gamma^\nu(P,k)D_G(P+K), \\
i\Lambda_{\mu\nu}(Q) &= \lambda \int_K H^{(0)}_{\mu\rho} D_G(K+Q)\Delta^{\rho\sigma}(K)H_{\sigma\nu}(K,Q),
\end{aligned} \tag{4.44}$$

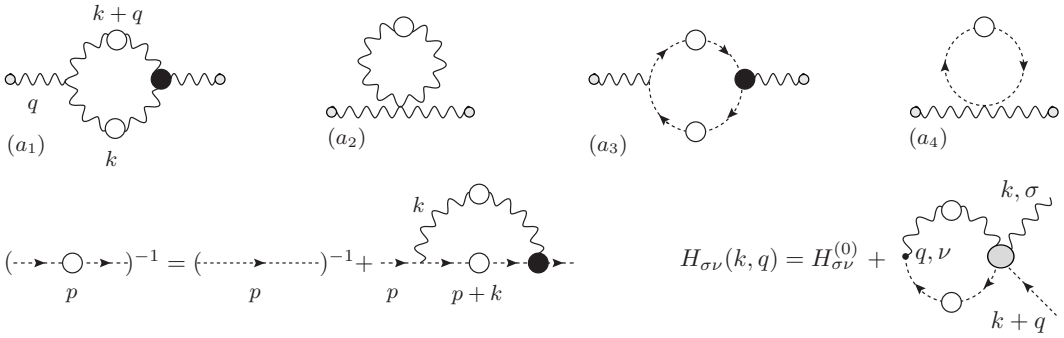

Figure 4.5: The new DSEs for the gluon-ghost system.

where $P_{\mu\nu} = g_{\mu\nu} - \frac{Q_\mu Q_\nu}{Q^2}$ is the transverse projector, $\lambda = g^2 C_A$, $G(Q^2)$ is the $g_{\mu\nu}$ component of the auxiliary two point function $\Lambda_{\mu\nu}(Q)$. The function $H_{\sigma\nu}$ appears as a consequence of the Slavnov-Taylor identity (STI) at all orders that is respected by the standard three-gluon vertex, and is related to the full gluon-ghost vertex by $Q^\sigma H_{\sigma\nu}(P,R,Q) = -i\Gamma_\nu(P,Q,R)$.
In order to satisfy the Ward identities, there appears an explicit condition upon a_i's (these coefficients appear when we consider the gluon propagator to first order as is shown in Fig. 4.5), i.e., a presence of massless pole term $1/Q^2$.
Longitudinally bound-state poles are known to be instrumental for obtaining $\Delta^{-1}(0) \neq 0$.
With this, the authors of Ref. [85] find integral equations which are solved numerically. In the solution, the renormalization constants are fixed in the usual way

$$\Delta^{-1}(\mu^2)\big|_{\mu^2\sim M_z^2} = \mu^2, \qquad D_G^{-1}(\mu^2)\big|_{\mu^2\sim M_z^2} = \mu^2, \qquad G(\mu^2)\big|_{\mu^2\sim M_z^2} = 0. \tag{4.45}$$

They found an IR behavior of the gluon propagator given by

$$\Delta^{-1}(0) = \frac{\lambda(T_g + T_c)}{[1+G(0)]^2}, \tag{4.46}$$

where

$$\begin{aligned} T_g &= \frac{15}{4}\int_k \Delta(k) - \frac{3}{2}\int_k k^2\Delta^2(k), \\ T_c &= -2\int_k D_G(k) + \int_k k^2 D_G^2(k). \end{aligned} \tag{4.47}$$

We can verify the pQCD behavior of this limit. We have the general perturbative

gluon propagator:

$$\Delta^{-1}_{pert}(Q^2) = Q^2 + i\Pi(Q^2) = Q^2 \sum_{m=0}^{\infty} \tilde{\delta}_m \ln^m(Q^2/\mu^2)\alpha_s^m \tag{4.48}$$

$$\Rightarrow \Delta_{pert}(Q^2) = (Q^2)^{-1} \sum_{n=0}^{\infty} \delta_n \ln^n(Q^2/\mu^2)\alpha_s^n$$

Here we have $\int_k \Delta(k) \sim \int_k \frac{\ln^n k}{k^2}$ for $n = 1, 2, \ldots$ (the procedure for $(D_G)_{pert}(k)$ is the same). Therefore, the pQCD gluon propagator in the IR has the well known limit

$$\Delta^{-1}_{pert}(0) = 0 \tag{4.49}$$

However, non-perturbatively $\Delta^{-1}(0)$ does not have to vanish, provided that the quadratically divergent integrals defining it can be properly regulated and made finite, without introducing counterterms of the form $m_0^2(\Lambda^2_{UV})A^2_\mu$, which are forbidden by the local gauge invariance of the fundamental QCD Lagrangian. Motivated by these arguments, the T_g constant is regularized only where pQCD does not hold, in the form

$$16\pi^2 T_g^{reg} = \frac{15}{4}\int_0^s dy y[\Delta(y) - \Delta_{pert}(y)] - \frac{3}{2}\int_0^s dy y^2[\Delta^2(y) - \Delta^2_{pert}(y)], \tag{4.50}$$

and analogously for T_c.

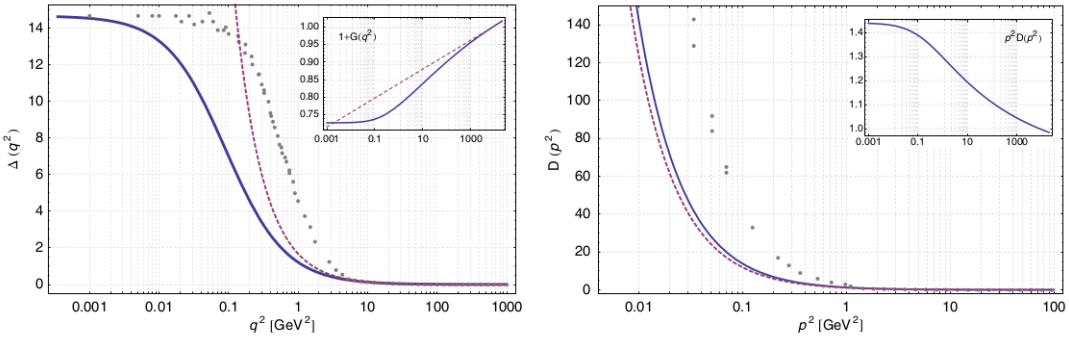

Figure 4.6: Left Panel: The Gluon propagators obtained from the solution of the DSE system(continuous line) compared to lattice [94]; the dashed line is the perturbative behavior. Right Panel: The ghost propagators from DSE (continuous line), the one-loop result (dashed line), and the corresponding lattice data [94] .

The procedure in order to fix the s variable is the following [85]: (i) Choose a boundary condition: $\Delta(0) = C > 0$; (ii) Obtain with the aforementioned assumption a regularized gluon propagator: $\Delta^{-1}_{reg}(0)$; (iii) Check that $\Delta^{-1}_{reg}(0) = C^{-1}$ is satisfied;

if it is not, follow with the next step: (iv) Choose a new C and repeat the procedure. Of course, there always exists the possibility to fix s and see what is the value for $\Delta(0)$.
Results: $C = 14.7\text{GeV}^{-2} \Rightarrow s \approx 10\text{GeV}^2$ (this is the preferred value for C from lattice simulations at the origin, see Left Panel in Fig. 4.6).
We note that if C increases, s decreases (for example, with $C = 50\text{GeV}^{-2} \Rightarrow s \approx 1\text{GeV}^2$).
From the fitting it was deduced:

$$\Delta^{-1}(Q^2) = a + b(Q^2)^{c-1} \Rightarrow \left\{ \begin{array}{cccc} & a & b & c \\ Lattice & 0.07 & 0.15 & 2.54 \\ DSE & 0.07 & 0.77 & 2.01 \end{array} \right. \tag{4.51}$$

This approach satisfies the Kugo-Ojima confinement criterium [88] in the form (that are essentially (4.33a) and (4.33b) without the effects of Gribov copies as in (4.34)):

- The non-perturbative gluon propagator being finite in the IR, is automatically less singular than a single pole (this criteria was checked above).
- The non-perturbative ghost propagator should be more singular in the IR than a simple pole.

In order to check the second criterium for DSE, we must to have $\gamma > 0$ in $P^2 D_G(P^2) = c_1 (P^2)^{-\gamma}$ and the authors of Ref. [85] found from the fit (see the Right Panel in Fig. 4.6) the value $\gamma = 0.02$ within the range $P^2 \leq 10\text{GeV}^2$. Therefore, this approach satisfied the second criterium, too, although at the borderline of balidity.
It is interesting that there is another better fit, that is

$$P^2 D_G(P^2) = \kappa_1 - \kappa_2 \ln(P^2 + \kappa_3) \tag{4.52}$$

where $\kappa_1 = 1.3$, $\kappa_2 = 0.05$ and $\kappa_3 = 0.05$, and this does not fulfill the KO criterium (4.33b).

4.3 Calculus with Variuos Dispersion Relations in FAPT

Now, we want to analyze the analyticity of the Gluon propagator in two different approaches, namely the subtracted and unsubtracted dispersion relation.
The subtracted concept is based on the idea of removing possible non-analytic contributions (singularities) to the gluon propagator.
It is interesting to evaluate both methods for the gluon propagator $D(Q^2)$, and for its dressing function $Z(Q^2) \equiv Q^2 D(Q^2)$.

4.3.1 Unsubtracted Dispersion Relation

For the first case $D(Q^2)$ we have the imaginary part (using Eq. (4.7)) given by:

$$\begin{aligned}\rho_D(\sigma) \equiv \mathrm{Im}D(-\sigma - i\epsilon) &= -c_v \mathrm{P}\left[\frac{1}{\sigma}\right] \mathrm{Im}\left\{\sum_{n=0}^{N-1} d_n a_{pt}^{n+\nu}(-\sigma - i\epsilon)\right\} + \pi c_v \delta(\sigma) \times \\ &\quad \mathrm{Re}\left\{\sum_{n=0}^{N-1} d_n a_{pt}^{n+\nu}(-\sigma - i\epsilon)\right\} \\ &= -c_v \frac{1}{\sigma}\sum_{n=0}^{N-1} d_n \rho_{n+\nu}^{(pt)}(\sigma) + c_v \pi\delta(\sigma)\sum_{n=0}^{N-1} d_n r_{n+\nu}^{(pt)}(\sigma). \quad (4.53)\end{aligned}$$

Here, by definition, the discontinuity function in terms of the perturbative coupling is $\rho_{n+\nu}^{(pt)}(\sigma) = \mathrm{Im}\left\{a_{pt}(-\sigma - i\epsilon)\right\}$ and $r_{n+\nu}^{(pt)}(\sigma) = \mathrm{Re}\left\{a_{pt}^{n+\nu}(-\sigma - i\epsilon)\right\}$.
With this, the analytic gluon propagator is

$$\begin{aligned}D^{(an.)}(Q^2) &= \frac{1}{\pi}\int_0^\infty \frac{d\sigma \rho_D(\sigma)}{\sigma + Q^2} \\ &= -c_v \frac{1}{\pi}\sum_{n=0}^{N-1} d_n \int_0^\infty d\sigma \frac{1}{\sigma}\frac{\rho_{n+\nu}^{(pt)}(\sigma)}{\sigma + Q^2} + \Delta_\delta(Q^2) \\ &= c_v \frac{1}{Q^2}\sum_{n=0}^{N-1} d_n \frac{1}{\pi}\int_0^\infty \frac{d\sigma \rho_{n+\nu}^{(pt)}(\sigma)}{\sigma + Q^2} - c_v \frac{1}{Q^2}\sum_{n=0}^{N-1} d_n \frac{1}{\pi}\int_0^\infty \frac{d\sigma \rho_{n+\nu}^{(pt)}(\sigma)}{\sigma} + \Delta_\delta(Q^2) \\ &= \frac{1}{Q^2} c_v \sum_{n=0}^{N-1} d_n \left(\mathcal{A}_{n+\nu}(Q^2) - \mathcal{A}_{n+\nu}(0)\right) + \Delta_\delta(Q^2) \quad (4.54)\end{aligned}$$

In the last line we used the dispersion relations for the analytic coupling $\mathcal{A}_{n+\nu}$ given by the well known Frectional Analytic Perturbation Theory (FAPT). And we note that $\Delta_\delta(Q^2) = 0$ (that corresponds to the second term in the r.h.s of (4.53) integrated as in (4.54)).
On the other hand, if we apply the (unsubtracted) dispersion relation to $Z(Q^2) = Q^2 D(Q^2)$ (instead of $D(Q^2)$), we have (following the same procedure as before):

$$\begin{aligned}Z^{(an.)}(Q^2) &= \frac{1}{\pi}\int_0^\infty \frac{d\sigma \rho_Z(\sigma)}{\sigma + Q^2} \\ &= c_v \frac{1}{\pi}\sum_{n=0}^{N-1} d_n \int_0^\infty \frac{d\sigma \rho_{n+\nu}^{(pt)}(\sigma)}{\sigma + Q^2} \\ &= c_v \sum_{n=0}^{N-1} d_n \mathcal{A}_{n+\nu}(Q^2) \quad (4.55)\end{aligned}$$

In this case the gluon propagator takes the form (the tilde superscript is only to differentiate from the first case):

$$\tilde{D}^{(an.)}(Q^2) \equiv \frac{1}{Q^2} Z^{(an.)}(Q^2) = \frac{1}{Q^2} c_v \sum_{n=0}^{N-1} d_n \mathcal{A}_{n+\nu}(Q^2). \tag{4.56}$$

4.3.2 Subtracted Dispersion Relation

Here we follow the analogous way as in the previous subsection, but now we subtract by hand a possible non-analytic term in the propagator at $Q^2 = \kappa^2$, we have for the first case:

$$\begin{aligned}
D(Q^2) &= D(\kappa^2) + \frac{\kappa^2 - Q^2}{\pi} \int_0^\infty \frac{d\sigma \rho_D(\sigma)}{(\sigma + \kappa^2)(\sigma + Q^2)} \\
&= D(\kappa^2) - c_v \frac{\kappa^2 - Q^2}{\pi} \sum_{n=0}^{N-1} d_n \int_0^\infty d\sigma \frac{1}{\sigma} \frac{\rho^{(pt)}_{n+\nu}(\sigma)}{(\sigma + \kappa^2)(\sigma + Q^2)} \\
&= D(\kappa^2) + c_v \sum_{n=0}^{N-1} d_n \left\{ \frac{1}{Q^2} \frac{1}{\pi} \int_0^\infty d\sigma \frac{\rho^{(pt)}_{n+\nu}(\sigma)}{\sigma + Q^2} \right. \\
&\quad \left. - \frac{\kappa^2 - Q^2}{Q^2 \kappa^2} \frac{1}{\pi} \int_0^\infty d\sigma \frac{\rho^{(pt)}_{n+\nu}(\sigma)}{\sigma} - \frac{1}{\kappa^2} \frac{1}{\pi} \int_0^\infty d\sigma \frac{\rho^{(pt)}_{n+\nu}(\sigma)}{\sigma + \kappa^2} \right\} \\
&= D(\kappa^2) + \frac{1}{Q^2} c_v \sum_{n=0}^{N-1} d_n \left(\mathcal{A}_{n+\nu}(Q^2) - \mathcal{A}_{n+\nu}(0) \right) \\
&\quad + \frac{1}{\kappa^2} c_v \sum_{n=0}^{N-1} d_n \left(\mathcal{A}_{n+\nu}(0) - \mathcal{A}_{n+\nu}(\kappa^2) \right).
\end{aligned} \tag{4.57}$$

And for the second case (subtracted dispersion relation applied to $Z(Q^2) = Q^2 D(Q^2)$):

$$\begin{aligned}
Z^{(an.)}(Q^2) &= Z^{(an.)}(\kappa^2) + (Q^2 - \kappa^2) \frac{1}{\pi} \int_0^\infty d\sigma \frac{\rho_Z(\sigma)}{(\sigma + \kappa^2)(\sigma + Q^2)} \\
&= Z^{(an.)}(\kappa^2) - (Q^2 - \kappa^2) c_v \sum_{n=0}^{N-1} d_n \frac{1}{\pi} \int_0^\infty d\sigma \frac{\rho^{(pt)}_{n+\nu}(\sigma)}{(\sigma + \kappa^2)(\sigma + Q^2)}
\end{aligned} \tag{4.58}$$

At this stage, it is easy to relate with the FAPT analytic coupling if we note that

$$\mathcal{A}_{n+\nu}(Q^2) - \mathcal{A}_{n+\nu}(\kappa^2) = -(Q^2 - \kappa^2) \frac{1}{\pi} \int_0^\infty \frac{d\sigma \rho^{pt}_{n+\nu}(\sigma)}{(\sigma + Q^2)(\sigma + \kappa^2)}. \tag{4.59}$$

So, we have finally

$$Z^{(an.)}(Q^2) \;=\; Z^{(an.)}(\kappa^2) + c_v \sum_{n=0}^{N-1} d_n (\mathcal{A}_{n+\nu}(Q^2) - \mathcal{A}_{n+\nu}(\kappa^2)). \tag{4.60}$$

So the gluon propagator takes the form (the tilde superscript is only to differentiate from the first case):

$$\tilde{D}^{(an.)}(Q^2) \equiv \frac{1}{Q^2} Z^{(an.)}(Q^2) = \frac{\kappa^2}{Q^2} \tilde{D}^{(an.)}(\kappa^2) + \frac{1}{Q^2} c_v \sum_{n=0}^{N-1} d_n (\mathcal{A}_{n+\nu}(Q^2) - \mathcal{A}_{n+\nu}(\kappa^2)) \tag{4.61}$$

It is interesting to note that, if we take the limit $\kappa^2 = 0$ we recover Eq. (4.54).

4.3.3 Non-Zero Dynamic Mass of Gluon

Following the same steps as in the previous subsection, we can find an explicit expression to the massive gluon propagator. Starting from Eq. (4.3) in the dispersion relation we obtain:

$$D^{(an.)}_{MG}(Q^2) = c_v \sum_{n=0}^{N-1} d_n \frac{1}{Q^2 + M^2} \left(\mathcal{A}_{n+\nu}(Q^2) - \frac{1}{\pi} \mathrm{P} \left[\int_0^\infty \frac{d\sigma \rho^{(pt)}_{n+\nu}(\sigma)}{\sigma - M^2} \right] + r^{(pt)}_{n+\nu}(M^2) \right) \tag{4.62}$$

We note that, when the gluon mass vanishes, we recover the unsubtracted gluon propagator (4.54). Another interesting point here is the limit when the mass parameter tends to zero (note that we take the propagator in the form (4.4) and with the final expression (4.7), so we are neglecting the mass term effects in the Callan-Symanzik ecuation) we find

$$D^{(an.)}_{MG}(Q^2) \;\approx\; c_v \sum_{n=0}^{N-1} d_n \frac{1}{Q^2 + M^2} \left(\mathcal{A}_{n+\nu}(Q^2) - \mathcal{A}_{n+\nu}(-M^2) \right) \tag{4.63}$$

$$\;\approx\; c_v \sum_{n=0}^{N-1} d_n \frac{1}{Q^2 + M^2} \left(\mathcal{A}_{n+\nu}(Q^2) - \mathcal{A}_{n+\nu}(0) \right). \tag{4.64}$$

On the other hand, when we perform the analytization of dressing funtion $Z(Q^2)$, instead of $D(Q^2)$, we obtain

$$\tilde{D}^{(an.)}_{MG}(Q^2) \approx c_v \sum_{n=0}^{N-1} d_n \frac{1}{Q^2 + M^2} \mathcal{A}_{n+\nu}(Q^2). \tag{4.65}$$

4.3.4 Numerical Results

Before presenting our results, we note that our results should be compared with the lattice data for the unquenched case ($N_f = 3$), Ref. [97], in the available interval of $Q \equiv \sqrt{Q^2}$: 0.1 GeV $< Q \lesssim 10$ GeV. This is so because the (F)APT formalism requires $N_f \geq 3$. Namely, the thresholds in the (F)APT formalism are understood to be implemented in general at $Q^2 = m_q^2$ (m_q is the corresponding quark mass) in the underlying pQCD coupling $a(Q^2)$, and the latter coupling has Landau singularities at energies $0 < Q^2 \lesssim m_s^2$ (m_s is the strange quark mass) and even at $Q^2 > m_s^2$.

We work with the gluon propagator (4.3), which has FAPT-holomorphic dressing function (4.56) and a dynamical gluon mass M, Eq. (4.65). The free parameters are c_v and M. We are choosing certain two points of the (low-Q) lattice data and adjust the free parameters (c_v and M) so that our curve goes through these two points; the two chosen points are also varied, so as to obtain (visually) the best curve. This approach is applied in the analytic (FAPT) and in the pQCD case.

In this context, we mention that a variant of APT was applied to the dressing function in Ref. [96], but in a more naive manner since the FAPT approach was not known at the time; and the dynamical gluon mass effect was not included.

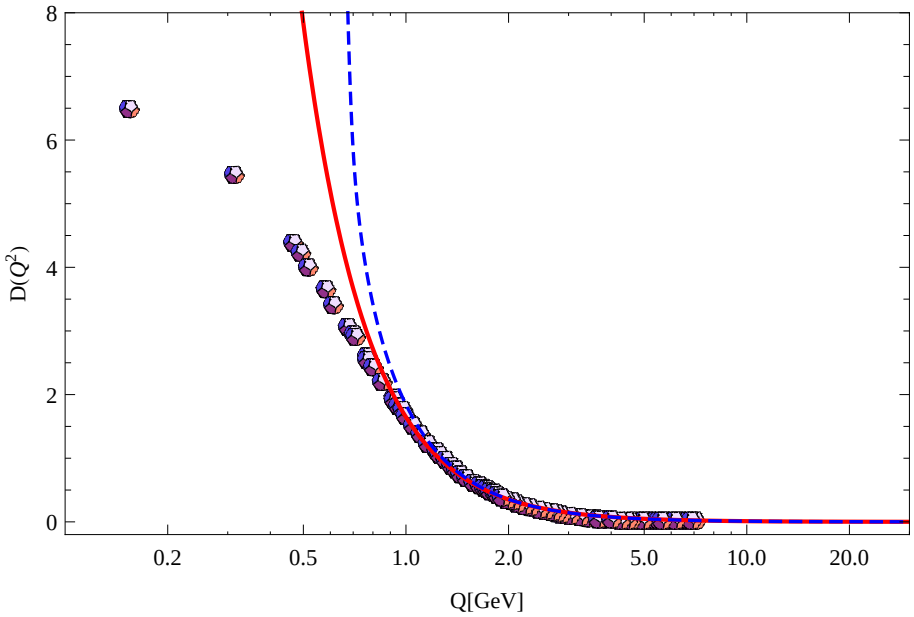

Figure 4.7: Analytic gluon propagator (4.3) with the dynamical effective gluon mass parameter $M = 0$ and $c_v = 5.10$ (continuous line), in comparison with unquenched lattice data taken from Ref. [97], where $N_f = 2 + 1$. Further, the (two-loop) pQCD result is presented as well, with $c_v = 4.55$ (dashed line).

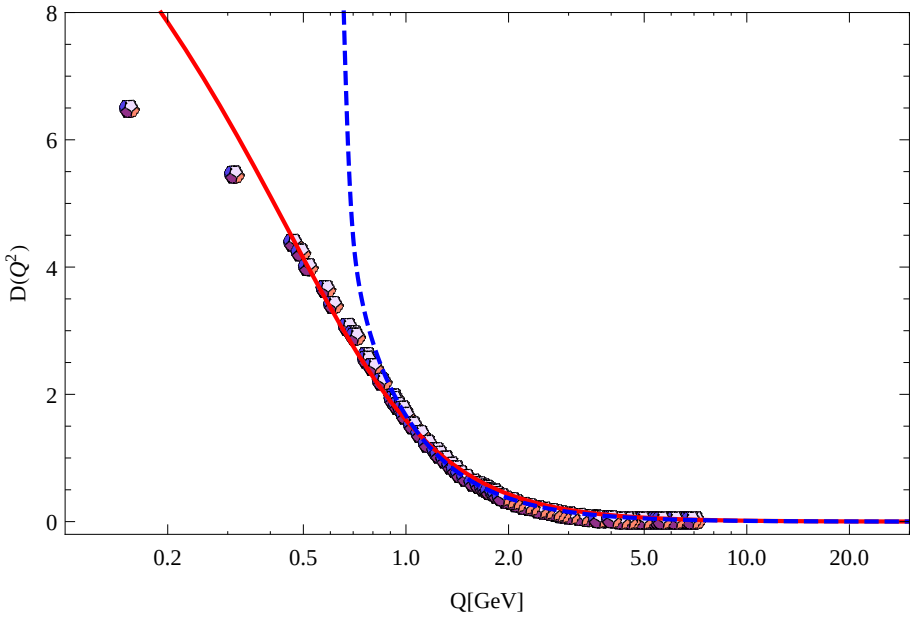

Figure 4.8: The same as in Fig. 4.7, but now the dynamical effective gluon mass parameter M is nonzero: the analytic propagator (4.3) (continuous line) has $M^2 = 0.382$ GeV^2 and $c_v = 6.81$. The pQCD result (dashed line), i.e., Eq. (4.65) with (4.7), has $M^2 = 0.211$ GeV^2 and $c_v = 4.98$.

In Fig. 4.7, we compare with the lattice data at low positive Q^2 ($Q \equiv \sqrt{Q^2}$) when fixing $M = 0$ in $D(Q^2)$ of Eq. (4.3), while the other parameter c_v is fixed by a lattice point. We include also a (two-loop) pQCD result, where in $a(Q^2)$ we use the same Lambert scale: $\Lambda_{\rm L.}(N_f = 3) = 0.581$ GeV.

In Fig. 4.8 both parameters, M and c_v, are varied in Eq. (4.3) so as to get the best possible agreement with the lattice data. For additional comparisons, a representative pQCD curve with $M \neq 0$ [i.e., Eq. (4.65) with (4.7)] is included, where we use the aforementioned Lambert scale.

In Fig. 4.7 we see that the analytization alone (and $M = 0$) gives us results which are good down to approximately 0.8 GeV; this is an improvement with respect to pQCD. But we wanted to go beyond and see what is the effect of including a (small) dynamical effective mass M of gluon, Eqs. (4.65) and (4.3). We find that the best mass parameter is $M^2 \approx 0.382$ GeV^2, see Fig. 4.8. It turns out that this value is consistent with the values of M obtained in Refs. [76].[1]

We see from Fig. 4.8 that the massive FAPT-analytic version is applicable for mo-

[1]In Refs. [76], $M(Q^2)$ and $Z(Q^2)$ were considered as Q^2-dependent functions with specific Ansätze, and the resulting propagator was fitted to the lattice results.

menta down to $Q \approx 0.4$ GeV ($Q^2 \approx 0.15$ GeV^2), but not below that. This is consistent with the conclusions about the applicability of the APT approach in Bjorken Polarized Sum Rule at low Q, Ref. [98], where the authors included other nonperturbative effects via higher-twist terms.

We note that in our approach, when we want to reproduce lattice results for lower momenta Q, the mass parameter M is getting bigger and is accompanied with a worse behavior at higher Q values. Therefore, we intend to improve this approach in the future, by using a Q^2-dependent dynamical mass $M(Q^2)$ of the gluon. However, the applicability of (F)APT will probably restrict from below the values of Q: $Q > Q_{\rm min}$ (> 0).

4.3.5 Summary

In this work, we evaluated the gluon propagator in the Landau gauge at low spacelike momenta Q^2. We used the two-loop solution of the Callan-Symanzik equation for the dressing function $Z(Q^2)$. The nonperturbative effects were incorporated in the form of the analytization procedure $a^\nu(Q^2) \mapsto \mathcal{A}_\nu(Q^2)$ for the (noninteger) powers of the QCD coupling $a(Q^2)$, within Fractional Analytic Perturbation Theory (FAPT) with $N_f = 3$; and by incorporation of a constant dynamical effective gluon mass M in the propagator. The obtained expression Eq. (4.3) has two free parameters: the normalization constant c_v and the dynamical gluon mass M. We compared the obtained results with the unquenched lattice results ($N_f = 3$) at low positive Q^2. In comparison with pQCD results, the analytization clearly improved the behavior of the propagator at low Q. The additional introduction of the dynamical effective gluon mass further improved the low-Q behavior. We used the FAPT with $N_f = 3$, because in FAPT it is apparently not possible to define unambiguously the theory for $N_f < 3$.

The main results can be summarized as follows:

1. We performed an analytization procedure (numerical FAPT) for the dressing function of gluon propagator in the Landau gauge. The dressing function was obtained from the two-loop Callan-Symanzik equation, and this (pQCD) procedure introduces one free parameter c_v which is an overall normalization constant.

2. In addition, we introduced a (constant) dynamical effective gluon mass M in the propagator, as suggested by various DSE studies of gluon propagator in the Landau gauge.

3. We compared the obtained results with the unquenched lattice data of the propagator, by varying the free parameters c_v and M.

4. In the nonmassive ($M = 0$) case, the analytic gluon propagator is in agreement with the unquenched lattice data down to $Q^2 \approx 0.6$ GeV^2 ($Q \equiv \sqrt{Q^2} \approx 0.8$ GeV), while the massive ($M > 0$) analytic gluon propagator agrees with the lattice data down to $Q^2 \approx 0.15$ GeV^2 ($Q \approx 0.4$ GeV).

5. The values that we found for our fit are $c_v = 5.10$ for the nonmassive case; and $c_v = 6.81$ and $M^2 = 0.382$ GeV^2 ($M \approx 0.62$ GeV) for the massive case, where this value of the dynamical effective gluon mass M is similar to the values found in the literature.

We intend to continue this work in various directions: perform the analytization procedure within other QCD models such as the two-delta analytic QCD model of Ref. [54] and the analytic QCD models with effective mass in the coupling (cf. Refs. [99–104]); allow Q^2-dependence in the dynamical effective gluon mass M; and compare with DSE results (numerically and theoretically).

Chapter 5

Heavy Quarkonia

5.1 Introduction

We will apply two anQCD models of $(a_{\rm pt})_{\rm an.} \equiv \mathcal{A}_1$, namely APT of Chapter 2, and the 2δanQCD model of Section 3.3, to evaluations of the perturbation series of the binding energy $E_{q\bar{q}}$ of heavy quarkonia ($\Upsilon(1S)$ and $J/\psi(1S)$) and of the quark pole mass m_q based on the work of Ref. [105]. In this way, we will evaluate the masses of these quarkonia $M_{q\bar{q}} = 2m_q + E_{q\bar{q}}$ as functions of the ($\overline{\rm MS}$) quark mass $\overline{m}_q$. In the APT model of analytic QCD, we will need to evaluate not just the integer power analogs $(a^n_{\rm pt})_{\rm an.APT} \equiv \mathcal{A}^{\rm (APT)}_n$ (hereafter through this chapter we will use this notation in order to not distinguish with general analytic models), but also the analogs of the logarithmic terms $(a^n_{\rm pt} \ln^k a_{\rm pt})_{\rm an.APT} \equiv \mathcal{A}^{\rm (APT)}_{n,k}(Q^2)$ whose evaluation uses the approach of FAPT (see Chapter 2.7).

As input parameter we use the renormalon-free quark mass $\overline{m}_q$ ($\equiv \overline{m}_q(\mu^2 = \overline{m}_q^2)$) of the corresponding quark $q = b, c$ (also called the $\overline{\rm MS}$ quark mass), and the anQCD coupling of the model. Since the quarkonia masses are well measured, we can extract the values of $\overline{m}_q$. We also perform the same analysis in pQCD in the corresponding renormalization schemes.

We will evaluate the binding energy $E_{q\bar{q}}$ and of the quark pole mass m_q, in terms of the mass $\overline{m}_q$ and of the couplings. Furthermore, we explain how the cancellation of the leading infrared renormalon in the sum $2m_q + E_{q\bar{q}}$ allows us to separate the ultrasoft from the soft part of the binding energy. The numerical results and the extractions of the masses $\overline{m}_b$ and $\overline{m}_c$ will be presented. The evaluations are performed in the two aforementioned analytic models (F)APT and 2δanQCD, and in pQCD in the

corresponding two renormalization schemes ($\overline{\rm MS}$, and in the scheme of 2δanQCD called here the Lambert scheme). And Finally we summarize our results and draw certain conclusions.

The higher order couplings $A_\nu \equiv \left(a_{\rm pt}^\nu\right)_{\rm an}$ in 2δanQCD model are obtained according to the construction for general anQCD models, for general (noninteger) ν and for the couplings $\mathcal{A}_{\nu,k} \equiv \left(a_{\rm pt}^\nu \ln^k a_{\rm pt}\right)_{\rm an}$.

The analytization of expansions now consists simply in the replacements

$$a_{\rm pt}^\nu(\mu^2) \;\mapsto\; \left(a_{\rm pt}^\nu(\mu^2)\right)_{\rm an} = \mathcal{A}_\nu(\mu^2)\;, \tag{5.1a}$$

$$a_{\rm pt}^\nu(\mu^2)\ln^k a_{\rm pt}(\mu^2) \;\mapsto\; \left(a_{\rm pt}^\nu(\mu^2)\ln^k a_{\rm pt}(\mu^2)\right)_{\rm an} = \mathcal{A}_{\nu,k}(\mu^2)\;. \tag{5.1b}$$

In the FAPT procedure of Chapter 2.7, applicable only in APT, usually the truncation in the loop expansion ($\leq a_{\rm pt}^{\ell+1}$) is applied to the running coupling $a_{\rm pt}(\mu^2)$, which is then reflected in the spectral functions Im $a_{\rm pt}^\nu(-\sigma - i\epsilon)$ and Im$[a_{\rm pt}^\nu(-\sigma - i\epsilon)\ln^k a_{\rm pt}(-\sigma - i\epsilon)]$ that take the "simple" form:

$$a_{\rm pt}^\nu(Q^2) = \frac{1}{\pi}\int_{\sigma=-\Lambda_{\rm L}^2-\eta}^{\infty} \frac{d\sigma\ {\rm Im}\ a_{\rm pt}^\nu(-\sigma - i\epsilon)}{(\sigma + Q^2)}, \tag{5.2}$$

and $\eta \to +0$. And

$$\left(a_{\rm pt}^\nu(Q^2)\right)_{\rm an}^{(({\rm F})\rm APT)} \equiv \mathcal{A}_\nu^{(({\rm F})\rm APT)}(Q^2) = \frac{1}{\pi}\int_{\sigma=0}^{\infty} d\sigma \frac{{\rm Im}\ a_{\rm pt}^\nu(-\sigma - i\epsilon)}{(\sigma + Q^2)}\;. \tag{5.3}$$

5.2 Perturbation expansion for heavy $q\bar{q}$ ground state energy

5.2.1 General formulas

The analysis of nonrelativistic potential is the starting point for the determination of the ground state energy of $\bar{q}q$ and thus of the mass of such systems. The main input in these calculations is the mass $\overline{m}_q(\overline{m}_q^2)$ (here denoted simply as $\overline{m}_q$), also called $\overline{\rm MS}$ quark mass. The masses of the heavy quarkonia $\bar{q}q$ [$\Upsilon(1S)$ when $q = b$, $J/\psi(1S)$ when $q = c$] are well measured, and this allows us to extract the corresponding mass $\overline{m}_q$. By evaluating an observable, such as the quark-antiquark binding energy here, within anQCD models, at least part of the (chirality-conserving) nonperturbative effects get included in the leading-twist term via the analytization.

The coefficients in the (leading-twist) perturbation expansion of the ground state binding energy $E_{q\bar{q}}$ (i.e., with: $n = 1$ and $\ell = 0$) of heavy quarkonium $q\bar{q}$ in powers of $a_{\rm pt}$ were obtained up to all terms $\mathcal{O}(a_{\rm pt}^4)$ in Ref. [106], the terms $\mathcal{O}(a_{\rm pt}^5 \ln a_{\rm pt})$ in Ref. [107], and all terms up to $\mathcal{O}(a_{\rm pt}^5)$ (including logarithmic) are given in Ref. [108]. The last term ($\sim a_{\rm pt}^5$) is now completely known since the parameter a_3 from the static potential is now known, Refs. [109, 110]. The general structure of the (leading-twist term of the) ground state binding energy in pQCD is

$$\begin{aligned} E_{q\bar{q}}^{(\rm pt)} &= -\frac{4}{9} m_q \pi^2 a_{\rm pt}^2(\mu^2) \Big\{ 1 + a_{\rm pt}(\mu^2) \left[K_{1,0} + K_{1,1} L_{\rm pt}(\mu^2) \right] + a_{\rm pt}^2(\mu^2) \left[K_{2,0} \right. \\ &\quad \left. + K_{2,1} L_{\rm pt}(\mu^2) + K_{2,2} L_{\rm pt}^2(\mu^2) \right] + a_{\rm pt}^3(\mu^2) \left[K_{3,0,0} + K_{3,0,1} \ln a_{\rm pt}(\mu^2) \right. \\ &\quad \left. + K_{3,1} L_{\rm pt}(\mu^2) + K_{3,2} L_{\rm pt}^2(\mu^2) + K_{3,3} L_{\rm pt}^3(\mu^2) \right] + \mathcal{O}(a_{\rm pt}^4) \Big\} \ , \end{aligned} \tag{5.4}$$

where

$$L_{\rm pt}(\mu^2; m_q^2) = \frac{1}{2} \ln \left(\frac{\mu^2}{((4\pi/3) m_q)^2 a_{\rm pt}^2(\mu^2)} \right) \ , \tag{5.5}$$

μ^2 is the (square of the) renormalization scale, m_q is the pole mass of the quark, and the coefficients $K_{j,k}$ can be obtained by combining the results of the mentioned literature. The typical scale of the process is a soft reference scale Q_s^2 ($\equiv -q^2$), which is a typical quark-antiquark momentum transfer inside the quarkonium ($Q_s^2 \sim m_q^2 \alpha_s^2$) and can be fixed by convention. The soft renormalization scale $\mu^2 \equiv \mu_s^2$ can then be varied around Q_s^2

$$\mu^2 \equiv \mu_s^2 = \kappa Q_s^2 \quad (\kappa \sim 1; Q_s^2 \sim m_q^2 \alpha_s^2) \ . \tag{5.6}$$

The quarkonium mass is then

$$M_{q\bar{q}} = 2 m_q + E_{q\bar{q}}(m_q) \ . \tag{5.7}$$

In principle, the input quantity here could be the quark pole mass m_q. However, this mass m_q, in contrast to the mass $\overline{m}_q$, suffers from the strong infrared renormalon ambiguity (at Borel parameter value $b = 1/2$, $\Rightarrow \delta m_q \sim \Lambda_{\rm QCD}$). This ambiguity must cancel in the physical sum [Eq. (5.7)].

It is more convenient to use as input a renormalon ambiguity-free input mass, such as $\overline{m}_q$, and we will do this.

In the case of the bottom quark, before we relate the pole mass m_b with the mass $\overline{m}_b$, at renormalization energies $\mu = \overline{m}_b$ where $N_f = 4$ (and where the charm quark mass is considered zero, i.e., decoupled), the effects δm_b of the nonzero massa $m_c \neq 0$ have to be subtracted, and they are [111]

$$(\delta m_b)_{m_c} = (\delta m_b)_{m_c}^{(1)} + (\delta m_b)_{m_c}^{(2)} \approx 0.025 \pm 0.005 \ {\rm GeV} \ . \tag{5.8}$$

These effects were calculated in Ref. [111] in pQCD, at the hard renormalization scale $\mu^2 = \overline{m}_b^2$. We checked that they do not get significantly modified in APT and in the 2δanQCD model.

The pole mass m_q and the mass $\overline{m}_q$ are then related via the relation

$$\frac{m_q - \delta m_q}{\overline{m}_q} = 1 + \frac{4}{3}\left(a_{\rm pt}(\overline{m}_q^2) + r_1 a_{\rm pt}^2(\overline{m}_q^2) + r_2 a_{\rm pt}^3(\overline{m}_q^2) + r_3 a_{\rm pt}^4(\overline{m}_q^2)\right) + \mathcal{O}(a_{\rm pt}^5) \ , \quad (5.9)$$

where δm_q is zero when $q = c$, and is given by Eq. (5.8) when $q = b$

$$\delta m_q \equiv \left\{ \begin{array}{ll} (\delta m_b)_{m_c} & (q = b) \\ 0 & (q = c) \end{array} \right\} \ . \quad (5.10)$$

The coefficient $R_0 = 4/3$ was obtained in Ref. [112]. Also the coefficients $r_1(\overline{m}_q^2)$, and $r_2(\overline{m}_q^2)$ are known (Refs. [113], [114–116], respectively) they are given in Eqs. (A.1) in Appendix A, and N_f in these coefficients is the number of flavors of quarks lighter than q. Specifically, the values are: $r_1 = 7.739$ and $r_2 = 87.224$ for $N_f = 3$; and $r_1 = 6.958$ and $r_2 = 70.659$ for $N_f = 4$. On the other hand, in Appendix A we estimate the values of r_3 to a reasonably high level of precision (with less than 4 % uncertainty) by a method which uses the structure of the leading infrared renormalon (at $b = 1/2$) of the quantity $m_q/\overline{m}_q$: $r_3(N_f = 3) = 1339.4$, $r_3(N_f = 4) = 987.3$.

While the relation (5.9) is written here at the "hard" renormalization scale $\mu^2 = \overline{m}_q^2$, it is straightforward to reexpress the sum on the right-hand side of Eq. (5.9) at a different, lower, scale μ^2. In Appendix A this reexpression is presented explicitly, under the assumption that during the lowering of the scale, $\overline{m}_q^2 \to \mu^2$, we do not cross the quark threshold. The goal is to express in the perturbation expansion of the binding energy (5.4), where the renormalization scale is soft, the pole mass m_q via the mass $\overline{m}_q$, and for this we need the relation (5.9) at the soft renormalization scale. It turns out that for the $b\bar{b}$ system the hard scale is $\overline{m}_b \approx 4$ GeV, i.e., the scale where $N_f = 4$; and the soft scale, Eq. (5.6), is $\mu_s \approx 2$ GeV, i.e., the scale where it is more reasonable to expect $N_f = 3$.[1] In this case, we take into account also the (three-loop) quark threshold transition $N_f = 4 \mapsto 3$ at $\mu^2 = (2m_c)^2$, Ref. [117]. We thus obtain the relation (5.9) reexpressed at the soft scale μ_s^2 of Eq. (5.6)

$$\begin{aligned} m_q(\overline{m}_b^2; \mu_s^2) \ &= \ \delta m_q + \overline{m}_q \left\{ 1 + \frac{4}{3} a_{\rm pt}(\mu_s^2) \left[1 + a_{\rm pt}(\mu_s^2) r_1(\mu_s^2) + a_{\rm pt}^2(\mu_s^2) r_2(\mu_s^2) \right.\right. \\ & \left.\left. + a_{\rm pt}^3(\mu_s^2) r_3(\mu_s^2) \right] + \mathcal{O}(a_{\rm pt}^5) \right\} \ . \end{aligned} \quad (5.11)$$

Further, the renormalization scheme can also be varied in this relation and in the relations (5.4)-(5.5), i.e., the changes of the scheme parameters $c_j = \beta_j/\beta_0$ $(j = 2, 3)$

[1] Usually, the quark thresholds are taken at $2m_q$. In the case of $N_f = 4 \mapsto 3$ transition, this is about 2.5 GeV, above the soft scale of the $b\bar{b}$ system.

from the usual $\overline{\rm MS}$ scheme to other schemes affect correspondingly the values of the coupling $a_{\rm pt}(\mu_s^2)$ and of the coefficients. We recall that in (F)APT the chosen scheme here is $c_2 = c_3 = \cdots = 0$; in the 2δanQCD model and in Lambert pQCD, the scheme is $c_2 = -4.76^{+2.66}_{-0.97}$ and $c_j = c_2^{j-1}/c_1^{j-2}$ for $j \geq 3$. The relationship between $a_{\rm pt}$'s at two different scales and in two different renormalization schemes is summarized in Appendix B, where we also summarize the (three-loop) connection of $a_{\rm pt}$'s across the quark threshold.

After performing all these transformations, we can rewrite the original expansion (5.4) for $E_{q\bar{q}}$ in terms of the $\overline{m}_q \equiv \overline{m}_q(\overline{m}_q^2)$ mass, with the coupling $a_{\rm pt}$ at any soft renormalization scale μ_s and in any chosen renormalization scheme $(c_2, c_3, \ldots)$

$$E_{q\bar{q}}^{\rm (pt)}(Q_s^2; \overline{m}_q^2; N_f = 3) = -\frac{4}{9}(\overline{m}_q + \delta m_q)\pi^2 a_{\rm pt}^2(\mu_s^2)\Big\{1 + a_{\rm pt}(\mu_s^2)\left[\mathcal{K}_{1,0} + \mathcal{K}_{1,1}\mathcal{L}_{\rm pt}(\mu_s^2)\right] + a_{\rm pt}^2(\mu_s^2)\left[\mathcal{K}_{2,0} + \mathcal{K}_{2,1}\mathcal{L}_{\rm pt}(\mu_s^2) + \mathcal{K}_{2,2}\mathcal{L}_{\rm pt}^2(\mu_s^2)\right] + a_{\rm pt}^3(\mu_s^2)\left[\mathcal{K}_{3,0,0} + \mathcal{K}_{3,0,1}\ln a_{\rm pt}(\mu_s^2) + \mathcal{K}_{3,1}\mathcal{L}_{\rm pt}(\mu_s^2) + \mathcal{K}_{3,2}\mathcal{L}_{\rm pt}^2(\mu_s^2) + \mathcal{K}_{3,3}\mathcal{L}_{\rm pt}^3(\mu_s^2)\right] + \mathcal{O}(a_{\rm pt}^4)\Big\}\,, \tag{5.12}$$

where $\mu_s^2 = \kappa Q_s^2$ ($\kappa \sim 1$ being the soft renormalization scale parameter), and the logarithm contains now $\overline{m}_q$ mass

$$\mathcal{L}_{\rm pt}(\mu_s^2; \overline{m}_q^2) \;=\; \frac{1}{2}\ln\left(\frac{\mu_s^2}{\left[(4\pi/3)(\overline{m}_q + \delta m_q)\right]^2 a_{\rm pt}^2(\mu_s^2)}\right)\,. \tag{5.13}$$

We note that the new (renormalon-ambiguity-free) mass which appears naturally in this expansion is not exactly the mass $\overline{m}_q$, but rather

$$\widetilde{m}_q \equiv \overline{m}_q + \delta m_q = \left\{ \begin{array}{ll} \overline{m}_b + (\delta m_b)_{m_c} & (q = b) \\ \overline{m}_c & (q = c) \end{array} \right\}\,, \tag{5.14}$$

where $(\delta m_b)_{m_c}$ is given by Eq. (5.8) when $q = b$.

The mentioned soft "process scale" Q_s^2 ($\sim \overline{m}_q^2\alpha_s^2$) can be regarded, at least formally, to be a variable complex scale. Therefore, the binding energy $E_{q\bar{q}}(Q_s^2; \overline{m}_q^2)$ is, formally, a spacelike observable analytic in Q_s^2; and the dependence on the renormalization scale parameter κ disappears when the number of terms in the expansion is infinite. The analytization of $E_{q\bar{q}}^{\rm (pt)}(Q_s^2; \overline{m}_q^2)$ of Eq. (5.12), according to Eqs. (5.1) [or, in (F)APT: Eq. (5.3)], then leads to

$$E_{q\bar{q}}^{\rm (an)}(Q_s^2; \overline{m}_q^2) = -\frac{4}{9}\widetilde{m}_q\pi^2\Big\{\mathcal{A}_2(\kappa Q_s^2) + \left[\mathcal{K}_{1,0}\mathcal{A}_3(\kappa Q_s^2) + \mathcal{K}_{1,1}\mathcal{B}_{3,1}(\kappa Q_s^2)\right] + \left[\mathcal{K}_{2,0}\mathcal{A}_4(\kappa Q_s^2) + \mathcal{K}_{2,1}\mathcal{B}_{4,1}(\kappa Q_s^2) + \mathcal{K}_{2,2}\mathcal{B}_{4,2}(\kappa Q_s^2)\right] + \left[\mathcal{K}_{3,0,0}\mathcal{A}_5(\kappa Q_s^2) + \mathcal{K}_{3,0,1}\mathcal{A}_{5,1}(\kappa Q_s^2) + \mathcal{K}_{3,1}\mathcal{B}_{5,1}(\kappa Q_s^2) + \mathcal{K}_{3,2}\mathcal{B}_{5,2}(\kappa Q_s^2) + \mathcal{K}_{3,3}\mathcal{B}_{5,3}(\kappa Q_s^2)\right] + \mathcal{O}(\mathcal{A}_{6,4})\Big\}\,, \tag{5.15}$$

where we use, for simplicity, the general notation of Eqs. (5.1a)-(5.1b) for $\mathcal{A}_\nu$'s ($\nu = k$ integer now) [in (F)APT: Eq. (5.3)], and denote by $\mathcal{B}_{n+2,j}$ the following:

$$\begin{aligned}\mathcal{B}_{n+2,j}(\kappa Q_s^2) &= \left(a_{\rm pt}^{n+2}(\kappa Q_s^2) \frac{1}{2^j} \ln^j \left(\frac{\kappa Q_s^2}{((4\pi/3)\overline{m}_q)^2 a_{\rm pt}^2(\kappa Q_s^2)} \right) \right)_{\rm an} \\ &= \frac{1}{2^j} \sum_{s=0}^{j} \left(\begin{array}{c} j \\ s \end{array} \right) (-2)^s \, \bar{f}^{j-s}(\kappa Q_s^2) \mathcal{A}_{n+2,s}(\kappa Q_s^2) \, , \end{aligned} \tag{5.16}$$

where $\bar{f} \equiv \ln[\kappa Q_s^2/(4\pi/3)^2/\overline{m}_q^2]$, and $\mathcal{A}_{n+2,s}$ are defined as: $\mathcal{A}_{n+2,s} \equiv (a^{n+2}(Q^2) \ln^s a(Q^2))_{an}$. In FAPT we have

$$\mathcal{A}_{n,s}(Q^2) = \frac{1}{\pi} \int_0^\infty \frac{d\sigma {\rm Im} \left\{ a^n \ln^s a(Q'^2 = -\sigma - i\epsilon) \right\}}{\sigma + Q^2}. \tag{5.17}$$

In general anQCD, such as 2δanQCD, we have (3.61). On the other hand, $\mathcal{A}_{n,k}(Q^2) \equiv \left(a^n(Q^2) \ln^k a(Q^2)\right)_{an}$ are obtained by the use of the relation

$$\mathcal{A}_{n,k}(Q^2) = \frac{\partial^k}{\partial \nu^k} \mathcal{A}_{n+\nu}(Q^2) \Big|_{\nu=0} , \tag{5.18}$$

where this relation is the consequence of the identity

$$a^n \ln^k a \equiv \frac{\partial^k}{\partial \nu^k} a^{n+\nu} \Big|_{\nu=0} . \tag{5.19}$$

Here, $j = 1, \ldots, n$, therefore $\mathcal{B}_{n+2,j}(\kappa Q_s^2) \to 0$ faster than $a_{\rm pt}^2(\kappa Q_s^2)$ when $|Q_s^2| \to \infty$, by asymptotic freedom.

The relation (5.11) in its analytized form is

$$\begin{aligned} m_q(\overline{m}_b^2; \mu_s^2) &= \delta m_q + \overline{m}_q \Big\{ 1 + \frac{4}{3} \left[\mathcal{A}_1(\mu_s^2) + r_1(\mu_s^2) \mathcal{A}_2(\mu_s^2) + r_2(\mu_s^2) \mathcal{A}_3(\mu_s^2) \right. \\ &\quad \left. + r_3(\mu_s^2) \mathcal{A}_4(\mu_s^2) \right] + \mathcal{O}(\mathcal{A}_5) \Big\} \, . \end{aligned} \tag{5.20}$$

Since this relation includes at its highest order the term $\sim \mathcal{A}_4$ ($\sim a_{\rm pt}^4$), in general analytic QCD it is consistent to use in Eq. (5.20) for the expressions $\mathcal{A}_n$ ($n = 1, 2, 3, 4$) those given in Eq. (3.61) with the sum there truncated at (and including) $\widetilde{\mathcal{A}}_4$ ($\sim \mathcal{A}_4 \sim a_{\rm pt}^4$). On the other hand, the expression (5.15) for the binding energy includes at its highest order the terms $\sim \mathcal{A}_5$ (more precisely, $\sim \mathcal{A}_{5,3}$), therefore it is consistent to use there for the expressions $\mathcal{A}_n$ ($2 \le n \le 5$) those of Eq. (3.61) [or Eqs. (**??**)] with the sum truncated at (and including) $\widetilde{\mathcal{A}}_5$, and expressions $\mathcal{A}_{n,k}$ of Eq. (5.18) truncated at (and including) $\partial^k \widetilde{\mathcal{A}}_{\nu+5}/\partial \nu^k|_{\nu=0}$ ($\sim a_{\rm pt}^n \ln^k a_{\rm pt}$), where $k = 1, 2, 3$.

The mentioned soft reference scale Q_s^2 ($\sim \overline{m}_q^2 \alpha_s^2$) can be fixed in pQCD, by convention, by the condition that all the logarithmic terms in the expansion (5.12) disappear

$$Q^2_{s,\mathrm{pt}} = (4\pi/3)^2 \widetilde{m}_q^2 a^2_{\mathrm{pt}}(Q^2_{s,\mathrm{pt}}) \ , \tag{5.21}$$

where $\widetilde{m}_q$ is defined in Eq. (5.14). This type of condition, in analytic QCD, would correspond to fixing the soft reference scale Q_s by requiring $\mathcal{B}_{n+1,j}(Q_s^2) = 0$, for various n's and $j = 1, \ldots, n$. This fixing is not unique since it depends on n and j. Our convention will be that the leading logarithmic term in Eq. (5.15) is zero at such scale

$$\mathcal{B}_{3,1}(Q_s^2) = 0 \ . \tag{5.22}$$

It will turn out that this condition has a solution in the case of $b\bar{b}$ ($\Upsilon(1S)$) in the 2δanQCD model, but not in $J/\psi(1S)$ in that model, and not in any case of the (F)APT model. In such respective cases, we will use simply the following simpler analogs of the pQCD condition (5.21):

$$Q_s^2 = (4\pi/3)^2 \widetilde{m}_q^2 \widetilde{\mathcal{A}}_2(Q_s^2) \quad (J/\psi(1S) \text{ in } 2\delta\text{anQCD}) \ , \tag{5.23}$$

$$Q^2_{s,(\mathrm{(F)APT})} = (4\pi/3)^2 \widetilde{m}_q^2 \mathcal{A}_2^{(\mathrm{(F)APT})}(Q^2_{s,(\mathrm{(F)APT})}) \quad (\mathrm{(F)APT}) \ . \tag{5.24}$$

These measures of the typical momentum scale of the (nonrelativistic) quark inside the quarkonium are rather low, ≈ 2 GeV in $\Upsilon(1S)$, and $\lesssim 1$ GeV in $J/\psi(1S)$. In pQCD such scales are problematic, because they are not far away from the unphysical (Landau) singularities of $a_{\mathrm{pt}}(Q^2)$; in analytic QCD models, no such problems appear in principle.

5.2.2 Separation of the soft and ultrasoft contributions

The pole mass m_q and the static potential $V(r)$ both contain the leading infrared renormalon ($b = 1/2$) singularities, and cancellation of these singularities takes place in the sum $2m_q + V(r)$ [118,120,121]. As a consequence, this cancellation must take place also in the quarkonium mass $2m_q + E_{q\bar{q}}$ [111,119,122,145–147], more specifically, in the sum $2m_q + E_{q\bar{q}}(s)$ where $E_{q\bar{q}}(s) = \langle 1|V(r)|1\rangle$ [$\sim V(r_s)$] is the soft part of the binding energy $E_{q\bar{q}}$, and $|1\rangle$ denotes the (ground) state of the quarkonium. The typical soft distance r_s in the quarkonium is $\sim 1/\sqrt{Q_s^2} \sim 1/(\overline{m}_q \pi a)$, where $a = a_{\mathrm{pt}}$ or $\mathcal{A}_1$. Since $V(r_s) \propto 1/r_s$, we have $E_{q\bar{q}}(s)/\overline{m}_q \sim V(r_s)/\overline{m}_q \propto 1/(r_s \overline{m}_q) \sim (\pi a)$. This leads to the so called "power mismatch" in the renormalon cancellation in the pQCD expansion of the sum $(2m_q + E_{q\bar{q}}(s))/\overline{m}_q$ [124] (see also: [122]): the terms $\sim a^n$ in $2m_q/\overline{m}_q$ tend to cancel numerically the terms $\sim a^{n+1}$ in $E_{q\bar{q}}(s)/\overline{m}_q$. Therefore, since the binding energy $E_{q\bar{q}}$ is now known up to $\sim a^5_{\mathrm{pt}}$, it is very convenient to have the relation $m_q/\overline{m}_q$ up to $\sim a^4$, i.e., to have a good estimate for the coefficient r_3 and

to use it, so that the effects of renormalon cancellation in $2m_q + E_{q\bar{q}}(s)$ can be seen numerically more clearly. This was the main reason for performing the analysis in Appendix A resulting in estimates of r_3, Eq. (A.13). This cancellation, term by term, should be numerically more precise (at sufficiently high orders) if the renormalization scales μ_s used in $m_q/\overline{m}_q$ and in $E_{q\bar{q}}(s)/\overline{m}_q$ [Eqs. (5.11) and (5.12)] are taken to be equal. This renormalon cancellation will be our guiding principle for the separation of the soft (s) and the ultrasoft (us) part in the binding energy

$$E_{q\bar{q}} = E_{q\bar{q}}(s) + E_{q\bar{q}}(us) \ . \tag{5.25}$$

Typical us scales are $\mu_{us} \sim \overline{m}_q \alpha_s^2$, and the us part of the binding energy is $\sim \overline{m}_q a^5 \ln a$. We can parametrize the s-us separation by a dimensionless parameter $k_{s/us}$ such that the s-us factorization scale μ_f is written as

$$\mu_f = k_{s/us} \overline{m}_q \alpha_s(Q_s)^{3/2} \left[\approx k_{s/us} (Q_s Q_{us})^{1/2}\right] \ , \tag{5.26}$$

where $Q_{us} \sim \overline{m}_q \alpha_s^2$ is a (chosen) us reference scale. It is expected that usually $k_{s/us} \sim 1$, but it does not have to be so always. The us part can be rewritten, in terms of $k_{s/us}$ as (cf. Ref. [145])

$$E^{(\rm pt)}_{q\bar{q}}(us) = -\frac{4}{9} \widetilde{m}_q \pi^2 \left[\mathcal{K}_{3,0,0}(us) a^5_{\rm pt}(\mu^2_{us}) + \mathcal{K}_{3,0,1}(us) a^5_{\rm pt}(\mu^2_{us}) \ln a_{\rm pt}(\mu^2_{us}) + \mathcal{O}(a^6_{\rm pt})\right] \ , \tag{5.27}$$

and in analytic QCD correspondingly

$$E^{(\rm an)}_{q\bar{q}}(us) = -\frac{4}{9} \widetilde{m}_q \pi^2 \left[\mathcal{K}_{3,0,0}(us) \mathcal{A}_5(\mu^2_{us}) + \mathcal{K}_{3,0,1}(us) \mathcal{A}_{5,1}(\mu^2_{us}) + \mathcal{O}(\mathcal{A}_6)\right] \tag{5.28}$$

where $\mu_{us} = \kappa_{us} Q_{us}$ is a us renormalization scale ($\kappa_{us} \sim 1$), and the two us coefficients are

$$\mathcal{K}_{3,0,1}(us) = 7.098 \pi^3 \ , \quad \mathcal{K}_{3,0,0}(us) = \left[27.512 + 7.098 \ln \pi - 14.196 \ln(k_{s/us})\right] \pi^3 \ . \tag{5.29}$$

The expansion of the soft (s) part $E_{q\bar{q}}(s)$ of the binding energy is then, according to Eq. (5.25), the same as the expansions (5.12) and (5.15), with the exception of the replacements[2] of two coefficients $\mathcal{K}_{3,0,0}$ and $\mathcal{K}_{3,0,1}$

$$E^{(\rm pt,an)}_{q\bar{q}}(s) = E^{(\rm pt,an)}_{q\bar{q}} \left(\mathcal{K}_{3,0,0} \mapsto \mathcal{K}_{3,0,0} - \mathcal{K}_{3,0,0}(us); \mathcal{K}_{3,0,1} \mapsto \mathcal{K}_{3,0,1} - \mathcal{K}_{3,0,1}(us)\right) \ . \tag{5.30}$$

The s-us factorization, i.e., the parameter $k_{s/us}$, will then be determined, in each model, by requiring that the leading infrared renormalon cancellation in $2m_q + E_{q\bar{q}}(s)$

[2]The coefficients $\mathcal{K}_{3,0,0}(us)$ and $\mathcal{K}_{3,0,1}(us)$, representing the leading part of the (quasi)observable $E_{q\bar{q}}(us)$, are renormalization scale (μ_{us}) and scheme independent.

be exact at the last available order, i.e., that the $\mathcal{O}(a^4)$ term in $2m_q(Q_s^2, \overline{m}_q^2)$ and the term $\mathcal{O}(a^5)$[3] in $E_{q\bar{q}}(s; Q_s^2; \overline{m}_q^2)$ cancel exactly.

The us part of the quarkonium mass, $E_{q\bar{q}}(us; Q_{us}^2; \overline{m}_q^2)$, will be evaluated in each case according to a procedure which takes into account those problems of low-scale evaluations which appear in the considered model (2δanQCD, pQCD, (F)APT).

We recall that the binding energy $E_{q\bar{q}}(s)$ is a Euclidean quantity because it depends on spacelike quark-antiquark momentum transfer q ($q^2 = -\vec{q}^2 \equiv -Q^2 < 0$). Analytization of such quantities must follow the procedure (5.1). On the other hand, the quark pole mass m_q is a Minkowskian quantity because it depends on the timelike pole momentum ($q^2 \equiv -Q^2 = m_q^2 > 0$). We note that our analytization procedure for the quark pole mass is again the procedure (5.1): $a_{\rm pt}^n(\overline{m}_q^2) \mapsto \mathcal{A}_n(\overline{m}_q^2)$ in the relation (5.9) [and then reexpressing $\mathcal{A}_n(\overline{m}_q^2)$ via $\mathcal{A}_k(\mu_s^2)$'s at a lower soft scale μ_s^2, for renormalon cancellation]. This procedure, for the Minkowskian quantities, is analogous to the fixed order perturbation theory (FOPT) in pQCD, Ref. [123], where the couplings in the corresponding contour integral, on the contour $Q^2 = \overline{m}_q^2 \exp(i\phi)$, are Taylor-expanded around the spacelike point $Q^2 = \overline{m}_q^2 > 0$. As a result, the kinematic π^2-terms appear in the expansion coefficients r_j.

Another analytization of the pole mass expansion would involve contour integration of the corresponding Euclidean quantity with (exact) RGE-running couplings along the contour, cf. Ref. [125]. This procedure is analogous to the Contour Improved Perturbation Theory (CIPT) in pQCD; in such a case, the aformentioned π^2 terms are effectively resummed, Refs. [126,127]. We decided not to pursue this CIPT type of analytization, because it is technically more demanding due to the additional running of the mass factor $\overline{m}_q(\mu^2)$; and because in this approach the renormalon cancellation mechanism, due to the mentioned resummations, probably changes its practical form. This problem remains to be addressed in the future.

5.3 Numerical results

5.3.1 Bottom mass extraction

In this section, we extract from the mass of $b\bar{b}$ quarkonium the mass $\overline{m}_b \equiv \overline{m}_b(\overline{m}_b^2)$ in (F)APT, 2δanQCD model, and in pQCD in two renormalization schemes ($\overline{\rm MS}$ and in the Lambert scheme of 2δanQCD). For this, we use the relation between $\overline{m}_b$ and the well-measured mass of the $b\bar{b}$ quarkonium $\Upsilon(1S)$ [56]

$$2m_b(\overline{m}_b^2; \mu_s^2) + E_{b\bar{b}}(s; Q_s^2; \overline{m}_b^2; \mu_s^2, N_f = 3) + E_{b\bar{b}}(us; Q_{us}^2; \overline{m}_b^2; \mu_{us}^2) = M_{\Upsilon(1S)}^{(\rm exp)} \ . \quad (5.31)$$

[3]The latter term includes all $\mathcal{O}(a^5 \ln^k a)$ terms ($k = 0, 1, 2, 3$).

The dependence on the (soft) renormalization scale $\mu_s^2 = \kappa_s Q_s^2$ in the pole mass m_b and in the soft binding energy $E_{b\bar{b}}(s)$ occurs due to the truncation of the series for these two quantities. For the same reason, the ultrasoft binding energy $E_{b\bar{b}}(us)$ has strong dependence on the ultrasoft renormalization scale μ_{us}^2 ($= \kappa_{us} Q_{us}^2$) due to the drastic truncation of this quantity at its leading order ($\sim a^5 \ln a$). As mentioned in the previous Section, the separation of the s and us parts of the binding energy will be performed here by determining the s-us separation parameter $k_{s/us}$, Eqs. (5.25)-(5.30), by the requirement of cancellation of the leading renormalon in $2m_b + E_{b\bar{b}}(s)$.

In contrast to the other three models, (F)APT gives a very small central value for the s-us separation parameter $k_{s/us} \approx 6 \times 10^{-10}$. This reflects the difficulty in the (F)APT scenario to exactly enforce the leading renormalon cancellation of the $\sim \mathcal{A}_4$ term of $2m_b$ with the corresponding $\sim \mathcal{A}_5$ term of $E_{b\bar{b}}(s)$. If, on the other hand, we impose in (F)APT the condition $k_{s/us} \sim 1$, more specifically the central value $k_{s/us} = 1$ and variation in the interval $(0.1, 10.)$, the results change somewhat, the central extracted value of $\overline{m}_b$ increases by about 0.050 GeV, and the absolute values of the us part of the binding energy and of various other uncertainties of $\overline{m}_b$ get reduced. We will consider in (F)APT only the natural range ~ 1 of the s-us separation parameter, $k_{s/us} = 1.0^{+9.0}_{-0.9}$, rather than the exceedingly small values of $k_{s/us}$ required by the exact renormalon cancellation. In the other three models (2δanQCD, and in Lambert and $\overline{\rm MS}$ pQCD), the renormalon cancellation is imposed without any problems, resulting in the values of $k_{s/us}$ within the interval between 10^{-1} and 10^{1}.

In the previous section we mentioned that we take $N_f = 3$ for the number of active flavors in the binding energy, i.e., in this case the m_c mass is considered to be infinite (decoupled). It turns out that, while the effects of the finiteness of m_c cannot be neglected in the relation between m_b and $\overline{m}_b$, Eqs. (5.8)-(5.9), these effects can be safely neglected in the binding energy $E_{b\bar{b}}(N_f = 3)$; cf. Ref. [111] based on Refs. [113, 128, 129].

Application of the formalism described in Chapter 2 and 3 for the calculation of the couplings of the analytic QCD models (F)APT and 2δanQCD, and in Sec. 5.2 for the calculation of $2m_b$, $E_{b\bar{b}}(s)$ and $E_{\bar{b}b}(us)$ in terms of these couplings, then gives us the following results (see Ref. [105] for details):

$$\begin{aligned}
\overline{m}_b(\text{(F)APT}) &= \left\{ 4.155 \pm 0.002_{(us)} + \begin{pmatrix} +0.005 \\ -0.004 \end{pmatrix}_{(s/us)} + \begin{pmatrix} -0.019 \\ +0.020 \end{pmatrix}_{(\Lambda)} \right. \\
&\quad \left. + \begin{pmatrix} -0.004 \\ +0.002 \end{pmatrix}_{(\mu_s)} \mp 0.005_{(m_c)} \right\} \text{GeV} \qquad (5.32a) \\
&= 4.155 \pm 0.022 \text{ GeV} , \qquad (5.32b)
\end{aligned}$$

with $Q_{s,(\text{(F)APT})} = 1.60; \text{GeV}$ and $k_{s/us} = 1.0$.

$$\overline{m}_b(2\delta\text{anQCD}) = \left\{4.353 + \begin{pmatrix} -0.068 \\ +0.071 \end{pmatrix}_{(us)} + \begin{pmatrix} +0.015 \\ -0.016 \end{pmatrix}_{(s/us)} \mp 0.005_{(\alpha_s)} + \begin{pmatrix} -0.023 \\ +0.034 \end{pmatrix}_{(c_2)} + \begin{pmatrix} +0.017 \\ -0.025 \end{pmatrix}_{(\mu_s)} \mp 0.005_{(m_c)}\right\} \text{GeV} \quad (5.33a)$$

$$= 4.353 \pm 0.084 \text{ GeV} , \quad (5.33b)$$

with $Q_s = 2.08$ GeV and $k_{s/us} = 0.238$.
We will comment on the above uncertainties below. For completeness, we give here also the results of the same kind of analysis in pQCD, first in the Lambert renormalization scheme (i.e., the scheme as used in 2δanQCD: $c_2 = -4.76$, $c_j = c_2^{j-1}/c_1^{j-2}$ for $j \geq 3$); and in the (four-loop) $\overline{\text{MS}}$ scheme:

$$\overline{m}_b(\text{pQCDLamb.}) = \left\{4.382 + \begin{pmatrix} -0.091 \\ +0.097 \end{pmatrix}_{(us)} + \begin{pmatrix} -0.013 \\ +0.017 \end{pmatrix}_{(s/us)} \pm 0.010_{(\alpha_s)} + \begin{pmatrix} +0.027 \\ -0.008 \end{pmatrix}_{(c_2)} + \begin{pmatrix} -0.002 \\ -0.041 \end{pmatrix}_{(\mu_s)} \mp 0.005_{(m_c)}\right\} \text{GeV} \quad (5.34a)$$

$$= 4.382 \pm 0.111 \text{ GeV} , \quad (5.34b)$$

with $Q_{s,\text{pt}} = 1.73$ GeV and $k_{s/us} = 0.306$.

$$\overline{m}_b(\text{pQCD}\overline{\text{MS}}) = \left\{4.505 + \begin{pmatrix} -0.177 \\ +0.200 \end{pmatrix}_{(us)} + \begin{pmatrix} -0.082 \\ +0.084 \end{pmatrix}_{(s/us)} + \begin{pmatrix} +0.031 \\ -0.027 \end{pmatrix}_{(\alpha_s)} + \begin{pmatrix} -0.004 \\ -0.075 \end{pmatrix}_{(\mu_s)} \mp 0.005_{(m_c)}\right\} \text{GeV} \quad (5.35a)$$

$$= 4.505 \pm 0.231 \text{ GeV} , \quad (5.35b)$$

with $Q_{s,\text{pt}} = 1.87$ GeV and $k_{s/us} = 0.248$.
The value of the s-us separation parameter $k_{s/us}$ was determined in all cases by the aforementioned renormalon cancellation in the sum $M_{\Upsilon(1S)}(s) = 2m_b + E_{b\bar{b}}(s; k_{s/us})$, except in the (F)APT case, as discussed above. Below we present these resulting sums

$$M_{\Upsilon(1S)}(s; \text{(F)APT}) = 8.361 + 0.993 + 0.107 + 0.006 - 0.013 \text{ GeV} \quad (5.36a)$$

$$E_{b\bar{b}}(us; \text{(F)APT}) = 0.006 \mp 0.003 \text{ GeV} , \quad (\overline{m}_b = 4.155 \text{ GeV}, \ k_{s/us} = 1.0) ; \quad (5.36b)$$

$$M_{\Upsilon(1S)}(s; 2\delta\text{anQCD}) = 8.756 + 0.868 + 0.151 + 0.040 + 0.000 \text{ GeV} \quad (5.37a)$$
$$E_{b\bar{b}}(us; 2\delta\text{anQCD}) = -0.355 \pm 0.151 \text{ GeV} , \quad (\overline{m}_b = 4.355 \text{ GeV}, \ k_{s/us} = 0.238) ; \quad (5.37b)$$

$$M_{\Upsilon(1S)}(s; \text{pQCDLamb.}) = 8.814 + 0.925 + 0.107 - 0.031 + 0.000 \text{ GeV} \quad (5.38a)$$
$$E_{b\bar{b}}(us; \text{pQCDLamb.}) = -0.355 \pm 0.201 \text{ GeV} , \quad (\overline{m}_b = 4.382 \text{ GeV}, \ k_{s/us} = 0.306) ; \quad (5.38b)$$

$$M_{\Upsilon(1S)}(s; \text{pQCD}\overline{\text{MS}}) = 9.060 + 0.991 + 0.136 - 0.109 + 0.000 \text{ GeV} \quad (5.39a)$$
$$E_{b\bar{b}}(us; \text{pQCD}\overline{\text{MS}}) = -0.617 \pm 0.394 \text{ GeV} , \quad (\overline{m}_b = 4.505 \text{ GeV}, \ k_{s/us} = 0.248) ; \quad (5.39b)$$

We can see from Eqs. (5.36a)-(5.39a) explicitly that for the chosen corresponding central values of the parameter $k_{s/us}$ the renormalon cancellation is exact in the last term [the fifth term, named $t_5(s)$] in the sum for the soft mass $M_{\Upsilon(1S)}(s)$, except in the case of (F)APT where $k_{s/us} = 1.0$ was chosen and the cancellation in $t_5(s)$ is approximate.

The extracted values of $\overline{m}_b$, Eqs. (5.32)-(5.35), have a strong uncertainty coming from the ultrasoft (us) regime and from the related s/us separation. The origin of this uncertainty lies in the strong dependence of the us binding energy $E_{b\bar{b}}(us; \mu^2_{us})$ on the us renormalization scale μ_{us} and on the s-us separation parameter $k_{s/us}$, cf. Eqs. (5.26)-(5.29). The behavior of the us binding energy $E_{b\bar{b}}(us; \mu^2_{us})$ in the three models (2δanQCD, and pQCD in the two schemes), as a function of the us renormalization scales μ_{us} in the low-momentum regime, is presented in Fig. 5.1(a), and in the case of (F)APT in Fig. 5.1(b). In the 2δanQCD model and in pQCD, we do not consider the scales μ_{us} below $(\mu_{us})_{\min} = 1.1$ GeV, because at $\mu_{us} \approx 1.1$ GeV the coupling $\mathcal{A}_5(\mu_{us})$ ($= \widetilde{\mathcal{A}}_5(\mu_{us})$ in our approach) in the 2δanQCD model reaches a local maximum, indicating that the model may not necessarily give reliable values of $\mathcal{A}_5$ and $\mathcal{A}_{5,1}$ below such scales. Therefore, in general, we will not consider μ_{us} lower than 1.1 GeV, in the 2δanQCD model and in pQCD. $E_{b\bar{b}}(us; mu^2_{us})$ in 2δanQCD reaches a local minimum at μ_{us} slightly above 1.1 GeV. Therefore, we estimate the us part of the binding energy in the 2δanQCD model in the following way [we use the notation $E_{b\bar{b}}(us; \mu^2_{us})$]:

$$E_{b\bar{b}}(us; 2\delta\text{anQCD}) = \frac{1}{2}\left[E_{b\bar{b}}(us; Q^2_s) + (E_{b\bar{b}}(us))_{\min}\right] \pm \frac{1}{2}\left[E_{b\bar{b}}(us; Q^2_s) - (E_{b\bar{b}}(us))_{\min}\right] , \quad (5.40)$$

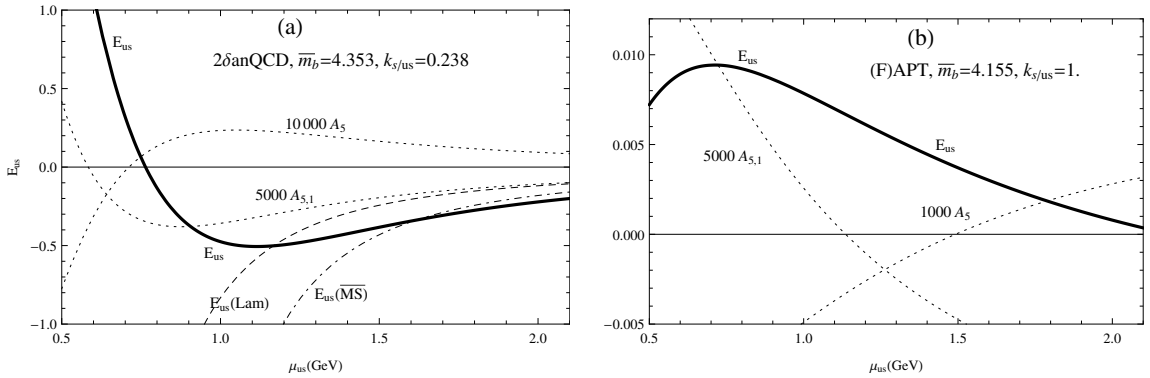

Figure 5.1: (a) Ultrasoft binding energy $E_{b\bar{b}}(us)$ (in GeV) as a function of the us renormalization scale μ_{us}, for the central input values of the 2δanQCD model for the $\Upsilon(1S)$ system ($\overline{m}_b = 4.353$ GeV; $k_{s/us} = 0.238$; $c_2 = -4.76$; $s_0 = 23.06$): solid line for 2δanQCD; dashed line for Lambert pQCD ($c_2 = -4.76$); dash-dotted line for the four-loop $\overline{\rm MS}$ pQCD ($c_2 = 4.471$). For all three curves the same $\overline{m}_b$ and $k_{s/us}$ values are used. Also included are the properly rescaled 2δanQCD couplings $\mathcal{A}_5$ and $\mathcal{A}_{5,1}$ as functions of the scale μ ($= \mu_{us}$). (b) Same as in (a), but for the (F)APT model (with $c_2 = 4.471$), with the corresponding central values of that model ($\overline{m}_b = 4.155$ GeV and $k_{s/us} = 1$). In all the curves $N_f = 3$ was taken.

where the soft reference scale Q_s was determined by the condition (5.22), and gave $Q_s \approx 2.08$ GeV.

In the two pQCD approaches, $E_{b\bar{b}}(us)$ decreases monotonously when μ_{us} decreases below the soft reference scale $Q_{s,\rm pt}$ of Eq. (5.21). For pQCD in the Lambert scheme ($c_2 = -4.76$), with central values of the input parameters, the soft reference scale turns out to be $Q_{s,\rm pt} \approx 1.73$ GeV, and the us binding energy at $(\mu_{us})_{\rm min} = 1.1$ GeV reaches the value of -0.56 GeV. In the $\overline{\rm MS}$ scheme, however, $E_{b\bar{b}}(us; 1.1^2 {\rm GeV}^2) \approx -1.5$ GeV, which is exceedingly low and indicates failure of the method already at such scales, due to vicinity of Landau singularities of the running coupling.[4] Therefore, in $\overline{\rm MS}$ we take as the minimal acceptable scale $(\mu_{us})_{\rm min} = 1.2$ GeV, where $E_{b\bar{b}}(us; 1.2^2 {\rm GeV}^2) \approx -1.0$ GeV (and $Q_{s,\rm pt} \approx 1.87$ GeV) when the central values of the input parameters are used. Thus, in pQCD we estimate the us binding energy as

$$E_{b\bar{b}}(us) = \frac{1}{2}\left[E_{b\bar{b}}(us; Q^2_{s,\rm pt}) + E_{b\bar{b}}(us; (\mu^2_{us})_{\rm min})\right] \pm \frac{1}{2}\left[E_{b\bar{b}}(us; Q^2_{s,\rm pt}) - E_{b\bar{b}}(us; (\mu^2_{us})_{\rm min})\right] , \tag{5.41}$$

[4] It turns out that the Landau cut in the perturbative coupling $a_{\rm pt}(\mu^2)$ starts in the four-loop ($N_f = 3$) $\overline{\rm MS}$ scheme already at about $\mu = \Lambda_{\rm L} \approx 0.607$ GeV. In the Lambert scheme [Eq. (1.24) with the central value $c_2 = -4.76$] there is one pole at $\mu = \Lambda_{\rm p} \approx 0.262$ GeV; the cut begins at an even lower value $\mu = \Lambda_{\rm L.} \approx 0.208$ GeV. The 2δanQCD coupling $\mathcal{A}_1(\mu^2)$ has, of course, no Landau singularities (poles and cuts), although it almost coincides with the Lambert pQCD coupling $a_{\rm pt}(\mu^2)$ at higher scales $|\mu^2| > 1$ GeV^2, Ref. [54].

with $(\mu_{us})_{\rm min} = 1.1$ GeV and 1.2 GeV in the Lambert and $\overline{\rm MS}$ schemes, respectively.

In the (F)APT case, on the other hand, Q_s is fixed according to Eq. (5.24) and gives, for the central input parameter values, the value $Q_{s,(({\rm F})\rm APT)} \approx 1.60$ GeV. In (F)APT no practical problems appear at scales $\mu_{us} < 1.1$ GeV. $E_{b\bar{b}}(us, ({\rm F})\rm APT)$ reaches a moderate maximum value of 0.009 GeV at $\mu_{us} \approx 0.7$ GeV for the chosen central value $k_{s/us} = 1.0$. Therefore, we estimate the us part of the binding energy in (F)APT in the following way:

$$\begin{aligned} E_{b\bar{b}}(us; ({\rm F})\rm APT) &= \frac{1}{2}\left[E_{b\bar{b}}(us; Q^2_{s,(({\rm F})\rm APT)}) + (E_{b\bar{b}}(us))_{\rm max}\right] \\ &\pm \frac{1}{2}\left[E_{b\bar{b}}(us; Q^2_{s,(({\rm F})\rm APT)}) - (E_{b\bar{b}}(us))_{\rm max}\right] \ . \end{aligned} \tag{5.42}$$

In Eqs. (5.32)-(5.35), the uncertainties in $\overline{m}_b$ originating from these determinations of the us binding energy are denoted by the subscript (us).

The related uncertainties for the extracted values of $\overline{m}_b$ originate from the variation of the s-us separation parameter $k_{s/us}$, and are denoted by the subscript (s/us) in Eqs. (5.32)-(5.35). The parameter $k_{s/us}$ was varied in such a way that the last [fifth, $t_5(s)$] term in the series for the soft mass $M_{\Upsilon(1S)}(s)$ [cf. Eqs. (5.36a)-(5.39a)] varies between the penultimate term $t_4(s)$ of these series, and its negative $-t_4(s)$, these two cases correspond to the upper and the lower entry of (s/us) uncertainty of $\overline{m}_b$, respectively. In the (F)APT case the exact renormalon cancellation was not achieved and the parameter $k_{s/us}$ was varied between 0.1 and 10, i.e., $k_{s/us} = 1.0^{+9.0}_{-0.9}$.

The other uncertainty in the determination of $\overline{m}_b$ comes from the uncertainty of the Λ scale. In (F)APT it comes from $\overline{\Lambda}_5 = 0.260 \pm 0.030$ GeV and is denoted by the subscript (Λ) in Eq. (5.32a). In the 2δanQCD model and in the two pQCD approaches (the Lambert scheme and $\overline{\rm MS}$ scheme), this uncertainty comes from $\alpha_s(M_Z^2; \overline{\rm MS}) = 0.1184 \pm 0.007$ [56] and is denoted by the subscript (α_s) in Eqs. (5.33a), (5.34a), and (5.35a).

Yet another uncertainty of $\overline{m}_b$, in the 2δanQCD model and in Lambert scheme pQCD, comes from the variation of the (Lambert) renormalization scheme parameter $c_2 = -4.76^{+2.66}_{-0.97}$, and is denoted in Eqs. (5.33a) and (5.34a) by the subscript (c_2). The scheme in (F)APT was fixed by the underlying pQCD solution: $c_2 = c_3 = \cdots = 0$, i.e., effectively the two-loop solution.

The uncertainty due to the variation of the soft renormalization scale μ_s was denoted in Eqs. (5.32)-(5.35) by the subscript (μ_s). We varied μ_s^2 around the central value $(Q_s^2)_{\rm centr.}$ of the soft reference scale, between $2(Q_s^2)_{\rm centr.}$ and $(1/2)(Q_s^2)_{\rm centr.}$. The scale $(Q_s^2)_{\rm centr.}$ is determined by Eqs. (5.21), (5.22) and (5.24) in pQCD, 2δanQCD and (F)APT, respectively, for central values of the input parameters $\overline{m}_b$, $k_{s/us}$, etc.

Finally, the uncertainty $\delta m_b(m_c \neq 0) = \pm 0.005$ GeV due to nonzero c mass [Eq. (5.8; cf. also Eqs. (5.11)-(5.14)] results in the uncertainties ∓ 0.005 GeV of $\overline{m}_b$, denoted in Eqs. (5.32)-(5.35) by the subscript (m_c).

We see in Eqs. (5.32)-(5.35) that the largest resulting uncertainty in the determination of $\overline{m}_b$ is the one originating from the uncertainty of the determination of the us binding energy (except in (F)APT where $|E_{b\bar{b}}(us)|$ values are small). These uncertainties are larger in the two pQCD approaches, due to the influence of the nearby (unphysical) Landau singularities in the running couplings. The contribution of the us regime to the quarkonium mass, in the 2δanQCD model and in pQCD, increases the predicted value of $\overline{m}_b$. This is so because the us binding energies are in these cases significant and negative; cf. also Fig. 5.1(a). If we had ignored the existence and separation of the us contributions, i.e., if we had used in the entire binding energy $E_{b\bar{b}}$ simply a common soft renormalization scale $\mu_s \sim Q_s$, the predicted values of $\overline{m}_b$ in the 2δanQCD model and in Lambert and $\overline{\rm MS}$ pQCD would have decreased, by -0.068, -0.091, and -0.177 GeV, respectively, as can be deduced from the us-origin uncertainties in Eqs. (5.33a)-(5.35a). On the other hand, in (F)APT the choice $\mu_{us} = Q_{s,(\rm (F)APT)}$ would only slightly increase the central value of $\overline{m}_b$, by 0.002 GeV [cf. Eq. (5.32a)], basically because the values of $|E_{b\bar{b}}(us)|$ in (F)APT are much smaller; cf. Fig. 5.1(b).

We wish to address here briefly the question of nonperturbative (NP, higher-twist) contribution to the quarkonium mass. In the heavy quark system such as $b\bar{b}$, the NP contribution can be estimated, and in the leading order it comes from the gluon condensate and is given by [130]

$$E_{b\bar{b}}(us)^{(\rm NP)} \approx \overline{m}_b \pi^2 \frac{624}{425} \left(\frac{4\pi}{3} \overline{m}_b \right)^{-4} \frac{1}{a^4_{\rm pt}(\mu^2_{us})} \langle \frac{\alpha_s}{\pi} G_{\mu\nu} G^{\mu\nu} \rangle \ . \tag{5.43}$$

The factor $1/a^4_{\rm pt}(\mu^2_{us})$ in (four-loop) $\overline{\rm MS}$ pQCD is unreliable for realistic us scales $\mu_{us} \approx 1$ GeV, due to the vicinity of the Landau singularities (cf. footnote 4). In the 2δanQCD model, for purposes of estimation, we replace $1/a^4_{\rm pt}(\mu^2_{us})$ by $1/\mathcal{A}_4(\mu^2_{us})$ or by $1/\widetilde{\mathcal{A}}_4(\mu^2_{us})$. In the interval (1.1 GeV $< \mu_{us} <$ 1.3 GeV) we have $\mathcal{A}_4 \sim \widetilde{\mathcal{A}}_4 \sim 10^{-4}$; the couplings $\mathcal{A}_4$ and $\widetilde{\mathcal{A}}_4$ cover in this interval the values between 0.5×10^{-4} and 2×10^{-4}. For these values, and using the central value of the gluon condensate $\langle (\alpha_s/\pi) G^2 \rangle = 0.009$ GeV^2 [131] (cf. also Refs. [133] and [132]), and for $\overline{m}_b = 4.3$ GeV, we obtain the following estimate:

$$E_{b\bar{b}}(us)^{(\rm NP)} = 0.05^{+0.05}_{-0.02} \ \text{GeV} \ . \tag{5.44}$$

This effect is relatively small and has large uncertainties. If we take it into account, then the central extracted values of $\overline{m}_b$ in this subsection decrease somewhat, the decrease being $(\triangle \overline{m}_b)_{(\rm NP)} \approx (-0.025^{-0.025}_{+0.010})$ GeV.

We wish to comment briefly on the following aspect: the results of this subsection show that the extracted values $\overline{m}_b$ and various uncertainties $\delta\overline{m}_b$ are similar in the 2δanQCD model and the corresponding Lambert pQCD. The main reason for this lies in the fact that the scheme parameters (c_j, $j \geq 2$) are the same in both frameworks, and that the two corresponding running couplings practically merge at high momenta $|Q^2| > \Lambda^2$: $\mathcal{A}_1(Q^2) - a_{\rm pt}(Q^2) \sim (\Lambda^2/Q^2)^5$. Nonetheless, the evaluation methods for these two cases differ somewhat due to the different types of truncations involved. In pQCD, the quantities $2m_b$ and $E_{b\bar{b}}$ were calculated as truncated series of powers $a_{\rm pt}^n$, truncated at $a_{\rm pt}^4$ and $a_{\rm pt}^5$, respectively. In the 2δanQCD model, they were effectively calculated as series in logarithmic derivatives $\widetilde{\mathcal{A}}_n$, truncated at $\widetilde{\mathcal{A}}_4$ and $\widetilde{\mathcal{A}}_5$, respectively; namely, the analytic power analogs $\mathcal{A}_n$ in $2m_q$ were evaluated as a series in $\widetilde{\mathcal{A}}_k$'s up to $k = 4$, and in $E_{b\bar{b}}$ as a series in $\widetilde{\mathcal{A}}_k$'s up to $k = 5$.

For comparison, we present in Table 5.1 a list of extracted values of $\overline{m}_b$ (and $\overline{m}_c$) by various methods in the literature: lattice calculations, sum rules (pQCD+OPE), and from meson spectra (pQCD). The latter pQCD calculations account for the renormalon cancellation, but most of them either do not consider the ultrasoft contributions, or they include them unseparated from the soft contributions (using the same scale in the soft and the ultrasoft). We can see that (F)APT results agree with those of the usual pQCD calculations of the quarkonium spectrum and those of the sum rules (pQCD+OPE). The 2δanQCD results are incompatible with those results, but are compatible with the results of lattice calculations. The same can be claimed for the estimates of our pQCD approach (in the Lambert and $\overline{\rm MS}$ schemes), but the uncertainties there, coming principally from the ultrasoft sector, are larger, especially in $\overline{\rm MS}$ scheme.

5.3.2 Charm mass extraction

In this case, $q\bar{q} = c\bar{c}$, and the quarkonium mass is now $M_{J/\psi(1S)} = 3.0969$ GeV [56]. We basically repeat the analysis as in the case of $b\bar{b}$. There are some differences, though (see Ref. [105]):

- The relation (5.9) is now at $N_f = 3$; therefore, the transition to the relation at the soft renormalization scales, Eq. (5.11), which is also at $N_f = 3$, has now no threshold transition complication.
- The typical soft reference scales [Eqs. (5.21) and (5.23)] are now significantly lower: $Q_s \approx 1$ GeV or even lower (in the $b\bar{b}$ case we had: $Q_s \approx 2$ GeV). This, in conjunction with our suggestion that the considered models 2δanQCD and pQCD (in the Lambert and $\overline{\rm MS}$ schemes) are not necessarily to be trusted at scales below 1.1 GeV, implies that the typical soft renormalization scales μ_s

Table 5.1: Values of $\overline{m}_b$ and $\overline{m}_c$ masses extracted from lattice calculations, sum rules (pQCD+OPE) or from quarkonium spectrum (pQCD).

reference (year)	method	$\overline{m}_b$ (GeV)	$\overline{m}_c$ (GeV)
ETM (2011) [134, 135]	lattice ($N_f = 2$)	4.29 ± 0.14 ([134])	1.28 ± 0.04 ([135])
GST (2008) [136]	lattice (quenched)	4.42 ± 0.06	–
DGPS (2006) [137]	lattice (quenched)	4.347 ± 0.048	–
DGPTP (2003) [138]	lattice (quenched)	4.33 ± 0.10	1.319 ± 0.028
Narison (2011) [139]	sum rules	4.177 ± 0.011	1.261 ± 0.016
HPQCD (2010) [141]	sum rules[a]	4.164 ± 0.023	1.279 ± 0.006
CKMM *et al.* (2009) [140]	sum rules	4.163 ± 0.016	1.279 ± 0.013
PS (2006) [142]	sum rules	4.19 ± 0.06	–
BCS (2006) [143]	sum rules	4.205 ± 0.058	1.295 ± 0.015
LKW (2011) [144]	spectrum	$4.18^{+0.05}_{-0.04}$	$1.28^{+0.07}_{-0.06}$
CCG (2003) [145]	spectrum	4.24 ± 0.07	–
Lee (2003) [146]	spectrum	4.20 ± 0.04	–
BSV (2001) [111]	spectrum	$4.19 \pm 0.02 \pm 0.025$	–
Pineda 2001 [147]	spectrum	$4.210 \pm 0.090 \pm 0.025$	$1.210 \pm 0.070 \pm 0.079$
This work	spectrum	4.16 ± 0.02 ((F)APT)	1.257 ± 0.012 ((F)APT)
		4.35 ± 0.08 (2δanQCD)	1.266 ± 0.017 (2δanQCD)
		4.38 ± 0.11 (pQCD Lamb.)	1.265 ± 0.027 (pQCD Lamb.)
		4.50 ± 0.23 (pQCD $\overline{\text{MS}}$)	1.272 ± 0.078 (pQCD $\overline{\text{MS}}$)

[a]Uses sum rules with lattice input.

should be chosen significantly higher than Q_s. We choose $\mu_s^2 = (3 \pm 1)Q_s^2$ in these three models. In this case, the lowest possible soft scale, $(\mu_s)_{\rm min} = \sqrt{2}Q_s$ is slightly above 1.1 GeV. In (F)APT, the soft renormalization scale will also be varied in this way, giving, however, somewhat lower central value for the renormalization scale:, $\mu_s = \sqrt{3}Q_{s,(({\rm F})\rm APT)} \approx 1.004$ GeV.[5] The scale variation $\mu_s^2 = (3 \pm 1)Q_s^2$ results in small uncertainties $(\delta \overline{m}_c)_{(\mu_s)}$ of the extracted mass $\overline{m}_c$, but these uncertainties may be underestimated because $\mu_s^2 > Q_s^2$.

- In general, the cancellation of the leading renormalon now implies for the s-us separation parameter $k_{s/us}$ such values for which the absolute values of $E_{c\bar{c}}(us)$ are significantly smaller than in the $b\bar{b}$ case, and consequently, the us ambiguities are smaller. Since we now use for the central choice of the soft renormalization scale $\mu_s^2 = 3Q_s^2$, $E_{c\bar{c}}(us)$ is calculated in the 2δanQCD model and in pQCD in the following way:

$$E_{c\bar{c}}(us) = \frac{1}{2}\left[E_{c\bar{c}}(us; 3Q_s^2) + E_{c\bar{c}}(us; 1.1^2 {\rm GeV}^2)\right] \pm \frac{1}{2}\left[E_{c\bar{c}}(us; 3Q_s^2) - E_{c\bar{c}}(us; 1.1^2 {\rm GeV}^2)\right] \ , \quad (5.45)$$

  where the soft reference scale Q_s in the 2δanQCD model is determined by Eq. (5.23)[6] and in pQCD by Eq. (5.21). In (F)APT, we do not have practical problems at low scales $\mu < 1.1$ GeV, and the us energy as a function of low scale μ_{us} turns out to have a moderate local maximum and a moderate local minimum; hence we use

$$E_{c\bar{c}}(us; ({\rm F})\rm APT) = \frac{1}{2}\left[E_{c\bar{c}}(us)_{\rm max} + E_{c\bar{c}}(us)_{\rm min}\right] \pm \frac{1}{2}\left[E_{b\bar{b}}(us)_{\rm max} - E_{c\bar{c}}(us)_{\rm min}\right] \ , \quad (5.46)$$

  where these values are quite small: in the central case ($\overline{m}_c = 1.257$, $k_{s/us} = 1.0$), the local maximum is $E_{c\bar{c}}(us)_{\rm max} \approx +0.003$ GeV and is reached at $\mu_{us} \approx 0.71$ GeV, and the local minimum is $E_{c\bar{c}}(us)_{\rm min} \approx -0.006$ GeV and is reached at very low scale $\mu_{us} \approx 0.11$ GeV [cf. Fig. 5.2(b)].

- The exact renormalon cancellation requirement in (F)APT gives again an exceedingly small value of the s-us separation parameter, $k_{s/us} \approx 3 \times 10^{-9}$. In (F)APT we vary the parameter $k_{s/us}$ again around its central chosen value 1.0, in the interval between 0.1 and 10.x, just as it was done in the $b\bar{b}$ case of (F)APT.

The described behavior of the $E_{c\bar{c}}(us; \mu_{us}^2)$ in the analytic 2δanQCD model and in pQCD in the two schemes, as a function of the ultrasoft scales μ_{us}, is presented in

[5] If we used in (F)APT a lower definition of the central renormalization scale, $\mu_s = Q_{s,(({\rm F})\rm APT)}$ (≈ 0.58 GeV), the predicted central value of $\overline{m}_c$ would go up by only 0.005 GeV.

[6] Note that in the 2δanQCD model in the $c\bar{c}$ case the condition (5.22) cannot be fulfilled.

Fig. 5.2(a), and in the case of (F)APT in Fig. 5.2(b). Comparing Figs. 5.2(a) and

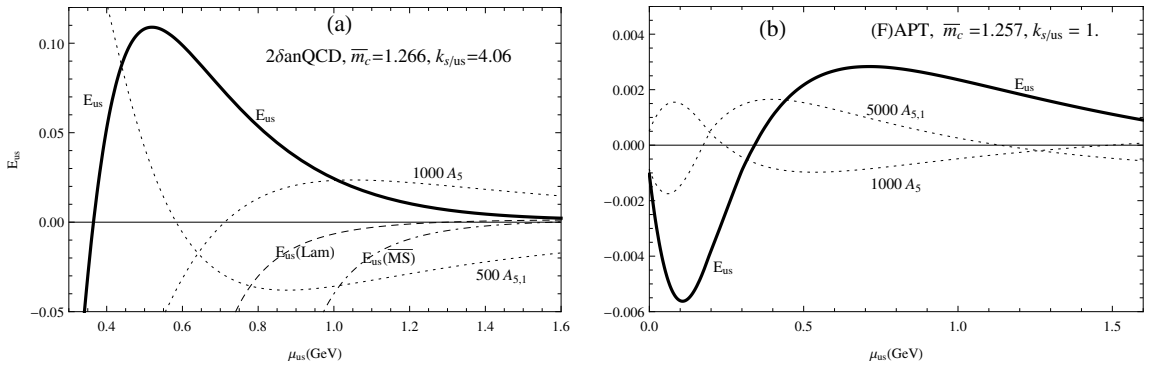

Figure 5.2: (a) Ultrasoft binding energy $E_{c\bar{c}}(us)$ (in GeV) as a function of the us renormalization scale μ_{us}, for the central input values of the 2δanQCD model for the $J/\psi(1S)$ system ($\overline{m}_c = 1.266$ GeV; $k_{s/us} = 4.06$; $c_2 = -4.76$; $s_0 = 23.06$): solid line for 2δanQCD; dashed line for Lambert pQCD ($c_2 = -4.76$); dash-dotted line for the four-loop $\overline{\rm MS}$ pQCD ($c_2 = 4.471$). For all three curves the same $\overline{m}_c$ and $k_{s/us}$ values are used. Included are the properly rescaled 2δanQCD couplings $\mathcal{A}_5(\mu_{us}^2)$ and $\mathcal{A}_{5,1}(\mu_{us}^2)$ as functions of the scale μ_{us}. (b) Same as in (a), but for the (F)APT model (with $c_2 = 4.471$), with the corresponding central values of that model ($\overline{m}_c = 1.257$ GeV and $k_{s/us} = 1$). In all the curves $N_f = 3$ was taken.

(b), we see that $|E_{c\bar{c}}(us)| \sim 10^{-2}$-$10^{-1}$ GeV in the 2δanQCD model, and $\sim 10^{-3}$ GeV in (F)APT. Furthermore, comparing with the corresponding curves in Figs. 5.1(a) and (b) for the $b\bar{b}$, we can see that in the 2δanQCD model and in the two pQCD approaches, the absolute values $|E_{c\bar{c}}(us)|$ are by almost two orders of magnitude smaller than $|E_{b\bar{b}}(us)|$, principally because the renormalon cancellation gives us in the two cases significantly different s-us separation parameter values: $k_{s/us}(c\bar{c}) = 4.06$ and $k_{s/us}(b\bar{b}) = 0.238$. Further, the values of $|E_{q\bar{q}}(us)|$ (for $q = c, b$) in pQCD are larger than in the 2δanQCD model, especially in $\overline{\rm MS}$ pQCD. In the (F)APT case, the values of $|E_{q\bar{q}}(us)|$ ($q = c, b$) are quite small, being in $c\bar{c}$ case smaller by almost one order of magnitude. All this is reflected also in the numerical results of this and of the previous subsection.

The resulting extracted values of $\overline{m}_c$ are

$$\overline{m}_c(\text{(F)APT}) = \left\{1.257 \mp 0.002_{(us)} \mp 0.002_{(s/us)} \mp 0.011_{(\Lambda)} \right. \quad (5.47a)$$
$$\left. \mp 0.002_{(\mu_s)}\right\} \text{ GeV} = 1.257 \pm 0.012 \text{ GeV} , \quad (5.47b)$$

with $\sqrt{3}Q_{s,(\text{(F)APT})} = 1.00$GeV and $k_{s/us} = 1.0$.

$$\overline{m}_c(2\delta\text{anQCD}) = \Big\{1.266 \pm 0.003_{(us)} \pm 0.007_{(s/us)} \mp 0.005_{(\alpha_s)} + \begin{pmatrix} -0.014 \\ +0.003 \end{pmatrix}_{(c_2)} \tag{5.48a}$$

$$+ \begin{pmatrix} -0.002 \\ +0.005 \end{pmatrix}_{(\mu_s)} \Big\} \text{ GeV} = 1.266 \pm 0.017 \text{ GeV} , \tag{5.48b}$$

with $\sqrt{3}Q_s = 1.42$ GeV and $k_{s/us} = 4.06$.

$$\overline{m}_c(\text{pQCDLamb.}) = \Big\{1.265 \pm 0.001_{(us)} + \begin{pmatrix} +0.021 \\ -0.021 \end{pmatrix}_{(s/us)} \mp 0.004_{(\alpha_s)}$$

$$\pm 0.000_{(c_2)} + \begin{pmatrix} -0.003 \\ +0.015 \end{pmatrix}_{(\mu_s)} \Big\} \text{ GeV} \tag{5.49a}$$

$$= 1.265 \pm 0.027 \text{ GeV} , \tag{5.49b}$$

with $\sqrt{3}Q_s = 1.38$ GeV and $k_{s/us} = 5.59$.

$$\overline{m}_c(\text{pQCD}\overline{\text{MS}}) = \Big\{1.272 \mp 0.011_{(us)} + \begin{pmatrix} +0.066 \\ -0.075 \end{pmatrix}_{(s/us)} \mp 0.002_{(\alpha_s)} \tag{5.50a}$$

$$+ \begin{pmatrix} -0.003 \\ +0.017 \end{pmatrix}_{(\mu_s)} \Big\} \text{ GeV} = 1.272 \pm 0.078 \text{ GeV} , \tag{5.50b}$$

with $\sqrt{3}Q_s = 1.58$ GeV and $k_{s/us} = 3.08$.
Below we show the renormalon cancellation in the sum for the soft mass $M_{J/\psi(1S)}(s) = 2m_c + E_{c\bar{c}}(s)$ for the central input values of parameters $\overline{m}_c$, μ_s $(= \sqrt{3}Q_s)$ and $k_{s/us}$; separately we present also $E_{c\bar{c}}(us)$.

$$M_{J/\psi(1S)}(s; (\text{F})\text{APT}) = 2.513 + 0.354 + 0.146 + 0.062 + 0.023 \text{ GeV} \tag{5.51a}$$

$$E_{c\bar{c}}(us; (\text{F})\text{APT}) = -0.001 \pm 0.004 \text{ GeV} , \tag{5.51b}$$

with $\overline{m}_c = 1.257$ GeV and $k_{s/us} = 1.0$.

$$M_{J/\psi(1S)}(s; 2\delta\text{anQCD}) = 2.531 + 0.296 + 0.157 + 0.103 + 0.000 \text{ GeV} \tag{5.52a}$$

$$E_{c\bar{c}}(us; 2\delta\text{anQCD}) = 0.010 \mp 0.006 \text{ GeV} , \tag{5.52b}$$

with $\overline{m}_c = 1.266$ GeV and $k_{s/us} = 4.06$).

$$M_{J/\psi(1S)}(s; \text{pQCDLamb.}) = 2.530 + 0.293 + 0.161 + 0.099 + 0.000 \text{ GeV} \tag{5.53a}$$

$$E_{c\bar{c}}(us; \text{pQCDLamb.}) = 0.013 \mp 0.003 \text{ GeV} , \tag{5.53b}$$

with $\overline{m}_c = 1.265$ GeV and $k_{s/us} = 5.59$.

$$M_{J/\psi(1S)}(s; \text{pQCD}\overline{\text{MS}}) = 2.544 + 0.302 + 0.185 + 0.099 + 0.000 \text{ GeV} \quad (5.54a)$$
$$E_{c\bar{c}}(us; \text{pQCD}\overline{\text{MS}}) = -0.034 \pm 0.024 \text{ GeV} , \quad (5.54b)$$

with $\overline{m}_c = 1.272$ GeV and $k_{s/us} = 3.08$.

The nonperturbative (NP) contribution coming from the gluon condensate, cf. Eq. (5.43) for the $b\bar{b}$ system in the previous subsection, is unreliable for the lighter $c\bar{c}$ system, since the next-to-leading corrections are in this case large and tend to make the result unreliable, cf. Ref. [148].

Comparing the results for $\overline{m}_c$ in this subsection with those for $\overline{m}_b$ in the previous subsection, we see that the soft-ultrasoft separation parameter $k_{s/us}$ in the 2δanQCD model and pQCD is now larger: $k_{s/us} \approx$ 3-5, while in $\overline{m}_b$ case we had $k_{s/us} \approx$ 0.2-0.3. This is a consequence of the requirement of the leading renormalon cancellation. As a result, the ultrasoft contributions to the $J/\psi(1S)$ mass are by an order of magnitude smaller (in absolute value) than those to the $\Upsilon(1S)$ mass, surprisingly. The extracted values of $\overline{m}_c$ thus suffer from less (ultrasoft) uncertainty than the extracted values of $\overline{m}_b$. On the other hand, in (F)APT, the ultrasoft sector is always suppressed, a consequence of the suppressed (F)APT couplings in the infrared.

The extracted values of $\overline{m}_c$ obtained in this work, in all four models, are compatible with all those obtained in the literature (from lattice, sum rules, and spectrum calculations), as can be seen from Table 5.1.

5.4 Summary

The use of the analytic QCD models was motivated by the fact that the typical soft (s) momentum scales Q_s in the ground bound states of quarkonia are low ($Q_s \approx 2$ GeV and 1 GeV, for $b\bar{b}$ and $c\bar{c}$, respectively), and that the typical ultrasoft (us) momentum scales Q_{us} are even lower. This, in conjunction with the fact that Landau singularities of the pQCD coupling $a_{\text{pt}}(Q^2)$ reach relatively high momenta: $Q \approx 0.61$ GeV in the usual (four-loop) $\overline{\text{MS}}$ scheme (with $c_2 \equiv \beta_2/\beta_0 = 4.471$), and $Q \approx 0.26$ GeV in the Lambert scheme ($c_2 = -4.76$). So we can apply in analytic QCD generally more natural renormalization scales at which the pQCD couplings are sometimes "out of control."
Analytic QCD approaches which at high energies follow the pQCD behavior closely (such as the 2δanQCD model) indicate that the ultrasoft regime in the $\Upsilon(1S)$ quarkonium ($b\bar{b}$) is important. Our approach, together with the leading renormalon cancellation condition, gives us clues about how to estimate the effects of the ultrasoft regimes

in pQCD. In both the 2δanQCD model and in pQCD we obtain, as a consequence, extracted values of $\overline{m}_b$ which are significantly higher ($\overline{m}_b \geq 4.3$ GeV) than most of those ($\overline{m}_b \approx 4.2$ GeV) obtained in the sum rule approaches (which use pQCD+OPE) and in the usual pQCD calculations of meson spectra. These approaches usually either do not include the ultrasoft contributions, or they include them unseparated from the soft contributions (i.e., the ultrasoft and soft scales are set to be equal). As an additional consequence, the uncertainties in the extracted values of $\overline{m}_b$ in our approach are dominated by the ultrasoft sector and are, especially in pQCD in the $\overline{\text{MS}}$ scheme, larger than in the usual pQCD approaches. Further, the extracted values of $\overline{m}_b$ in the 2δanQCD model, $\overline{m}_b \approx (4.35 \pm 0.08)$ GeV, are compatible with those of lattice calculations; cf. Table 5.1. On the other hand, the 2δanQCD model indicates that the ultrasoft regime in the $J/\Psi(1S)$ quarkonium ($c\bar{c}$) is less important, principally because the leading renormalon cancellation condition results in smaller ultrasoft coefficients in this system. The extracted values, $\overline{m}_c \approx (1.27 \pm 0.02)$ GeV, are compatible with those of pQCD (or pQCD+OPE) approaches, and those of the lattice calculations. On the other hand, the (F)APT of Shirkov *et al.*, suppresses the infrared contributions because the higher order couplings in (F)APT are more strongly suppressed in the infrared than the 2δanQCD couplings. The extracted values in (F)APT, $\overline{m}_b \approx (4.16 \pm 0.02)$ GeV and $\overline{m}_c \approx (1.26 \pm 0.01)$ GeV, are compatible with those obtained from the sum rules and from the usual pQCD spectrum calculations.

Chapter 6

Deep Inelastic Scattering

The goal in this chapter is to apply FAPT to the calculation of moments of structure functions, and to see the effects of analytization in low-Q^2 region of DIS [149]

6.1 Elastic Electron-Muon Scattering

The process of initial interest is the $e-\mu$ scattering, since this process will give us the notion of how to deal with the calculus of cross sections and how relate this simple process (simple in the sense of that is the well known special case of lepton-lepton scatternig) with others more complicated.
In Fig.1 we show the scattering of $e(k)+\mu(p) \to e(k')+\mu(p')$ in the lowest order of perturbation theory.
We know that the nonpolarized cross section is proportional to the square of the amplitude summed over final spins and averaged over initial spins, this can be written as

$$d\sigma = \frac{1}{4} \sum_{r,s,r',s'} |F_{sr;s'r'}|^2 \equiv \left(\frac{e^2}{q^2}\right)^2 L_{\mu\nu} M^{\mu\nu}, \tag{6.1}$$

where $L_{\mu\nu}$ is the symmetric electronic (leptonic) tensor:

$$\begin{aligned} L_{\mu\nu} &= 2\left[k'_\mu k_\nu + k'_\nu k_\mu + (m_e^2 - kk')g_{\mu\nu}\right] \\ &= 2\left[k'_\mu k_\nu + k'_\nu k_\mu + \frac{q^2}{2} g_{\mu\nu}\right], \end{aligned} \tag{6.2}$$

and $M_{\mu\nu}$ is the symmetric muon tensor:

$$M_{\mu\nu} = 2\left[p'^\mu p^\nu + p'^\nu p^\mu + \frac{q^2}{2} g_{\mu\nu}\right]. \tag{6.3}$$

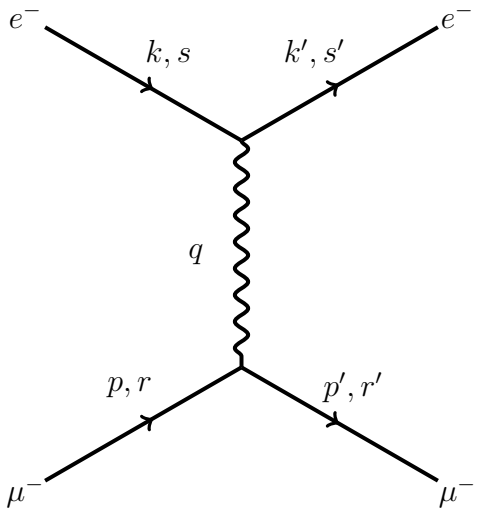

Figure 6.1: The lowest order contribution (one-photon exchange approximation) for $e\mu$ scattering amplitude.

Contracting these two tensors (neglecting the electron mass in the ultrarelativistic limit and considering the system such that the muon is in the rest frame: $p^\mu = (M, \vec{0})$), the following nonpolarized cross section is obtained

$$\frac{d\sigma}{d\Omega} = \left\{ \frac{\alpha^2}{4E^2 \sin^4(\theta/2)} \frac{E'}{E} \cos\left(\frac{\theta}{2}\right) \right\} \times \left(1 - \frac{q^2 \tan^2\left(\frac{\theta}{2}\right)}{2M^2} \right), \tag{6.4}$$

where θ is the scattering angle of the electron and $\alpha = e^2/4\pi$ is the electromagnetic fine structure constant. And we separate the cross section in two factors, the first one representing the typical non-structure contribution and the second factor appears due to the spin-1/2 nature of the muon.
Similar to the $e\mu \to e\mu$ scattering case is the $e^+e^- \to \mu^+\mu^-$ scattering, whose non-polarized cross section is obtained in a similar way

$$\frac{d\sigma}{d\Omega} = \frac{\alpha^2}{4q^2}(1 + \cos^2\theta), \tag{6.5}$$

where $q^2 = s$ is the square of the e^+e^- energy in the center of mass system of e^+e^-, and θ is the angle between e^+ and μ^+ in this system.

6.2 Electron-Neutron Scattering

6.2.1 Elastic *e-n* Scattering

The process of interest as a first approximation to the deep inelastic scattering (DIS) is the elastic *en* scattering (in general *lepton-hadron*) depicted in Fig. 2.
The matrix elements of the vertex function have the general covariant structure

$$\bar{u}(P')\Gamma_\mu u(P) = \bar{u}(P')\left[A\gamma_\mu + BP'_\mu + CP_\mu + iDP'^\nu\sigma_{\mu\nu} + iEP^\nu\sigma_{\mu\nu}\right]u(P), \qquad (6.6)$$

with constants A, B, C, D and E depending on Lorentz-invariant quantities, namely the momentum transfer square q^2 and the nucleon (hadron) mass M_N^2.
The general expression (6.6) can be reduced to a more compact structure when taking into account the gauge invariance

$$\bar{u}(P')\Gamma_\mu u(P) = \bar{u}(P')\left[A(q^2)\gamma_\mu + iB(q^2)q^\nu\sigma_{_\mu\nu}\right]u(P). \qquad (6.7)$$

Using (6.7) in the cross section calculus, we identify

$$\begin{aligned} W_{\mu\nu} &= \frac{1}{2}\sum_{S,S'}\left[\bar{u}(P')\Gamma_\mu u(P)\right]^*\left[\bar{u}(P')\Gamma_\mu u(P)\right] \\ &\equiv \left(-g_{\mu\nu} + \frac{q_\mu q_\nu}{q^2}\right)W_1(Q^2) + \left(P_\mu - q_\mu\frac{P\cdot q}{q^2}\right)\left(P_\nu - q_\nu\frac{P\cdot q}{q^2}\right)\frac{W_2(Q^2)}{M_N^2} \end{aligned} \qquad (6.8)$$

where

$$\begin{aligned} W_1(Q^2) &= (-q^2)\left(A(q^2) + 2M_N B(q^2)\right)^2 = Q^2\left(A(Q^2) + 2M_N B(Q^2)\right)^2, \\ W_2(Q^2) &= 4M_N^2\left(A^2(Q^2) + B^2(Q^2)Q^2\right), \end{aligned} \qquad (6.9)$$

with the spacelike notation for the momentum transfer energy $Q^2 = -q^2$ (> 0). We note that the gauge invariance relation is satisfied $q^\mu W_{\mu\nu} = q^\nu W_{\mu\nu} = 0$.
The leptonic part is the same as before (see Eq. (6.2) where $k \mapsto p$), with $m_e \neq 0$ for the moment.
Finally, the unpolarized cross section is obtain in the form

$$\frac{d^2\sigma}{dE'd\Omega} = \frac{E'}{E}\frac{\alpha^2}{Q^4}L^{\mu\nu}W_{\mu\nu}, \qquad (6.10)$$

in the n-rest frame (or laboratory system), where $P_\mu = (M_N, \vec{0})$, $p_\mu = (E, \vec{p})$ and $p'_\mu = (E', \vec{p}')$. This can be written in the well known "*Rosenbluth formula*" form as in QED:

$$\frac{d^2\sigma}{dE'd\Omega} = 4E'^2\frac{\alpha^2}{Q^4}\left[2\sin^2\left(\frac{\theta}{2}\right)W_1(Q^2) + \cos^2\left(\frac{\theta}{2}\right)W_2(Q^2)\right]. \qquad (6.11)$$

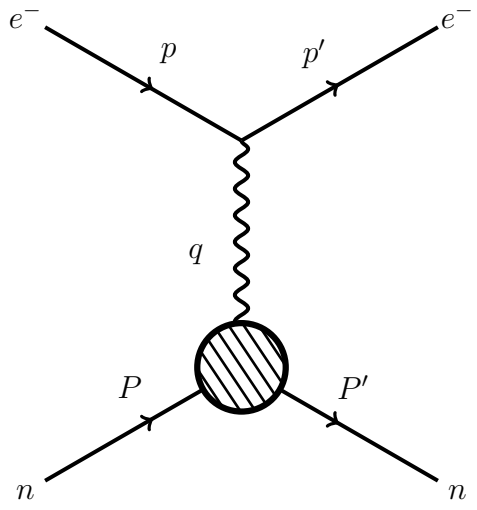

Figure 6.2: Elastic en scattering amplitude in the lowest order approximation.

Here, θ is the angle between the electrons (initial and final) in the n-rest frame. The main difference between the behavior of cross sections in the case of scattering on a pointlike particle (lepton) μ and a particle with internal structure (hadron) n is the strong dependence on Q^2 in the $W_{1,2}$ functions (later we will identify them in terms of structure functions).

6.2.2 Inelastic *e-n* Scattering

In the inelastic case, the change in comparison with the general structure of the expression (6.8) is that now the Lorentz invariant quantities (q^2 and $P \cdot q$) are independent of each other. Therefore, we express $W_{\mu\nu}$ in the general case as (maintaining the gauge, parity and time invariance)

$$W_{\mu\nu} = \left(-g_{\mu\nu} + \frac{q_\mu q_\nu}{q^2}\right) W_1(Q^2, \nu) + \left(P_\mu - q_\mu \frac{P \cdot q}{q^2}\right)\left(P_\nu - q_\nu \frac{P \cdot q}{q^2}\right) \frac{W_2(Q^2, \nu)}{M_N^2}, \tag{6.12}$$

where the explicit Lorentz invariant independent quantities are

$$q^2 = (p - p')^2 = -Q^2, \qquad \nu = P \cdot q. \tag{6.13}$$

The leptonic (tensor) is given by (6.2) (with $k \mapsto p$, $k' \mapsto p'$). When we replace these expression for $W_{\mu\nu}$ in (6.12) and for $L_{\mu\nu}$ in (6.2) replacing into the unpolarized cross

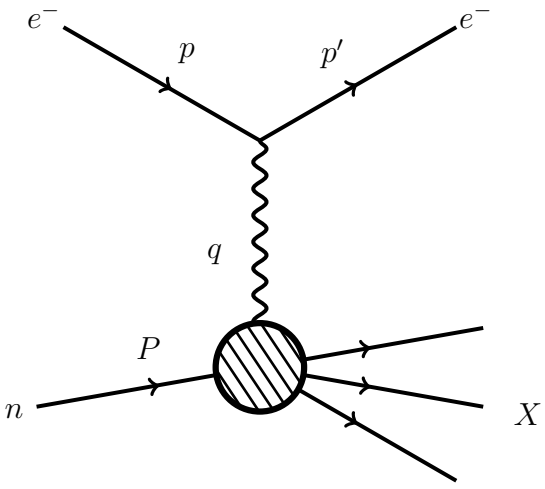

Figure 6.3: Inelastic *en* scattering amplitude to the lowest order approximation.

section (6.10) we obtain

$$\begin{aligned}\frac{d^2\sigma}{dE'd\Omega} &= \frac{E'\alpha^2}{EQ^4}2(2p^\mu p^\nu - g^{\mu\nu}p\cdot p')\left[\left(-g_{\mu\nu}+\frac{q_\mu q_\nu}{q^2}\right)W_1(Q^2,\nu)\right.\\ &\left.+\left(P_\mu - q_\mu\frac{P\cdot q}{q^2}\right)\left(P_\nu - q_\nu\frac{P\cdot q}{q^2}\right)\frac{W_2(Q^2,\nu)}{M_N^2}\right], \qquad (6.14)\end{aligned}$$

where $p_\mu = (E,\vec{p})$ and $p'_\mu = (E',\vec{p'})$.
We neglect the electron mass and take into account that we are working in the laboratory system, i.e., the nucleon is at rest before the collision: $P_\mu = (M_N,\vec{0})$, $\nu = P\cdot q = M_N(E-E')$. Finally, we introduce the angle θ in the form: $\vec{p}\cdot\vec{p'} = EE'\cos\theta$ (scattering angle of the electron with respect to the initial direction), which implies $Q^2 = 4EE'\sin^2(\theta/2)$.
With the considerations presented above, the scattering cross section is:

$$\frac{d^2\sigma}{dEd\Omega} = 4E'^2\frac{\alpha^2}{Q^4}\left[2\sin^2\left(\frac{\theta}{2}\right)W_1(Q^2,\nu)+\cos^2\left(\frac{\theta}{2}\right)W_2(Q^2,\nu)\right]. \qquad (6.15)$$

Using this final expression we can extract the structure functions $W_{1,2}$ from the experiment, where the (partial) cross section is measured at various θ and E'.
We can consider the same process, but from another point of view (other formalism), Using the local current operators:

$$\begin{aligned}W_{\mu\nu}(P,q) &= \frac{1}{4\pi}\sum_{pol.}\int d^4x e^{iq\cdot x}\langle P|\hat{J}_\mu(x)\hat{J}_\nu(0)|P\rangle\\ &= \frac{1}{4\pi}\sum_{pol.}\int d^4x e^{iq\cdot x}\langle P|[\hat{J}_\mu(x),\hat{J}_\nu(0)]|P\rangle, \qquad (6.16)\end{aligned}$$

where $|P\rangle$ is the vector state of the nucleon with momentum P and $\hat{J}$ is the electromagnetic current operator. In fact, from here it is straightforward to find the general structure (6.12) due to electromagnetic current conservation ($q_\mu W_{\mu\nu} = 0$ as was noted before) and it is straightforward to find the cross section (6.15).
This form, in terms of an algebra of local current, will be useful in the Operator Product Expantion (OPE) formalism.
In order to obtain the structure function information from the experiment, it is convenient to choose as the second parameter the ratio $x = Q^2/2\nu$ (as was noted by Bjorken [156]) rather than ν; x is called the Bjorken or scaling variable.
It is possible to deduce the range of the Bjorken variable $0 < x \leq 1$ from the following properties:

1. Elastic Scattering:

$$x = \frac{Q^2}{2\nu} = \frac{-q^2}{2P \cdot q} = \frac{-q^2}{-q^2} = 1$$

2. For the lighter produced state ($M_X > M_N$):

$$x = \frac{Q^2}{2\nu} = \frac{Q^2}{M_X^2 - M_N^2 + Q^2} = \frac{1}{1 + \frac{M_X^2 - M_N^2}{Q^2}} \approx 1 - \frac{M_X^2 - M_N^2}{Q^2}.$$

   This last approximation was made in the high energy assumption ($Q^2 \gg 0$) and implies that $x \leq 1$.

3. From (2) and with the physical range: $Q^2 > 0$ and $M_X^2 - M_N^2 > 1$ we have $x > 0$.

With this new variable x, we define (for convenience) the new structure functions

$$\begin{aligned} F_1(Q^2, x) &= M_N W_1(Q^2, x), \\ F_2(Q^2, x) &= \frac{\nu}{M_N} W_2(Q^2, x), \end{aligned} \tag{6.17}$$

and we define

$$y \equiv \frac{\nu}{M_N E}, \tag{6.18}$$

that is the fraction of the energy that the electron transfers to the hadron (nucleon). We will give an interpretation of x when we consider the parton model.
The cross section can be written in terms of the Bjorken variable

$$\frac{d^2\sigma}{dE' d\Omega} = \frac{E'}{2\pi M_N E y} \frac{d^2\sigma}{dx dy}, \tag{6.19}$$

where

$$\frac{d^2\sigma}{dxdy} = \frac{8\pi M_N E\alpha^2}{Q^4}\left[xy^2F_1(Q^2,x) + \left(1 - y - \frac{M_N xy}{2E}\right)F_2(Q^2,x)\right]. \tag{6.20}$$

The first experiment on charged lepton DIS at SLAC in 1968 [158] (and these data confirmed the convenience of the choice of the new variable x) provided us the following information for $Q^2 > 1\text{GeV}^2$:

$$\begin{aligned} F_1(Q^2,x) &\approx F_1(x), \\ F_2(Q^2,x) &\approx F_2(x), \end{aligned}$$

and

$$F_2 \approx 2xF_1.$$

We will see that these results can be confirmed theoretically, the first one via Bjorken scaling property and the second one with the Callan-Gross relation.

6.3 The Parton Model

The SLAC experiment (that Bjorken scaling take place) can be explained by the following proposal by Feynman [157]: "each hadron (in SLAC there were protons as target hadrons) contains some constituents called partons as pointlike spin-1/2 free objects".
We can formulate the parton model by considering the hadron (nucleon) as being made up of (three) partons, each of them participating in the scattering with e^-. Since each parton is assumed to be a point-like object with spin 1/2, it takes on the role of μ^- in the $e^-\mu^-$ scattering, where now $\nu = M_N(E - E')$ and $Q^2 = 4EE'\sin^2(\theta/2)$. Eq. (6.4) can be written as

$$\frac{d\sigma_i}{d\Omega} = \frac{\alpha^2 q_i^2}{4E^2}\frac{1}{\sin^4(\theta/2)}\frac{\left[\cos^2(\theta/2) - \frac{q^2}{2M_i^2}\sin^2(\theta/2)\right]}{1 + \frac{2E}{M_i}\sin^2(\theta/2)}, \tag{6.21}$$

where $q_i e_0$ is the electric charge and M_i the mass of the parton i.
At this point arises an evident problem: the partons can't stay at rest as we have assumed until now (in the laboratory system). It is easy to see this problem taking the momentum of parton i by

$$P_{i,\mu} = \xi_i P_\mu + \Delta P_{i,\mu}. \tag{6.22}$$

Here, the first term in the r.h.s of (6.22) represents the fraction of the hadron momentum that carries the parton i and the second term is the motion of the parton

inside the nucleon.
In order to solve the aforementioned problem, we can find a system where the nucleon has a very fast motion, called "Lorentz system" or "infine momentum frame" (see [150]) depending on the literature.
In this assumption the partons move very slow with respect to the hadron (nucleon in our case).
Taking the approximation of massless partons $M_i \approx 0$ as a good estimate in comparison with the experiment, we obtain

$$\begin{aligned} \frac{d\sigma_i}{dQ^2} &= \frac{4\pi\alpha^2 q_i}{Q^4}\left(\frac{(p+P_i)^4+(p'-P_i)^4}{2(p+P_i)^4}\right) \\ &\equiv \frac{4\pi\alpha^2 q_i}{Q^4}\left(\frac{s_i^2+u_i^2}{2s_i^2}\right), \end{aligned} \tag{6.23}$$

where the Mandelstam variables (that are the invariant quantities in our process) are

$$\begin{aligned} s_i &= (p+P_i)^2 = (p'+P_i')^2, \\ u_i &= (p'-P_i)^2 = (p+P_i')^2. \end{aligned} \tag{6.24}$$

We can change to a new frame system, namely "Breit system", where:

$$\begin{gathered} q_\mu = (0,0,0,\sqrt{-q^2}) = (0,0,0,\sqrt{Q^2}), \\ P_\mu = (\tilde{P},0,0,-\tilde{P}); \qquad \tilde{P} \gg M_N; \qquad P^2 = 0 \approx M_N^2. \end{gathered} \tag{6.25}$$

From Eq. (6.23), with conditions (6.25), the elastic electron-parton scattering can be rewritten as

$$\frac{d\sigma_i}{dQ^2} = \frac{4\pi\alpha^2 q_i^2}{Q^4}\left(\frac{s^2+u^2}{2s^2}\right). \tag{6.26}$$

6.3.1 Callan-Gross Relation

In order to compare with inelastic scattering, we need to rewrite (6.26) in terms of x and y. For this purpose, we note that $P_i'^2 \approx 0 = (P_i+q)^2 = (\xi_i P+q)^2 \approx 2\xi_i P\cdot q + q^2$, that leads to the following important result:

$$\xi_i = \frac{Q^2}{2P\cdot q} = x. \tag{6.27}$$

This means that the Bjorken variable x represents (only in the Breit system) the fraction of the total hadron momentum that carries the struck parton i.
Based on this conclusion, we have

$$\frac{d\sigma_i}{dxdy} = \delta(\xi_i - x)\frac{d\sigma_i}{dy}. \tag{6.28}$$

And as $Q^2 = 2(P \cdot q)x = 2M_N(E - E')x = 2M_N Exy = sxy$, we have

$$dQ^2 = sxdy = s\frac{Q^2}{s+u}dy. \tag{6.29}$$

Therefore, putting (6.28) and (6.29) into (6.26), we obtain

$$\frac{d\sigma_i}{dxdy} = \frac{2\pi\alpha^2 q_i^2}{Q^4}\frac{(s^2+u^2)}{s^2}\delta(\xi_i - x)\frac{Q^2 s}{s+u}. \tag{6.30}$$

Finally, we sum over all partons i and all possible fractions of momentum ξ_i, with

$$\int_0^\infty d\xi_i f(\xi_i) \tag{6.31}$$

where $f(\xi_i)$ is the weight function or the distribution of probability to find a parton i with momentum $\xi_i P$ in the hadron.
From these considerations, the total cross section is given by

$$\frac{d^2\sigma}{dxdy} = \frac{2\pi\alpha^2 s}{Q^4}\frac{(s^2+u^2)}{s^2}\sum_i f_i(x)q_i^2 x. \tag{6.32}$$

On the other hand, when rewriting (6.20) in terms of invariant variables, we have

$$\frac{d^2\sigma}{dxdy} = \frac{4\pi\alpha^2 s}{Q^4}\left[xy^2 F_1(Q^2,x) + \left(1 - y - \frac{xyM_N^2}{s}\right)F_2(Q^2,x)\right] \tag{6.33}$$

From the fact that $F_{1,2}$ are dimensionless, it is natural to assume that they depend on x (that is known as "scaling" and was found by Bjorken [156] and Feynman [157] in terms of the quark parton model (QPM)):

$$F_1(Q^2,x) = F_1(x); \qquad F_2(Q^2,x) = F_2(x). \tag{6.34}$$

Using this, and equating (6.32) with (6.33), we obtain

$$F_1(x) = \frac{1}{2}\sum_i f_i(x)q_i^2; \qquad F_2(x) = \sum_i f_i(x)q_i^2 \cdot x. \tag{6.35}$$

Therefore, we deduce the well known Callan-Gross relation [159] (as was noted before):

$$F_2(x) = 2xF_1(x) \tag{6.36}$$

6.4 DGLAP Equations

6.4.1 Motivation

First, we will show the central reason for the need to consider gluons (i.e., QCD) in our description of DIS.
We denote by $q(x)$ ($\bar{q}(x)$) the momentum distribution function for a quark flavor q (antiquark $\bar{q}$), where $q = u, d$. The structure functions are

$$\begin{aligned} F_2^{ep}(x) &= \sum q^p(x) q_i^2 x = \frac{4}{9}(u^p(x) + \bar{u}^p(x))x + \frac{1}{9}(d^p(x) + \bar{d}^p(x))x, \\ F_2^{en}(x) &= \sum q^n(x) q_i^2 x = \frac{4}{9}(u^n(x) + \bar{u}^n(x))x + \frac{1}{9}(d^n(x) + \bar{d}^n(x))x. \end{aligned} \quad (6.37)$$

Due to the isospin symmetry, we can relate the momentum distribution functions of the quarks inside the proton (p) with the quarks inside the neutron (n) in the form: $u^p(x) = d^n(x) \equiv u(x)$ and $d^p(x) = u^n(x) \equiv d(x)$. Therefore, the total structure function is given by

$$\begin{aligned} F_2(x) &= \frac{1}{2}\left(F_2^{ep}(x) + F_2^{en}(x)\right) \\ &= \frac{5}{18}[(u(x) + \bar{u}(x)) + (d(x) + \bar{d}(x))]x. \end{aligned} \quad (6.38)$$

Now, the total moment due to the partons ($P_\mu^{(\text{parton})}$) which we have considered until now is

$$P_\mu^{(parton)} = \int_0^1 dx (x P_\mu^{(\text{parton})})[u(x) + \bar{u}(x) + d(x) + \bar{d}(x) + s(x) + \ldots]. \quad (6.39)$$

This implies

$$\int_0^1 dx x[u(x) + \bar{u}(x) + d(x) + \ldots] = 1 \quad (6.40)$$

Therefore with (6.38), we obtain

$$\frac{18}{5}\int_0^1 dx F_2(x) = 1 \quad (6.41)$$

When we test experimentally, we sum over all possible x values of the structure function, and the result is one half, instead of 1 as in (6.41). We have an expression for the total momentum that is incomplete. Therefore, we need to add to the total momentum the momentum carried by the interaction partons, i.e., "gluons".
With this, we conclude that we must take the radiative corrections to the DIS into account, and with this we will obtain the well known DGLAP (Dokshitzer-Gribov-Lipatov-Altarelli-Parisi) integro-differential equations.

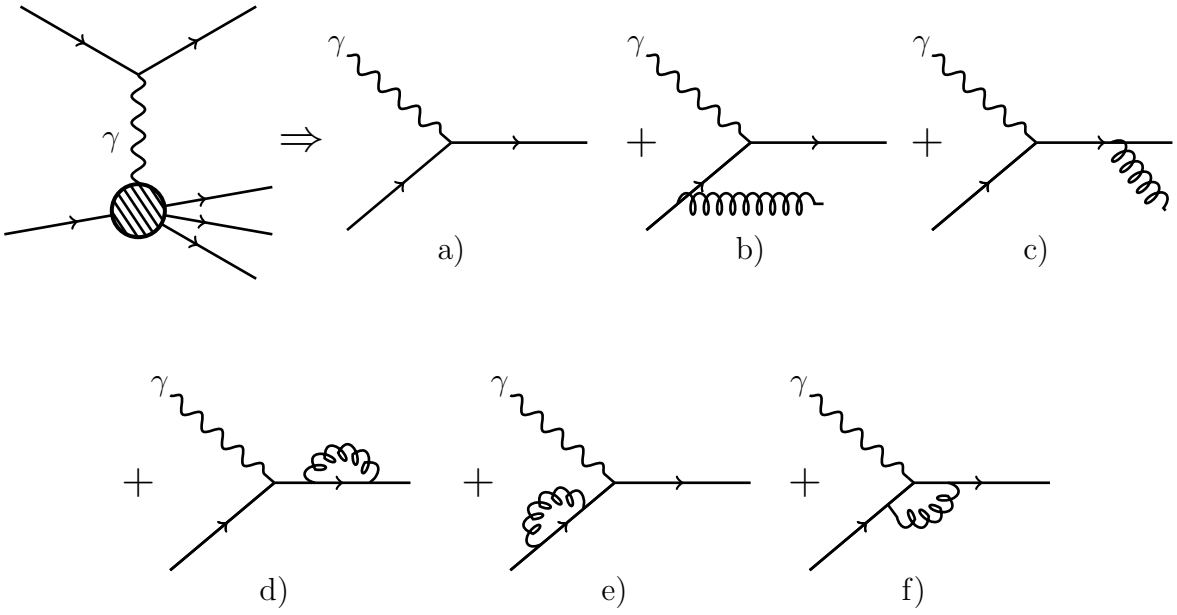

Figure 6.4: The first Feynman diagrams for radiative corrections in DIS, where DIS involves scattering of photon off a quark. We denote by q, p, P and K the four-momenta of the photon, quark, hadron and gluon respectively. a) free quark (parton model); b) and c) radiation of a gluon ("gluon Bremsstrahlung") for the incoming and outgoing quark respectively, d) and e) first correction to the quark propagator, and f) gluon loop for quark-photon vertex.

6.4.2 DGLAP: Taking Radiative Corrections Into Account

As mentioned, DGLAP equations are the radiative corrections to the distribution functions in the parton model of DIS. For this purpose, we take the lowest correction (leading order in perturbation theory). This is the emission of a gluon before and after the photon interaction with the quark (parton) in question inside the hadron. We identify this as "gluon Bremsstrahlung" (like in QED). This contribution is shown in Fig. 6.4b and Fig. 6.4c, respectively. Hereafter we use the notation q, p, P and K for the four-momenta of the photon, quark, hadron and gluon respectively.

These two first corrections are governed by the following current operators:

$$\begin{aligned} J_\mu^{(b)}(x) &= \int \bar{\psi}(x) Q_f \gamma_\mu S(x-y) \frac{\lambda^a}{2} g G_\nu^a \gamma^\nu \psi(y) d^4y, \\ J_\mu^{(c)}(x) &= \int \bar{\psi}(y) \frac{\lambda^a}{2} g \gamma_\mu G^{a\nu} S(y-x) Q_f \gamma^\mu \psi(x) d^4y, \end{aligned} \tag{6.42}$$

where $S(x-y)$ is the quark propagator, $G_\mu^a(x)$ the gluon field, λ^a the Gell-Mann

matrices, and Q_f the electric charge of the quark with flavor f.
Here we have eigenvalues and not operators, since when the quarks are free particles, we can replace the nucleon state $|N\rangle$ by free quark state $|\psi\rangle$ in the hadronic function ($\hat{J}_\mu|\psi\rangle = J_\mu|\psi\rangle$). The current correlator in the nucleon is

$$\begin{aligned} W_{\mu\nu} &= \frac{1}{2\pi}\int d^4x \mathrm{e}^{iqx}\frac{1}{2}\sum_{pol.}\langle N|\hat{J}_\mu(x)\hat{J}_\nu(0)|N\rangle, \\ &= \frac{1}{2\pi}\int d^4x \mathrm{e}^{iqx}\frac{1}{2}\sum_{pol.}\sum_{part.} J_\mu(x)J_\nu(0). \end{aligned} \tag{6.43}$$

Neglecting the quark masses and replacing (6.42) in (6.43) ($J_\mu(x) = J_\mu^{(b)}(x)+J_\mu^{(c)}(x)$) we have

$$W_{\mu\nu} = \frac{g^2Q_f^2}{3(2\pi)^3}S_{\mu\nu}\Theta(k_0)\Theta(p_0+q_0-k_0)\delta(k^2)\delta[(p+q-k)^2], \tag{6.44}$$

where S_μ^μ and $p^\mu p^\nu S_{\mu\nu}$ (since we contract the hadronic with the leptonic part, only these two quantities survive in the calculus) in terms of Mandelstam variables are given by

$$\begin{aligned} S_\mu^\mu &= -8\left(\frac{2\nu-Q^2}{t}+\frac{t}{2\nu-Q^2}+\frac{2Q^2(2\nu+t)}{t(2\nu-Q^2)}\right) \\ &= -8\left(\frac{s}{t}+\frac{t}{s}-2\frac{Q^2u}{st}\right), \end{aligned} \tag{6.45}$$

$$p^\mu p^\nu S_{\mu\nu} = -4(2\nu+t) = 4u \tag{6.46}$$

where

$$\begin{aligned} t &= (p-k)^2 \simeq -2p\cdot k, \\ s &= (p+q)^2 \simeq 2p\cdot q, \\ u &= (q-k)^2 \simeq -2p\cdot(q-k), \\ Q^2 &= -q^2 \simeq 2(q+p)\cdot(p-k). \end{aligned} \tag{6.47}$$

Combinig (6.45) and (6.46) with (6.44), we obtain

$$\begin{aligned} p^\mu p^\nu W_{\mu\nu} &= \frac{4}{3}\alpha_s\frac{Q_f^2}{8\pi}2\nu, \\ W_\mu^\mu &= \frac{4}{3}\alpha_s\frac{Q_f^2}{4\pi}\left(2\frac{1+x^2}{1-x}\ln\left(\frac{\lambda^2x}{Q^2}\right)-\frac{1}{1-x}+4\frac{x}{1-x}\right), \end{aligned} \tag{6.48}$$

with $x = Q^2/2\nu$, λ^2 is the cutoff that appears from $-\lambda^2$ in the integral.
In this treatment with gluons, there appears an explicit dependence on Q^2 as a new

variable in the structure functions [160].
In order to identify the structure functions $F_{1,2}$, we write

$$W_{\mu\nu} = \left(-g_{\mu\nu} + \frac{q_\mu q_\nu}{q^2}\right) F_1 + \frac{1}{\nu}\left(p_\mu - q_\mu \frac{p\cdot q}{q^2}\right)\left(p_\nu - q_\nu \frac{p\cdot q}{q^2}\right) F_2. \tag{6.49}$$

This is the same expression as the one obtained by inserting (6.17) into (6.12) but now we forget the factor $1/M_N$ for convenience, since we are taking massless quarks. Comparing (6.48) with (6.49), we obtain

$$\begin{aligned} p^\mu p^\nu W_{\mu\nu} &= \frac{Q^2}{8x^3}(F_2 - 2xF_1) = \frac{4}{3}\alpha_s \frac{Q_f^2}{8\pi} 2\nu, \\ W_\mu^\mu &= -3F_1 + \frac{F_2}{2x} \\ &= \frac{4}{3}\alpha_s \frac{Q_f^2}{4\pi}\left(2\frac{1+x^2}{1-x}\ln\left(\frac{\lambda^2 x}{Q^2}\right) - \frac{1}{1-x} + 4\frac{x}{1-x}\right). \end{aligned} \tag{6.50}$$

Therefore

$$\begin{aligned} F_1(x,Q^2) &= -\frac{1}{2}W_\mu^\mu + \frac{2x^2}{Q^2} p^\mu p^\nu W_{\mu\nu}, \\ F_2(x,Q^2) &= -xW_\mu^\mu + 12\frac{x^3}{Q^2} p^\mu p^\nu W_{\mu\nu}. \end{aligned} \tag{6.51}$$

In Eqs (6.50)-(6.51) we can see an explicit violation of the Callan-Gross relation (6.36). Generalization of (6.35) when we introduce the Q^2 dependence gives ($X = Q^2/2P_N\cdot q$, $x = Q^2/2p\cdot q$ and Q_i the charge of the ith parton)

$$\begin{aligned} F_2(X,Q^2) &= \sum_i f_i(X,Q^2) Q_i^2 X \\ &= \sum_i \int_0^1 d\xi_i f_i(\xi_i, Q^2) Q_i^2 \xi_i \delta(\xi_i - X) \end{aligned} \tag{6.52}$$

where

$$p_\mu = \xi_i P_\mu, \qquad \int_0^1 d\xi_i f(\xi_i) = 1. \tag{6.53}$$

Here, ξ_i represents the fraction of the total momentum (hadron momentum) that carry the parton i, and $f(\xi_i)$ is the density of probability to have a parton i with momentum $p_\mu = \xi_i P\mu$.
Each quark has its own structure function in the form (6.52). Therefore, if we want to obtain the nucleon structure function, we need to sum over all quark structure

functions:

$$\begin{aligned} F_2(X,Q^2) &= \sum_i \int_0^1 d\xi_i F_2^i(\xi_i,Q^2) Q_i^2 \xi_i \delta(\xi_i - X) \\ &= \sum_i \int_0^1 d\xi_i f_i(\xi_i)\xi_i \int_0^1 \delta(X - x\xi_i) F_2^i(\xi_i,Q^2), \end{aligned} \tag{6.54}$$

since $x = X/\xi_i$.
Now, we need an explicit form of the Q^2-dependence of the structure function. From (6.50) and (6.51), we have $F_2^i = F_2$ from the first radiative correction (corresponding only to gluon Bremsstrahlung, i.e., diagrams b and c in Fig. 6.4)

$$\begin{aligned} \Delta F_2(x,Q^2) &= \frac{4}{3}\alpha_s x \frac{Q_f^2}{4\pi}\left(6x + 2\frac{1+x^2}{1-x}\ln\left(\frac{\lambda^2 x}{Q^2}\right) - \frac{1}{1-x} + \frac{x}{1-x}\right) \\ &\simeq -\frac{4}{3}\alpha_s Q_f^2 \frac{x}{2\pi}\frac{1+x^2}{1-x}\ln(\lambda^2 Q^2) \end{aligned} \tag{6.55}$$

valid for $Q^2 \gg 1\text{GeV}^2$.
Therefore, the Q^2 variation gives: (the variation is between two energies Q_{in}^2 and Q_{fin}^2)

$$\begin{aligned} \Delta F_2(x,Q_{fin}^2,Q_{in}^2) &\equiv \Delta F_2(x,Q_{fin}^2) - \Delta F_2(x,Q_{in}^2) \\ &= \sum_i \int_0^1 d\xi_i f(\xi_i)\xi_i \int_0^1 dx \delta(X - x\xi_i)\Delta F_2^i(x,Q_{fin}^2,Q_{in}^2) \\ &= \frac{4}{3}\alpha_s \frac{1}{2\pi}\sum_i Q_i^2 \int_X^1 d\xi_i f(\xi_i)\frac{X}{\xi_i}\frac{1+(X/\xi_i)^2}{1-(X/\xi_i)}\ln\left(\frac{Q_{fin}^2}{Q_{in}^2}\right) \end{aligned} \tag{6.56}$$

Finally, including the corrections d, e and f of Fig. 6.4 we obtain:

$$\Delta F_2(x,Q_{fin}^2,Q_{in}^2) = \frac{4}{3}\frac{\alpha_s}{2\pi}\sum_i Q_i^2 \ln\left(\frac{Q_{fin}^2}{Q_{in}^2}\right)\int_X^1 d\xi_i f(\xi_i)\frac{X}{\xi_i}\left[\frac{1+(X/\xi_i)^2}{1-(X/\xi_i)}\right]_+, \tag{6.57}$$

where for a regular function $F(z)$ we have introduced the notation

$$\int_0^1 F(z)\left[\frac{1+z^2}{1-z}\right]_+ = \int_0^1 F(z)\left[F(z) - F(1)\right]\frac{1+z^2}{1-z}. \tag{6.58}$$

From (6.56) (not forgetting where this expression arises from), we have:

$$x\Delta F_2^i(x,Q_{fin}^2,Q_{in}^2) = \frac{4}{3}\frac{\alpha_s}{2\pi}\ln\left(\frac{Q_{fin}^2}{Q_{in}^2}\right)\int_x^1 d\xi_i F_2^i(\xi_i)\frac{x}{\xi_i}\left[\frac{1+(x/\xi_i)^2}{1-(x/\xi_i)}\right]_+. \tag{6.59}$$

Introducing the notation $y \equiv \xi = \xi_i$ (hereafter, we will omit the index "i"), $t(Q^2) \equiv \ln\left(\frac{Q^2}{Q_0^2}\right)$ and $P_{qq}(z) \equiv \frac{4}{3}\left[\frac{1+z^2}{1-z}\right]_+$, we rewrite (6.59)

$$\frac{\Delta F_2(x,t)}{\Delta t} = \frac{\alpha_s}{2\pi}\int_x^1 \frac{dy}{y} F_2(y) P_{qq}(x/y). \tag{6.60}$$

Therefore, for small Δt, we have a coupling α_s that depends on Q^2 too (from pQCD). And transforming from discrete to continuum, we obtain the Dokshitzer-Gribov-Lipatov-Altarelli-Parisi (DGLAP) integro-differential [161] equations for $F_2(x,t)$:

$$\frac{dF_2(x,t)}{dt} = \frac{\alpha_s(t)}{2\pi}\int_x^1 \frac{dy}{y} F_2(y,t) P_{qq}\left(\frac{x}{y}\right) \tag{6.61}$$

Due to the fact that DGLAP equation is restricted to the perturbative regime, the strong coupling must be small. This implies that radiative processes appear at high and therefore take place (appear physically) only for very short time.
In this sense, P_{qq} represents the probability that the struck quark inside the hadron appears (or that the hadron splits up). For this reason we call P_{qq} "splitting function". In general, it is straightforward to see that P_{ab} corresponds to the breaking up of a parton of kind "a" into a parton of kind "b" when Q^2 increases. From the general expression for the DGLAP equation

$$\frac{\partial F_2(x_b,Q^2)}{\partial \ln Q^2} = \frac{\alpha_s(Q^2)}{2\pi}\sum_b \int_{x_b}^1 P_{ab}\left(\frac{x_b}{x_a}\right) F_2(x_a,Q^2)\frac{dx_a}{x_a}. \tag{6.62}$$

It is convenient to define the following complete quark and anti-quark distributions [$q(x) = \sum_i q_i(x)$ and $\bar{q}(x) = \sum_i \bar{q}_i(x)$, respectively]:

$$\begin{aligned}
\Sigma(x) &= q(x) + \bar{q}(x), \\
\Delta_{ij}(x) &= q_i(x) - q_j(x), \\
\bar{\Delta}_{ij}(x) &= \bar{q}_i(x) - \bar{q}_j(x), \\
V(x) &= q(x) - \bar{q}(x), \\
G(x) &= \text{gluon distribution.}
\end{aligned} \tag{6.63}$$

Note that $\Sigma(x)$ transforms as a singlet in the flavor symmetry group SU(4) of (u, d, c, s); and $\Delta_{ij}(x)$, $\bar{\Delta}_{ij}(x)$ and $V(x)$ are non-singlet under flavor symmetry. Therefore, $\Sigma(x)$ is called singlet distribution function, and $\Delta_{ij}(x)$, $\bar{\Delta}_{ij}(x)$ and $V(x)$ non-singlet distribution functions. They have their corresponding DGLAP equations

$$\begin{aligned}
\frac{d\Delta_{ij}(x,t)}{dt} &= \frac{\alpha_s(t)}{2\pi}\int_x^1 \frac{dy}{y}\Delta_{ij}(y,t) P_{qq}\left(\frac{x}{y}\right), \\
\frac{d\Sigma(x,t)}{dt} &= \frac{\alpha_s(t)}{2\pi}\int_x^1 \frac{dy}{y}\left[\Sigma(y,t) P_{qq}\left(\frac{x}{y}\right) + 2N_f G(y,t) P_{qG}\left(\frac{x}{y}\right)\right], \\
\frac{dG(x,t)}{dt} &= \frac{\alpha_s(t)}{2\pi}\int_x^1 \frac{dy}{y}\left[\Sigma(y,t) P_{Gq}\left(\frac{x}{y}\right) + G(y,t) P_{GG}\left(\frac{x}{y}\right)\right],
\end{aligned} \tag{6.64}$$

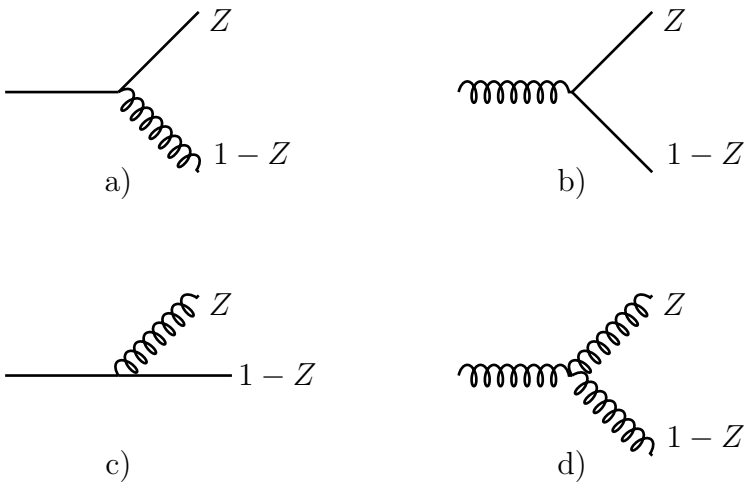

Figure 6.5: All processes to first order that describe the splitting functions: a) $P_{qq}(Z)$, b) $P_{qG}(Z)$, c) $P_{Gq}(Z)$, d) $P_{GG}(Z)$

where the splitting functions P_{qG}, P_{Gq} and P_{GG} correspond to the remaining processes that were not considered until now (see Fig. 6.5). The splitting functions were calculated in [161].
The relation between SFs (e.g. F_2) and parton distribution functions (q_i, G) is in general a convolution

$$F_2(x,Q^2) = x\int_0^1 \frac{dy}{y}\sum_i e_i^2 q_i(y,Q^2)C_q\left(\frac{x}{y},a(Q^2)\right) + \sum_j e_j^2 G(y,Q^2)C_g\left(\frac{x}{y},a(Q^2)\right), \tag{6.65}$$

where C_q and C_g are the (Wilson) coefficient functions which will be consider in the next sections. At the parton level $C_q(z,a) = \delta(1-z)$, $C_g = 0$, while at the beyond-the -parton level we have

$$\begin{aligned} C_q(z,a(Q^2)) &= \delta(1-z) + \frac{1}{2}a(Q^2)C_q^1(z) + \mathcal{O}(a^2), \\ C_g(z,a(Q^2)) &= \frac{1}{2}a(Q^2)C_g^1(z) + \mathcal{O}(a^2), \end{aligned} \tag{6.66}$$

where, us usual, $a(Q^2) \equiv \alpha_s/\pi$.
The SF $F_2(x,Q^2)$ has the nonsinglet (NS) and singlet (S) part, $F_2 = F_2^{NS} + F_2^S$. For $x \geq 0.25$ only the NS part contributes. We will approximate $F_2 \approx F_2^{NS}$.

The experimental evidence of the scaling behavior as well as their violation is depicted in Fig. 6.6. We see that at high energies ($Q^2 \gtrsim 10\text{GeV}^2$) the structure function $F_2(x,Q^2)$ (of the proton) is approximately independent of Q^2 for $x \gtrsim 0.005$. Therefore, the parton model is applied in this range of Q^2 and x: $Q^2 > 10\text{GeV}^2$ and

$x > 0.005$.
For very small x ($x \lesssim 0.005$), $F_2(x, Q^2)$ increases as Q^2 increases (in the regime of high energies). On the other hand, for large x ($x \gtrsim 0.7$), $F_2(x, Q^2)$ decreases as Q^2 increases. In this last range, parton model is not valid and we must consider another approach, namely QCD [inclusion of interactions between partons (quarks)] via gluons.

6.5 OPE and DIS

We will deduce in a more clear way (in order to find the generalization) the expansion into bilocal operators known as operator product expansion [163] (OPE). We start with the free field case.
The considered hadronic tensor is

$$\begin{aligned} W_{\mu\nu} &= \frac{1}{2\pi}\int d^4x \mathrm{e}^{iqx}\frac{1}{2}\sum_{pol}\langle N|\hat{J}_\mu(x)\hat{J}_\nu(0)|N\rangle \\ &= \frac{1}{2\pi}\int_{x^2\geq 0} d^4x \mathrm{e}^{iqx}\frac{1}{2}\sum_{pol}\langle N|[\hat{J}_\mu(x),\hat{J}_\nu(0)]|N\rangle, \end{aligned} \tag{6.67}$$

where in the second line we used $\langle N|\hat{J}_\mu(x)\hat{J}_\nu(0)|N\rangle = 0$ if $x^2 \geq 0$.
For free fields we have the current $\hat{\bar{J}}_\mu(x) = \hat{\bar{\psi}}(x)\gamma_\mu\hat{\psi}(x)$. Therefore:

$$[\hat{J}_\mu(x),\hat{J}_\nu(0)] = \hat{\bar{\psi}}(x)\gamma_\mu S(x)\gamma_\nu\hat{\psi}(0) - \hat{\bar{\psi}}(0)\gamma_\nu S(x)\gamma_\mu\hat{\psi}(x), \tag{6.68}$$

where the quark propagator is

$$\begin{aligned} S(x) &\equiv \{\hat{\psi}(x),\hat{\bar{\psi}}(0)\} = (i\gamma_\mu\partial^\mu + m)i\Delta(x) \\ &\approx \gamma_\mu\partial^\mu\frac{1}{2\pi}\epsilon(x_0)\delta(x^2), \end{aligned} \tag{6.69}$$

where the last approximation was made for $x^2 \mapsto 0$ and $\epsilon(x_0) \equiv sgn(x_0)$ is the sign function.
With this propagator we obtain

$$[\hat{J}_\mu(x),\hat{J}_\nu(0)] = \left(\hat{\bar{\psi}}(x)\gamma_\mu\gamma_\lambda\gamma_\nu\hat{\psi}(0) - \hat{\bar{\psi}}(0)\gamma_\nu\gamma_\lambda\gamma_\mu\hat{\psi}(x)\right)\frac{1}{2\pi}\partial^\lambda\epsilon(x_0)\delta(x^2). \tag{6.70}$$

Performing a translation by $-x/2$ (since we have translation invariance) in the arguments

$$[\hat{J}_\mu(x),\hat{J}_\nu(0)] = \frac{1}{2}\left([\hat{J}_\mu(x/2),\hat{J}_\nu(-x/2)] + [\hat{J}_\nu(x/2),\hat{J}_\mu(-x/2)]\right), \tag{6.71}$$

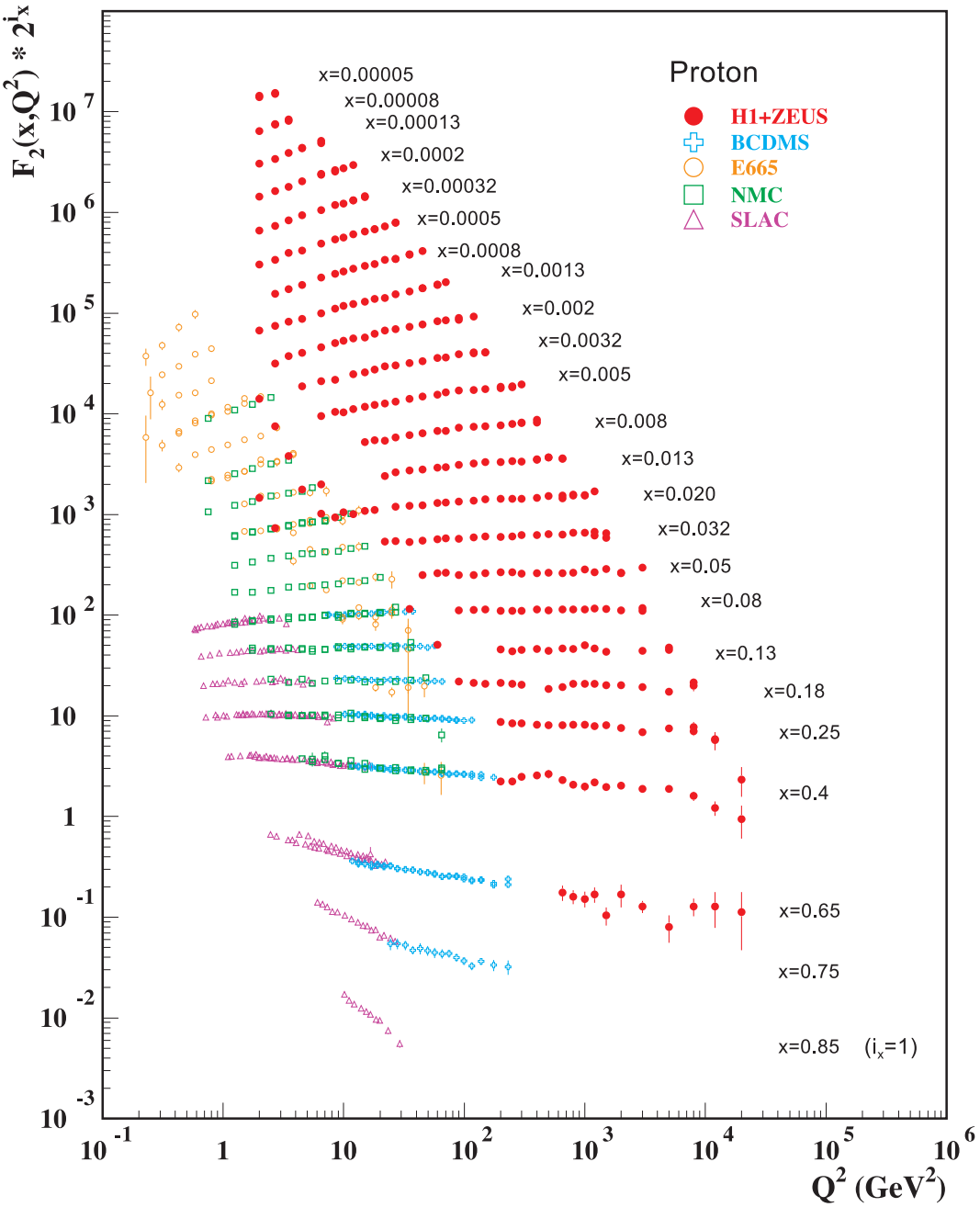

Figure 6.6: Non-singlet proton structure function $F_2(x, Q^2)$ versus Q^2. The authors (see Ref. [162] and reference therein), in order to present this plot without overlappings, multiplied $F_2(x, Q^2)$ by 2^{i_x}, where i_x is the number of x bin ($i_x = 1$ for $x = 0.85$, etc., up to $i_x = 24$ for $x = 0.00005$).

and using the relation of gamma functions:

$$\gamma_\mu\gamma_\lambda\gamma_\nu = (s_{\mu\lambda\nu\beta} + i\epsilon_{\mu\lambda\nu\beta})\gamma^\beta, \tag{6.72}$$

we obtain

$$\begin{aligned}\langle N|[\hat{J}_\mu(x/2), \hat{J}_\nu(-x/2)]|N\rangle &= \frac{1}{2\pi}\partial^\lambda\epsilon(x_0)\delta(x^2)\Big\{s_{\mu\lambda\nu\beta}\langle N|\hat{\bar{\psi}}(x/2)\gamma^\beta\hat{\psi}(-x/2) \\ &\quad -\hat{\bar{\psi}}(x/2)\gamma^\beta\hat{\psi}(-x/2)|N\rangle + i\epsilon_{\mu\lambda\nu\beta}\langle N|\hat{\bar{\psi}}(x/2)\gamma_5\gamma^\beta\hat{\psi}(-x/2) \\ &\quad -\hat{\bar{\psi}}(x/2)\gamma_5\gamma^\beta\hat{\psi}(-x/2)|N\rangle\Big\}. \end{aligned}\tag{6.73}$$

The first term corresponds to the UV divergencies (purely perturbative), and the second one (the term in $\{\ldots\}$) is a finite part (nonperturbative). All divergent factors will be absorbed into the well-known Wilson coefficient.
In order to extract the coefficients, we expand the bilocal operator $\hat{\bar{\psi}}(x/2)\hat{\psi}(-x/2)$ into a sum of local operators, by performing a translation (due to translation invariance of the theory, like Schr'odinger picture in quantum mechanics), and obtain

$$W_{\mu\nu} = \frac{1}{2\pi}\int_{x^2\geq 0} d^4x \mathrm{e}^{iqx}\sum_{nodd}\frac{1}{n!}\prod_{j=1}^{n}\left(\frac{x}{2}\right)^{\mu_j} s_{\mu\alpha\nu}{}^{\beta}\,\frac{1}{2}\sum_{pol}\langle N|\hat{O}_{\mu_1\mu_2\ldots\mu_n\beta}|N\rangle\frac{1}{\pi}\partial^\alpha(\epsilon(x_0)\delta(x^2)) \tag{6.74}$$

where $\hat{O}_{\mu_1\mu_2\ldots\mu_n\beta}(0) = \hat{\bar{\psi}}(0)\overleftrightarrow{\partial}_{\mu_1}\overleftrightarrow{\partial}_{\mu_2}\ldots\overleftrightarrow{\partial}_{\mu_n}\gamma_\beta\hat{\psi}(0)$, with $\overleftrightarrow{\partial}_\mu \equiv \partial_\mu - \overleftarrow{\partial}_\mu$.
Now, as a consequence of Lorentz covariance we can use the following expansion:

$$\frac{1}{2}\sum_{pol}\langle N|\hat{O}_{\mu_1\mu_2\ldots\mu_n\beta}(0)|N\rangle = A^{(n)}\cdot P_{\mu_1}P_{\mu_2}\cdots P_{\mu_n}P_\beta + \cdots. \tag{6.75}$$

where we neglect the singular terms, which are less important in the Bjorken limit. Using this one obtains

$$W_{\mu\nu} = \frac{1}{2\pi}\int_{x^2\geq 0} d^4x \mathrm{e}^{iqx}\sum_{nodd}\frac{1}{n!}\left[\frac{x\cdot P}{2}\right]^n s_{\mu\alpha\nu}{}^{\beta}\,P_\beta A^{(n)}\frac{1}{\pi}\partial^\alpha(\epsilon(x_0)\delta(x^2)). \tag{6.76}$$

When this is rewritten with the help of Fourier transform of

$$\sum_{nodd}\frac{1}{n!}\left[\frac{x\cdot P}{2}\right]^n\frac{A^{(n)}}{n!} = -\int d\xi \mathrm{e}^{ix\cdot\xi P}f(\xi), \tag{6.77}$$

we obtain

$$\begin{aligned} W_{\mu\nu} &= -2\int d\xi\; s_{\mu\alpha\nu}{}^{\beta}\,P_\beta f(\xi)(q+\xi P)^\alpha\delta\left[(q+\xi P)^2\right]\epsilon(q_0+\xi P_0) \\ &= -2\; s_{\mu\alpha\nu}{}^{\beta}\,P_\beta f(x)\frac{x}{Q^2}(q+xP)^\alpha, \end{aligned}\tag{6.78}$$

where the second line is obtained since $(q+\xi P)^2 \approx -Q^2 + 2\nu\xi = \frac{Q^2}{x}(\xi - x)$.
Finally, due to the current conservation ($q^\mu L_{\mu\nu} = q^\nu L_{\mu\nu} = 0$) and the fact that we are interested in $W_{\mu\nu}L^{\mu\nu}$ (which is proportional to the cross section) we discard terms proportional to q_μ (or q_ν) in $W_{\mu\nu}$, thus obtaining

$$\begin{aligned} W_{\mu\nu} &\approx -2\frac{x}{Q^2}f(x)\left[-g_{\mu\nu}(xM^2+\nu) + 2xP_\mu P_\nu\right] \\ &\approx -2\frac{x}{Q^2}f(x)\left[-\nu g_{\mu\nu} + 2xP_\mu P_\nu\right] \end{aligned} \tag{6.79}$$

We discard such terms also in the general form of $W_{\mu\nu}$ in (6.49):

$$W_{\mu\nu} = -g_{\mu\nu}F_1(x,Q^2) + \frac{1}{\nu}P_\mu P_\nu F_2(x,Q^2). \tag{6.80}$$

Comparing (6.79) with (6.80) we obtain

$$\begin{aligned} F_1(x,Q^2) &= -2\frac{x}{Q^2}\nu f(x), \\ \frac{F_2(x,Q^2)}{\nu} &= -4\frac{x^2}{Q^2}f(x). \end{aligned} \tag{6.81}$$

Therefore, the Callan-Gross relation [159], Eq. (6.36), is satisfied (scaling behavior holds for free field as was seen above)

6.5.1 Generalization: Taking quark interaction into account

In the bilocal operator, we need to expand now, in covariant derivatives $\hat{D}_\mu$ in (6.75), instead of the usual derivatives ∂_μ. For simplicity we take $\overleftrightarrow{\partial}_\mu \sim 2\partial_\mu \mapsto 2\hat{D}_\mu$. Therefore, in general (6.74) takes the form

$$\begin{aligned} W_{\mu\nu} &= \frac{1}{2\pi}\int d^4x e^{iqx}\sum_{j,n}\Big\{-g_{\mu\nu}x^{\mu_1}x^{\mu_2}\cdots x^{\mu_n} i^n C^{(n)}_{1,j}(x) \\ &\quad + \left(g_{\mu\mu_1}g_{\nu\mu_2}x^{\mu_3}\cdots x^{\mu_n}\right) i^{n-2}C^{(n)}_{2,j}(x)\Big\}\frac{1}{2}\sum_{pol}\langle N|\hat{O}^{(n),j}_{\mu_1\ldots\mu_n\beta}|N\rangle, \end{aligned} \tag{6.82}$$

since $W_{\mu\nu} \sim g_{\mu\nu}, P_\mu P_\nu$; $s_{\mu\alpha\nu}{}^\beta P_\beta \sim g_{\mu\nu}, g_{\mu\mu_1}g_{\nu\mu_2}$. The interaction implies new divergencies, in this sense we replace in the general case the terms of the type: $\frac{1}{\pi}\partial^\alpha(\epsilon(x_0)\delta(x^2)) \mapsto i^n C^{(n)}_{1,j}(x), i^{n-2}C^{(n)}_{2,j}(x)$, and $\hat{O}^{(n)}_{\mu_1\ldots\mu_n\beta} \mapsto \frac{2^n}{2n!}\hat{D}_{\mu_1}\ldots\hat{D}_{\mu_n}\gamma_\beta = \hat{O}^{(n),j}_{\mu_1\ldots\mu_n\beta}$. As $\hat{O}^{(n),j}_{\mu_1\ldots\mu_n\beta}$ change the flavor of a quark and act on the gluon, we have three possibilities for this: an $SU(3)$ singlet operator (operator that acts upon quark states $j = S$); and $SU(3)$ octet operator (operator that acts upon quark states and can

change the flavor $j = NS$); and the operator related to gluon states ($j = G$).
As in the previous subsection, we take (6.75) to the leading term ($A^{(n)} \mapsto A^{(n),j}$). In the momentum space we obtain

$$W_{\mu\nu} = \frac{1}{2\pi}\sum_{j,n}\left[-g_{\mu\nu}\left(\frac{2q\cdot P}{Q^2}\right)^n (Q^2)^n\left(\frac{\partial}{\partial q^2}\right)^n \int d^4x \mathrm{e}^{iqx} C_{1,j}^{(n)}(x)\right.$$
$$\left. + \frac{P_\mu P\nu}{2q\cdot P}\left(\frac{2q\cdot P}{Q^2}\right)^{n-1}(Q^2)^{n-1}\left(\frac{\partial}{\partial q^2}\right)^{n-2}\int d^4x \mathrm{e}^{iqx} C_{2,j}^{(n)}(x)\right] A^{(n),j}. \qquad (6.83)$$

Comparing (6.83) with (6.80) we obtain the general structure function

$$\begin{aligned} F_1(x,Q^2) &= 2\sum_{j,n} x^{-n}\tilde{C}_{1,j}^{(n)}(Q^2)A^{(n),j}, \\ F_2(x,Q^2) &= 4\sum_{j,n} x^{-n+1}\tilde{C}_{2,j}^{(n)}(Q^2)A^{(n),j}, \end{aligned} \qquad (6.84)$$

where

$$\begin{aligned} \tilde{C}_{1,j}^{(n)}(Q^2) &= \frac{1}{4\pi}(Q^2)^n\left(\frac{\partial}{\partial q^2}\right)^n\int d^4x \mathrm{e}^{iqx} C_{1,j}^{(n)}(x), \\ \tilde{C}_{2,j}^{(n)}(Q^2) &= \frac{1}{16\pi}(Q^2)^{n-1}\left(\frac{\partial}{\partial q^2}\right)^{n-2}\int d^4x \mathrm{e}^{iqx} C_{2,j}^{(n)}(x). \end{aligned} \qquad (6.85)$$

As we noted before, the Wilson coefficients $\tilde{C}_{1,j}^{(n)}$ and $\tilde{C}_{2,j}^{(n)}$ are obtained from pQCD (in general they are divergent functions) and are independent on the hadronic contribution. $A^{(n),j}$ are obtained by non-perturbative methods.
It's usual to rearrange the general expression for $W_{\mu\nu}$ using the relation

$$T\left\{J_\mu(x)J_\nu(0)\right\} - T\left\{J_\mu(x)J_\nu(0)\right\}^\dagger = \epsilon(x_0)\left[J_\mu(x), J_\nu(0)\right], \qquad (6.86)$$

where $T\ldots$ denotes the time ordered function, and $\epsilon(x_0)$ is the sign function and for the Compton scattering is equal to one ($x_0 > 0$)

$$T_{\mu\nu} = i\int d^4x \mathrm{e}^{iqx}\langle p|T\left\{\hat{J}_\mu(x)\hat{J}_\nu(0)\right\}|p\rangle. \qquad (6.87)$$

This implies

$$\begin{aligned} T_{\mu\nu} &= \left(-g_{\mu\nu}+\frac{q_\mu q_\nu}{q^2}\right)\tilde{F}_1(x,Q^2) + \left(p_\mu - q_\mu\frac{p\cdot q}{q^2}\right)\left(p_\nu - q_\nu\frac{p\cdot q}{q^2}\right)\frac{\tilde{F}_2(x,Q^2)}{p\cdot q} \\ &\equiv \left(-g_{\mu\nu}+\frac{q_\mu q_\nu}{q^2}\right)\tilde{F}_L(x,Q^2) \\ &\quad + \left(-g_{\mu\nu}+p_\mu p_\nu\frac{4x^2}{q^2} - (p_\mu p_\nu + p_\nu p_\mu)\frac{2x}{q^2}\right)\tilde{F}_2(x,Q^2), \end{aligned} \qquad (6.88)$$

where $F_{1,2}(x,Q^2) \equiv \frac{1}{\pi}\mathrm{Im}\tilde{F}_{1,2}(x,Q^2)$, since $W_{\mu\nu} = \frac{1}{\pi}\mathrm{Im}T_{\mu\nu}$, and for convenience we choose a new structure function $\tilde{F}_L \equiv \tilde{F}_2 - 2x\tilde{F}_1$ (it measures how much the scaling is violated).
With the help of projector operators $p_\mu p_\nu$ and $g_{\mu\nu}$, we find

$$\frac{\tilde{F}_L}{2x} = \frac{4x^2}{Q^2}p^\mu p^\nu T_{\mu\nu}; \qquad \frac{\tilde{F}_2}{2x} = -\frac{\tilde{F}_L}{2x} - \frac{g^{\mu\nu}}{2}T_{\mu\nu}. \tag{6.89}$$

Therefore, the problem is reduced to calculate terms of the form $T\{J_\mu(x)J_\nu(0)\}$, since we will have:

$$i\int d^4x \mathrm{e}^{iqx}\langle p|T\left\{\hat{J}_\mu(x)\hat{J}_\nu(0)\right\}|p\rangle = \sum_i \left[\tilde{C}_i(Q^2,\mu^2)\hat{O}_i(\mu^2)\right], \tag{6.90}$$

where $\tilde{C}_i(Q^2,\mu^2) = i\int d^4x \mathrm{e}^{iqx}C_i(x,\mu^2)$ are the Wilson coefficients.

6.5.2 Renormalization Group of Wilson Coefficient

The renormalized Wilson coefficients are

$$\tilde{C}^{(n)}_{i,j}(Q^2,g,\mu)_R = \sum_k Z^{(n)}_{jk}(g_0,\mu)\tilde{C}^{(n)}_{i,k}(Q^2,g_0), \tag{6.91}$$

where $g = g(g_0,\mu^2,Q^2)$ and $i = 1,2$.
From independence of renormalization scale μ we obtain (hereafter we omit subscript "R")

$$\frac{d}{d\mu}\tilde{C}^{(n)}_{i,j}(Q^2,g,\mu) = 0. \tag{6.92}$$

From here, it's straightforward to deduce the RGE for the Wilson coefficients

$$\sum_l \left[\left(\beta(g)\frac{\partial}{\partial g} + \mu\frac{\partial}{\partial\mu}\right)\delta_{jl} + \gamma^{(n)}_{jl}\right]\tilde{C}^{(n)}_{i,l}(Q^2,g,\mu) = 0, \tag{6.93}$$

where

$$\beta(g) = \frac{\partial g}{\partial\mu}, \qquad \gamma^{(n)}_{jl} = -\mu\sum_k \frac{\partial Z^{(n)}_{jk}}{\partial\mu}\left(Z^{(n)}_{jk}\right)^{-1}_{kl}. \tag{6.94}$$

Rewritten in terms of $t \equiv \frac{1}{2}\ln\frac{Q^2}{\mu^2}$, we have

$$\sum_l \left(\frac{d}{dt}\delta_{jl} + \gamma^{(n)}_{jl}\right)\tilde{C}^{(n)}_{i,l}(\bar{g}(g,t)) = 0, \tag{6.95}$$

giving

$$\tilde{C}^{(n)}_{i,l}(Q^2,g,\mu) = \sum_k \tilde{C}^{(n)}_{i,k}(Q^2,g,\mu)\mathrm{e}^{-\int_0^\infty dt'\gamma^{(n)}_{k,l}(\bar{g}(g,t'))}. \tag{6.96}$$

To the lowest order we have $\gamma^{(n)}_{k,l} = d^{(n)}_{k,l}\bar{g}^2 + \ldots$, $\bar{g}^2 = \frac{g^2}{1+2\beta_0 g^2 t}$, and we obtain

$$\begin{aligned}\tilde{C}^{(n)}_{i,l}(t,g) &= \sum_k C^{(n)}_{i,k}(Q^2,g,\mu)\left(\frac{\bar{g}^2(g,t)}{g^2}\right)^{d^{(n)}_{k,l}/2\beta_0} \\ &\sim \sum_k a^{(n)}_{i,l}\left(\frac{\bar{g}^2(g,t)}{g^2}\right)^{d^{(n)}_{k,l}/2\beta_0}.\end{aligned} \tag{6.97}$$

The last approximation was made for the high energy limit $t \gg 1$; $x \equiv cte$.

6.5.3 Moments of Structure Functions

We have identified in Eqs. (6.84) the structure functions in terms of Wilson coefficients. But a natural question arises: what is the explicit relation between these coefficients and the splitting functions? If we can answer this, the meaning of OPE will be clear (at least in the formal sense). A more general question that concerns us is what is the corresponding DGLAP equation?
In order to give an answer, we note that the inverse of Eqs. (6.84)are

$$\begin{aligned}2\sum_j \tilde{C}^{(n)}_{1,j}(Q^2)A^{(n),j} &= \frac{1}{2\pi i}\int_{\mathcal{C}} F_1(z,Q^2)z^{n-1}dz = 4\int_0^1 F_1(x,Q^2)x^{n-1}dx, \\ 4\sum_j \tilde{C}^{(n)}_{2,j}(Q^2)A^{(n),j} &= \frac{1}{2\pi i}\int_{\mathcal{C}} F_2(z,Q^2)z^{n-2}dz = 4\int_0^1 F_2(x,Q^2)x^{n-2}dx.\end{aligned} \tag{6.98}$$

Defining the moments of structure functions formally as

$$M_a(n,Q^2) = \int_0^1 F_a(x,Q^2)x^{n-2}dx = 2\pi i\sum_j \tilde{C}^{(n)}_{a;j}(Q^2)A^{(n),j} \tag{6.99}$$

we obtain:

$$\frac{\partial M_a(n,t)}{\partial t} = \frac{\alpha_s(t)}{2\pi}\sum_j M_{a,j}(n,t)D^{(n)}_j, \tag{6.100}$$

where $a = 1, 2$ (or $L, 2$) and $j = S; NS; G$ (the corresponding part of a that we are considering) and

$$\begin{aligned} D_{NS}^{(n)} &= -8\pi^2\gamma_{NS}^{(n)} = \int_0^\infty dz z^{n-1} P_{qq}(z), \\ D_{S}^{(n)} &= -8\pi^2\gamma_{S}^{(n)} = \int_0^\infty dz z^{n-1} \begin{pmatrix} P_{qq}(z) & P_{qG}(z) \\ P_{Gq}(z) & P_{GG}(z) \end{pmatrix}, \\ D_{G}^{(n)} &= -8\pi^2\gamma_{G}^{(n)} = \int_0^\infty dz z^{n-1} P_{GG}(z). \end{aligned} \tag{6.101}$$

The advantage of the moments approach is obvious, instead of integro-differential DGLAP equations we now have ordinary differential equations.

6.5.4 Anomalous Dimensions and Wilson coefficients

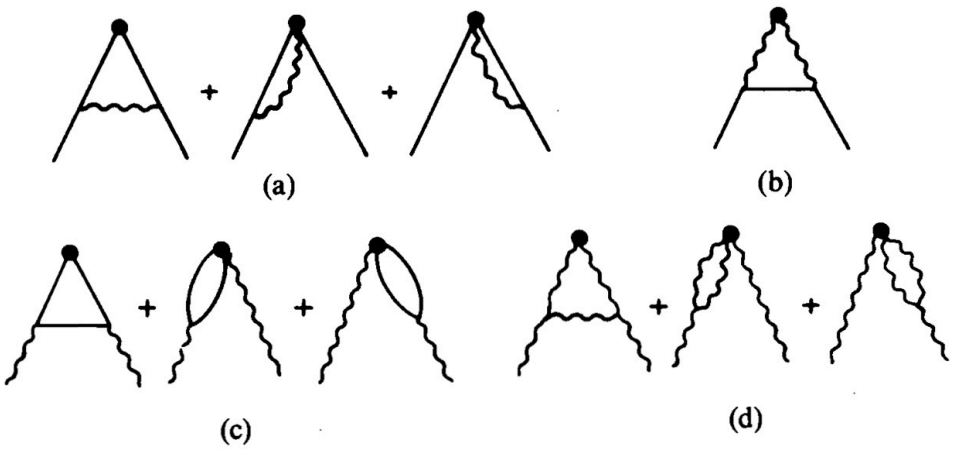

Figure 6.7: The lowest order contribution to the anomalous dimension, where (a) is $\gamma_{qq}^{0,n}$, (b) $\gamma_{qG}^{0,n}$, (c) $\gamma_{Gq}^{0,n}$ and (d) $\gamma_{GG}^{0,n}$. This figure was borrowed from [152]

In this subsection we only give a hint on how to obtain the anomalous dimensions $\gamma_j^{(n)}$ and Wilson coefficients, because the details go beyond the scope and purposes of this presentation.
When we renormalize the composite operator and obtain the corresponding RGE, we have the anomalous dimension (as perturbation expansion)

$$\begin{aligned} \gamma_{NS}^{(n)}(g) &= -\mu\frac{d}{d\mu}\ln Z_{NS}^{(n)} = \gamma_{NS}^{0,n}\frac{g^2}{16\pi^2} + O(g^4), \\ \gamma_{ab}^{(n)}(g) &= -\left(\mu\frac{d}{d\mu}\ln Z^{(n)}\right)_{ab} = \gamma_{ab}^{0,n}\frac{g^2}{16\pi^2} + O(g^4), \end{aligned} \tag{6.102}$$

where $a, b = q, G$. The corresponding diagrams for one loop are shown in Fig. (6.7). This gives (the calculation was performed to LO in Ref. [164]; and to NLO in Ref. [165])

$$\begin{aligned}
8\pi^2\gamma_{NS}^{0,n} &= 2C_F\left\{4S_1(n)+1-\frac{2}{n(n+1)}\right\},\\
8\pi^2\gamma_{qG}^{0,n} &= -4n_f\frac{n^2+n+2}{n(n+1)(n+2)},\\
8\pi^2\gamma_{Gq}^{0,n} &= -\frac{16}{3}\frac{n^2+n+2}{n(n^2-1)},\\
8\pi^2\gamma_{GG}^{0,n} &= 6\left\{\frac{1}{3}+4S_1(n)-\frac{4}{n(n-1)}-\frac{4}{(n+2)(n+1)}\right\}+\frac{4}{3}n_f,
\end{aligned} \tag{6.103}$$

where

$$S_\alpha(n)=\sum_{k=2}^{n}\frac{1}{k^\alpha}. \tag{6.104}$$

The calculus of the Wilson coefficients is more cumbersome, but the usual way is to calculate the virtual Compton amplitude $T_{\mu\nu}$, and $A^{(n),j}$ stands for the matrix element of the spin n non-singlet operator between quarks. The result in $\overline{MS}$ is given by (performed by several authors at NLO in Ref. [166] and NNLO in Ref. [167])

$$C_{NS}^{(1)}(n)=C_F\left\{2S_1(n)^2+3S_1(n)-2S_2(n)-\frac{2S_1(n)}{n(n+1)}+\frac{3}{n}+\frac{4}{n+1}+\frac{2}{n^2}-9\right\}. \tag{6.105}$$

6.6 Jacobi Polinomial Method

Once we know the moments, we can represent the SF $F_2(x,Q^2)$ with the help of Jacobi polynomials $\Theta_n^{\alpha\beta}(x)$ expansion method developed in Refs. [168], truncated at $n = N_{max}$:

$$F_{2,NS}(x,Q^2)=\omega^{\alpha\beta}(x)\sum_{n=0}^{N_{max}}\Theta_n^{\alpha\beta}(x)\sum_{j=0}^{n}C_j^{(n)}(\alpha,\beta)M_{2,NS}(j+2,Q^2). \tag{6.106}$$

Here $\omega^{\alpha\beta}(x)=x^\alpha(1-x)^\beta$ is the weight function and the parameters α,β will be obtained by fitting. The Jacobi polynomials $\Theta_n^{\alpha\beta}(x)$ appearing in the expansion are given by

$$\Theta_k^{\alpha\beta}(x)=\sum_{j=0}^{k}C_j^{(n)}(\alpha,\beta)x^j. \tag{6.107}$$

They satisfy the orthogonality relation:

$$\int_0^1 \omega^{\alpha\beta}(x)\Theta_k^{\alpha\beta}(x)\Theta_l^{\alpha\beta}(x) = \delta_{kl}. \tag{6.108}$$

If we know the moments $M_{2,NS}(n,Q^2)$, we obtain the SF $F_{2,NS}$ by evaluating the inverse Mellin transform (inverse of Eq. (6.99)). Choosing a convenient contour, it is given by

$$F_{2,NS}(x,Q^2) \equiv \mathcal{M}^{-1}\left\{M_{2,NS}(n,Q^2)\right\} = \frac{1}{2\pi i}\int_{c-i\infty}^{c+i\infty} x^{-n} M_{2,NS}(n,Q^2)dn, \tag{6.109}$$

where the integration is along a vertical line through $\mathrm{Re}(n) = c$. This integral allows direct numerical integration, leading to SF F_2.
Of course, the extension of the others SF, namely the complete $F_{1,2}$ (or $F_{L,2}$, and taking all S, NS and G part) is a direct replacement in formula (6.106) (directly in the sense of only change the prescriptions).

6.7 Analytic model in DIS

For our test of DGLAP (see Ref. [149] for details), we use the evolution of moments up to next-to-leading order. The non-singlet part of the moment, i.e., $M_{2,NS}$ up to this order is given by (solving the renormalization group equation for moments)

$$\begin{aligned}
\frac{M_{2,NS}(n,Q^2)}{M_{2,NS}(n,Q_0^2)} &= \frac{1 + C_{2,NS}^{(1)}(n)a_{pt}(Q^2)/4}{1 + C_{2,NS}^{(1)}(n)a_{pt}(Q_0^2)/4}\left(\frac{1 + (\beta_1/\beta_0)a_{pt}(Q^2)/4}{1 + (\beta_1/\beta_0)a_{pt}(Q_0^2)/4}\right)^{p(n)}\left[\frac{a_{pt}(Q_0^2)}{a_{pt}(Q^2)}\right]^{d_{NS}(n)} \\
&\simeq \frac{1 + \left(C_{2,NS}^{(1)}(n) + \frac{\beta_1}{\beta_0}p(n)\right)a_{pt}(Q^2)/4}{1 + \left(C_{2,NS}^{(1)}(n) + \frac{\beta_1}{\beta_0}p(n)\right)a_{pt}(Q_0^2)/4}\left[\frac{a_{pt}(Q^2)}{a_{pt}(Q_0^2)}\right]^{\delta_{NS}(n)}.
\end{aligned} \tag{6.110}$$

Here:

$$\delta_{NS}(n) = -d_{NS}(n) = \gamma_{NS}^{(0)}(n)/2\beta_0, \tag{6.111}$$

$$p(n) = \frac{1}{2}\left(\frac{\gamma_{NS}^{(1)}(n)}{\beta_1} - \frac{\gamma_{NS}^{(0)}(n)}{\beta_0}\right). \tag{6.112}$$

We consider in the evolution (6.110) the scale Q_0^2 as a reference scale at which the parton distribution functions (PDFs) are regarded as functions in x with parameters

which are fixed by the data. In particular, we use in the present work the data-based MSTW PDFs (see Ref. [169]), where:

$$xu_v(x,Q_0^2) = A_u x^{\eta_1}(1-x)^{\eta_2}(1+\epsilon_u\sqrt{x}+\gamma_u x), \quad (6.113)$$
$$xd_v(x,Q_0^2) = A_d x^{\eta_3}(1-x)^{\eta_4}(1+\epsilon_d\sqrt{x}+\gamma_d x), \quad (6.114)$$

The values of $A_{u,d}, \eta_k$ $(k=1,...,4)$, $\epsilon_{u,d}$ and $\gamma_{u,d}$ can be found in [169].
The implementation of APT analytic model is quite direct, rewriting Eq. (6.110) in the form:

$$M_{2,NS}(n,Q^2) = \frac{a_{pt}(Q^2)^{\delta_{NS}(n)} + \left(C_{2,NS}^{(1)}(n) + \frac{\beta_1}{\beta_0}p(n)\right) a_{pt}(Q^2)^{\delta_{NS}(n)+1}/4}{a_{pt}(Q_0^2)^{\delta_{NS}(n)} + \left(C_{2,NS}^{(1)}(n) + \frac{\beta_1}{\beta_0}p(n)\right) a_{pt}(Q_0^2)^{\delta_{NS}(n)+1}/4} M_{2,NS}(n,Q_0^2). \quad (6.115)$$

The analytization then gives

$$M_{2,NS}^{(an.)}(n,Q^2) = \frac{\mathcal{A}_{\delta_{NS}(n)}^{(2)}(Q^2) + \left(C_{2,NS}^{(1)}(n) + \frac{\beta_1}{\beta_0}p(n)\right) \mathcal{A}_{\delta_{NS}(n)+1}^{(2)}(Q^2)/4}{\mathcal{A}_{\delta_{NS}(n)}^{(2)}(Q^2) + \left(C_{2,NS}^{(1)}(n) + \frac{\beta_1}{\beta_0}p(n)\right) \mathcal{A}_{\delta_{NS}(n)+1}^{(2)}(Q^2)/4} M_{2,NS}^{(an.)}(n,Q_0^2), \quad (6.116)$$

where $L_0 = \ln(Q_0^2/\Lambda^2)$ and $\alpha_s(Q_0^2)$ is a constant number given by fit of data. This analytic version of the evolution of moments can be applied at low energies without problems, since no Landau singularities appear.
We can use either the Jacobi Polynomial expansion (6.106), or directly in the inverse Mellin transform (6.109).

6.7.1 Numerical Result for pQCD and APT

Accuracy of the Jacobi Polynomial Method in x Variable

The evaluation of Structure Functions depends on the method we are using, and in this way it is indispensable to test the accuracy of our parametrization.
We used the Jacobi Polynomial method which gives us a good prediction for the evolution, as has been shown in previous works (see Refs. [168]). This method is applied directly on the Bjorken variable, but it affects the Q^2-dependence indirectly.
Therefore, it is necessary to verify the x-range applicability of the JP method. For this we must compare the JP approach (6.106) with respect to the "exact" numerical SFs, "exact" in the sense of the exact inverse Mellin moments via Eq. (6.109). We solved Eq. (6.109) numerically, but only to one-loop due to technical limitations.

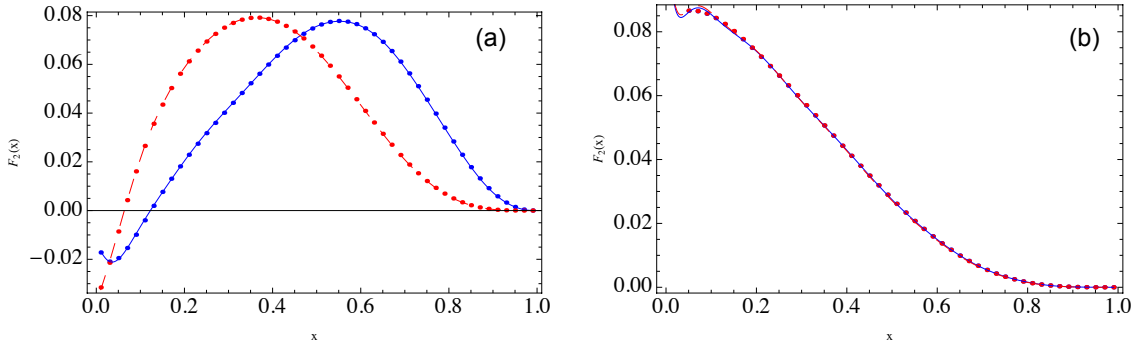

Figure 6.8: Non-singlet structure function $F_2(x)$ versus x at (a) LO , at energy scale $Q^2 = 0.3GeV^2$ and (b) $Q^2 = 100GeV^2$. The solid line represents the pQCD, the dashed line the FAPT in the JP method; and the dotted lines the corresponding exact Inverse Mellin transform behavior.

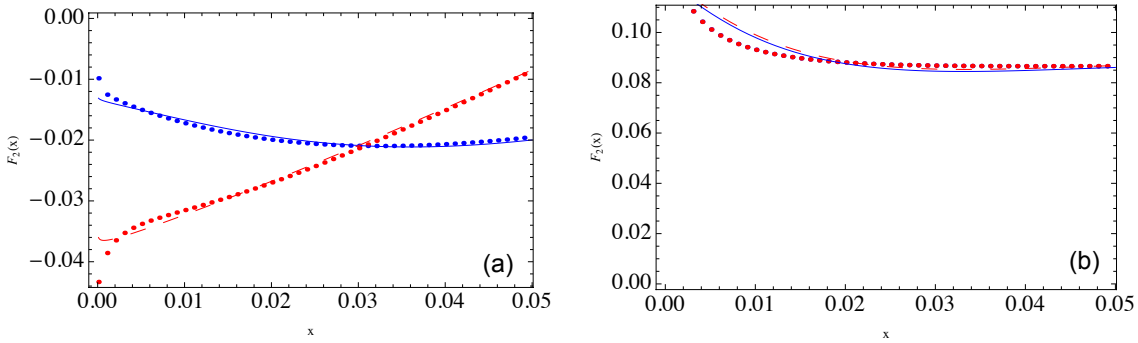

Figure 6.9: Non-singlet structure function $F_2(x)$ versus x at LO , at energy scale (a) $Q^2 = 0.3GeV^2$, and (b) $Q^2 = 100GeV^2$. The solid line represents pQCD, the dashed line FAPT in the JP method; and the dotted lines represent the corresponding exact Inverse Mellin transform.

In Fig. 6.8 the accuracy is apparently perfect. So, in order to clarify it, we perform a zoom in x, going to lower and lower x-region ($\sim 10^{-2}$). We see in Fig. 6.9 that JP method gradually loses precision starting at $x \sim 0.02$. Also, we can see that in this range, the difference between these two methods is approximatly 5%.

Numerical Structure Function $F_2(x, Q^2)$

The accuracy of the SF approximation by a finite number of Jacobi polynomials (N_{max}) depends on the choice of the weight function parameters. Therefore, we test the non-singlet SF given by the MSTW data, searching at $Q^2 = Q_0^2$ for the minimum

of:

$$\chi^2_{\alpha,\beta} = \left| \frac{F^{(theor.),N_{max}}_{\alpha,\beta}}{F^{(exp.)}} - 1 \right|^2 . \tag{6.117}$$

Here, we use Eqs. (6.99) and (6.110) at $Q^2 = Q_0^2$: $F(x,Q_0^2) \equiv F^{(exp.)}(x,Q_0^2) = \frac{1}{6}x\Delta(x,Q_0^2)$, and from Eq. (6.106) we define $F^{(theor.),N_{max}}_{\alpha,\beta}(x,Q_0^2) \equiv F^{N_{max}}_{\alpha,\beta}(x,Q_0^2)$.
For different values of N_{max}, we find the values of α and β that provide us with the best fit to the data.
We found at one loop: $N_{max} = 13$, $\alpha = 0.01124$ and $\beta = 3.033$ for $\chi^2 \approx 10^{-9}$, and at two loops (of course for even PDFs only): $N_{max} = 13$, $\alpha = 0.001$ and $\beta = 3.2314$ for $\chi^2 \approx 10^{-9}$, too.
For the evolution of the non-singlet moments, we need to take into account the values of $\Lambda^{n_f=3}_{1,2}$ at leading and NL order, which were taken from the data in [169], where: $\alpha_s^{(1loop)}(Q_0^2 = 1GeV^2) = 0.68183 \Rightarrow \Lambda_1^{n_f=3} = 0.359$ and $\alpha_s^{(2loop)}(Q_0^2 = 1GeV^2) = 0.49128 \Rightarrow \Lambda_2^{n_f=3} = 0.359$.
The couplings in pQCD and FAPT were calculated with the Mathematica package developed by Bakulev and Khandramai in Ref. [170], where the quarks thresholds were accounted for, leading to the global couplings. This was described briefly in Sec. 2.8.
With these considerations, we put Eqs. (6.110) and (6.116) in Eq. (6.106), obtaining the evolution of SFs up to NLO in pQCD or FAPT, respectively. We represent the obtained results in Fig. 6.10 in the range $0.25 \leq Q^2 \leq 100GeV^2$, and in 6.11 as a function of x.
First, in Fig. 6.10 we fix x at two differents values: $x = 0.25$ in (a.1) and (b.1), $x = 0.7$ in (a.2) and (b.2), where (a) and (b) represent the LO and NLO, respectively. In Fig. 6.11 we fix Q^2 at two different values: $Q^2 = 100GeV^2$ in (a.1) or (b.1), $Q^2 = 0.3GeV^2$ in (a.2) or (b.2), where (a) and (b) represent the LO and NLO, respectively.

We deduce the following main reasons for taking (F)APT seriously into account:

1. The stability of FAPT at low energies ($Q^2 < 1GeV^2$) is evident (see Fig. 6.10) this could give us some evidence of confinement, with $F_2(Q^2 = 0) \sim constant$ (which is almost independent of x).

2. $F_2(x,Q^2)$ at x fixed, is almost constant in the entire range of energies.

3. At high energies ($Q^2 \sim 100GeV^2$) we found that pQCD and FAPT are in agreement, see Fig. 6.11.

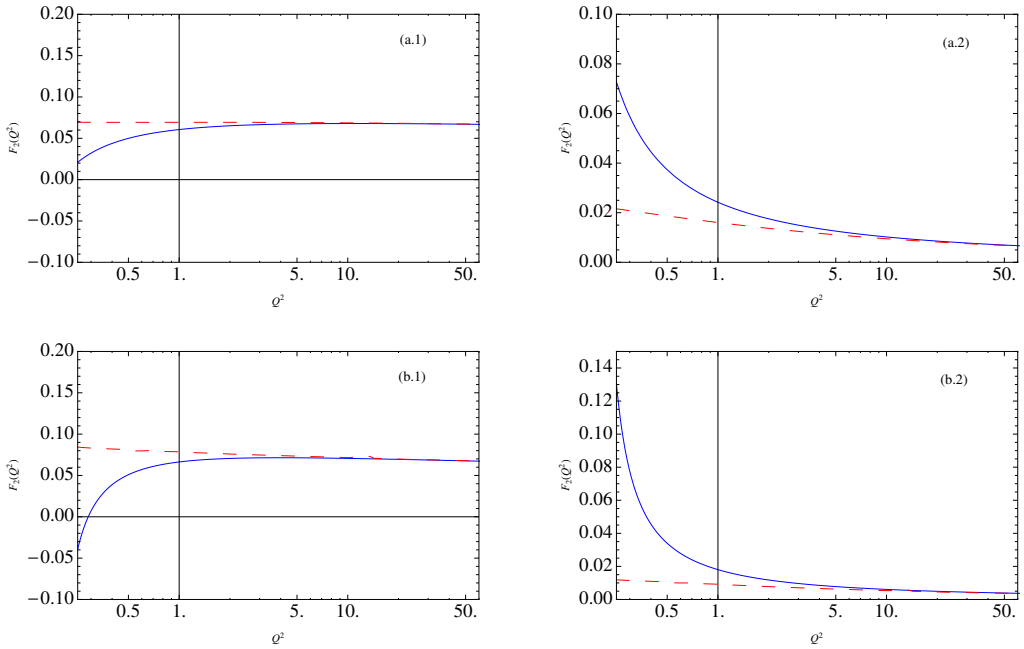

Figure 6.10: Non-singlet structure function $F_2(x)$ versus Q^2 at (a) LO and (b) NLO. The Bjorken parameter is $x = 0.25$ in (a.1) and (b.1), and $x = 0.7$ in (a.2) or (b.2). The solid line represents the pQCD and the dashed line the FAPT behavior.

It would be interesting to clarify in the future in more detail the behavior at very low energies ($Q^2 \sim 0.3GeV^2$). In Fig. 6.11 we can see that F_2 takes negative values at low x. This problem is more pronounced in the case of pQCD, where negative values start at $x \approx 0.2$, while in FAPT at $x \approx 0.05$. In this regime of low x, the Jacobi Polynomial method is not reliable. However, the method is not the main factor responsible for the negative values. Namely, we have seen that at very low x the Jacobi Polynomial method has a reasonable precision of about 5%. Moreover, the complete structure function includes the singlet and nonsinglet parts. Here we only took the nonsinglet part into account, since the complete SF is more cumbersome and is out of the scope and purpose of this analysis. Therefore, as this approximation is valid only at large values of x ($x \geq 0.25$), we must eventually incorporate the singlet part. Until now, this is the principal explanation for the appearance of negative values, and we will include the singlet part in future works. Another important issue is to add the Target Mass Contribution (TMC) and Higher Twist Contributions (HT) in our calculus, and test with other analytic QCD models that were mentioned in Chapter 3.

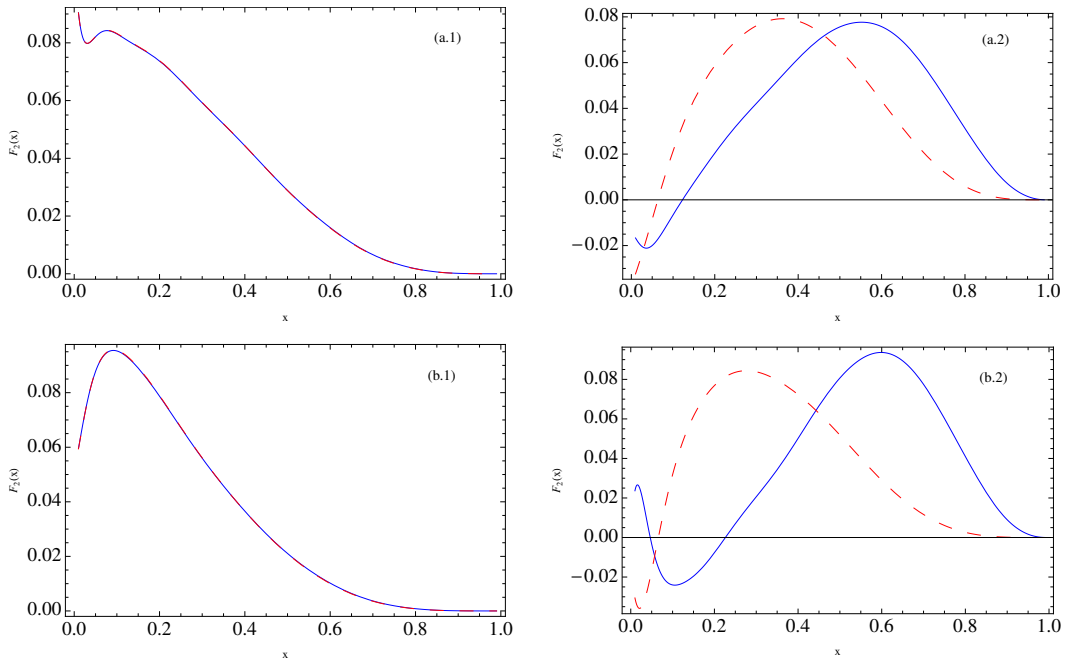

Figure 6.11: Non-singlet structure function $F_2(x)$ versus x at (a) LO and (b) NLO. The energy scale is $Q^2 = 100GeV^2$ in (a.1) or (b.1) and $Q^2 = 0.3GeV^2$ in (a.2) or (b.2). The solid line represents the pQCD and the dashed line the FAPT behavior.

Appendix A

Renormalon-based estimate of $\sim a_{\rm pt}^4$ coefficient

The term r_3 in the expansion of $m_q/\overline{m}_q$ in Eq. (5.9) can be estimated by a method closely related with the approach presented in Sec. II of Ref. [145]. The pQCD version of the sum in Eq. (5.9) can be reexpressed in terms of $a_{\rm pt}(\mu^2)$ at any other renormalization scale μ^2

$$S \equiv \frac{m_q}{\overline{m}_q} - 1 = \frac{4}{3} a_{\rm pt}(\mu^2) \left[1 + a_{\rm pt}(\mu^2) r_1(\mu^2) + a_{\rm pt}^2(\mu^2) r_2(\mu^2) + \mathcal{O}(a_{\rm pt}^3)\right] , \quad \text{(A.1a)}$$

$$r_1(\mu^2) = \kappa_1 + \beta_0 L_m(\mu^2) , \quad \text{(A.1b)}$$

$$r_2(\mu^2) = \kappa_2 + (2\kappa_1\beta_0 + \beta_1) L_m(\mu^2) + \beta_0^2 L_m^2(\mu^2) , \quad \text{(A.1c)}$$

$$(4/3)\kappa_1 = 6.248\beta_0 - 3.739 , \quad \text{(A.1d)}$$

$$(4/3)\kappa_2 = 23.497\beta_0^2 + 6.248\beta_1 + 1.019\beta_0 - 29.94 , \quad \text{(A.1e)}$$

where $L_m(\mu^2) = \ln(\mu^2/\overline{m}_q^2)$, while $\beta_0(N_f)$ and $\beta_1(N_f)$ are the renormalization scheme independent coefficients (1.8). Here, $N_f = N_\ell$ is the number of light active flavors (quarks with masses lighter than m_q).

Since r_1 and r_2 are explicitly known, the Borel transform $B_S(b)$ is known to order $\sim b^2$

$$B_S(b;\mu) = \frac{4}{3}\left[1 + \frac{r_1(\mu^2)}{1!\,\beta_0} b + \frac{r_2(\mu^2)}{2!\,\beta_0^2} b^2 + \mathcal{O}(b^3)\right] . \quad \text{(A.2)}$$

The function $B_S(b)$ has renormalon singularities at $b = 1/2, 3/2, 2, \ldots, -1, -2, \ldots$ [171–173]. The behavior of B_S near the leading infrared (IR) renormalon singularity $b = 1/2$ is determined by the resulting renormalon ambiguity of m_q. This ambiguity δm_q is a (QCD) scale which, having the dimension of energy and being renormalization scale and scheme independent, must be proportional to the QCD scale $\Lambda_{\rm QCD}$:

$\delta m_q = const \times \Lambda_{\rm QCD}$ [174]. This scale can be expressed in terms of $a_{\rm pt}(\mu^2)$ and μ (μ being any renormalization scale) in the form

$$\Lambda = const \times \mu \exp\left(-\frac{1}{2\beta_0 a_{\rm pt}(\mu)}\right) a_{\rm pt}(\mu)^{-\nu} c_1^{-\nu} \left[1 + \sum_{k=1}^{\infty} (2\beta_0)^k \nu(\nu-1)\cdots(\nu-k+1)\widetilde{c}_k a_{\rm pt}^k(\mu)\right] , \tag{A.3}$$

where

$$\nu = \frac{c_1}{2\beta_0} = \frac{\beta_1}{2\beta_0^2} , \tag{A.4a}$$

$$\widetilde{c}_1 = \frac{(c_1^2 - c_2)}{(2\beta_0)^2 \nu},$$

$$\widetilde{c}_2 = \frac{1}{2(2\beta_0)^4 \nu(\nu-1)} \left[(c_1^2 - c_2)^2 - 2\beta_0(c_1^3 - 2c_1c_2 + c_3)\right] , \tag{A.4b}$$

$$\widetilde{c}_3 = \frac{1}{6(2\beta_0)^6 \nu(\nu-1)(\nu-2)} \left[(c_1^2 - c_2)^3 - 6\beta_0(c_1^2 - c_2)(c_1^3 - 2c_1c_2 + c_3) + 8\beta_0^2(c_1^4 - 3c_1^2c_2 + c_2^2 + 2c_1c_3 - c_4)\right] . \tag{A.4c}$$

The above constants, expressed in terms of β_0 and of $c_j = \beta_j/\beta_0$, appear in the expansion of the residue of the Borel transform $B_S(b;\mu)$ at the pole $b = 1/2$

$$B_S(b;\mu) = N_m \pi \frac{\mu}{\overline{m}_q} \frac{1}{(1-2b)^{1+\nu}} \left[1 + \sum_{k=1}^{\infty} \widetilde{c}_k (1-2b)^k\right] + B_S^{(\rm an.)}(b;\mu) , \tag{A.5}$$

where $B_S^{(\rm an.)}(b;\mu)$ is analytic on the disk $|b| < 1$ and can be expanded in powers of b. The form of the representation (A.5) is called bilocal and was proposed in Ref. [146]. We can assume that the coefficients $\widetilde{c}_k$ are known up to $k = 3$, because the coefficient $c_4 = \beta_4/\beta_0$ (in the $\overline{\rm MS}$ scheme) is known to a large degree by Padé-related methods of Ref. [175]

$$\beta_4 = \frac{1}{4^5}(A_4 + B_4 N_f + C_4 N_f^2 + D_4 N_f^3 + E_4 N_f^4) \tag{A.6}$$

with $A_4 = 7.59 \times 10^5$, $B_4 = -2.19 \times 10^5$, $C_4 = 2.05 \times 10^4$, $D_4 = -49.8$, and $E_4 = -1.84$. This gives $c_4 = 123.7$ for $N_f = 3$, $c_4 = 97.2$ for $N_f = 4$, and $c_4 = 86.2$ for $N_f = 5$. The residue parameter N_m can be determined with high precision by using the idea of Refs. [176], i.e., by calculating:

$$N_m = \frac{\overline{m}_q}{\mu} \frac{1}{\pi} R_S(b = 1/2) , \tag{A.7}$$

where

$$R_S(b;\mu) \equiv (1-2b)^{1+\nu} B_S(b;\mu) , \tag{A.8}$$

and the first coefficients in the expansion in powers of b of this quantity are known from the known coefficients r_1 and r_2. We can use a combination of truncated perturbation series and Padé approximants [1/1] for $R_S(b)$, as presented in Ref. [177], and obtain

$$N_m \approx 0.575(N_f=3)\ , \quad \approx 0.555(N_f=4)\ , \quad \approx 0.533(N_f=5)\ . \tag{A.9}$$

with the uncertainties in these values of roughly ± 0.020.

In the bilocal expansion (A.5), the analytic part $B_S^{(\mathrm{an.})}(b;\mu)$ can be taken as a polynomial in b, i.e., a truncated expansion in powers of b. The coefficients of the latter expansion can be related with $r_j(\mu^2)$'s by equating the expansion of Eq. (A.5) in powers of b with the expansion (A.2), resulting in

$$B_S^{(\mathrm{an.})}(b;\mu) = h_0^{(m)} + \sum_{k\geq 1} \frac{h_k^{(m)}}{k!\ \beta_0^k} b^k\ , \tag{A.10a}$$

$$h_k^{(m)} = \frac{4}{3} r_k - \pi N_m \frac{\mu}{\overline{m}_q} (2\beta_0)^k \sum_{n\geq 0} \widetilde{c}_n \frac{\Gamma(\nu+k+1-n)}{\Gamma(\nu+1-n)}\ , \tag{A.10b}$$

where, by convention, $r_0 = \widetilde{c}_0 = 1$. The numbers $\widetilde{c}_n$ of Eqs. (A.4), which enter the sum in Eq. (A.10b), are known only up to $n=3$, because, in $\overline{\mathrm{MS}}$, only c_k up to $k=4$ are reasonably known (c_4 approximately, as mentioned). For $N_f=3$, these values are: $\widetilde{c}_1 = -0.1638$, $\widetilde{c}_2 = 0.2372$, $\widetilde{c}_3 = -0.1205$ (and $\nu = 0.3951$). For $N_f=4$, they are: $\widetilde{c}_1 = -0.1054$, $\widetilde{c}_2 = 0.2736$, $\widetilde{c}_3 = -0.1610$ (and $\nu = 0.3696$). And for $N_f=5$ they are: $\widetilde{c}_1 = 0.0238$, $\widetilde{c}_2 = 0.3265$, $\widetilde{c}_3 = -0.2681$ (and $\nu = 0.3289$). Therefore, the sums in (A.10b) are truncated at $n=3$.

Theoretically, the pole closest to the origin in $B_S^{(\mathrm{an.})}(b;\mu)$ is at $b=-1$, at least in the large-β_0 approximation.[1] Since in $B_S^{(\mathrm{an.})}(b;\mu)$ the coefficients $h_k^{(m)}(\mu^2)$ for $k=0,1,2$ are known [because $r_1(\mu^2)$ and $r_2(\mu^2)$ are known], we can construct the Padé $[1/1]_{B_S^{(\mathrm{an.})}}(b)$ and check the pole of it. It turns out that this Padé, at the natural scale $\mu = \overline{m}_q$, has the pole at $b = -1.09, -0.96, -1.12$, for $N_f = 3,4,5$, respectively, reflecting correctly the theoretical expectation.[2] We can extend further this reasoning and obtain the next coefficient $h_3^{(m)}$ (at $\mu = \overline{m}_q$) by requiring that the Padé $[2/1]_{B_S^{(\mathrm{an.})}}(b)$ has the pole at $b=-1$. This gives us

$$h_3^{(m)}(\overline{m}_q^2) = -25.18(N_f=3)\ ,\ -28.28(N_f=4)\ ,\ -35.62(N_f=5)\ . \tag{A.11}$$

[1] Nonetheless, there is a possibility that at two-loop order the kinetic term contributes to an IR renormalon at $b=+1$ in $B_S(b)$, cf. Ref. [178].

[2] However, the μ dependence of this position is rather strong. For example, when μ^2 varies by 10 % around $\overline{m}q^2$, the pole position in [1/1] varies between -1.6 and -0.7 in the $N_f=3$ case, between -1.2 and -0.7 in the $N_f=4$ case, and between -1.26 and -1.00 in the $N_f=5$ case.

If constructing with these values of $h_3^{(m)}$ the other possible Padé approximant of index 3, namely $[1/2]_{B_S^{(\rm an.)}}(b)$, it turns out that the nearest to origin pole of such Padé is then at $b = -1.003, -1.001, -1.008$, for $N_f = 3, 4, 5$, respectively. This indicates that the obtained values of $h_3^{(m)}$, Eq. (A.11), are consistent.[3] Using these values, we obtain from the relation (A.10b) (with the natural choice $\mu^2 = \overline{m}_q^2$) at $k = 3$ an estimate for r_3

$$\frac{4}{3} r_3(\overline{m}_q^2) \;\; = \;\; h_3^{(m)}(\overline{m}_q^2) + \pi N_m (2\beta_0)^3 \sum_{n=0}^{3} \widetilde{c}_n \frac{\Gamma(\nu + 4 - n)}{\Gamma(\nu + 1 - n)} \; . \tag{A.12}$$

This gives us numerically the following estimates (we recall that $N_f \equiv N_\ell = 3, 4, 5$ for c, b, t quark, respectively):

$$\frac{4}{3} r_3 = 1785.9 (N_f = 3) \; , \; 1316.4 (N_f = 4) \; , \; 920.1 (N_f = 5) \; . \tag{A.13}$$

The principal origin of the uncertainties in these expressions is the uncertainty in the residue parameter N_m (roughly ± 0.020, i.e., less than 4 %), implying an uncertainty in r_3 of a few percent (below 4 %).

An analysis similar to this one has been performed in Ref. [147]. There, however, the term $\widetilde{c}_3$ and the coefficients $h_k^{(m)}$ were not included in the analysis. The results of Ref. [147] are: $(4/3) r_3 = 1818.6, 1346.7, 947.9.$, for $N_f \equiv N_\ell = 3, 4, 5$, respectively. These results are by about 2-3% higher than ours [Eq. (A.13)]. In another approach, applying the effective charge method (ECH) of Refs. [180] to a Euclidean analog of the quantity m_q, an approach using the idea of Ref. [181] extended in Ref. [125] to the mass-dependent Minkowskian quantities, the authors of Ref. [127] obtained for these coefficients the estimates $1281.05, 986.097, 719.339$, respectively. These quantities are by about 22-28% lower than ours. On the other hand, the corresponding estimates in Ref. [125] are $1544.1, 1091.0, 718.74$, respectively.[4]

[3] We used for the $\overline{\rm MS}$ scheme coefficient c_4 the estimated values (A.6), with $c_4 = 123.7, 97.2, 86.2$, for $N_f = 3, 4, 5$, respectively, from Ref. [175]. Simpler Padé-based estimates of c_4 were obtained in Ref. [179]: $c_4 = 40, 70$ for $N_f = 4, 5$, respectively (and a large negative and uncertain value $c_4 = -850$ for $N_f = 3$). The $c_4 = 40$ value (for $N_f = 4$) in this case differs substantially from the value $c_4 = 97.2$. If we repeat for the $c_4 = 40$ value ($N_f = 4$) the same procedure described above, we obtain $\widetilde{c}_4 \approx 0.0055$ (for $c_4 = 97.2$ we got: $\widetilde{c}_4 = -0.1610$); hence the expressions of $h_k^{(m)}(\overline{m}_q^2)$ of Eq. (A.10b) change, and the pole of $[1/1]_{B_S^{(\rm an.)}}(b)$ becomes $b \approx -5.9$ (before: $b \approx -0.96$), not close to the theoretical pole $b = -1$. Furthermore, from the requirement that $[2/1]_{B_S^{(\rm an.)}}(b)$ has the pole at $b = -1$ we now get $h_3^{(m)}(\overline{m}_q^2) = 4.10$ (before: -28.28), and using this value of $h_3^{(m)}$ in the Padé $[1/2]_{B_S^{(\rm an.)}}(b)$ we obtain the pole nearest to the origin $b = 1.94$ (before: $b = -1.001$). This indicates that the estimate $c_4 = 40$ (for $N_f = 4$) is not giving results consistent with the theoretical expectations of the renormalon structure of $B_S^{(\rm an.)}$.

[4] At the time, the coefficient r_2 was not known, and the authors of Ref. [125] used in the estimates

of $(4/3)r_3$ the analogously ECH-estimated values of $(4/3)r_2 = 124.1, 97.729, 73.616$, respectively (the exact values are $116.30, 94.21, 73.43$).

Appendix B

Variation of pQCD coupling with scales and schemes

In this appendix we give the relation between $a_0 \equiv a_{\rm pt}(Q_0^2; c_2^{(0)}, c_3^{(0)}, \ldots)$ and $a \equiv a_{\rm pt}(Q^2; c_2, c_3, \ldots)$, where the latter is expressed as power expansion of the former

$$\begin{aligned} a &= a_0 + a_0^2(-x) + a_0^3(x^2 - c_1 x + \delta c_2) \\ &+ a_0^4 \left(-x^3 + \frac{5}{2} c_1 x^2 - c_2^{(0)} x - 3x\delta c_2 + \frac{1}{2}\delta c_3 \right) \\ &+ a_0^5 \Bigg[x^4 - \frac{13}{3} c_1 x^3 + \left(\frac{3}{2} c_1^2 + 3c_2^{(0)} + 6\delta c_2 \right) x^2 \\ &+ (-c_3^{(0)} - 3c_1\delta c_2 - 2\delta c_3) x + \left(\frac{1}{3} c_2^{(0)} \delta c_2 + \frac{5}{3} (\delta c_2)^2 - \frac{1}{6} c_1 \delta c_3 + \frac{1}{3}\delta c_4 \right) \Bigg] \\ &+ \mathcal{O}(a_0^6) \ , \end{aligned} \tag{B.1}$$

where we denote

$$a \equiv a_{\rm pt}(Q^2; c_2, c_3, \ldots) \ , \quad a_0 \equiv a_{\rm pt}(Q_0^2; c_2^{(0)}, c_3^{(0)}, \ldots) \ , \tag{B.2a}$$

$$x \equiv \beta_0 \ln \frac{Q^2}{Q_0^2}, \quad \delta c_k \equiv c_k - c_k^{(0)} \ . \tag{B.2b}$$

For the purposes of our paper, it is sufficient to consider in the above relation (B.1) terms up to (including) terms $\sim a_0^4$.

The three-loop threshold connection of $a_{\rm pt}$ in the $\overline{MS}$ scheme at the threshold scale $\mu_{\rm thr}^2 = (\mathcal{K}\overline{m}_c)^2$ (where $\mathcal{K} \sim 1$; usually $\mathcal{K} = 2$) can be written as the following relation between $a_{\rm pt}(\mu_{\rm thr}^2 + 0; N_f = 4) \equiv a_+$ and $a_{\rm pt}(\mu_{\rm thr}^2 - 0; N_f = 3) \equiv a_-$:

$$a_+ = a_- \left[1 + x_1 a_- + x_2 a_-^2 + x_3 a_-^3 + \mathcal{O}(a_-^4) \right] \ , \tag{B.3}$$

where

$$x_1 \;=\; -k_1 \;, \qquad x_2 = -k_2 + 2k_1^2 \;, \qquad x_3 = -k_3 + 5k_1k_2 - 5k_1^3 \;, \tag{B.4}$$

and the coefficients k_j were calculated in Ref. [117]

$$\begin{aligned} k_1 &= -\frac{1}{6}\ell_h \;, \qquad k_2 = \frac{1}{36}\ell_h^2 - \frac{19}{24}\ell_h + \frac{11}{72} \;, \\ k_3 &= -\frac{1}{216}\ell_h^3 - \frac{131}{576}\ell_h^2 + \frac{(-6793 + 281N_\ell)}{1728}\ell_h \\ &\quad + \left(-\frac{82043}{27648}\zeta(3) + \frac{564731}{124416} - \frac{2633}{31104}N_\ell\right) \;, \end{aligned} \tag{B.5}$$

where $\ell_h = \ln(\mu_{\rm thr}^2/\overline{m}_c^2) = \ln \mathcal{K}^2$, and N_ℓ in Eq. (B.5) is the number of light quark flavors, i.e., $N_\ell = 3$ in the considered case of transition from $N_f = 4$ to $N_f = 3$.

Bibliography

[1] N.N. Bogoliubov and D.V. Shirkov, *Introduction to the Theory of Quantum Fields*, New York, Wiley, 1959; 1980.

[2] G. Cvetič and I. Kondrashuk, JHEP **1112**, 019 (2011) [arXiv:1110.2545 [hep-ph]].

[3] R. M. Corless, G. H. Gonnet, D. E. G. Hare, D. J. Jeffrey, D. E. Knuth, "On the Lambert W function," Adv. Comput. Math. **5**, 329-359 (1996).

[4] E. Gardi, G. Grunberg and M. Karliner, JHEP **9807**, 007 (1998) [hep-ph/9806462]; B. A. Magradze, arXiv:hep-ph/9808247.

[5] D. S. Kourashev, arXiv:hep-ph/9912410; D. S. Kurashev and B. A. Magradze, Theor. Math. Phys. **135**, 531 (2003) [Teor. Mat. Fiz. **135**, 95 (2003)].

[6] B. A. Magradze, Few Body Syst. **40**, 71 (2006) [hep-ph/0512374].

[7] D. V. Shirkov, Eur. Phys. J. C **22**, 331 (2001) [hep-ph/0107282].

[8] S. Weinberg, Phys. Lett. B **91** (1980) 51;

[9] B. A. Ovrut and H. J. Schnitzer, Phys. Lett. B **100** (1981) 403.

[10] W. Wetzel, Nucl. Phys. B **196** (1982) 259 ;
W. Bernreuther and W. Wetzel, Nucl. Phys. B **197** (1982) 228 [Erratum-ibid. B **513** (1998) 758];
W. Bernreuther, Z. Phys. C **20** (1983) 331.

[11] S. A. Larin, T. van Ritbergen and J. A. M. Vermaseren, Nucl. Phys. B **438** (1995) 278 [hep-ph/9411260].

[12] K. G. Chetyrkin, B. A. Kniehl and M. Steinhauser, Phys. Rev. Lett. **79** (1997) 2184 [hep-ph/9706430];
K. G. Chetyrkin, B. A. Kniehl and M. Steinhauser, Nucl. Phys. B **510** (1998) 61 [hep-ph/9708255].

[13] N.N. Bogoliubov and D.V. Shirkov, *Introduction to the Theory of Quantum Fields*, New York, Wiley, 1959; 1980.

[14] R. Oehme, Int. J. Mod. Phys. A **10**, 1995 (1995) [arXiv:hep-th/9412040].

[15] S. Bethke, Prog. Part. Nucl. Phys. **58**, 351 (2007) [hep-ex/0606035].

[16] D. V. Shirkov and I. L. Solovtsov, hep-ph/9604363; Phys. Rev. Lett. **79**, 1209 (1997) [arXiv:hep-ph/9704333].

[17] I. L. Solovtsov and D. V. Shirkov, Phys. Lett. B **442**, 344 (1998) [hep-ph/9711251].

[18] I. L. Solovtsov and D. V. Shirkov, Theor. Math. Phys. **120**, 1220 (1999) [Teor. Mat. Fiz. **120**, 482 (1999)] [hep-ph/9909305].

[19] D. V. Shirkov, Theor. Math. Phys. **119**, 438 (1999) [Teor. Mat. Fiz. **119**, 55 (1999)] [hep-th/9810246].

[20] D. V. Shirkov and I. L. Solovtsov, Theor. Math. Phys. **150**, 132 (2007) [hep-ph/0611229].

[21] A. P. Bakulev, Phys. Part. Nucl. **40**, 715 (2009) [arXiv:0805.0829 [hep-ph]].

[22] D. V. Shirkov, Theor. Math. Phys. **127**, 409 (2001) [hep-ph/0012283]; Eur. Phys. J. C **22**, 331 (2001) [hep-ph/0107282].

[23] K. A. Milton and I. L. Solovtsov, Phys. Rev. D **55**, 5295 (1997) [hep-ph/9611438].

[24] K. A. Milton and O. P. Solovtsova, Phys. Rev. D **57**, 5402 (1998) [hep-ph/9710316].

[25] D. V. Shirkov, hep-ph/0009106.

[26] A. V. Radyushkin, JINR Rapid Commun. **78**, 96 (1996) [hep-ph/9907228].

[27] G. Cvetic and A. V. Kotikov, J. Phys. G **39**, 065005 (2012) [arXiv:1106.4275 [hep-ph]].

[28] A. P. Bakulev, S. V. Mikhailov and N. G. Stefanis, Phys. Rev. D **72**, 074014 (2005) [Phys. Rev. D **72**, 119908 (2005)] [hep-ph/0506311].

[29] A. P. Bakulev, S. V. Mikhailov and N. G. Stefanis, Phys. Rev. D **75**, 056005 (2007) [Erratum-ibid. D **77**, 079901 (2008)] [hep-ph/0607040].

[30] K. A. Milton, I. L. Solovtsov and O. P. Solovtsova, Phys. Lett. B **415**, 104 (1997) [arXiv:hep-ph/9706409].

[31] A. V. Nesterenko, Phys. Rev. D **62**, 094028 (2000); Phys. Rev. D **64**, 116009 (2001); Int. J. Mod. Phys. A **18**, 5475 (2003);

[32] A. V. Nesterenko and J. Papavassiliou, Phys. Rev. D **71**, 016009 (2005); A. C. Aguilar, A. V. Nesterenko and J. Papavassiliou, J. Phys. G **31**, 997 (2005). J. Phys. G **32**, 1025 (2006) [arXiv:hep-ph/0511215]; A. V. Nesterenko, in *Proceedings of the Ninth Workshop on Nonperturbative QCD, Paris, France, 2007* [arXiv:0710.5878].

[33] A. I. Alekseev, Few Body Syst. **40**, 57 (2006) [arXiv:hep-ph/0503242].

[34] Y. Srivastava, S. Pacetti, G. Pancheri and A. Widom, in *Proceedings of e^+e^- Physics at Intermediate Energies, SLAC, Stanford, CA, USA, 30 April - 2 May 2001, pp T19* [arXiv:hep-ph/0106005].

[35] G. Cvetič and C. Valenzuela, J. Phys. G **32**, L27 (2006) [arXiv:hep-ph/0601050].

[36] G. Cvetič and C. Valenzuela, Phys. Rev. D **74**, 114030 (2006) [arXiv:hep-ph/0608256].

[37] K. A. Milton, I. L. Solovtsov, O. P. Solovtsova and V. I. Yasnov, Eur. Phys. J. C **14**, 495 (2000) [arXiv:hep-ph/0003030].

[38] M. A. Shifman, A. I. Vainshtein and V. I. Zakharov, Nucl. Phys. B **147**, 385 (1979); Nucl. Phys. B **147**, 448 (1979).

[39] G. Cvetič, R. Kögerler, C. Valenzuela, J. Phys. G **G37**, 075001 (2010) [arXiv:0912.2466 [hep-ph]]; Phys. Rev. **D82**, 114004 (2010) [arXiv:1006.4199 [hep-ph]].

[40] G. Cvetič and H. E. Martínez, J. Phys. G **36**, 125006 (2009) [arXiv:0907.0033 [hep-ph]].

[41] S. Peris, Phys. Rev. D **74**, 054013 (2006) [arXiv:hep-ph/0603190].

[42] B. A. Magradze, Few Body Syst. **48**, 143 (2010) [Erratum-ibid. **53**, 365 (2012)] [arXiv:1005.2674 [hep-ph]].

[43] R. Barate *et al.* [ALEPH Collaboration], Eur. Phys. J. C **4**, 409 (1998).

[44] S. Schael *et al.* [ALEPH Collaboration], Phys. Rept. **421**, 191 (2005) [arXiv:hep-ex/0506072].

[45] K. Ackerstaff *et al.* [OPAL Collaboration], Eur. Phys. J. C **7**, 571 (1999) [arXiv:hep-ex/9808019].

[46] S. Peris, M. Perrottet and E. de Rafael, JHEP **9805**, 011 (1998) [arXiv:hep-ph/9805442].

[47] Y. L. Dokshitzer, G. Marchesini and B. R. Webber, Nucl. Phys. B **469**, 93 (1996) [arXiv:hep-ph/9512336].

[48] G. Cvetič and C. Valenzuela, Phys. Rev. D **77**, 074021 (2008) [arXiv:0710.4530 [hep-ph]].

[49] C. Amsler *et al.* [Particle Data Group], Phys. Lett. B **667**, 1 (2008).

[50] A. P. Bakulev, Phys. Part. Nucl. **40**, 715 (2009) (in Russian) [arXiv:0805.0829 [hep-ph]]; A. P. Bakulev, S. V. Mikhailov and N. G. Stefanis, JHEP **1006**, 085 (2010) [arXiv:1004.4125 [Unknown]].

[51] G. Cvetič and R. Kögerler, Phys. Rev. D **63**, 056013 (2001) [arXiv:hep-ph/0006098].

[52] P. M. Stevenson, Phys. Rev. D **23**, 2916 (1981).

[53] C. Contreras, G. Cvetič, O. Espinosa and H. E. Martínez, Phys. Rev. D **82**, 074005 (2010) [arXiv:1006.5050].

[54] C. Ayala, C. Contreras and G. Cvetic, Phys. Rev. D **85**, 114043 (2012) [arXiv:1203.6897 [hep-ph]].

[55] MATHEMATICA 8.0.4, Wolfram Co.

[56] K. Nakamura *et al.* [Particle Data Group], J. Phys. G **37**, 075021 (2010).

[57] A. Erdélyi, W. Magnus, F. Oberhettinger and F. G. Tricomi, *Higher Transcendental Functions, Vol. I*, McGraw-Hill Book Company, Inc., New York-Toronto-London. 1953; note that they use for $\mathrm{Li}_{\nu'}(z)$ the Lerch function notation: $\mathrm{Li}_{\nu'}(z) = z\,\Phi(z,\nu',1) \equiv F(z,\nu')$.

[58] A. P. Prudnikov, Yu. A. Brychkov, and O. I. Marichev, *Integrals and Series, Vol. 3: More Special Functions*, New York, Gordon and Breach (1989); I. S. Gradshteyn and I. M. Ryzhik, *Table of Integrals, series, and Products*, 7th edition, edited by A. Jeffrey and D. Zwillinger, Academic Press, London, 2007

[59] A. V. Kotikov, V. G. Krivokhizhin and B. G. Shaikhatdenov, arXiv:1008.0545 [hep-ph], Phys. Atom. Nucl. **75**, 507 (2012)

[60] M. Davier, S. Descotes-Genon, A. Höcker, B. Malaescu and Z. Zhang, Eur. Phys. J. C **56**, 305 (2008) [arXiv:0803.0979 [hep-ph]].

[61] B. L. Ioffe, Prog. Part. Nucl. Phys. **56**, 232 (2006) [arXiv:hep-ph/0502148].

[62] K. Maltman and T. Yavin, Phys. Rev. D **78**, 094020 (2008) [arXiv:0807.0650 [hep-ph]].

[63] G. Grunberg, Phys. Rev. D **29**, 2315 (1984); Phys. Lett. B **95**, 70 (1980) [Erratum-ibid. B **110**, 501 (1982)]; Phys. Rev. D **40**, 680 (1989).

[64] S. J. Brodsky, G. P. Lepage and P. B. Mackenzie, Phys. Rev. D **28**, 228 (1983); S. J. Brodsky, C. -R. Ji, A. Pang and D. G. Robertson, Phys. Rev. D **57**, 245 (1998) [hep-ph/9705221]; G. Grunberg, Phys. Rev. D **46**, 2228 (1992).

[65] D. V. Shirkov, Phys. Part. Nucl. Lett. **10**, 186 (2013) [arXiv:1208.2103 [hep-th]].

[66] G. Cveti?, arXiv:1311.7611 [hep-ph], to appear in Phys. Rev. D.

[67] G. Cvetic and R. Kogerler, Phys. Rev. D **84**, 056005 (2011) [arXiv:1107.2902 [hep-ph]].

[68] G. Cvetic, Nucl. Phys. B **517**, 506 (1998) [hep-ph/9711406].

[69] P. Allendes, C. Ayala and G. Cvetič, arXiv:1401.1192 [hep-ph].

[70] M. Frasca, Int. J. Mod. Phys. A **22**, 2433 (2007) [hep-th/0611276].

[71] M. Frasca, arXiv:0704.3260 [hep-th]. M. Frasca, Phys. Rev. D **73**, 027701 (2006) [Erratum-ibid. D **73**, 049902 (2006)] [hep-th/0511068]. M. Frasca, Int. J. Mod. Phys. A **22**, 1727 (2007) [hep-th/0610148].

[72] M. Frasca, Phys. Lett. B **670**, 73 (2008) [arXiv:0709.2042 [hep-th]].

[73] A. C. Aguilar and A. A. Natale, JHEP **0408**, 057 (2004) [hep-ph/0408254].

[74] M. Frasca, arXiv:0711.3860 [hep-th].

[75] A. Sternbeck, E. -M. Ilgenfritz, M. Muller-Preussker, A. Schiller and I. L. Bogolubsky, PoS LAT **2006**, 076 (2006) [hep-lat/0610053].

[76] P. Bicudo and O. Oliveira, PoS LATTICE **2010**, 269 (2010) [arXiv:1010.1975 [hep-lat]].

O. Oliveira and P. Bicudo, J. Phys. G **38**, 045003 (2011) [arXiv:1002.4151 [hep-lat]].

[77] J. M. Cornwall, Phys. Rev. D **26**, 1453 (1982).

[78] J. R. Forshaw, J. Papavassiliou and C. Parrinello, Phys. Rev. D **59**, 074008 (1999) [hep-ph/9808392].

[79] J. H. Field, Phys. Rev. D **66**, 013013 (2002) [hep-ph/0101158].

[80] I. L. Bogolubsky, E. M. Ilgenfritz, M. Muller-Preussker and A. Sternbeck, Phys. Lett. B **676**, 69 (2009) [arXiv:0901.0736 [hep-lat]].

[81] D. B. Leinweber *et al.* [UKQCD Collaboration], Phys. Rev. D **60**, 094507 (1999) [Erratum-ibid. D **61**, 079901 (2000)] [hep-lat/9811027].

[82] P. J. Silva and O. Oliveira, Nucl. Phys. B **690**, 177 (2004) [hep-lat/0403026].

[83] A. C. Aguilar, A. A. Natale and P. S. Rodrigues da Silva, Phys. Rev. Lett. **90**, 152001 (2003) [hep-ph/0212105].

[84] A. C. Aguilar and J. Papavassiliou, Phys. Rev. D **77**, 125022 (2008) [arXiv:0712.0780 [hep-ph]].

[85] A. C. Aguilar, D. Binosi and J. Papavassiliou, Phys. Rev. D **78**, 025010 (2008) [arXiv:0802.1870 [hep-ph]].

[86] D. Binosi and J. Papavassiliou, JHEP **0811**, 063 (2008) [arXiv:0805.3994 [hep-ph]].

[87] A. C. Aguilar and J. Papavassiliou, Phys. Rev. D **81**, 034003 (2010) [arXiv:0910.4142 [hep-ph]].

[88] T. Kugo and I. Ojima, Prog. Theor. Phys. Suppl. **66**, 1 (1979); N. Nakanishi and I. Ojima, *Covariant Operator Formalism of Gauge Theories and Quantum Gravity,* Lecture Notes in Physics Vol. 27 (World Scientific, Singapore, 1990).

[89] D. Zwanziger, Nucl. Phys. B **364**, 127 (1991); Nucl. Phys. B **378**, 525 (1992).

[90] C. Lerche and L. von Smekal, Phys. Rev. D **65**, 125006 (2002) [hep-ph/0202194].

[91] V. N. Gribov, Nucl. Phys. B **139**, 1 (1978); see also R. F. Sobreiro and S. P. Sorella, hep-th/0504095.

[92] J. C. Taylor, Nucl. Phys. B **33**, 436 (1971).

[93] A. Cucchieri and T. Mendes, PoS **LAT2007**, 297 (2007).

[94] I. L. Bogolubsky, E. M. Ilgenfritz, M. Muller-Preussker and A. Sternbeck, PoS **LAT2007**, 290 (2007).

[95] D. Binosi and J. Papavassiliou, Phys. Rev. D **77**, 061702 (2008)

[96] B. A. Magradze, Conf. Proc. C **980518**, 158 (1999) [hep-ph/9808247].

[97] P. O. Bowman, U. M. Heller, D. B. Leinweber, M. B. Parappilly, A. Sternbeck, L. von Smekal, A. G. Williams and J. -b. Zhang, Phys. Rev. D **76**, 094505 (2007) [hep-lat/0703022 [HEP-LAT]]; A. C. Aguilar, D. Binosi and J. Papavassiliou, Phys. Rev. D **86**, 014032 (2012) [arXiv:1204.3868 [hep-ph]].

[98] V. L. Khandramai, R. S. Pasechnik, D. V. Shirkov, O. P. Solovtsova and O. V. Teryaev, Phys. Lett. B **706**, 340 (2012) [arXiv:1106.6352 [hep-ph]].

[99] Yu. A. Simonov, Phys. Atom. Nucl. **58**, 107 (1995) [Yad. Fiz. **58**, 113 (1995)] [hep-ph/9311247]; arXiv:1011.5386 [hep-ph]; Phys. Atom. Nucl. **65**, 135 (2002) [Yad. Fiz. **65**, 140 (2002)] [hep-ph/0109081].

[100] A. M. Badalian and D. S. Kuzmenko, Phys. Rev. D **65**, 016004 (2002) [hep-ph/0104097]; A. M. Badalian, Phys. Atom. Nucl. **63**, 2173 (2000) [Yad. Fiz. **63**, 2269 (2000)].

[101] B. Badelek, J. Kwiecinski and A. Stasto, Z. Phys. C **74**, 297 (1997) [hep-ph/9603230].

[102] A. V. Kotikov, V. G. Krivokhizhin and B. G. Shaikhatdenov, Phys. Atom. Nucl. **75**, 507 (2012) [arXiv:1008.0545 [hep-ph]].

[103] D. V. Shirkov, Phys. Part. Nucl. Lett. **10**, 186 (2013) [arXiv:1208.2103 [hep-th]].

[104] E. G. S. Luna, A. L. dos Santos and A. A. Natale, Phys. Lett. B **698**, 52 (2011) [arXiv:1012.4443 [hep-ph]].

[105] C. Ayala and G. Cvetic, Phys. Rev. D **87**, no. 5, 054008 (2013) [arXiv:1210.6117 [hep-ph]].

[106] A. Pineda and F. J. Yndurain, Phys. Rev. D **61** (2000) 077505; Phys. Rev. D **58** (1998) 094022.

[107] N. Brambilla, A. Pineda, J. Soto and A. Vairo, Phys. Lett. B **470**, 215 (1999) [hep-ph/9910238].

[108] A. A. Penin and M. Steinhauser, Phys. Lett. B **538** (2002) 335 [arXiv:hep-ph/0204290].

[109] A. V. Smirnov, V. A. Smirnov and M. Steinhauser, Phys. Rev. Lett. **104**, 112002 (2010) [arXiv:0911.4742 [hep-ph]].

[110] C. Anzai, Y. Kiyo and Y. Sumino, Phys. Rev. Lett. **104**, 112003 (2010) [arXiv:0911.4335 [hep-ph]].

[111] N. Brambilla, Y. Sumino and A. Vairo, Phys. Rev. D **65** (2002) 034001 [arXiv:hep-ph/0108084].

[112] R. Tarrach, Nucl. Phys. B **183**, 384 (1981).

[113] N. Gray, D. J. Broadhurst, W. Grafe and K. Schilcher, Z. Phys. C **48** (1990) 673; L. V. Avdeev and M. Y. Kalmykov, Nucl. Phys. B **502**, 419 (1997) [arXiv:hep-ph/9701308].

[114] K. G. Chetyrkin and M. Steinhauser, Phys. Rev. Lett. **83**, 4001 (1999).

[115] K. G. Chetyrkin and M. Steinhauser, Nucl. Phys. B **573**, 617 (2000).

[116] K. Melnikov and T. v. Ritbergen, Phys. Lett. B **482**, 99 (2000).

[117] K. G. Chetyrkin, B. A. Kniehl and M. Steinhauser, Phys. Rev. Lett. **79**, 2184 (1997) [arXiv:hep-ph/9706430].

[118] A. H. Hoang, M. C. Smith, T. Stelzer and S. Willenbrock, Phys. Rev. D **59** (1999) 114014 [arXiv:hep-ph/9804227].

[119] N. Brambilla, Y. Sumino and A. Vairo, Phys. Lett. B **513**, 381 (2001) [hep-ph/0101305].

[120] N. Brambilla, A. Pineda, J. Soto and A. Vairo, Nucl. Phys. B **566** (2000) 275 [arXiv:hep-ph/9907240].

[121] M. Beneke, Phys. Lett. B **434** (1998) 115 [arXiv:hep-ph/9804241].

[122] Y. Kiyo and Y. Sumino, Phys. Lett. B **496**, 83 (2000) [hep-ph/0007251]; Phys. Rev. D **67**, 071501 (2003) [arXiv:hep-ph/0211299].

[123] M. Beneke and M. Jamin, JHEP **0809**, 044 (2008) [arXiv:0806.3156 [hep-ph]].

[124] A. H. Hoang, Z. Ligeti and A. V. Manohar, Phys. Rev. Lett. **82**, 277 (1999) [arXiv:hep-ph/9809423]; Phys. Rev. D **59**, 074017 (1999) [arXiv:hep-ph/9811239].

[125] K. G. Chetyrkin, B. A. Kniehl and A. Sirlin, Phys. Lett. B **402**, 359 (1997) [hep-ph/9703226].

[126] A. V. Radyushkin, JINR E2-82-159 (1982), JINR Rapid Commun. **78**, 96 (1996) [hep-ph/9907228]; N. V. Krasnikov and A. A. Pivovarov, Phys. Lett. B **116**, 168 (1982); S. G. Gorishnii, A. L. Kataev and S. A. Larin, Sov. J. Nucl. Phys. **40**, 329 (1984) [Yad. Fiz. **40**, 517 (1984)].

[127] A. L. Kataev and V. T. Kim, Phys. Part. Nucl. **41**, 946 (2010) [arXiv:1001.4207 [hep-ph]].

[128] D. Eiras and J. Soto, Phys. Lett. B **491**, 101 (2000) [arXiv:hep-ph/0005066].

[129] A. H. Hoang, arXiv:hep-ph/0008102.

[130] M. B. Voloshin, Nucl. Phys. B **154**, 365 (1979); H. Leutwyler, Phys. Lett. B **98**, 447 (1981); M. B. Voloshin, Sov. J. Nucl. Phys. **36**, 143 (1982) [Yad. Fiz. **36**, 247 (1982)].

[131] B. L. Ioffe and K. N. Zyablyuk, Eur. Phys. J. C **27**, 229 (2003) [arXiv:hep-ph/0207183].

[132] G. Cvetič and C. Villavicencio, Phys. Rev. D **86**, 116001 (2012) [arXiv:1209.2953 [hep-ph]].

[133] B. V. Geshkenbein, B. L. Ioffe and K. N. Zyablyuk, Phys. Rev. D **64**, 093009 (2001) [arXiv:hep-ph/0104048]; B. L. Ioffe, Prog. Part. Nucl. Phys. **56**, 232 (2006) [arXiv:hep-ph/0502148].

[134] P. Dimopoulos *et al.* [ETM Collaboration], JHEP **1201**, 046 (2012) [arXiv:1107.1441 [hep-lat]].

[135] B. Blossier *et al.* [ETM Collaboration], Phys. Rev. D **82**, 114513 (2010) [arXiv:1010.3659 [hep-lat]].

[136] D. Guazzini, R. Sommer and N. Tantalo, JHEP **0801**, 076 (2008) [arXiv:0710.2229 [hep-lat]].

[137] M. Della Morte, N. Garron, M. Papinutto and R. Sommer, JHEP **0701**, 007 (2007) [hep-ph/0609294].

[138] G. M. de Divitiis, M. Guagnelli, R. Petronzio, N. Tantalo and F. Palombi, Nucl. Phys. B **675**, 309 (2003) [hep-lat/0305018].

[139] S. Narison, Phys. Lett. B **706**, 412 (2012) [arXiv:1105.2922 [hep-ph]]; Phys. Lett. B **707**, 259 (2012) [arXiv:1105.5070 [hep-ph]].

[140] K. G. Chetyrkin, J. H. Kühn, A. Maier, P. Maierhofer, P. Marquard, M. Steinhauser and C. Sturm, Phys. Rev. D **80**, 074010 (2009) [arXiv:0907.2110 [hep-ph]].

[141] C. McNeile, C. T. H. Davies, E. Follana, K. Hornbostel and G. P. Lepage, Phys. Rev. D **82**, 034512 (2010) [arXiv:1004.4285 [hep-lat]].

[142] A. Pineda and A. Signer, Phys. Rev. D **73**, 111501 (2006) [hep-ph/0601185].

[143] R. Boughezal, M. Czakon and T. Schutzmeier, Phys. Rev. D **74**, 074006 (2006) [hep-ph/0605023].

[144] A. Laschka, N. Kaiser and W. Weise, Phys. Rev. D **83**, 094002 (2011) [arXiv:1102.0945 [hep-ph]].

[145] C. Contreras, G. Cvetič and P. Gaete, Phys. Rev. D **70** (2004) 034008 [arXiv:hep-ph/0311202].

[146] T. Lee, JHEP **0310**, 044 (2003) [arXiv:hep-ph/0304185].

[147] A. Pineda, JHEP **0106**, 022 (2001) [arXiv:hep-ph/0105008].

[148] A. Pineda, Nucl. Phys. B **494**, 213 (1997) [hep-ph/9611388].

[149] C. Ayala and S. V. Mikhailov, "Calculation of Structure Function in analytic QCD models with Jacobi polynomials method", to be submitted.

[150] F. J. Yndurain, Quantum Chromodynamics (An Introduction to the Theory of Quarks and Gluons) (Springer-Verlag, Berlin, 1983).

[151] W. Greiner, S. Schramm and E. Stein, Quantum Chromodynamics (Springer, 2006).

[152] T. Muta, Foundations Of Quantum Chromodynamics (An Introduction to Perturbative Methods in Gauge Theories) (World Scientific Lecture Notes in Physics, 2009).

[153] F. Halzen and A. D. Martin, Quarks and Leptons (An Introductory Course in Modern Particle Physics) (Wiley, 1984).

[154] V. G. Krivokhizhin and A. V. Kotikov, Phys. Atom. Nucl. **68** (2005) 1873 [Yad. Fiz. **68** (2005) 1935]; V. G. Krivokhizhin and A. V. Kotikov, Phys. Part. Nucl. **40**, 1059 (2009).

[155] A. J. Buras, Rev. Mod. Phys. **52**, 199 (1980).

[156] J. D. Bjorken, Phys. Rev. **179**, 1547 (1969).

[157] R. P. Feynman, Phys. Rev. Lett. **23**, 1415 (1969).

[158] W. K. H. Panofsky, 1968, *Proceedings of the* 14^{th} *International Conference on High Energy Physics* , Vienna, p.23 (Editors J. Prentki and J. Steinberger, CERN Geneva).

[159] C. G. Callan, Jr. and D. J. Gross, Phys. Rev. Lett. **22**, 156 (1969).

[160] G. Altarelli, Phys. Rept. **81**, 1 (1982).

[161] V. N. Gribov and L. N. Lipatov, Sov. J. Nucl. Phys. **15**, 438 (1972) [Yad. Fiz. **15**, 781 (1972)]; L. N. Lipatov, Sov. J. Nucl. Phys. **20**, 94 (1975) [Yad. Fiz. **20**, 181 (1974)]; G. Altarelli and G. Parisi, Nucl. Phys. B **126**, 298 (1977); Y. L. Dokshitzer, Sov. Phys. JETP **46**, 641 (1977) [Zh. Eksp. Teor. Fiz. **73**, 1216 (1977)].

[162] J. Beringer *et al.* [Particle Data Group Collaboration], Phys. Rev. D **86**, 010001 (2012).

[163] K. G. Wilson, Phys. Rev. **179**, 1499 (1969).

[164] E. G. Floratos, D. A. Ross and C. T. Sachrajda, Nucl. Phys. B **129**, 66 (1977) [Erratum-ibid. B **139**, 545 (1978)]; A. Gonzalez-Arroyo, C. Lopez and F. J. Yndurain, Nucl. Phys. B **153**, 161 (1979).

[165] J. Blumlein and J. A. M. Vermaseren, Phys. Lett. B **606**, 130 (2005) [hep-ph/0411111]; S. A. Larin, P. Nogueira, T. van Ritbergen and J. A. M. Ver-

maseren, Nucl. Phys. B **492**, 338 (1997) [hep-ph/9605317]; S. Moch, J. A. M. Vermaseren and A. Vogt, Nucl. Phys. B **688**, 101 (2004) [hep-ph/0403192].

[166] R. L. Kingsley, Nucl. Phys. B **60**, 45 (1973); T. F. Walsh and P. M. Zerwas, Phys. Lett. B **44**, 195 (1973); A. De Rujula, S. L. Glashow, H. D. Politzer, S. B. Treiman, F. Wilczek and A. Zee, Phys. Rev. D **10**, 1649 (1974); E. Witten, Nucl. Phys. B **104**, 445 (1976); A. De Rujula, H. Georgi and H. D. Politzer, Annals Phys. **103**, 315 (1977); M. Calvo, Phys. Rev. D **15**, 730 (1977); I. Hinchliffe and C. H. Llewellyn Smith, Nucl. Phys. B **128**, 93 (1977); G. Altarelli, R. K. Ellis and G. Martinelli, Nucl. Phys. B **143**, 521 (1978) [Erratum-ibid. B **146**, 544 (1978)]; J. Abad and B. Humpert, Phys. Lett. B **77**, 105 (1978); J. Kubar-Andre and F. E. Paige, Phys. Rev. D **19**, 221 (1979); E. G. Floratos, D. A. Ross and C. T. Sachrajda, Nucl. Phys. B **152**, 493 (1979).

[167] W. L. van Neerven and E. B. Zijlstra, Phys. Lett. B **272**, 127 (1991); E. B. Zijlstra and W. L. van Neerven, Phys. Lett. B **273**, 476 (1991); E. B. Zijlstra and W. L. van Neerven, Phys. Lett. B **297**, 377 (1992); E. B. Zijlstra and W. L. van Neerven, Nucl. Phys. B **383**, 525 (1992); W. L. van Neerven and E. B. Zijlstra, Nucl. Phys. B **382**, 11 (1992) [Erratum-ibid. B **680**, 513 (2004)]; J. A. M. Vermaseren, A. Vogt and S. Moch, Nucl. Phys. B **724**, 3 (2005) [hep-ph/0504242].

[168] V. G. Krivokhizhin, S. P. Kurlovich, V. V. Sanadze, I. A. Savin, A. V. Sidorov and N. B. Skachkov, Z. Phys. C **36**, 51 (1987); Z. Phys. C **48**, 347 (1990).

[169] A. D. Martin, W. J. Stirling, R. S. Thorne and G. Watt, Eur. Phys. J. C **63**, 189 (2009) [arXiv:0901.0002 [hep-ph]].

[170] A. P. Bakulev and V. L. Khandramai, arXiv:1204.2679 [hep-ph].

[171] I. I. Bigi, M. A. Shifman, N. G. Uraltsev and A. I. Vainshtein, Phys. Rev. D **50** (1994) 2234 [arXiv:hep-ph/9402360].

[172] M. Beneke and V. M. Braun, Nucl. Phys. B **426** (1994) 301 [arXiv:hep-ph/9402364].

[173] M. Beneke, Phys. Rept. **317** (1999) 1.

[174] M. Beneke, Phys. Lett. B **344**, 341 (1995) [arXiv:hep-ph/9408380].

[175] J. Ellis, I. Jack, D. R. T. Jones, M. Karliner and M. A. Samuel, Phys. Rev. D **57**, 2665 (1998) [arXiv:hep-ph/9710302].

[176] T. Lee, Phys. Rev. D **56** (1997) 1091 [arXiv:hep-th/9611010]; Phys. Lett. B **462** (1999) 1 [arXiv:hep-ph/9908225].

[177] G. Cvetič, J. Phys. G **30**, 863 (2004) [hep-ph/0309262].

[178] M. Neubert, Phys. Lett. B **393**, 110 (1997) [hep-ph/9610471].

[179] V. Elias, T. G. Steele, F. Chishtie, R. Migneron and K. B. Sprague, Phys. Rev. D **58**, 116007 (1998) [arXiv:hep-ph/9806324].

[180] G. Grunberg, Phys. Lett. **95B**, 70 (1980), **110B**, 501(E) (1982); **114B**, 271 (1982); Phys. Rev. D **29**, 2315 (1984); N. V. Krasnikov, Nucl. Phys. B **192**, 497 (1981) [Yad. Fiz. **35**, 1594 (1982)]. A. L. Kataev, N. V. Krasnikov, and A. A. Pivovarov, Nucl. Phys. **B198**, 508 (1982); A. Dhar and V. Gupta, Phys. Rev. D **29**, 2822 (1984); V. Gupta, D. V. Shirkov, and O. V. Tarasov, Int. J. Mod. Phys. A **06**, 3381 (1991).

[181] A. L. Kataev and V. V. Starshenko, Mod. Phys. Lett. A **10**, 235 (1995) [hep-ph/9502348].